UNIVERSITEIT VAN PRETORIA
UNIVERSITY OF PRETORIA
YUNIBESITHI YA PRETORIA

DEVELOPMENT OF APPROPRIATE SYNTHETIC DESIGN STORMS FOR SMALL CATCHMENTS IN GAUTENG, SOUTH AFRICA

JACOBUS VAN STADEN MOUTON

A dissertation submitted in partial fulfilment of the requirements for the degree of

MASTER OF SCIENCE (APPLIED SCIENCE: WATER RESOURCES)

In the

FACULTY OF ENGINEERING, BUILT ENVIRONMENT AND INFORMATION TECHNOLOGY

UNIVERSITY OF PRETORIA

February 2023

DISSERTATION SUMMARY

DEVELOPMENT OF APPROPRIATE SYNTHETIC DESIGN STORMS FOR SMALL CATCHMENTS IN GAUTENG, SOUTH AFRICA

J.V.S. MOUTON

Supervisor: Ms I. Loots

Co-Supervisor: Professor J.C. Smithers

Department: Civil Engineering

University: University of Pretoria

Degree: Master of Science (Applied Science: Water Resources)

Urban stormwater drainage networks are frequently analysed in dynamic rainfall-runoff simulation models. These models use a hypothetical rainstorm event (synthetic design storm) as input in the case of single event-based modelling. A significant number of methods to generate synthetic design storms are described in the literature and they are IDF based, mass-curve based, and stochastically based. However, due to the abundance of methods some engineers are likely to base their method choice on familiarity with a method and preference. This could lead to the selection of an inappropriate method that will generate unrealistic peak discharge results. Therefore, the need to develop appropriate synthetic design storms applicable to single event-based modelling of small urban catchments in South Africa was identified.

The aim of this study was to test the performance of the existing methods used for generation of design storms, and to identify the method, or methods, best suited for single event-based modelling of small urban catchments in the selected pilot study area, Gauteng. The specific objectives to meet the aim were to identify and assess the performance of currently available methods, and to propose improved procedures. The 5-min interval rainfall records obtained from the South African Weather Service (SAWS) were used for the analyses. The completeness of the data was assessed, at-site design rainfall was determined, storm events were identified and analysed to obtain the general storm parameters, and synthetic design storms were generated and compared with the observed storm events. The performance of each method was evaluated based on its shape and intensity, whereas the peak discharge and the runoff volume were evaluated using dynamic rainfall-runoff simulation models.

The Mean Absolute Relative Error (MARE) was used as a measure to determine the Goodness-of-Fit (GOF) between the observed and the simulated storm events. It was concluded that synthetic design storms are not representative of naturally occurring storm events. However, despite this shortcoming, the use of synthetic design storms in a single event-based model resulted in good peak discharge and runoff volume estimates. It, therefore, provides the engineer with the ability to assess the complex hydrological and hydraulic characteristics of an urban stormwater network in a timely manner. The results from the study indicate that the Chicago Design Storm (CDS) and SCS-SA are recommended for single event-based models in Gauteng. Both methods have the ability to generate site-specific synthetic design storms, but improvements were proposed in terms of: (a) estimating the Intensity-Duration-Frequency (IDF) regression coefficients, and (b) the development of Intermediate Curve (IC) values.

The estimates of the IDF regression coefficients for the CDS were determined from the design rainfall estimated by the Design Rainfall Estimation in South Africa (DRESA) software. The coefficients were determined using the Generalised Reduced Gradient (GRG) nonlinear algorithm in combination with the Root Mean Square Error (RMSE) formula. The RMSE was used to measure the GOF between DRESA and the Sherman (1931) IDF formula whilst the coefficients were simultaneously optimised. This methodology resulted in small relative errors between DRESA and the simulated intensities. The optimised regression coefficients and the average storm advancement coefficient of 0.38, determined for the Gauteng Province using Keifer and Chu's (1957) methodology, produced good results when applied to the simulation models. The IC values were developed for the SCS-SA curves following the assessment of the performance of the Type 3 curve for the province. In contrast to Weddepohl (1988), it was found that on average the rainfall distribution in the Gauteng province is closer to the Type 2 than the Type 3 distribution, with a significant variation observed across the province. Therefore, a method of linear interpolation between the standard type curves was developed to determine an intermediate curve. The Inverse Distance Weighting (IDW) method was used for the geographical interpolation of IC values. For more accurate modelling of an ungauged site an intermediate curve can be generated based on the IC value of the ungauged site. Guidance is provided for further refinement of both the CDS and the SCS-SA curves. This included the following: (a) investigating the effect of the advancement coefficient and total storm duration on the peak discharge and runoff volume estimates; (b) determining the impact missing data has on design rainfall estimation; (c) validating the General Extreme Value (GEV) probability distribution for short duration design rainfall; (d) finding an appropriate IDW exponent for determining IC values; and (e) expanding the investigation by determining the relevance of the CDS and SCS-SA on a national scale.

ABSTRACT

Title: Development of appropriate synthetic design storms for use in small urban catchments: Gauteng pilot study

Author: Mr J.v.S. Mouton

Supervisor: Ms I. Loots

Co-Supervisor: Professor J.C. Smithers

Department: Civil Engineering

University: University of Pretoria

Degree: Master of Science (Applied Science: Water Resources)

Urban stormwater drainage networks are frequently analysed in dynamic rainfall-runoff simulation models. These models use hypothetical rainstorm events (synthetic design storms) as input in the case of single event-based modelling. A significant number of methods to generate synthetic design storms are described in the literature. However, due to the abundance of methods some engineers are likely to base their method choice on familiarity with a method and preference. This could lead to the selection of an inappropriate synthetic design storm that will generate unrealistic peak discharge results. Therefore, the need to develop appropriate synthetic design storms applicable to single event-based modelling of small urban catchments in South Africa was identified. The aim of this study was to test the performance of the existing methods, and to identify the method, or methods, best suited for single event-based modelling of small urban catchments in the selected pilot study area. The completeness of the data was assessed, at-site design rainfall was determined, storm events were identified and analysed to obtain the general storm parameters, and synthetic design storms were generated and compared with the observed rainfall mass curves. The performance was evaluated based on the shape of the storm and the intensity, whereas the peak discharge and the runoff volume was evaluated using dynamic rainfall-runoff simulation models. The Mean Absolute Relative Error (MARE) was used as a measure to determine the Goodness-of-Fit (GOF) of the data. It was concluded that the Chicago Design Storm and SCS-SA curves are most suited for single event-based models. Improvements to the Chicago Design Storm and SCS-SA curves are proposed to better simulate design rainfall events and guidance is provided for further refinement.

DECLARATION

I, the undersigned hereby declare that:

- I understand what plagiarism is and I am aware of the University's policy in this regard;
- The work contained in this dissertation is my original work;
- I did not refer to the work of current or previous students, lecture notes, handbooks, or any other study material without proper referencing;
- Where other people's work has been used this has been properly acknowledged and referenced;
- I have not allowed anyone to copy any part of my dissertation;
- I have not previously in its entirety or part submitted this dissertation at any university for a degree.

DISCLAIMER:

The work presented in this report is that of the student alone. Students were encouraged to take ownership of their projects and to develop and execute their experiments with limited guidance and assistance. The content of the research does not necessarily represent the views of the supervisor or any staff member of the University of Pretoria, Department of Civil Engineering. The supervisor did not read or edit the final report and is not responsible for any technical inaccuracies, statements, or errors. The conclusions and recommendations given in the report are also not necessarily that of the supervisor, sponsors or companies involved in the research.

Signature of student: 

Name of student: J.v.S Mouton

Student number: 10 60 1776

Date: 10 Feb 2023

Supervisor: 

ACKNOWLEDGEMENTS

I wish to express my appreciation to the following organisations and persons who made this project dissertation possible:

a) This project dissertation is based on the analysis of the short duration rainfall data provided by the South African Weather Services (SAWS). Permission to use the material is gratefully acknowledged. The opinions expressed are those of the author and do not necessarily represent the policy of SAWS.

b) The Water Research Commission (WRC) for financial support.

c) The following persons are gratefully acknowledged for their assistance during the study:

   i) Mrs Cornelia Dighton, for her proof reading and editing, and
   ii) Mr Gerhard Munro, for his assistance with the Java application development.

d) Ms I. Loots, my supervisor, and Professor J.C. Smithers, my co-supervisor for their guidance and support.

e) My wife and children (Elsabé, Danielle, and Amoré) for their love and encouragement, and family for their support during the study.

TABLE OF CONTENTS

LIST OF TABLES

LIST OF FIGURES

LIST OF SYMBOLS

Acronym	Description
a	Time to peak intensity (min)
a^o	Dimensionless time to peak
ABS	Absolute relative error
AIC_T	Average Intermediate Curve per Recurrence Interval
AIC_t	Average Intermediate Curve per time step
AIC_G	Average Intermediate Curve for Gauteng
AMC	Antecedent Moisture Content
AMS	Annual Maximum Series
ARD	Average Relative Difference (%)
ARE_t	Average Relative Error per time step
ARE_S	Average Relative Error per station
ARS	Automatic Rainfall Station
AWS	Automatic Weather Station
CDS	Chicago Design Storm
CTMM	City of Tshwane Metropolitan Municipality
D	Total rainfall volume (mm)
DC	Distribution Curve
DC5	1:5 year Distribution Curve
DC10	1:10 year Distribution Curve
DC20	1:20 year Distribution Curve
DDF	Depth Duration Frequency
DRESA	Design Rainfall Estimation in South Africa
EPA	Environmental Protection Agency
GEV	General Extreme Value
GOF	Goodness-of-Fit
GRG	Generalised Reduced Gradient
GPRS	General Packet Radio Service
h	Maximum rainfall intensity (mm/h)

h^0	Dimensionless maximum intensity
HRU	Hydrological Research Unit
i	Storm intensity (mm/hour)
i_a	Intensity after the peak intensity (mm/hour)
i_{av}	Average intensity (mm/hour)
i_b	Intensity before the peak intensity (mm/hour)
IC	Intermediate Curve
ICT	Intermediate cumulative rainfall ratio per time step
i_p	Peak intensity (mm/hour)
IDF	Intensity Duration Frequency
IDF_A	Actual design rainfall intensity (mm/hour)
IDF_S	Simulated design rainfall intensity (mm/hour)
IDW	Inverse Distance Weighting
ILLUDAS	Illinois Urban Drainage Area Simulator
MAP	Mean annual precipitation (mm)
MARE	Mean Absolute Relative Error
MARE_I	Mean Absolute Relative Error of the average intensities
MARE_S	Mean Absolute Relative Error of the mass curve shapes
MDP	Maximum Dry Period (min)
MIDUSS	A Windows-based software program that generates hydrographs for complex drainage networks from single event storms.
MRD	Minimum Rainfall Depth (mm)
MRI	Minimum Rainfall Intensity (mm/hour)
MS	Microsoft
NOAA	National Oceanic and Atmospheric Administration
NRCS	National Resources Conservation Service
P	Total rainfall depth (mm)
P_a	Cumulative rainfall depth after the peak intensity (mm)
P_b	Cumulative rainfall depth before the peak intensity (mm)
PD	Probability Distribution

r	Storm advancement coefficient. The ratio of the storm duration of the peak intensity relative to the total storm duration
RE	Relative Error (%)
RD	Relative Difference (%)
REC	Rectangular hyetograph method
RI	Recurrence Interval (1:year)
RIM	Recurrence Interval Maximum
RIR	Recurrence Interval Ratio
RMSE	Root Mean Square Error
R^2	Coefficient of determination
SA(T2)	SCS-SA Type 2
SA(T3)	SCS-SA Type 3
SAWS	South African Weather Service
SCS	Soil Conservation Services
SCS-SA	SCS curves adapted for Southern African conditions
SPI	Smoothed Probability Inherited
SWMM	Stormwater Management Model
t_a	Storm duration after the peak intensity (min)
t_b	Storm duration before the peak intensity (min)
T_c	Critical storm duration (hour)
T_d	Total storm duration (min)
T_p	Time when peak intensity occurs (min)
TRI	Triangular hyetograph method
USA	United States of America
USDA	United States Department of Agriculture
μ	Mean of the dimensionless cumulative hyetograph ordinates
WO	Weather Office

1 INTRODUCTION

1.1 BACKGROUND

Engineers have for centuries concerned themselves with redirecting and managing stormwater runoff to address the persistent increase in demands associated with civilisation. As a result, flood estimation methods were developed which have evolved into sophisticated computer-aided stormwater simulation modelling. The hydrological and hydraulic behaviour of an urban stormwater drainage network is frequently simulated using software such as the Stormwater Management Model (SWMM), developed by the United States Environmental Protection Agency (EPA). The rainfall-runoff process of an urban network can be simulated effectively and accurately with SWMM which has become the preferred method in the United States and Canada (Watt and Marsalek, 2013). Simulations can be run on a continuous basis using observed rainfall data, but because of the scarcity of short duration rainfall data many urban stormwater and infrastructure designs are rather based on single event-based modelling using a hypothetical rainstorm event (synthetic design storm) as input.

A significant number of methods to generate synthetic design storms are described in the literature (Veneziano and Villani, 1999; Al-Saadi, 2002; Asquith et al., 2003; Prodanovic and Simonovic, 2004; Smith, 2004; Knoesen, 2005; Watt and Marsalek, 2013; Pan et al., 2017; Weesakul et al., 2017; Ramlall, 2020; Wartalska et al., 2020). However, due to the abundance of methods some engineers are likely to base their method choice on familiarity with a method and preference. This could lead to the selection of an inappropriate method that will generate unrealistic peak discharge results (Watt and Marsalek, 2013). The synthetic design storm concept has also received criticism in an earlier study (Adams and Howard, 1986) which states that it should be used with care due to the large potential for error. Therefore, the need to develop appropriate synthetic design storms for small urban catchments was identified.

The focus of this pilot study in the Gauteng Province of South Africa is to assess the performance of methods used to generate synthetic design storms for single event-based modelling, applicable to small urban catchments. This document describes the methodology followed and results obtained from considering existing methods, and (a) comparing them against recently measured 5-min rainfall data, and (b) applying them to a typical urban stormwater network, to identify the method, or methods, most suited for single event-based modelling in small urban catchments in the selected pilot study area.

1.2 AIMS AND OBJECTIVES OF THE STUDY

As described in the background, the selection of an appropriate synthetic design storm is essential for generating realistic peak discharge results in single event-based modelling. Therefore, the aim of this study was (a) to test the performance of the existing synthetic design storm generation methods, and (b) to identify the method, or methods, most suited for conditions in small catchments in Gauteng, using the 5-min interval rainfall records obtained from the South African Weather Service (SAWS). The specific objectives to meet the aim were to: (i) identify and assess the performance of appropriate methods, and (ii) propose improved procedures to generate accurate synthetic design storms.

1.3 SCOPE OF THE STUDY

The observed rainfall data collection was limited to automatic recording rainfall stations with 5-min interval measurements operated by the SAWS within the boundaries of Gauteng. The existing methods used by some engineers were identified during the Flood Hydrology course presented by the University of Pretoria in February 2020. Further methods were identified telephonically as well as during one-on-one interviews with leading experts in this field. Therefore, the existing methods considered in the literature review include the following:

a) Rectangular hyetograph (Mulvaney, 1851);

b) Chicago design storm (Keifer and Chu, 1957);

c) The Huff curves (Huff, 1967);

d) Unites States Department of Agriculture's Soil Conservation Services (SCS) synthetic storm distribution curves (SCS, 1973);

e) The expanded SCS version adapted for Southern African conditions (SCS-SA) synthetic storm distribution curves (Schulze, 1984);

f) Triangular hyetograph (Yen and Chow, 1980);

g) Daily rainfall disaggregation model for South Africa (Knoesen, 2005); and

h) HRU 1/72 time distribution for intermediate durations.

1.4 METHODOLOGY

The methods considered for estimating temporal distributions of design rainfall were evaluated against recently measured 5-min rainfall data, to find the synthetic design storm best suited for single event-based modelling of small, urbanised catchment areas, with the case study area of Gauteng as the geographical focus. The rainfall data were assessed, the Chicago Design Storm (CDS) and SCS-SA curves were refined, and also improved.

The rainfall data were collated and reviewed by conducting a missing data analysis, taking the time of the year when missing data occurs into consideration as described in Chapter 3. The data quality of each station was characterised according to the data period and missing data occurring during the 'wet' months. Independent storm events were identified considering an allowable dry period between rainfall spells, the rainfall depth, and the rainfall intensity of the storm event. The methods were refined by extracting the general storm parameters as described in Chapter 4. This includes the storm advancement coefficient relating to the CDS method, and the dimensionless time to peak relating to the Triangular method. The at-site design rainfall was estimated, using the Generalised Extreme Value (GEV) probability distribution, and the D-hour to 24-hour ratios determined. The ratios were compared with the SCS and SCS-SA curves, as well as the ratios of the standardised mass curves.

The methods were evaluated by comparing the synthetic design storms with the observed rainfall events as described in Chapter 5. Two aspects were evaluated, namely the shape of the mass curves, as well as the average intensities embedded in each synthetic design storm. This was achieved by non-dimensionalising each significant event in terms of rainfall and generating a synthetic storm event matching the total duration. The evaluation of the intensities was conducted by considering the ratios of average intensities of the standard time steps (5, 10, 15, 30, 45-min, etc.). The evaluation of the simulated peak discharge and runoff volume was undertaken following the synthetic design storm evaluation. This was achieved by simulating a hypothetical catchment that is representative of the catchment size targeted in this study. The simulated peak discharge and runoff volume generated with different synthetic design storms were compared with results from continuous simulation using observed rainfall data as input.

1.5 ORGANISATION OF THE REPORT

The report consists of the following chapters:

a) Chapter 1 : Introduction – This chapter provides the objective and scope of the study, as well as the methodology and the aim of this study.

b) Chapter 2 : Literature review – The literature review that was conducted on the existing methods in terms of their development, application, and limitations, is described in this chapter.

c) Chapter 3 : Research methodology – This chapter describes the data collection, quality assessment and storm event identification processes applied in this study.

d) Chapter 4 : Data analysis – This chapter describe several aspects relating to the generation of synthetic design storms which provides the foundation for the next chapter. The extraction of storm parameters, at-site design rainfall estimation, IDF regression coefficients, 24-hour rainfall distributions, SCS-SA curve ratio comparisons, SCS curve ratio comparisons, and standardised mass curves are described in this Chapter.

e) Chapter 5 : Evaluation of synthetic design storms – This chapter contains details of the synthetic design storm evaluation by comparison between mass curves and average intensities, as well as simulated peak discharge and runoff volumes.

f) Chapter 6 : Discussion, conclusion, and recommendations – This chapter presents a discussion of the results from the analyses and conclusions that emanated from this study. The proposed way forward is also described.

g) References.

h) Annexure A – This annexure provides an alternative development of the cumulative rainfall formulae for the DCS method.

i) Annexure B – At site design rainfall estimation of 16 stations in Gauteng.

2 LITERATURE REVIEW

2.1 BACKGROUND

A natural hydrological event, in its simplest form, starts with a hyetograph and ends with a hydrograph, each having many unique characteristics that are quantifiable, such as total volume, total duration, intensities and skewness (Adams and Howard, 1986). The link, being the catchment with its various characteristics and antecedent moisture conditions, determines the relationship between the hyetograph and hydrograph. For example, two different hyetographs with two identical catchments and antecedent conditions can result in differently shaped hydrographs, but with the same peak discharge. Conversely, two identical hyetographs with two different catchments and antecedent conditions can result in two different hydrographs with different peak discharges (Adams and Howard, 1986). Despite the uncertainties about this transitional stage that rainfall needs to pass through before runoff is generated, it is nevertheless assumed that the frequency of the hyetograph is identical to the frequency of the hydrograph. This unrealistic assumption is well documented by Adams and Howard (1986) who, as a result, states it should be used only in the strictest of circumstances due to the large potential for error associated with the synthetic design storm concept.

It is, therefore, important to simulate a storm event with the hyetograph shape that will most likely be representative of the natural rainfall event since the storm shape may have a significant impact on the peak discharge and total flood volume. It becomes more noticeable at catchments with a high percentage of areas that saturate quickly. This is due to the rapid decline of the infiltration capacity during the early part of a rainstorm, which then tends towards an approximately constant value after a few hours for the remainder of the event (Horton, 1933). If the peak intensity of a synthetic design storm is applied earlier during the storm event, the infiltration capacity might be higher, which will result in a lower peak flow result. Conversely, a storm event peaking later during the event is likely to result in higher flow results.

The existing methods covered in this study have a strong scientific basis which guides the classification into three categories, which is an adaptation of the four categories defined by Veneziano and Villani (1999), as follows (Figure 2.1):

a) Methods that are derived from the IDF curves:

   i) Methods based on a simple geometrical shape using a single point on the IDF curve. This category includes the rectangular and triangular methods;

   ii) Methods that use the entire IDF curve, which includes the CDS method and to a degree the SCS and SCS-SA curves;

b) Standardised mass curves generated directly from rainfall records, which includes the Huff and NOAA Atlas 14 curves; and

c) The simulation from a stochastic rainfall model, which includes the daily rainfall disaggregation model for South Africa.

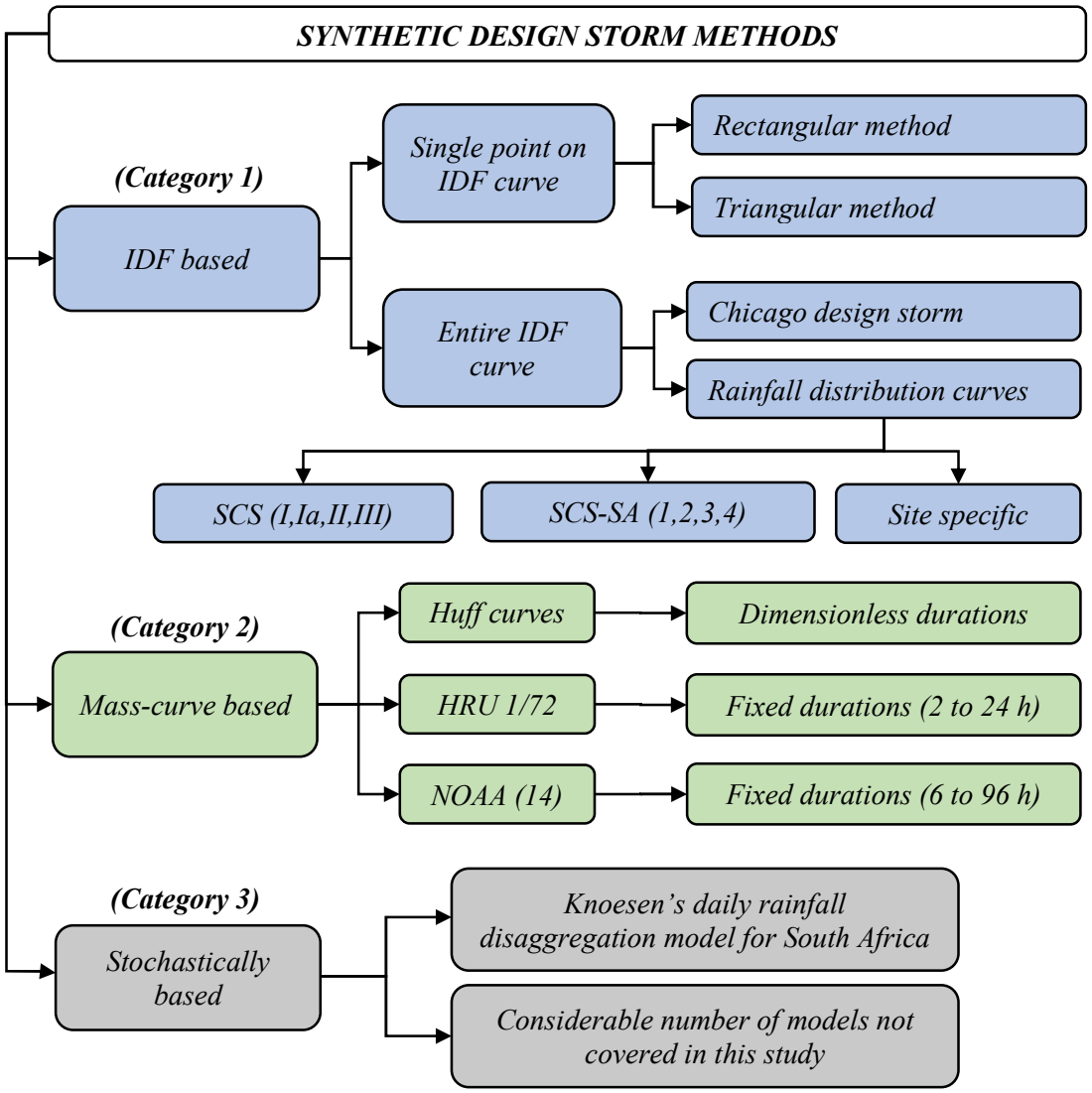

Figure 2.1: Categorization of design storm methods covered in the literature review (after Veneziano and Villani, 1999)

2.2 IDF BASED METHODS

2.2.1 Rectangular hyetograph

The Rectangular hyetograph (REC) method is commonly associated with the Rational Method, which is the most employed formula in engineering hydrology (Gomez and Sanchez, 2014), and it is used worldwide for flood protection design (Cordery and Pilgrim, 1993). This method assumes that the peak discharge occurs when the duration of the rainfall event is equal to the time of concentration of the catchment; that the rainfall intensity does not vary; and is distributed uniformly over the catchment (Smithers, 2012). The first principle of the Rational Method, the runoff coefficient, was concluded through the gradual development of flood estimation methods by researchers in the British Isles before the year 1850. Thomas Mulvaney presented the second principle, the time of concentration, and the method of estimating the peak discharge in 1851, which became known as the Rational Method (Gomez and Sanchez, 2014). With the development of the St. Venant equations for modelling surface flow towards the end of the 19th century (Boussinesq and Flamant, 1886) and the soil infiltration models, like the Green-Ampt model during the early 20th century (Green and Ampt, 1911), methods like the Unit Hydrograph (Sherman, 1932) were developed. This method in its simple form also assumes a uniform rainfall intensity distribution with a duration equal to or greater than the longest time of concentration.

2.2.2 Triangular hyetograph

The Triangular hyetograph (TRI) method was formulated by Yen and Chow (1980). The first-moment arm was calculated for the recorded hyetograph concerning the beginning of the rainstorm. It was related to a triangular representation of the hyetograph with an equal total rainfall volume and total storm duration. Each triangular hyetograph was non-dimensionalised in terms of the maximum intensity as well as the time to the maximum intensity, relative to the total storm duration. Yen and Chow (1980) considered the typically recorded hyetograph depicted in which depicts a typical hyetograph. Yen and Chow (1980) defined the first-moment arm concerning the beginning of the rainstorm in terms of Equation 2.1.

$$\bar{t} = \frac{\Delta t\left[\sum_{j=1}^{n}(j-0.5)d_j\right]}{\sum_{j=1}^{n} d_j} \qquad \text{(Equation 2.1)}$$

where:

$\bar{t}$ = first-moment arm of the hyetograph (minutes),

d_j = depth for the j-th time interval (mm),

Δt = equal time interval (minutes), and

n = number of time intervals for the rainstorm (Yen and Chow, 1980).

Yen and Chow (1980) considered the triangular hyetograph depicted in Figure 2.2, which is defined in terms of the total storm duration (T_d) and the maximum rainfall intensity (h).

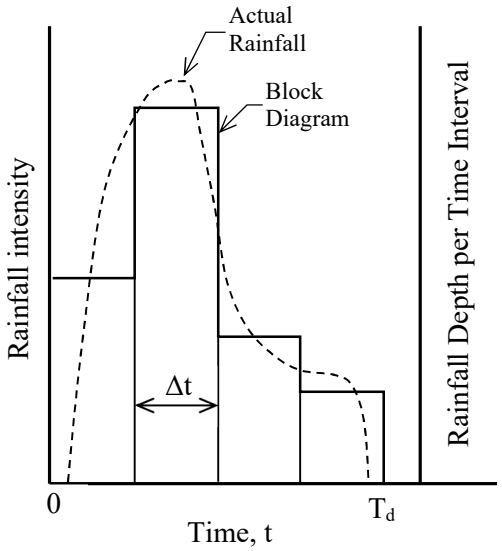

Figure 2.2: Example Hyetograph (Yen and Chow, 1980)

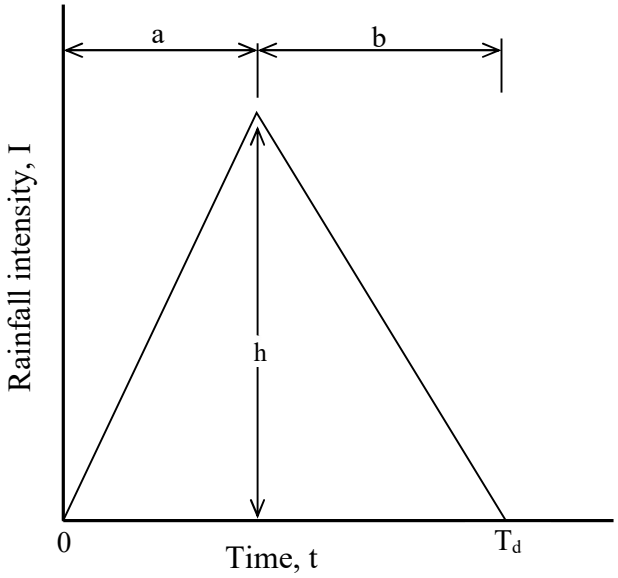

Figure 2.3: Triangular representation of the hyetograph (Yen and Chow, 1980)

The first-moment arm of the triangular hyetograph concerning the beginning of the rainstorm was expressed in terms of Equation 2.2 as follows.

$$\bar{t} = \frac{T_d + a}{3} \qquad \text{(Equation 2.2)}$$

Solving for the time to the peak intensity (a) of the triangular hyetograph yielded Equation 2.3 as follows:

$$a = 3\bar{t} - T_d \qquad \text{(Equation 2.3)}$$

Equation was solved using the first-moment arm and the total storm duration of the recorded hyetograph. The maximum intensity of the triangular hyetograph was expressed in terms of Equation 2.4 as follows:

$$h = \frac{2D}{T_d} \qquad \text{(Equation 2.4)}$$

where:

a = the time to peak intensity (min),

D = total rainfall volume (mm),

h = maximum rainfall intensity (mm/min), and

T_d = total storm duration (mins).

To generalise the geometric parameters of each hyetograph for all storm events, Yen and Chow (1980) non-dimensionalised the time to the peak intensity (a) and the maximum rainfall intensity (h) using Equation 2.5 and Equation 2.6 respectively:

$$a^o = \frac{a}{T_d} \qquad \text{(Equation 2.5)}$$

$$h^o = \frac{h}{\left(\frac{D}{T_d}\right)} = 2 \qquad \text{(Equation 2.6)}$$

where:

a^o = dimensionless time to the peak intensity, and

h^o = dimensionless maximum rainfall intensity.

Asquith et al. (2003) developed a method to estimate the rainstorm parameters using the dimensionless cumulative hyetograph ordinates and the fraction of storm duration. For fractions smaller and equal to the time to peak intensity, the quantile function Q(F) was expressed in terms of Equation 2.7, and for fractions larger than the time to peak the intensity was expressed in terms of Equation 2.8 as follow:

$$Q_1(0 \le F \le a^o) = \frac{1}{2}\frac{h}{a}F^2 \qquad \text{(Equation 2.7)}$$

$$Q_2(a^o < F \leq 1) = \frac{1}{2}h^o a^o + h^o(F - a^o) - \frac{1}{2}\frac{h}{b}(F - a^o)^2 \qquad \text{(Equation 2.8)}$$

By integration of the quantile functions and substitution of the dimensionless peak intensity, the mean of the dimensionless cumulative hyetograph ordinates was expressed in terms of Equation 2.9 as follows:

$$\mu = \frac{2 - a^o}{3} \qquad \text{(Equation 2.9)}$$

where:

F = fraction of storm duration,

Q_1 = dimensionless cumulative hyetograph ordinate for fractions of storm durations smaller and equal than a^o,

Q_2 = dimensionless cumulative hyetograph ordinate for fractions of storm durations larger than a^o,

μ = mean of the dimensionless cumulative hyetograph ordinates (Asquith et al. 2003).

Yen and Chow (1980) conducted a statistical analysis after the determination of the dimensionless parameters. The effect of different total storm durations, total rainfall volumes and different seasons, on the parameters were investigated by applying the triangular hyetograph method to rainstorms which were defined as periods of nonzero rainfall.

Altogether 7 484 rainstorms were analysed for three weather stations located in the USA: Boston, Urbana and Elizabeth City. The recorded hyetographs consisted of hourly recorded data. The mean values of the time to peak intensity considering different total storm durations, total rainfall volumes and seasons are depicted in Figure 2.4. Yen and Chow (1980) also determined that the triangular hyetograph method produces acceptably accurate design hyetographs and applied the method to the experimental data of Izzard (1946) as well as Yu and McNown (1964), which consists of measured runoff hydrographs from artificial catchments. Ellouze et al. (2009) conducted a similar investigation by analysing hourly recorded rainfall data, recorded between 1974 and 1997, at 10 rainfall stations located within a 7.74 km² catchment in central Tunisia. Altogether, 2 799 rainstorms were analysed. According to Ellouze et al (2009), the observed hyetographs conformed adequately with the synthetic hyetographs. Asquith et al. (2003) used a database of 1 659 storms for 91 small catchments with streamflow gauging stations in Texas. Using the model developed by Asquith et al. (2003), the storm parameters were estimated for two storm duration ranges, 0 to 24 hours, and 24 to 72 hours.

For each duration range, storms were classified into a sequence of integer depth intervals. The weighted averages of the mean of the dimensionless hyetographs were 0.59 and 0.55 respectively. The weighted averages were based on the number of storms in each depth interval. Applying Equation 2.6, the time to peak intensity was 0.23 and 0.35 respectively. The dimensionless cumulative hyetograph depicted in Figure 2.5, was calculated using the quantile functions before and after the peak intensity expressed in terms of Equations 2.7 and 2.8.

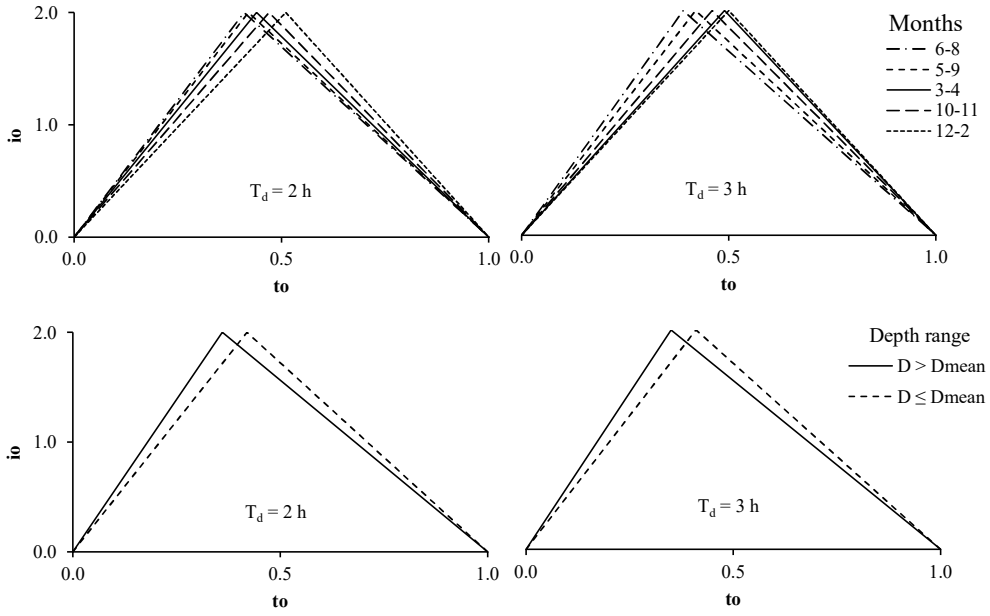

Figure 2.4: Mean values of a^o for nondimensional triangular hyetographs for Boston, Massachusetts (Yen and Chow, 1980)

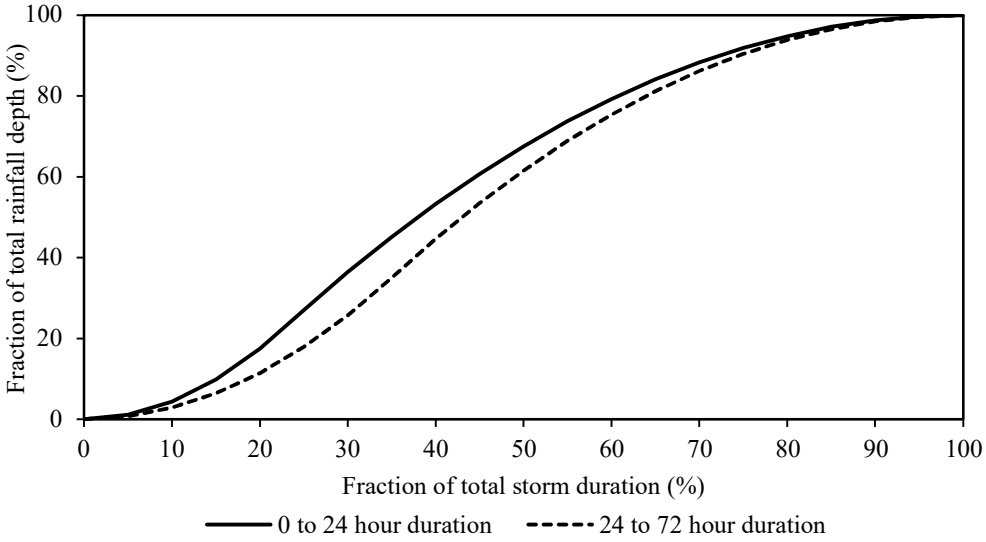

Figure 2.5: Dimensionless cumulative rainfall hyetographs for runoff producing storms having 0 to 24-hour and 24 to 72-hour durations computed by the triangular hyetograph model for Texas (Asquith et al, 2003)

2.2.3 Chicago Design Storm

The CDS method was developed for the City of Chicago by Keifer and Chu (1957) because of the rapid increase in urbanization that followed the end of World War II (Keifer and Chu,1957). As depicted in Figure 2.6 the method encompasses three important characteristics, namely:

a) Average intensity within the maximum storm duration,

b) Antecedent rainfall before the maximum duration, and

c) Location of peak intensity (Keifer and Chu, 1957).

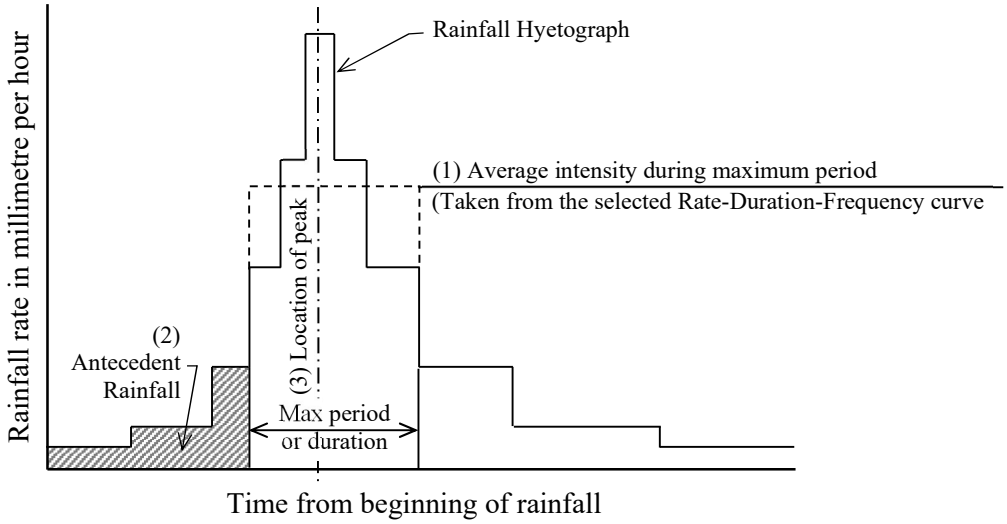

Figure 2.6: A rainfall hyetograph showing the three most important characteristics affecting the peak rate of runoff (Keifer and Chu, 1957)

The average rainfall intensities with associated probability or frequency of exceedance, are determined for particular storm durations using statistical analysis of historical rainfall data. These intensities concerning duration, expressed in terms of frequency of exceedance, are commonly known as IDF curves. The IDF curves have a sigmoidal shape which can be related to a mathematical function in the form of Equation 2.10 (Keifer and Chu, 1957) and Equation 2.11 (Watson, 1982, Smith, 2004; Silveira, 2017) as follows:

$$i_{av} = \frac{a}{t^b + c} \qquad \text{(Equation 2.10)}$$

And:

$$i_{av} = \frac{a}{(b + t)^c} \qquad \text{(Equation 2.11)}$$

where:

i_{av} = average rainfall intensity for a particular storm duration (mm/hour),

a,b,c = site specific constants, and

t = storm duration (min).

Keifer and Chu (1957) addressed the first characteristic of the average intensity within the maximum storm duration, with the intensity distribution function which was derived from the IDF curve, whereas the second and third characteristics of the CDS were represented by the storm advancement coefficient (r). The IDF curve, presented by Equation 2.10 was used to develop the intensity distribution (Keifer and Chu, 1957). However, the development was somewhat transformed using a formula, presented by Equation 2.11 also known as the Sherman formula (Sherman, 1931).

Preceded by various substitutions and differentiation, the intensity distribution of an advanced storm, which is a storm with the peak intensity located at the beginning of the event, was expressed in terms of Equation 2.12 as follows:

$$i = \frac{a[(1-c)t + b]}{(b+t)^{c+1}} \qquad \text{(Equation 2.12)}$$

The time before the peak intensity (t_b) and the time after the peak intensity (t_a) were expressed in terms of storm advancement coefficient in the form of Equations 2.13 and 2.14 as follows:

$$\frac{t_b}{t_d} = r$$
$$\therefore t_d = \frac{t_b}{r} \qquad \text{(Equation 2.13)}$$

And:

$$\frac{t_a}{t_d} = 1 - r$$
$$\therefore t_d = \frac{t_a}{1-r} \qquad \text{(Equation 2.14)}$$

Substituting the storm duration in Equation 2.12 with Equations 2.13 and 2.14, yielded the intensity distributions before and after the peak intensity in the form of Equation 2.15 and 2.16 as follows:

$$i_b = \frac{a\left[(1-c)\frac{t_b}{r} + b\right]}{\left(\frac{t_b}{r} + b\right)^{c+1}} \qquad \text{(Equation 2.15)}$$

And:

$$i_a = \frac{a\left[(1-c)\frac{t_a}{1-r}+b\right]}{\left(\frac{t_a}{1-r}+b\right)^{c+1}} \qquad \text{(Equation 2.16)}$$

where:

t_a = specific time interval after the peak,

t_b = specific time interval before the peak,

i_a = specific intensity after the peak intensity,

i_b = specific intensity before the peak intensity,

r = storm advancement coefficient (Smith, 2004; Watson, 1981).

The synthetic hyetograph for a completely advanced storm expressed by Equation 2.12 was illustrated graphically by Keifer and Chu (1957) as depicted in Figure 2.7. However, Watson (1981) illustrated the intensity distributions before and after the peak intensity, depicted in Figure 2.8, which were derived from the IDF curve and expressed in terms of Equations 2.15 and 2.16. The purpose of both these illustrations was to demonstrate that for any storm duration, the rainfall volume obtained from the IDF curve, is equal to the cumulative rainfall volume obtained from the hyetograph of the synthetic design storm.

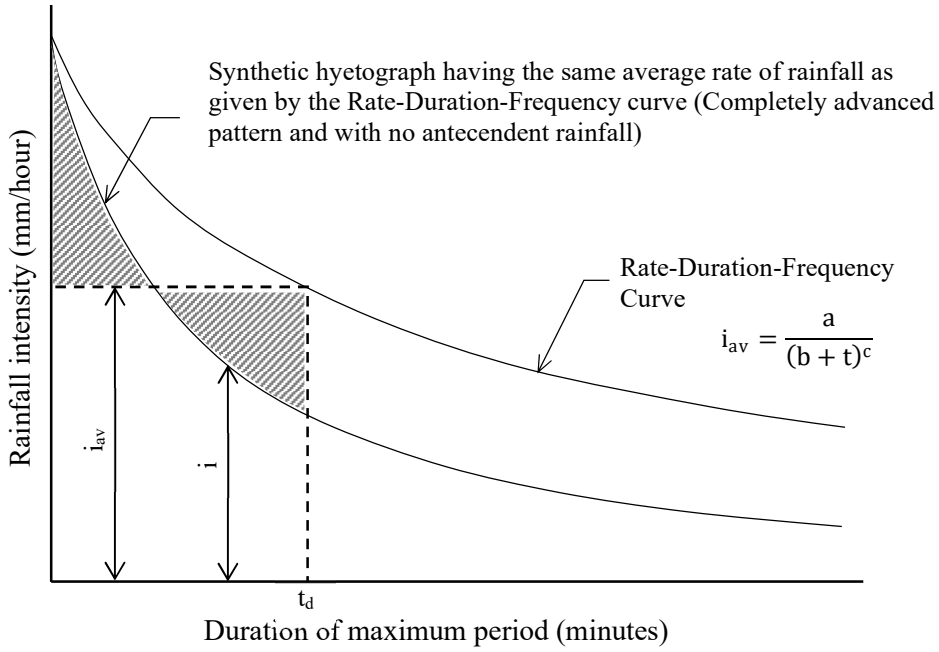

Figure 2.7: Development of a synthetic storm pattern from the Intensity-Duration-Frequency curve (Keifer and Chu, 1957)

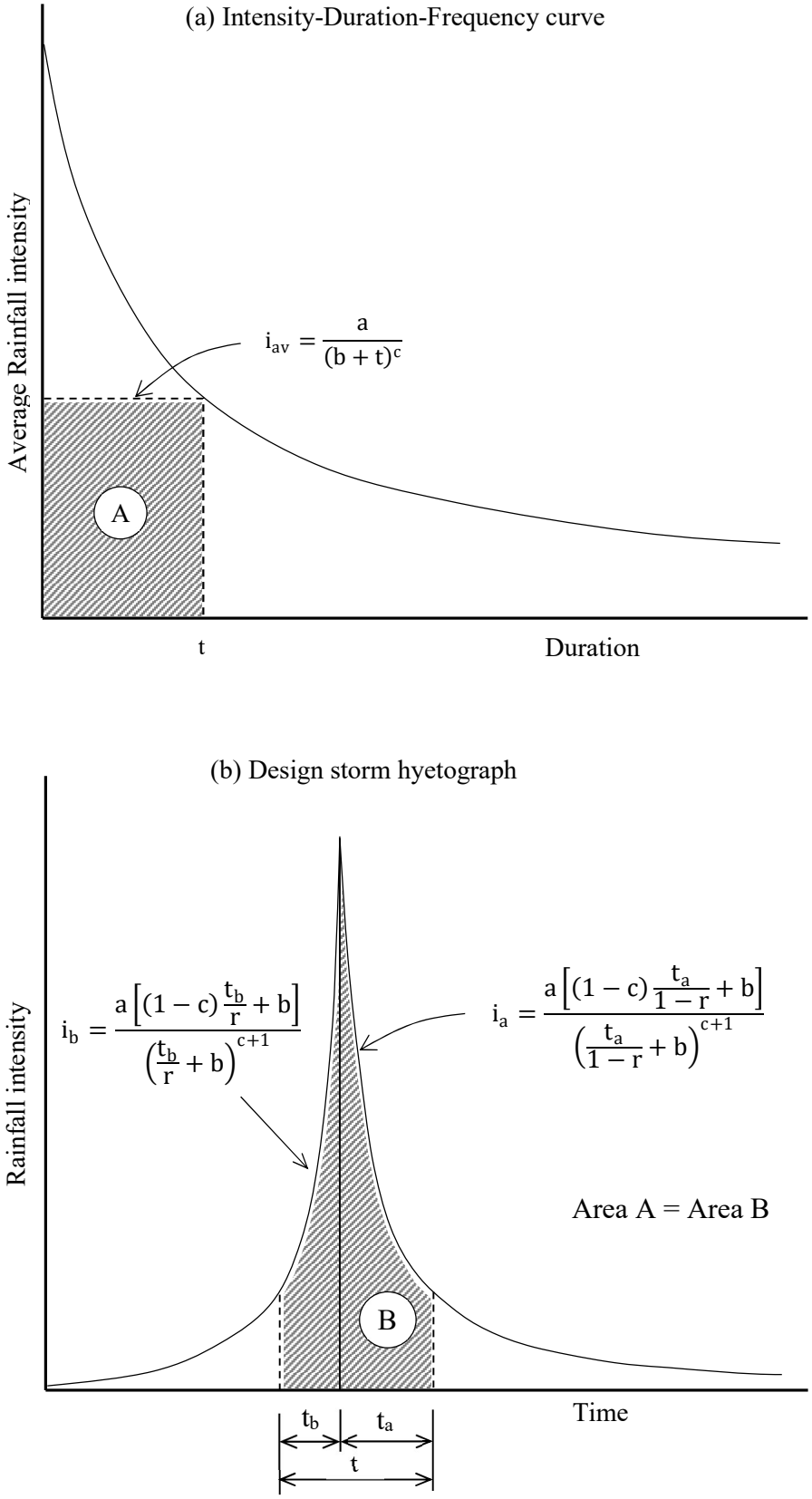

Figure 2.8: Chicago Design Storm (Watson, 1981)

By integrating Equation 2.15 and 2.16 from the beginning of the hyetograph to a time interval before and after the peak intensity, Silveira (2016) formulated two cumulative rainfall equations in the form of Equations 2.17 and 2.18. However, an alternative and simpler development of Equations 2.17 and 2.18 are presented in Annexure A.

$$P_b = r \cdot P - \frac{a(T_p - t_b)}{\left(b + \frac{T_p - t_b}{r}\right)^c} \qquad \text{(Equation 2.17)}$$

And:

$$P_a = r \cdot P + \frac{a(t_b - T_p)}{\left(b + \frac{t_b - T_p}{1 - r}\right)^c} \qquad \text{(Equation 2.18)}$$

where:

P = total rainfall depth (mm),

P_a = cumulative rainfall depth after the peak intensity (mm),

P_b = cumulative rainfall depth before the peak intensity (mm),

T_p = time when peak intensity occurs (minute), and

To address the second and third characteristic, Keifer and Chu (1957) calculated the storm advancement coefficient for different durations and weighted it in proportion to the antecedent rainfall volume. The average antecedent rainfall volume was calculated for the 15, 30, 60 and 120-min storm durations. Keifer and Chu (1957) considered the rainfall volume before the peak intensity, for which the antecedent rainfall volume was expressed in terms of the storm advancement coefficient. The storm advancement coefficient for the specific storm duration, using the average antecedent rainfall volume, was then calculated. The storm advancement coefficient was weighted proportionally to the average antecedent rainfall volume for specific storm durations and averaged for all durations. Following this approach they determined the advancement coefficient for the 15, 30, 60 and 120-minute storm durations for which the weighted average was 0.386. Watson (1981) determined the storm advancement coefficient for Norwood, Johannesburg from 28 significant storms also following this approach. For total storm durations of two and three hours, the storm advancement coefficient was 0.28 and 0.22, respectively. A graphical comparison was conducted between the CDS and two real storms, and an Illinois Urban Drainage Area Simulator (ILLUDAS) stormwater model was used to determine the peak discharges. Based on this limited extent of testing, it was concluded that the CDS is an adequate technique for predicting peak discharge. The second approach which was adopted for calculating the storm advancement coefficient was to ignore the second characteristic, which is the antecedent rainfall before the maximum duration.

Since the rainfall data was recorded in 5-min intervals, it was assumed that the peak intensity is located exactly in the middle of the peak 5-min interval (Keifer and Chu, 1957). Keifer and Chu (1957) determined the weighted average storm advancement coefficient for all durations considering only the location of the peak intensity and weighted proportionally to the duration. The weighted average was 0.375. Weesakul et al. (2017) conducted a similar investigation on rainfall data recorded at the meteorological station at the Asian Institute of Technology in Bangkok, Thailand, on data covering 21 years. The storm advancement coefficient was between 0.20 and 0.49.

2.2.4 SCS temporal distribution curves

Standard SCS temporal distribution curves, Types I and II, were first published in 1973 by the Soil Conservation Service (SCS), which later became the Natural Resources Conservation Services (NRCS). These two curves were developed from the generalised rainfall depth-duration relationships obtained from the US Weather Bureau technical papers (TP-42) published in 1961 (US Weather Bureau, 1961), of which Type II covers most of the USA. Types IA and III were later developed in the same way and were subsequently published by the NRCS in 1986 (Cronshey, 1986). The approximate geographic boundaries for the four SCS rainfall distributions are depicted in Figure 2.9. However, according to the National Engineering Handbook, little documentation is available that describes the development of Type II and other legacy rainfall distributions (NRCS, 2019). From the available information, the depth ratios relative to the 24-hour rainfall depth were plotted against the duration for several locations in each of the four regions and a curve was selected with the best fit (SCS, 1973).

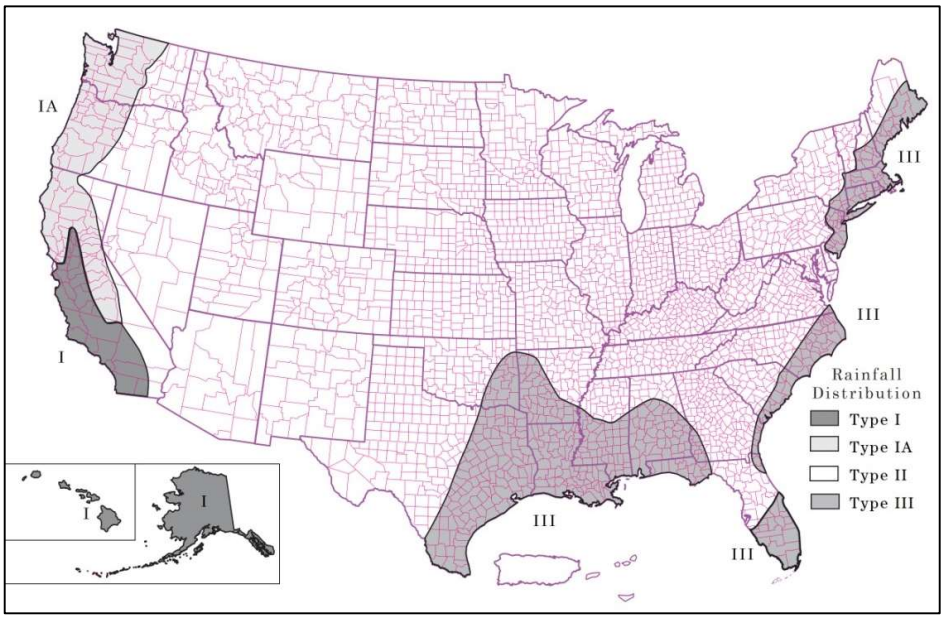

Figure 2.9: Approximate geographic boundaries for SCS rainfall distributions (Cronshey, 1986)

The curves were developed for each of the four regions by positioning the greatest 30-min rainfall depth at the 10-hour and 8-hour points for the Types I and IA respectively, and the 12-hour point for both the Types II and III curves. It is important to note that the positioning of the greatest 30-min rainfall depths at the 8-, 10- and 12-hour points were not based on any meteorological factors but rather design considerations (SCS, 1973). The second-largest 30-min depth was positioned 30-min later, and the third-largest 30-min depth was positioned at the preceding 30-min. The alternation of 30-min depths, which decrease in magnitude, was repeated until the smallest 30-min depths were located at the beginning and end of the 24-hour (SCS, 1973). The four SCS curves are depicted in Figure 2.10.

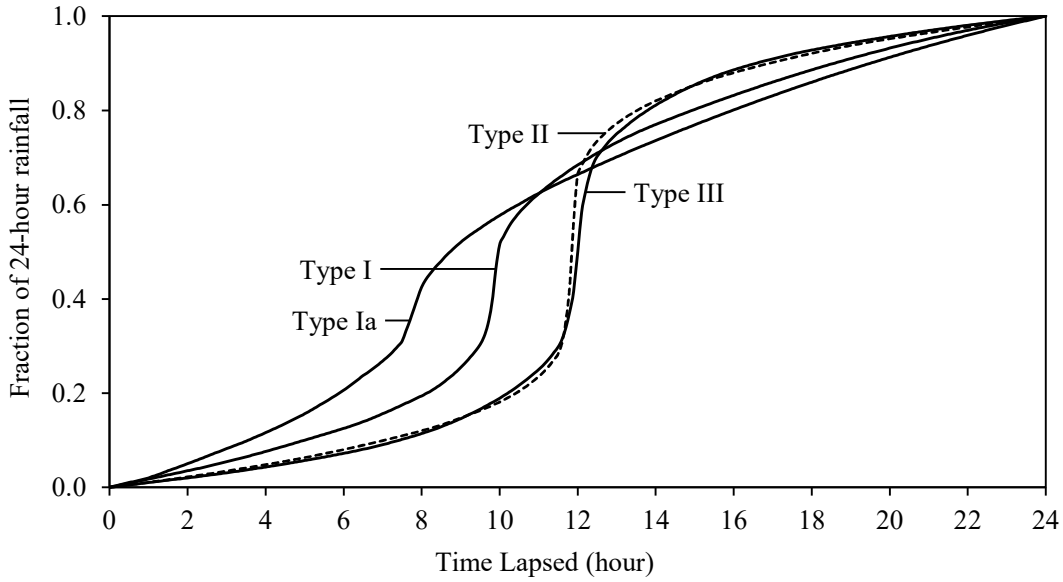

Figure 2.10: SCS Types I, IA, II and III rainfall distribution curves (Cronshey, 1986)

However, according to NRCS (2019), it was concluded that the use of the SCS curves is discontinued and replaced by the National Oceanic and Atmospheric Administration (NOAA) Atlas 14 curves. Locations in the USA that are already covered by the NOAA Atlas 14 data are depicted in Figure 2.11.

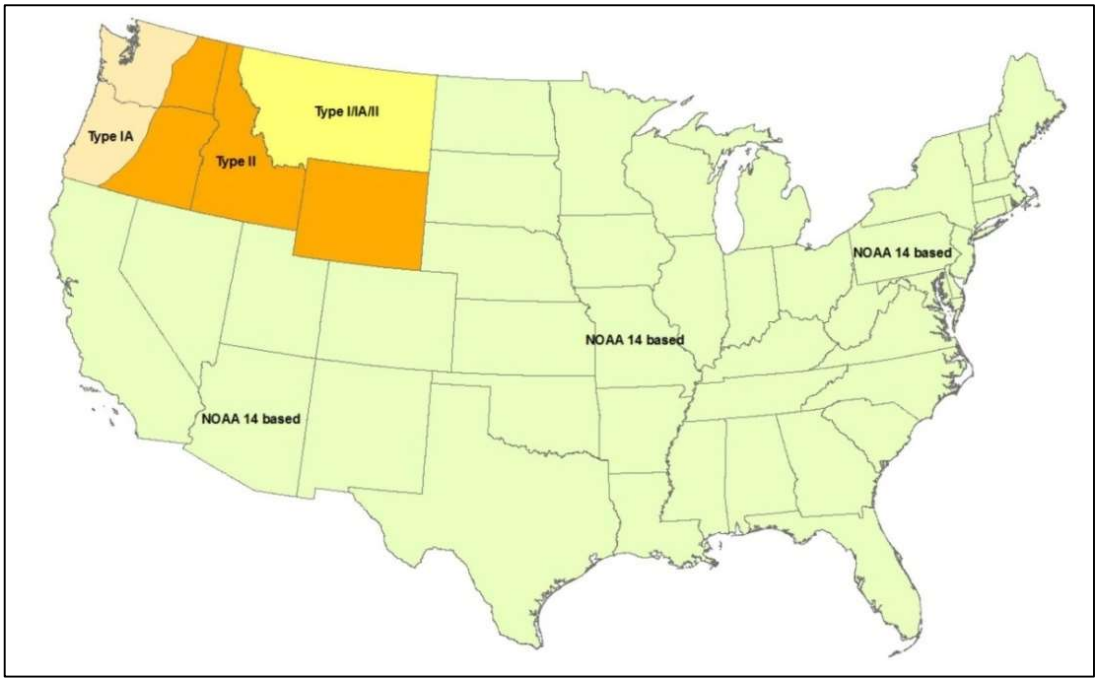

Figure 2.11: Map of States with updated synthetic rainfall distributions as of January 2016 (NRCS, 2019)

2.2.5 SCS-SA temporal distribution curves

The standard SCS Types I and II curves were originally adopted for use in South Africa (Schulze and Arnold, 1979), but the need for revised synthesised storm distributions for South Africa was identified after an analysis of digitised data for Natal (Schulze, 1984). The development of the SCS-SA synthetic rainfall distributions was based on the selection of four D-hour to one-day rainfall ratio range classes for various durations from 5-min to 24-hours, which became known as the SCS-SA synthetic rainfall distributions Type 1 to 4 (Weddepohl, 1988). The D-hour to one-day rainfall ratios for 40 autographic rainfall stations in South Africa were determined and the appropriate ratio range class was assigned to each station (Schmidt and Schulze, 1987). Based on this analysis a map was drawn, by linear interpolation, that represents the regionalisation of the four ratio range classes, depicted in Figure 2.12.

The D-hour to one-day rainfall ratios for the four distributions were represented by Equation 2.19 as follows:

$$R = \frac{a \cdot D}{(b + D)^c} \qquad \text{(Equation 2.19)}$$

where:

R = ratio of sub-daily to 24-hour design rainfall,

D = storm durations, and

a,b,c = regression constants summarised in Table 2.1 (Schmidt and Schulze, 1987).

Table 2.1: Regression constants for the four southern African synthetic rainfall distributions (Schmidt and Schulze, 1987)

Distribution Type	a	b	c
1	0.29935	0.059	0.62
2	0.45321	0.100	0.75
3	0.73402	0.230	0.90
4	1.01330	0.320	1.00

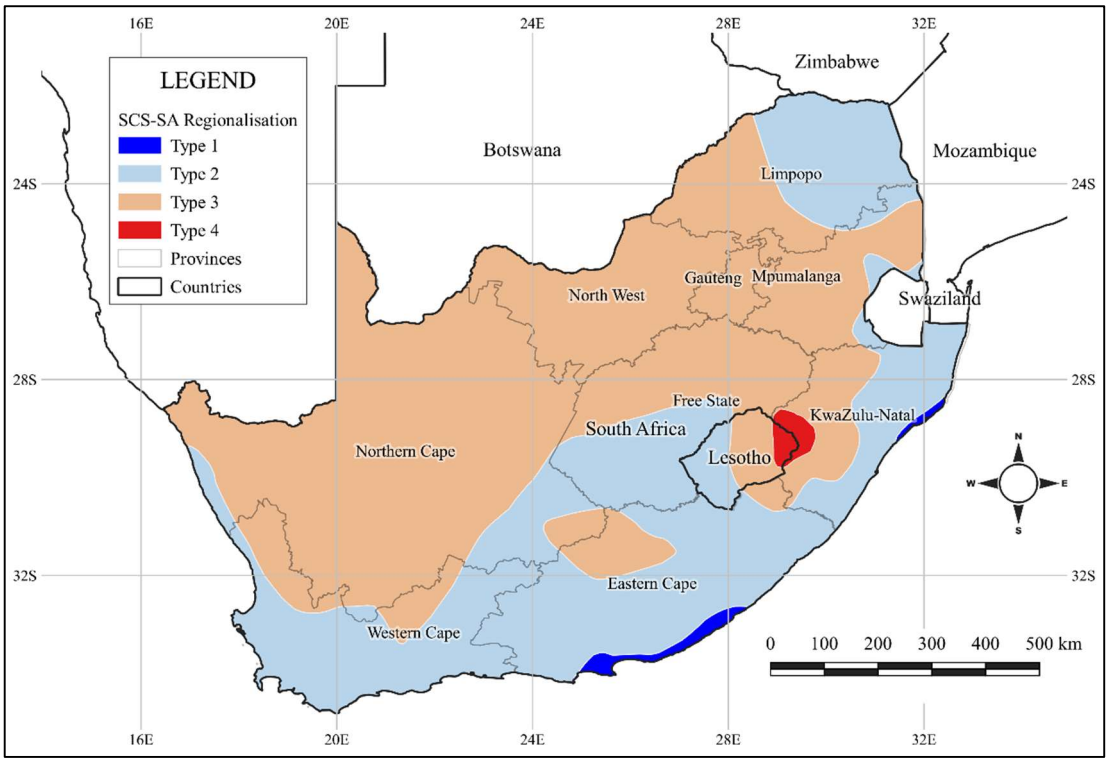

Figure 2.12: Regionalisation of synthetic rainfall distributions in southern Africa (After Weddepohl, 1988)

The rainfall distributions were derived by positioning the middle of the peak 5-min ratio at the 12-hour point, and distributing the ratios of increasing durations, equally on either side of the peak intensity. The cumulative rainfall distributions depicted in Figure 2.13, therefore represent the increase in intensity between consecutive durations from the start of the 24-hour duration up to the 12-hour point, followed by the decrease in intensity up to the end of the 24-hour duration. For example, the difference between the ratios of the 30-min before and 30-min after the peak intensity is equal to the ratio of the 1-hour ratio determined with Equation 2.19.

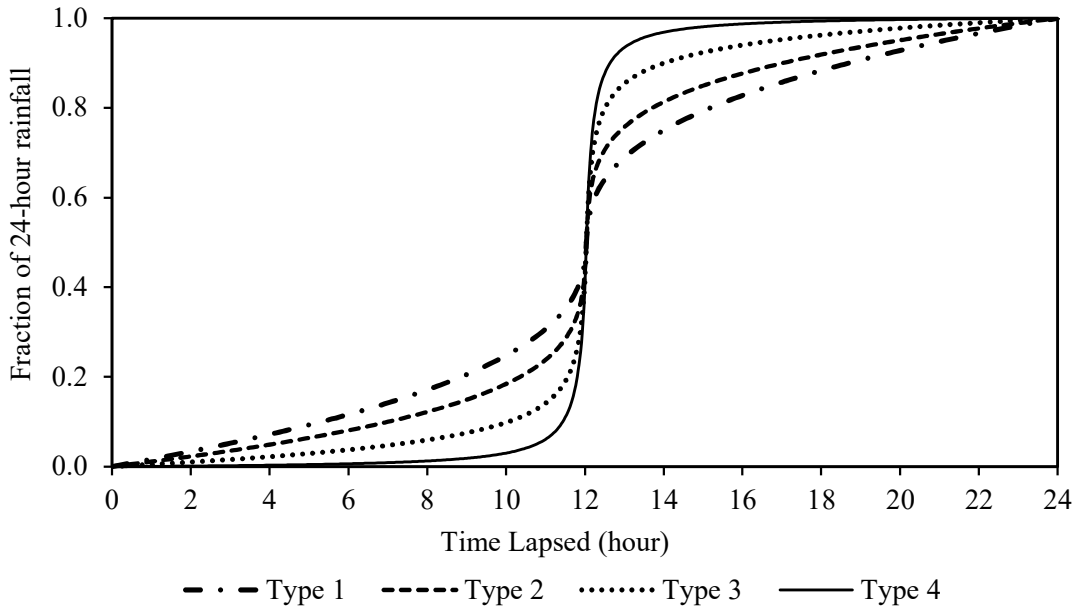

Figure 2.13: Time distributions of accumulated rainfall depth divided by total rainfall depths (Schmidt and Schulze, 1987)

More recently Smithers and Schulze (2002) demarcated the City of Tshwane Metropolitan Municipality (CTMM) into four distinct regions with similar distributions of short and long duration extreme rainfall. Males et al. (2004) then developed an integrated catchment management plan for the City of Tshwane Metropolitan Municipality (CTMM) by compiling a VisualSWMM model. It was found that the four regions conform to the SCS-SA Type 2 rainfall distributions by considering the ratio range classes defined by Weddepohl (1988).

2.3 MASS CURVE BASED METHODS

2.3.1 Huff curves

According to Bonta (1997), cited by Bonta and Shahalam (2003), the curves presented by Huff (1967) were developed by separating independent storms and non-dimensionalising each mass curve in terms of the total rainfall volume and total storm duration. The dimensionless mass curves were superimposed graphically showing the breakpoints at 0.02 intervals along the horizontal axis with the fraction of the total rainfall depth along the vertical axis, followed by the construction of curves with probability values from 10% to 90% (Bonta and Shahalam, 2003). This methodology of developing the Huff curves was, however, according to Bonta (2004), never documented which led to the formulated methodology presented by Bonta (1997). In terms of identifying independent rainstorms, Huff (1967) used a criterion of 6-hours as the minimum dry period to separate consecutive rainstorms (Huff, 1990), whereas Bonta (1997) determined a minimum dry period following the method of identification of independent rainstorms developed by Restrepo and Eagleson (1982).

The minimum threshold criterion for individual rainstorms was 25 mm (Huff, 1990). Typical dimensionless mass curves, also known as isopleths, which are lines connecting intersecting points with equal probabilities of dimensionless storm depths, developed by Bonta and Shahalam (2003) are depicted in Figure 2.14.

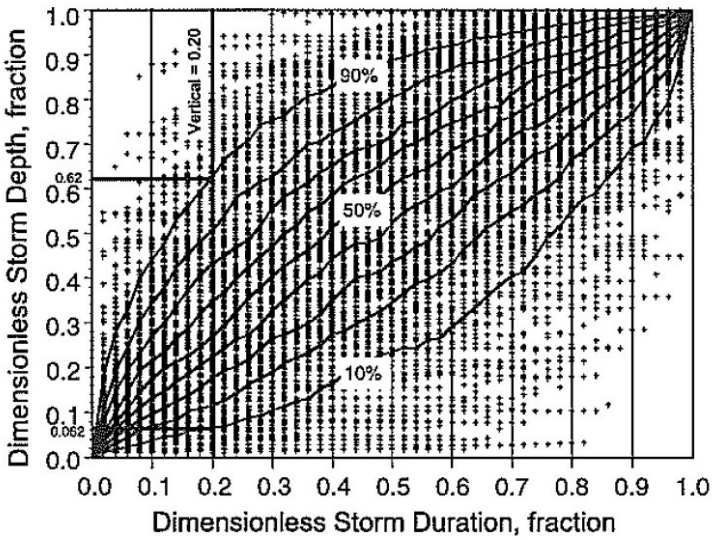

Figure 2.14: Dimensionless storm mass curve intersections with isopleths connecting equal probabilities of dimensionless storm depths (i.e., Huff curves) for a sample size of 322 May and June storms at Invercargill (base/smooth curves) (Bonta, 2003)

Huff (1967) investigated the time distributions from 261 storm events recorded in East-Central Illinois from 49 recording rain gauges over 12 years from 1955 to 1966. The rain gauges were distributed over 1 036 km². He divided the rainfall distributions between four quarters based on whether the heaviest rainfall within each storm event occurred in the first, second, third or fourth quarter of the total storm duration. The curves, with probability values from 10% to 90%, developed by Huff are depicted in Figure 2.15.

Huff (1990) further suggested that the first and second quartile distributions be used for storm durations of less than 12-hours, the third quartile for storm durations between 12 and 24-hours, and the fourth quartile for storm durations of more than 24-hours. It is suggested that the 50% percentile is likely applicable for most purposes.

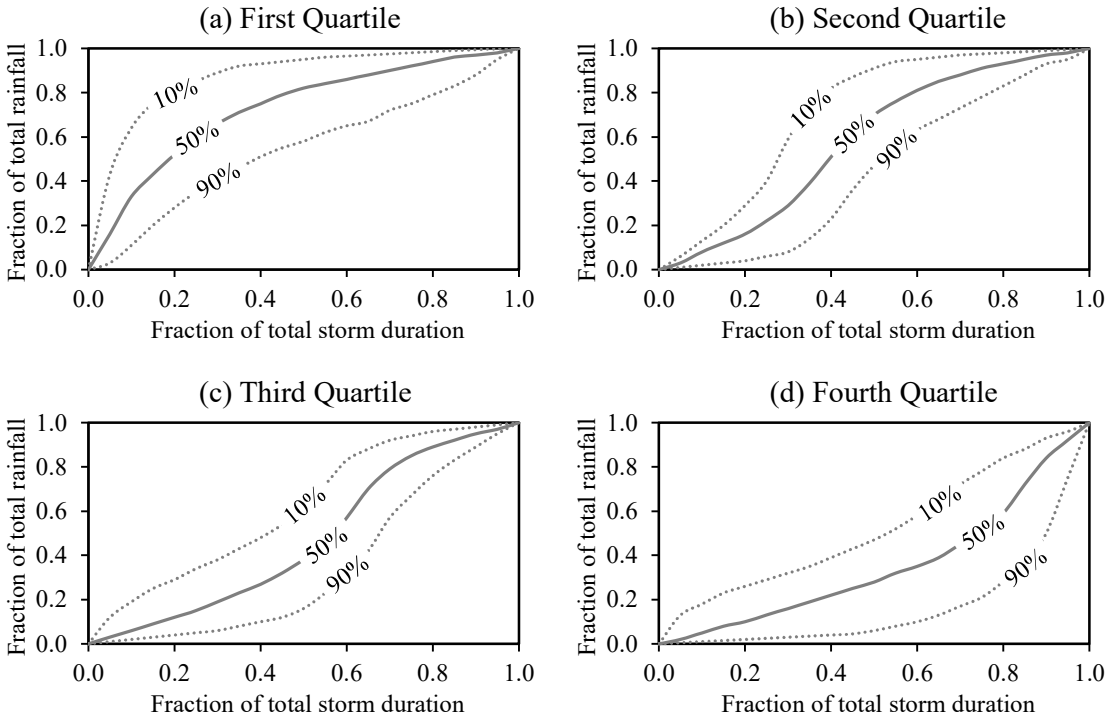

Figure 2.15: Huff curves (Huff, 1990)

2.3.2 NOAA Atlas 14 distribution curves

The NOAA Atlas 14 consists of a series of volumes that contains the estimates of the design rainfall for standard duration time steps and associated frequencies, together with 90% confidence intervals for the USA, similar to the design rainfall estimates developed by Smithers and Schulze (2000). Curves were also developed for four storm duration classes (6, 12, 24, and 96-hours), separated depending on which quartile the greatest percentage of the total rainfall occurred.

According to Bonnin et al. (2011) and Perica et al. (2018), the NOAA Atlas 14 curves were developed in the same way as the ones developed by Huff (1967), except that a storm event was defined in terms of a fixed duration. In other words, events always started with rainfall, but the end of the storm event was located after 6, 12, 24, and 96-hours respectively, irrespective of an event ending sooner (Bonnin et al. 2011). Therefore, many storm events ended sooner than the duration class which lead to events that were more front-loaded, compared to events selected based on the single event approach like Huff (1967). Typical 6-hour NOAA Atlas 14 storm distributions for the Interior Highlands region of the USA are depicted in Figure 2.16.

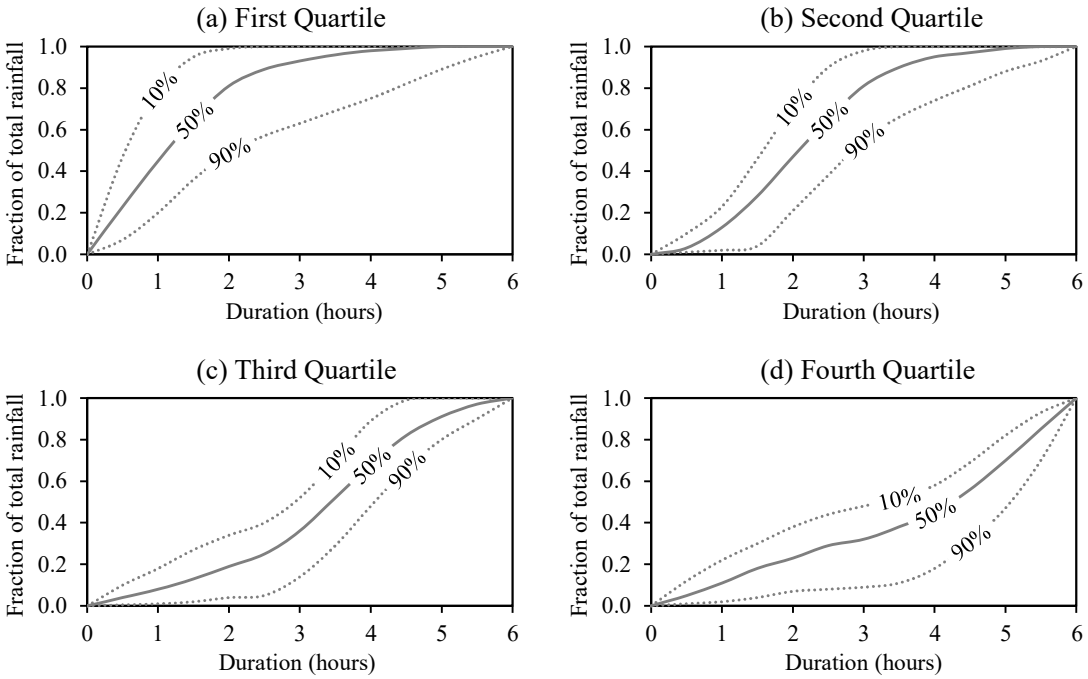

Figure 2.16: Typical 6-Hour temporal distribution curves for the Interior Highlands region (Perica et al., 2018)

Another approach to using the NOAA Atlas 14 design rainfall, is by developing a 24-hour rainfall distribution from the 5-min through to 24-hour design rainfall values, similar to the SCS-SA curves. The procedure involves the calculation of ratios of short durations to the 24-hour rainfall, that is distributed equally either side of 12-hours. Equations were developed to interpolate the design rainfall for durations in between the standard time steps (NRCS, 2019).

2.3.3 HRU curves

The HRU curves (HRU, 1972) were assessed by Watson (1981) and found the first type not appropriate for urban catchments since they were based on the analysis of hourly rainfall data, and the second type not applicable to the prediction of flood frequencies. Therefore, the HRU curves were not considered further in this study.

2.4 STOCHASTIC BASED METHODS

2.4.1 Daily rainfall disaggregation model for South Africa

Based on the work done by Boughton (2000), Knoesen (2005) developed and assessed a model to disaggregate daily rainfall into hourly rainfall for South Africa. A total of 157 stations, all of which had more than 10 years of hourly data were used to develop this model and to regionalise the distribution of the maximum hourly fraction. According to Boughton (2000), as cited by Knoesen (2005), the model treats each day as an independent event.

Therefore, only data of independent events of which all 24 hours from 00:00 to 00:00 with at least 1 mm rainfall recorded were used. The model is primarily based on the hourly fractions of the daily rainfall; the frequency of the maximum hourly fraction; the clustering of the other 23 hourly fractions; and the arrangement of the clusters into random daily temporal patterns. The average maximum fraction for each independent event was collated into 20 ranges.

The average highest 2-hour, 3-hour, 6-hour and 12-hour factions for each range of maximum hourly fraction were calculated. The second-highest hourly fraction added to the highest fraction was found to best approximate the 2-hour fraction, the third-highest to approximate the 3-hour fraction and so forth, which formed the clustered sequence (Knoesen, 2005). With the regionalisation of the model, the maximum hourly fraction of all the stations were collated into four revised ranges, and the average distribution of each range was calculated.

Using inverse distance weighting, a regionalised map was developed based on the mean value of the maximum hourly fraction. The map, depicted in Figure 2.17, is used to find the appropriate range for the site of interest.

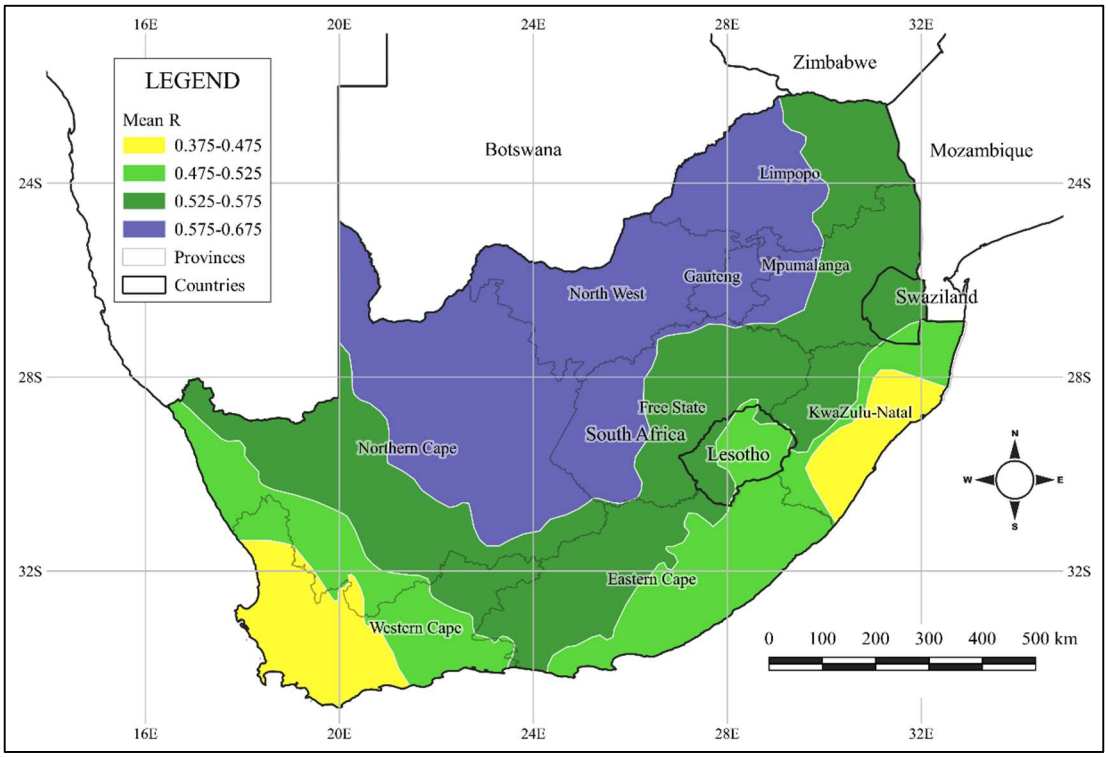

Figure 2.17: Regionalised map of the mean maximum hourly fraction (after Knoesen, 2005)

The advantage of this model is that it can be applied to a site where only daily recorded rainfall is available since short duration rainfall data are scarce compared to daily rainfall data. However, the disadvantage of this model is that the distribution of the highest fraction, considering the 20 ranges, and the 24 sequencings of the clustered fractions selected by Boughton (2000), results in 480 different temporal patterns (Knoesen, 2005), whereas the focus of this study is on single event modelling. Furthermore, this model disaggregates daily rainfall into hourly rainfall, whereas sub-hourly disaggregation would be more appropriate for this study. Based on this, this model was not considered.

2.4.2 Other stochastic based methods

Other stochastic based methods includes, but not limited to, the Bartlett-Lewis model and its variants, the Bartlett-Lewis Rectangular Pulse (BLRP), Modified BLRP model, Randomized BLMP model, and the BLRP Gamma model, as cited by Ramlall (2020). These methods were not covered in this study because of the focus being on single event-based modelling.

2.5 SUMMARY AND CRITICAL EVALUATION OF METHODS

Although the existing synthetic design storms were developed using the best data, technology, and engineering judgement available at the time, they have limitations. For example, the total precipitation volume is systematically underestimated by the REC (Arnell, 1982), and it was also realised that it gives a wrong shape of a hyetograph (Niemczynowicz, 1982). In terms of the TRI, Veneziano and Villani (1999) have noticed that, although it is quite simple and intuitive, it does not have a strong conceptual basis and may produce biased flow estimates. The CDS overestimates the peak discharge comparing with results from a continuous simulation modelling analysis (Malik and James, 2007). Veneziano and Viallani (1999) also state that it tends to overestimate the peak discharge because it produces an unrealistic single event. However, methods that use the entire IDF curve to generate a synthetic design storm hold much potential since the design rainfall has been regionalised by Smithers and Schulze (2000). Some of the variability and unique character of the rainfall pattern will therefore automatically be embedded in these methods.

In terms of Huff curves, Adamson (1981) suggested that it may be considered representative of regions in Southern Africa with similar rainfall climate and topography to the Mid-West of the USA. However, to determine the similarity, variables like latitude, longitude, altitude, distance from the sea, mean annual precipitation (MAP) need all to be considered. Sufficient data also exists which provide for an opportunity to develop similar type curves for the Gauteng province.

The standard SCS Types I and II curves were developed from data in the USA during the 1960s and 1970s. These curves are, however, in the process of being replaced by the NOAA Atlas 14 curves, which are regionalised curves for the USA, developed similarly to the Huff curves (NRCS, 2019), using the latest rainfall data. The standard SCS Types I and II curves were originally adopted for use in South Africa (Schulze and Arnold, 1979), but were further developed into four revised curves by Weddepohl (1988), as cited by Ramlall (2020). The four SCS-SA curves were regionalised, resulting in the SCS-SA Type 1, 2, 3 and 4 curves (Ramlall, 2020). Following the regionalisation map of the four SCS-SA curves, Type 3 applies to the Gauteng province, as well as the North-West, Northern Cape, and parts of the Eastern Cape, Mpumalanga, and Limpopo provinces. However, from practical experience, it appears that the Type 3 curve yields peak discharges that seem too high for specific sites in Gauteng when applied to a SWMM model (Males et al., 2004). This is partly due to too high ratios for the D-hour to one-day rainfall compared to the ratios calculated using the design rainfall of Smithers and Schulze (2000).

Despite the shortcomings, synthetic design storms together with Intensity-Duration-Frequency (IDF) curves are used extensively internationally in many urban stormwater designs and studies (Balbastre et al. 2019). This is because of the complex hydrological and hydraulic behaviour of an urban stormwater network which calls for the use of sophisticated computer-aided rainfall-runoff simulation modelling.

The inherent advantages of synthetic design storms are highlighted by Balbastre et al. (2019) which is summarised as follows:

a) It guarantees a uniform level of quality and operation standards.

b) It reduces and simplifies calculations, compared with continuous simulation modelling.

c) It provides a way of overcoming the problem of scarcity of short-duration rainfall data.

d) It can be regionalised which enhance its practicality.

To contextualise the advantages, the use of synthetic design storms for single event modelling is done with the intention that it will provide flow results that have the same frequency of exceedance then the statistical analysis of observed flow data. This is because observed flow data is hardly ever available and in the best of circumstances, will only be available at selective locations. In the case of a new stormwater network, observed flow data does not exist, and observed short duration rainfall data will provide the next best information in the form of a continuous simulation.

With the scarcity of short-duration rainfall data, the complexity of stochastic generated historic rainfall data, and the excessive time consumption of continuous simulation modelling, synthetic design storms have an important role to play in the design and assessment of urban stormwater networks. Therefore, a review of each of the synthetic design storms was provided in this chapter. Emphasis was placed on their development and the criteria and assumptions on which it was based, which provided the basis for the methodology that were followed to assess the applicability of the methods described in the next chapter. The methods that were considered appropriate after concluding the literature review were the REC, TRI, CDS, SCS rainfall distribution curves, SCS-SA rainfall distribution curves, and Huff curves.

3 RESEARCH METHODOLOGY

The first objective of this study is to identify and assess the performance of currently available methods to estimate synthetic design storms used as input for single-event modelling in the selected pilot study area. In order to achieve this objective, short-duration rainfall data for the study area had to be collated and reviewed, and applicable observed storm events identified. This chapter describes the data collection, quality assessment and storm event identification processes applied in this study.

3.1 SAWS RAINFALL DATA SOURCE

Rainfall data, recorded in 5-min intervals, were obtained from the SAWS for 35 stations situated in Gauteng. The stations consist of four Weather Office Stations (WO), 14 Automatic Weather Stations (AWS) and 17 Automatic Rain Stations (ARS). The locations of the stations are depicted in Figure 3.1 and their general details are summarised in Table 3.1.

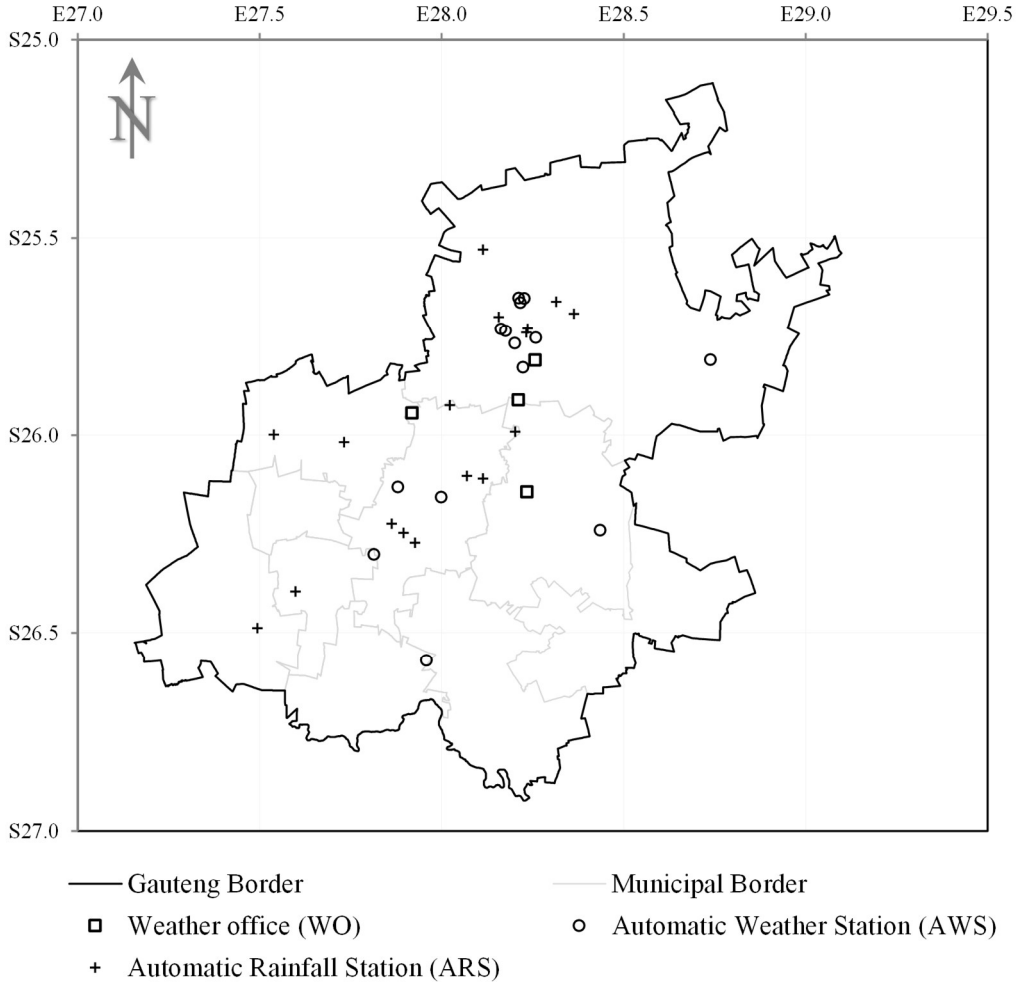

Figure 3.1: SAWS stations with short duration rainfall data in Gauteng

Table 3.1: SAWS short duration rainfall stations in Gauteng

ID	Name	Number	Latitude	Longitude	Type	Data Period (Years)
1	OR Tambo	0476399_0	26.1430 S	28.2346 E	WO	26.2
2	Lanseria	0512746_7	25.9436 S	27.9188 E	WO	10.7
3	Irene	0513385A2	25.9105 S	28.2106 E	WO	26.2
4	Bolepi House	0513439A1	25.8094 S	28.2564 E	WO	17.6
5	Vereeniging	0438784_3	26.5699 S	27.9582 E	AWS	26.2
6	Zuurbekom	0475528B7	26.3008 S	27.8136 E	AWS	6.3
7	Kloofendal	0475637_1	26.1308 S	27.8799 E	AWS	3.9
8	Jhb Bot Gardens	0475879_0	26.1566 S	27.9991 E	AWS	26.1
9	Springs	0476764_2	26.2395 S	28.4351 E	AWS	3.9
10	Bronkhorstspruit	0514408AX	25.8087 S	28.7386 E	AWS	11.7
11	Waterkloof AFB	0513379_8	25.8277 S	28.2235 E	AWS	7.9
12	Pretoria Unisa	0513346_0	25.7663 S	28.2005 E	AWS	26.2
13	Pretoria Proefplaas	0513435A4	25.7520 S	28.2585 E	AWS	9.9
14	Pretoria Pur	0513284_8	25.7351 S	28.1760 E	AWS	2.5
15	Pretoria TUT	0513253B3	25.7301 S	28.1627 E	AWS	1.9
16	Wonderboom RWY11	0513339B8	25.6516 S	28.2115 E	AWS	0.4
17	Wonderboom RWY24	0513369C4	25.6525 S	28.2272 E	AWS	0.4
18	Fochville Police	0474899_9	26.4877 S	27.4941 E	ARS	9.3
19	Westonaria Kloof	0475174_4	26.3944 S	27.5979 E	ARS	9.3
20	Goudkoppies	0475736B8	26.2715 S	27.9265 E	ARS	11.0
21	Dube	0475674_5	26.2466 S	27.8947 E	ARS	9.2
22	Dobsonville	0475613_X	26.2232 S	27.8626 E	ARS	9.2
23	Magaliesburg Police	0512090_5	25.9980 S	27.5386 E	ARS	9.2
24	Sterkfontein	0475361_8	26.0174 S	27.7317 E	ARS	11.2
25	Jhb Sandton	0476096_0	26.1026 S	28.0690 E	ARS	10.8
26	Alexandra Depot	0476156_X	26.1088 S	28.1130 E	ARS	9.2
27	Ivory Park	0513359_3	25.9906 S	28.2019 E	ARS	9.2
28	Diepsloot	0513025_X	25.9239 S	28.0218 E	ARS	9.2
29	Pta presidency	0513404_6	25.7394 S	28.2325 E	ARS	10.9
30	Pta Rietondale	0513404A0	25.7292 S	28.2361 E	ARS	9.7
31	Pta Mountain View	0513222_0	25.6994 S	28.1567 E	ARS	9.0
32	Baviaanspoort	0513611_4	25.6908 S	28.3633 E	ARS	9.3
33	Kameeldrift	0513550_3	25.6603 S	28.3144 E	ARS	9.8
34	Shosanguve	0550115_8	25.5289 S	28.1137 E	ARS	11.4
35	Wonderboom	0513369_0	25.6631 S	28.2166 E	AWS	10.6

Rainfall is recorded at all the stations using a tipping bucket rain gauge with a rainfall resolution of 0.2 mm. The rain gauge is equipped with a data logger which records the rainfall depth in 5-min intervals. The data is a continuous recording which will, therefore, contain zero value for each 5-min interval during periods of no rainfall. If the power supply is interrupted, the data logger will not record which will result in a gap in the dataset. The data recordings are described in detail in the next section.

3.2 DATA COLLATION

Each rain gauge is equipped with a solar panel and a General Packet Radio Service (GPRS) so that data can be remotely downloaded. Each AWS and ARS is assigned to a WO from where the data for the previous day's recordings are downloaded daily. The data goes through several quality checks before it gets uploaded into the SAWS database. If any discrepancies are noticed in the data during the quality checks, the rainfall recordings are manually deleted (Linnerts, 2022). Therefore, an interval will be present in the data set, but the rainfall column will be left blank. Typical deleted rainfall and missing intervals in a data set are depicted in Table 3.2.

Table 3.2: Typical short duration rainfall data set

Number	Name	Lat	Long	year	month	day	hour	min	Rain
.....	.....	.....	.....	.....	.....	.....	.....	.....	.....
0476399_0	JHB INT WO	-26,14	28,23	1994	12	31	1	35	0,0
0476399_0	JHB INT WO	-26,14	28,23	1994	12	31	1	40	0,0
0476399_0	JHB INT WO	-26,14	28,23	1994	12	31	1	45	0,0
0476399_0	JHB INT WO	-26,14	28,23	1994	12	31	1	50	0,0
0476399_0	JHB INT WO	-26,14	28,23	1994	12	31	1	55	0,0
0476399_0	JHB INT WO	-26,14	28,23	1994	12	31	2	0	0,0
0476399_0	JHB INT WO	-26,14	28,23	1994	12	1	2	5	0,0
0476399_0	JHB INT WO	-26,14	28,23	1994	12	1	2	10	0,0
0476399_0	JHB INT WO	-26,14	28,23	1995	1	1	2	15	0,0
0476399_0	JHB INT WO	-26,14	28,23	1995	1	1	2	20	0,0
0476399_0	JHB INT WO	-26,14	28,23	1995	1	1	2	25	0,0
.....	.....	.....	.....	.....	.....	.....	.....	.....	.....
0476399_0	JHB INT WO	-26,14	28,23	2000	10	20	17	15	0,2
0476399_0	JHB INT WO	-26,14	28,23	2000	10	20	17	20	0,0
0476399_0	JHB INT WO	-26,14	28,23	2000	10	20	17	25	0,0
0476399_0	JHB INT WO	-26,14	28,23	2000	10	20	17	30	0,0
0476399_0	JHB INT WO	-26,14	28,23	2000	10	20	17	35	
0476399_0	JHB INT WO	-26,14	28,23	2000	10	20	17	40	
0476399_0	JHB INT WO	-26,14	28,23	2000	10	20	17	45	
0476399_0	JHB INT WO	-26,14	28,23	2000	10	20	17	50	
0476399_0	JHB INT WO	-26,14	28,23	2000	10	20	17	55	
0476399_0	JHB INT WO	-26,14	28,23	2000	10	20	18	0	
0476399_0	JHB INT WO	-26,14	28,23	2000	10			5	
0476399_0	JHB INT WO	-26,14	28,23	2000	10			10	
0476399_0	JHB INT WO	-26,14	28,23	2000	10	20	18	15	
0476399_0	JHB INT WO	-26,14	28,23	2000	10	20	18	20	
0476399_0	JHB INT WO	-26,14	28,23	2000	10	20	18	25	
0476399_0	JHB INT WO	-26,14	28,23	2000	10	20	18	30	
0476399_0	JHB INT WO	-26,14	28,23	2000	10	20	18	35	0,0
0476399_0	JHB INT WO	-26,14	28,23	2000	10	20	18	40	0,0
.....	.....	.....	.....	.....	.....	.....	.....	.....	.....

Missing intervals

Deleted rainfall

3.3 DATA PROCESSING

The short duration rainfall data sets were processed using a Java application called the Rainfall Processor (Rain-Pro), which was developed using IntelliJ IDEA Community Edition 2019.1.3 and JDK 1.8 with JRE 1.8 (Munro, 2021). Subsequent analyses of the data was done using Microsoft (MS) Excel. The order in which the data was processed is summarised in the flow chart depicted in Figure 3.2. The process began with the short duration rainfall data of a station (RAW DATA SET.txt) as input for the Rain-Pro software, and the output consists of three files. The first was the PROCESSED.txt file, which consisted of the rainfall data, except for all intervals with zero rainfall. This file was used as input to the ANNUAL MAXIMUM SERIES.xlsx file, which provided the input for the STATISTICAL ANALYSIS.ssp file. This file provided the design rainfall estimations as described in Section 4.2. The PROCESSED.txt file was also used as input to the STORM FILTER.xlsx file, which applied the maximum dry period and the minimum rainfall depth criteria, described in Sections 3.6.1 and 3.6.2, respectively. After applying the maximum dry period and minimum rainfall depth criteria, the STORM FILTER.xlsx file provided the start and end dates of all individual events, which was used to create the STRIP DATES.txt file. The second output file of the Rain-Pro software, the MISSING_INTERVAL.txt file, contained the missing data which was subsequently used as input to the MISSING ANALYSER.xlsx file as described in Section 3.4. The third output file of the Rain-Pro software, the STATS.txt file provided a summary of the data set. This summary consisted of the total number of lines processed, the total number of lines with zero rainfall as well as lines with rainfall larger than zero, the start and end dates of the data set, the data period, and the total duration of missing data. The Rain-Pro software was executed for a second time, which extracted the individual events from the RAW DATA SET.txt file according to the STRIP DATES.txt file. The output from the Rain-Pro software, after the second run, consisted of the storm event files, 0M_EVENTS.txt, 15M_EVENTS.txt, etc., which contained the individual events according to the maximum dry period and minimum rainfall depth criteria. These files were used as input to the RI FILTER.xlsx file, which applied the minimum rainfall intensity criterion described in Section 3.6.3. The RI FILTER.xlsx file provided the start and end dates of the significant events, which was used to update the STRIP DATES.txt file. The Rain-Pro software was executed for the third time, and the storm event files were subsequently updated. These files contained the rainfall data of only the significant events which were used as input for the STORM PARAMETERS.xlsx file. This file determined the storm parameters described in Sections 4.1.2 and 4.1.3, respectively. The storm event files were also used as input for the SHAPE ASSESSMENT.xlsx and INTENSITY ASSESSMENT.xlsx files, which were used for the storm shape and average intensity assessments described in Sections 5.1 and 5.3.

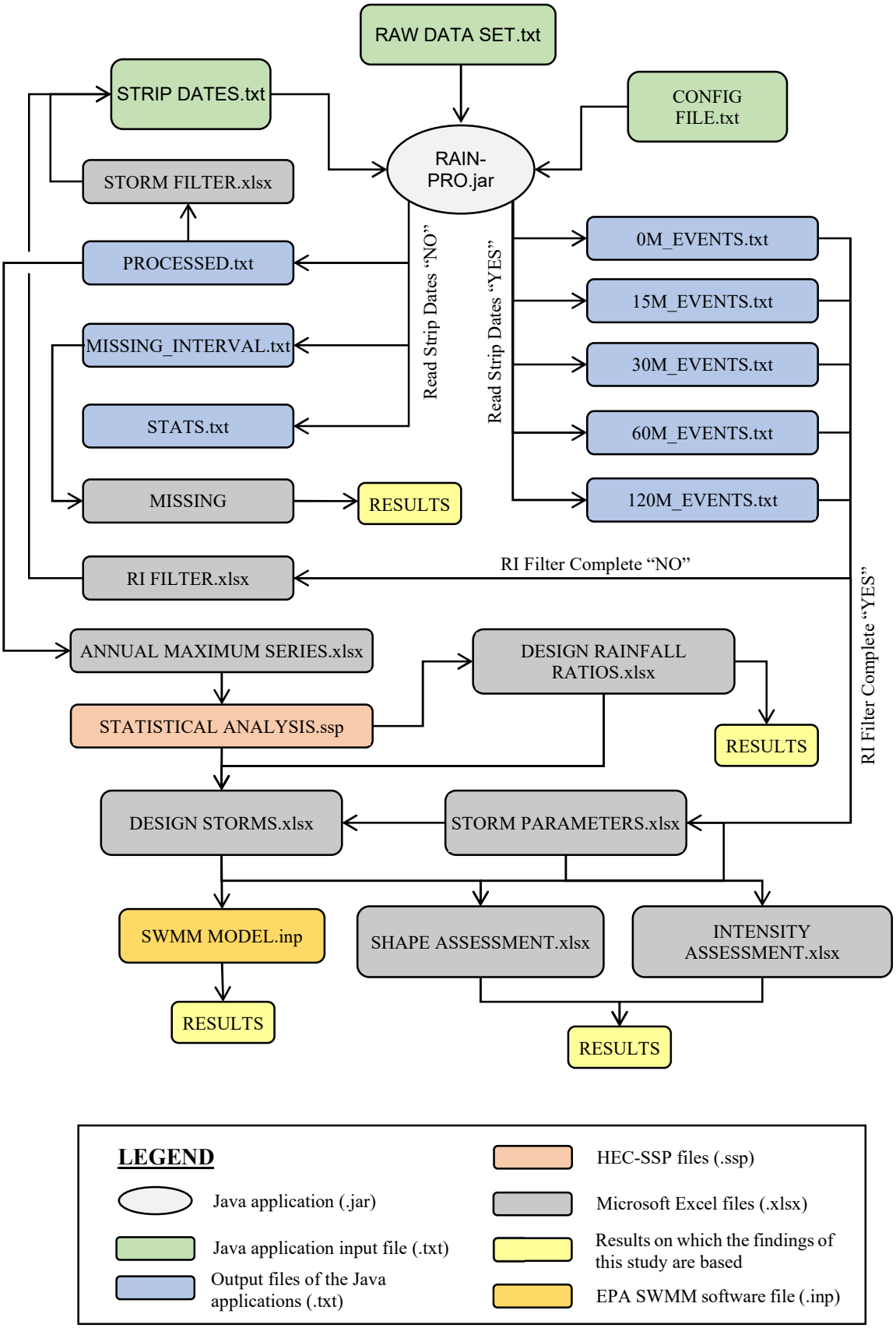

Figure 3.2: Data processing flow chart

3.4 MISSING DATA ANALYSIS

The missing data analysis was done by identifying missing periods of data, consisting of missing 5-min intervals, as well as intervals that had no rainfall value assigned, as indicated in Table 3.2. The information of all the missing periods of each station was written to a separate text file which was used for further processing in MS Excel. The time of the year when missing data occurs was taken into consideration. The average monthly rainfall, depicted in Figure 3.3, for the three stations situated at O.R. Tambo, Irene, and Jhb Bot Gardens, were used to guide this process. Also indicated in Figure 3.3 are the minimum and maximum values of the three stations, which indicates the variances in the average rainfall. Based on this analysis, the months of May to September were considered to be 'dry' months and hence missing data occurring during these months were assumed to be zero rainfall. Only missing data occurring during the 'wet' months were used for the classification of missing data in the assessment of data quality.

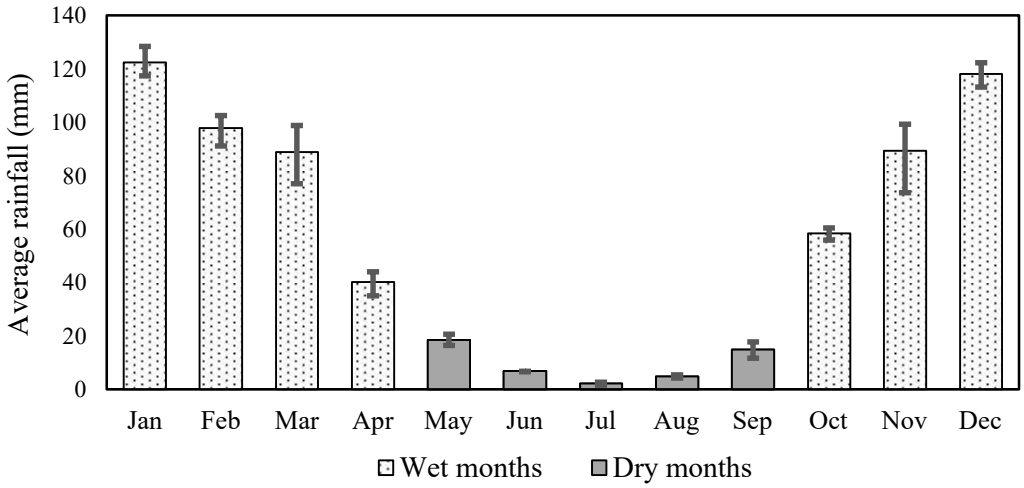

Figure 3.3: Average monthly rainfall for O.R. Tambo, Irene and Jhb Bot Gardens

The data quality of each station was characterised according to the criteria summarised in Table 3.3 and the results are summarised in Table 3.4. Stations with data periods of more than 20 years and periods of missing data during 'wet' months of less than 5% were classified as stations with good data sets. These stations were used to determine the storm parameters and design rainfall estimation described in Sections 4.1.2 and 4.1.3, respectively. They were also used for the shape and intensity assessments, as well as the continuous simulation modelling described in Chapter 5. Data periods of less than 20 years but more than 10 years, and missing data of less than 20%, were classified as Average data sets. These stations were considered to be less reliable and were only used for the design rainfall estimation. Data periods of less than 10 years, and missing data of more than 20%, were classified as poor sets. These stations were omitted from this study due to the data sets being incomplete. In total 35 stations were assessed, with five having good data sets, 11 average, and 19 poor.

Table 3.3: Data quality classification criteria

Description		Data period		
		years ≥ 20	20 > years ≥ 10	10 > years
Missing data during wet months	≤ 5%	Good	Average	Poor
	≤ 20%	Average	Poor	Poor
	> 20%	Poor	Poor	Poor

Table 3.4: Missing data analysis summary

ID	Name	Data period (years)	Missing data (%)		Data quality
			All year round	Wet months	
1	Jhb OR Tambo	26.2	1.9	1.0	Good
2	Lanseria	10.7	1.1	1.0	Poor #
3	Irene	26.2	1.2	0.7	Good
4	Bolepi House	17.6	16.3	10.6	Average
5	Vereeniging	26.2	6.9	5.2	Good
6	Zuurbekom	6.3	1.4	0.6	Poor
7	Kloofendal	3.9	17.9	17.0	Poor
8	Jhb Bot Tuine	26.1	4.1	2.8	Good
9	Springs	3.9	55.7	31.7	Poor
10	Bronkhorstspruit	11.7	3.5	3.0	Average
11	Waterkloof AFB	7.9	7.6	7.0	Poor
12	Pretoria Unisa	26.2	8.6	4.7	Good
13	Pta Proefplaas	9.9	1.4	1.1	Average
14	Pretoria Pur	2.5	18.3	3.3	Poor
15	Pretoria TUT	1.9	23.5	19.6	Poor
16	Wonderb. RWY11	0.4	17.0	16.3	Poor
17	Wonderb. RWY24	0.4	10.1	8.8	Poor
18	Fochville Police	9.3	2.2	2.0	Poor #
19	Westonaria Kloof	9.3	13.4	7.8	Average
20	Goudkoppies	11.0	6.5	4.2	Average
21	Dube	9.2	9.2	5.8	Average
22	Dobsonville	9.2	25.5	17.2	Poor #
23	Magalies Police	9.2	40.0	18.8	Poor #
24	Sterkfontein	11.2	11.8	6.8	Average
25	Jhb Sandton	10.8	8.2	7.1	Poor #
26	Alexandra Depot	9.2	7.3	6.1	Average
27	Ivory Park	9.2	20.4	12.4	Poor #
28	Diepsloot	9.2	3.9	2.6	Average
29	Pta presidency	10.9	35.1	23.2	Poor
30	Pta Rietondale	9.7	51.5	31.3	Poor
31	Pta Mount. View	9.0	42.1	23.0	Poor
32	Baviaanspoort	9.3	38.0	22.6	Poor
33	Kameeldrift	9.8	52.7	31.6	Poor
34	Shosanguve	11.4	13.2	9.3	Average
35	Wonderboom	10.6	4.5	3.5	Average

Data appear to be unreliable as described in Section 3.5 and were subsequently downgraded.

3.5 RAINFALL DATA VERIFICATION

Historically SAWS recorded daily rainfall at 08:00 using a standard rain gauge that is independent of the automatic rain gauge. However, this is no longer the case in Gauteng (Linnerts, 2022). The accuracy of the 5-min data could, therefore, not be determined using the daily rainfall records as an independent verification method, and an alternative methodology was developed.

The assessment of the data quality was conducted by comparing the annual rainfall of each station, in hydrological years, with the data of reliable stations. The annual rainfall from O.R Tambo and Irene was used as baselines because of their long data periods and least missing data. A subjective assessment was conducted whereby a data set was thought to be unreliable if significant deviations from the baselines were observed. It generally applied to average stations because of their small sample sizes which led to the downgrading of six stations' classification from 'average' to 'poor'.

The comparison between each station's annual rainfall with the baselines are depicted in Figure 3.4 to Figure 3.6. For example, at Lanseria in 2010/11 to 2012/13, substantial deviations from the baselines were observed with a small percentage of missing data periods in the same year. The deviations were attributed to poor quality and, therefore, Lanseria's classification was downgraded. Similarly, Fochville, Dobsonville, Magalies, Sandton, and Ivory Park were also downgraded. The substantial deviations in their short data period will have a significant effect on design rainfall estimation and, therefore, these stations were downgraded. The remainder of the stations were assumed sufficiently accurate to conduct this study. The substantial deviations at Dobsonville and Magalies could be attributed to a large percentage of missing data periods during the same year. However, further research on the cause of the substantial deviations is needed as the majority of stations are affected. The data quality classification criteria provided in Table 3.3 considers the missing data during wet months of the entire data period and could be further developed to consider missing data during an individual year. The data quality in this study was objectively assessed with the criteria provided in Table 3.3, but also partially subjectively assessed with the downgrading of the six stations due to the substantial deviations. The consequences of the total and annually missing data as well as the substantial deviations, in terms of design rainfall estimation, should be investigated and incorporated into the quality classification. The data quality classification criteria could be further developed which will provide a more objectively assessment of the data quality.

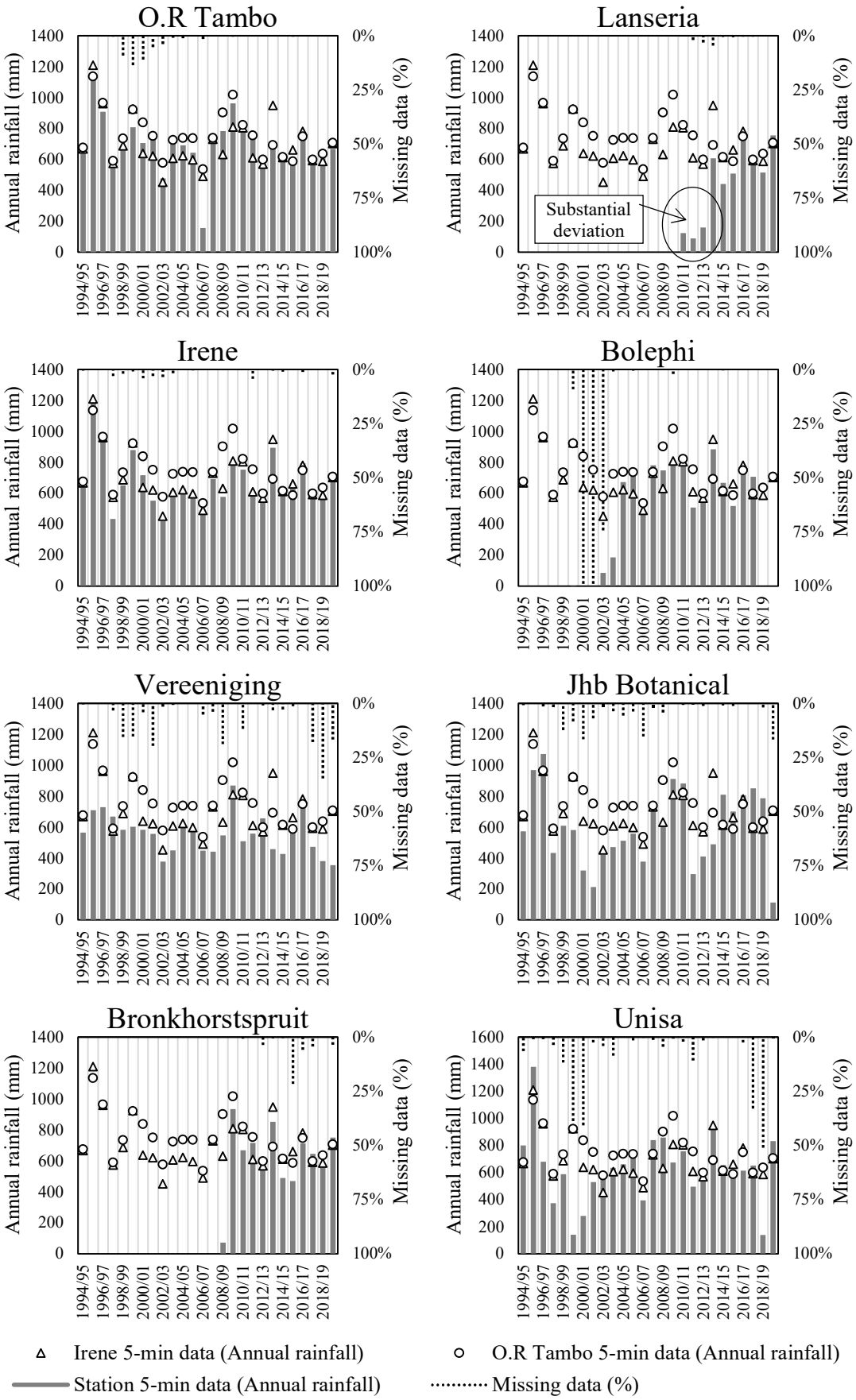

Figure 3.4: Comparison between annual rainfalls and missing data (1 of 3)

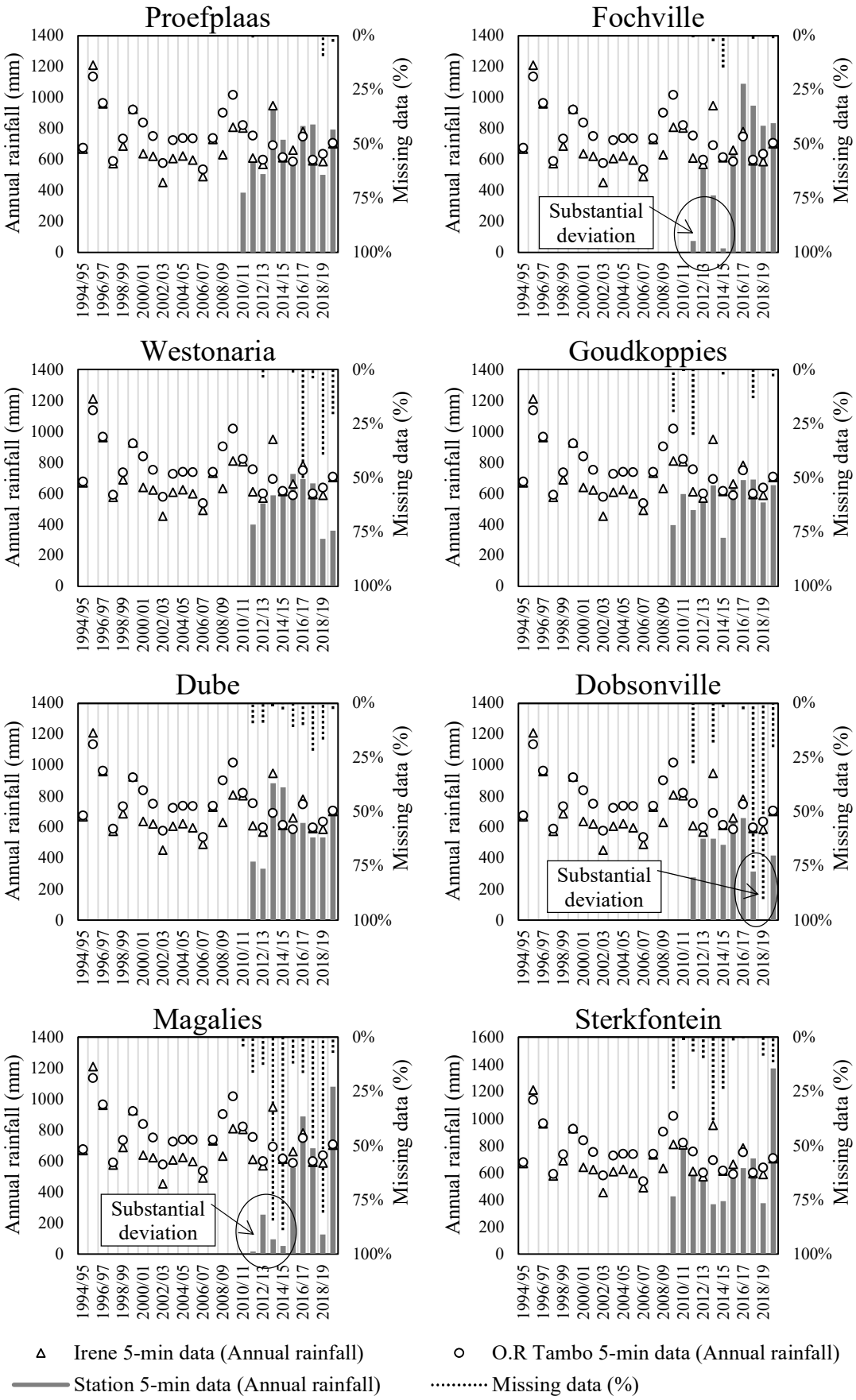

Figure 3.5: Comparison between annual rainfalls and missing data (2 of 3)

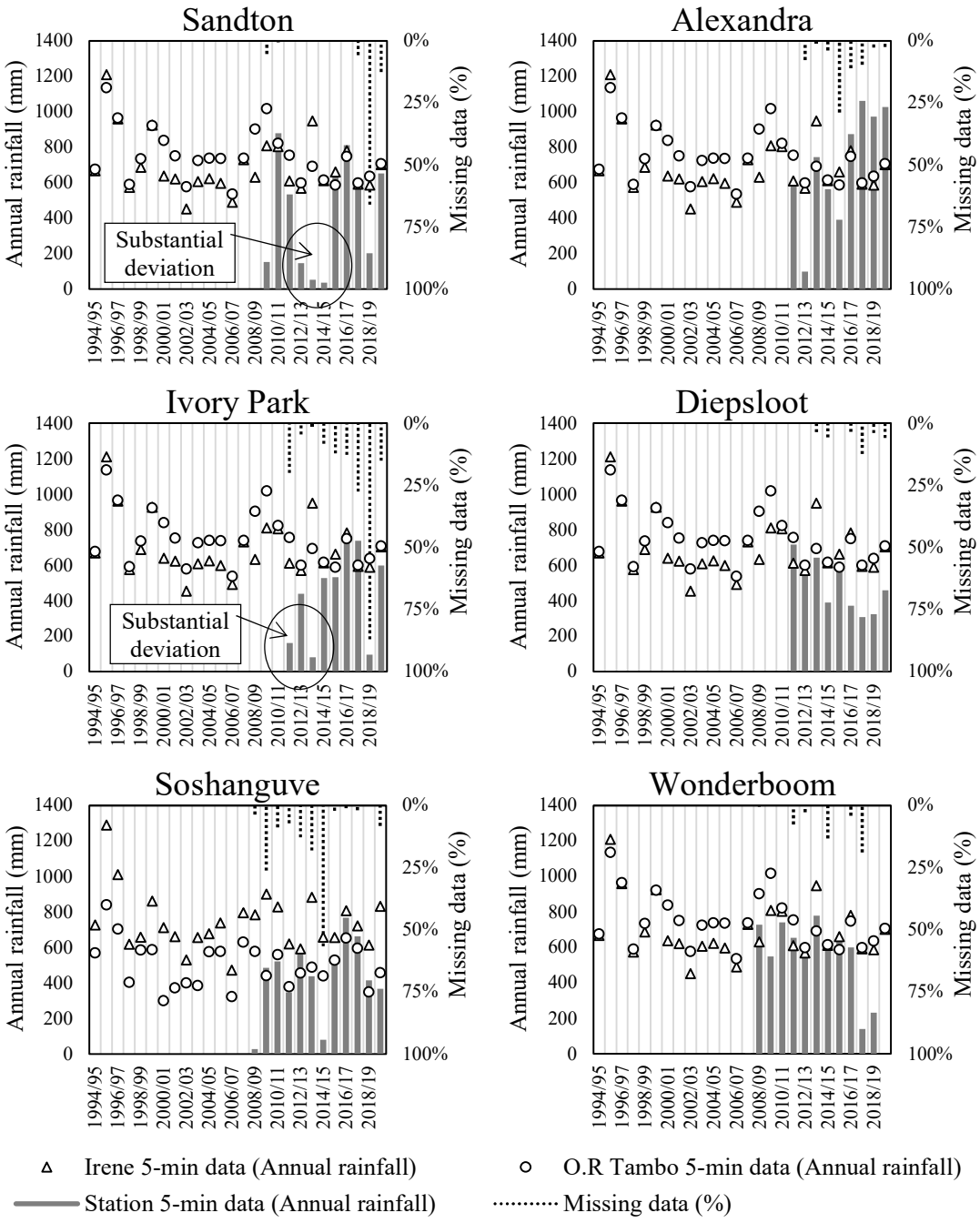

Figure 3.6: Comparison between annual rainfalls and missing data (3 of 3)

3.6 STORM EVENT IDENTIFICATION

A single event-based methodology was adopted for this study to identify independent storm events. Generally, this methodology consists of defining an allowable Maximum Dry Period (MDP) between rainfall spells, as well as a Minimum Rainfall Depth (MRD) threshold. This methodology was adapted by the addition of a third threshold criterion that is related to the Minimum Rainfall Intensity (MRI) of the storm event. The three criteria and the results are described in this section.

3.6.1 Maximum dry period

The MDP criterion refers to the threshold period of no rainfall that occurs between two rainfall spells. If the dry period exceeds the MDP threshold, the two spells are considered two separate events. Conversely, if the dry period is less than the MDP, the two spells are considered one event. This concept is depicted in Figure 3.7.

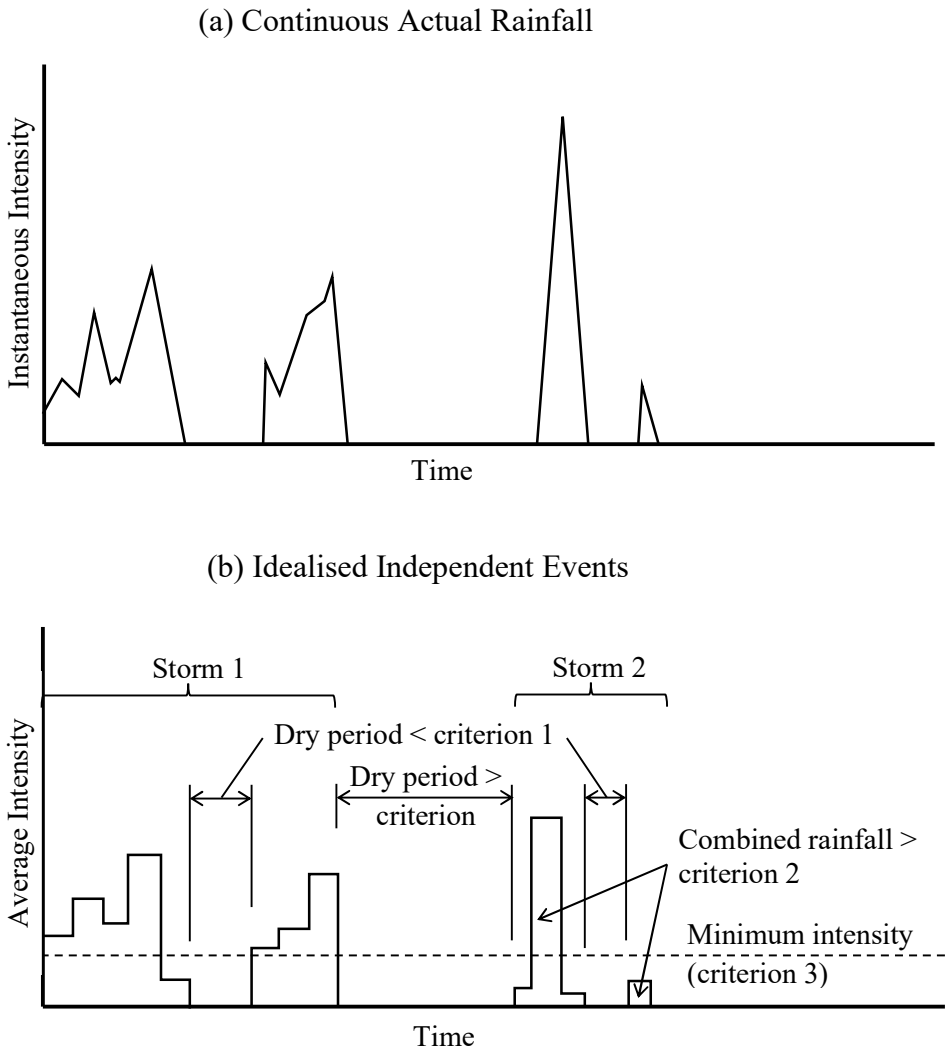

Figure 3.7: Idealised independent events (after Restrepo and Eagleson, 1982)

Different dry periods are documented in the literature. For example, Huff (1967) used a maximum of 6-hours to separate independent rainfall events. Ramlall (2020) initially used 6-hours as the MDP but found that events frequently included extensive periods of low to zero rainfall. Subsequently, the MDP was reduced to 1-hour which resulted in an improved coefficient of determination (R^2) between total rainfall depth and total storm duration. The MDP can also be determined by considering the statistical independence of events using an empirical relation for estimating the minimum time between independent events (Restrepo and Eagleson, 1982). This process involves the computation of the mean and standard deviation of dry periods in a continuous rainfall data set. In an iterative process, the smallest dry periods are omitted until the mean and standard deviation is equal (Bonta, 2004). However, for this study, the MDP was systematically increased from 0 to 120-min to identify idealised independent events on which the assessments were conducted. In other words, each data set was assessed from start to finish using the 0-min MDP criterion. Then a second assessment was conducted on the same data set but with a 15-min MDP criterion, then the 30-min MDP, and so forth. The total rainfall depth and total storm duration of a particular storm event could therefore differ depending on the MDP used to distinguish between idealised events. MDPs longer than 120-min could also be considered but because of the effect on the storm duration, which would increase as the MDP increase, the MDP was limited to 120-min for this study. The storm duration in relation to different MDPs, for example, at O.R Tambo are depicted in Figure 3.8. This indicates a constant increase in the average, median and maximum storm duration when the MDP is increased, considering only the MDP criterion to identify independent storm events. However, an appropriate MDP is selected in Section 4.1.1 by considering: (1) the correlation between total rainfall depth and total storm duration, and (2) the reaction time of a catchment.

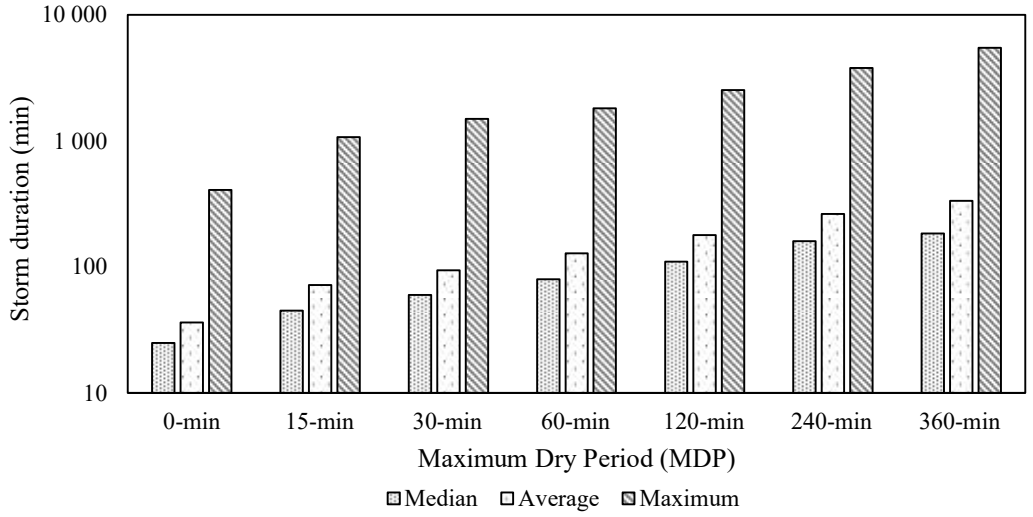

Figure 3.8: Storm duration in relation to the MDP at O.R Tambo

3.6.2 Minimum rainfall depth

Following the separation of the continuous rainfall data into individual storm events, the total rainfall of each event was considered. A storm event was ignored if the total rainfall was less than 10 mm. The MRD of 10 mm was selected considering the design rainfall obtained from the Design Rainfall Estimation in South Africa (DRESA) software (Smithers and Schulze, 2003), which implements the procedures to estimate design rainfall in South Africa per Smithers and Schulze (2000). For example, the 5 and 10-min design rainfall for the O.R Tambo station with a Recurrence Interval (RI) of two years, depicted in Figure 3.9, are 8.8 and 12.7 mm, respectively.

This implies that if the total rainfall for a 2-year RI event was less than 10 mm, the total duration of the event was between five and 10 minutes, which would have been recorded in only one or two 5-min intervals. The location of the peak intensity of such an event will therefore be either at the beginning or the end of the event whereas it is expected for the peak to be somewhere within the event. The second argument is that if the total rainfall of 10 mm was achieved over a longer period, the intensities would be lower than the 5-min design rainfall with a 2-year RI. Therefore, limiting the minimum rainfall to 10 mm to select events ensured that insignificant storm events were eliminated early during the storm event identification process.

User selection has the following criteria:
Coordinates: Latitude: 26 degrees 9 minutes; Longitude: 28 degreess 14 minutes
Durations requested: 5 m, 10 m, 15 m, 30 m, 45 m, 1 h, 1.5 h, 2 h, 4 h, 6 h, 8 h, 10 h, 12 h, 16 h, 20 h, 24
Return Periods requested: 2 yr, 5 yr, 10 yr, 20 yr, 50 yr, 100 yr, 200 yr
Block Size requested: 1 minutes

Gridded values of all points within the specified block

Latitude (°)	Latitude (')	Longitude (°)	Longitude (')	MAP (mm)	Altitude (m)	Duration (m/h/d)	Return Period (years) 2	2L	2U	5	5L	5U	10
26	10	28	13	722	1675	5 m	8.8	7.1	10.5	12.1	9.8	14.5	14.7
						10 m	12.7	10.0	15.3	17.5	13.9	21.1	21.1
						15 m	15.7	12.3	19.1	21.6	17.0	26.3	26.1
						30 m	20.1	16.0	24.1	27.7	22.1	33.3	33.5
						45 m	23.2	18.7	27.7	32.1	25.8	38.3	38.8
						1 h	25.7	20.9	30.6	35.5	28.9	42.3	43.0
						1.5 h	29.8	24.4	35.1	41.1	33.7	48.5	49.7
						2 h	33.0	27.2	38.8	45.5	37.6	53.5	55.1
						4 h	39.5	33.5	45.5	54.6	46.2	62.9	66.0
						6 h	43.9	37.8	50.0	60.7	52.2	69.1	73.3
						8 h	47.4	41.2	53.5	65.4	56.9	73.9	79.1
						10 h	50.2	44.0	56.4	69.3	60.8	77.8	83.8
						12 h	52.7	46.4	58.8	72.7	64.2	81.2	87.9
						16 h	56.8	50.6	62.9	78.4	69.9	86.8	94.7
						20 h	60.2	54.1	66.2	83.1	74.7	91.4	100.4
						24 h	63.1	57.1	69.1	87.1	78.9	95.4	105.3

Figure 3.9: Typical design rainfall estimation results for O.R. Tambo obtained from the DRESA software

3.6.3 Minimum rainfall intensity

The MRI was the final criterion that was applied before an event could be classified as a significant event. The RI of each storm event was estimated using the DRESA software. The ninety per cent upper (U) and lower (L) bounds for the design rainfall values were not considered for this investigation. The depth-frequency relationship for the design rainfall was approximated using an exponential function. The 5-min design rainfall for the O.R Tambo station, for example, is depicted in Figure 3.10 as well as the fitted exponential regression line. This indicates a good approximation of the design rainfall with $R^2 = 0.9963$. Similar results were obtained for all the stations and, therefore, the exponential function was used to apply the MRI criterion.

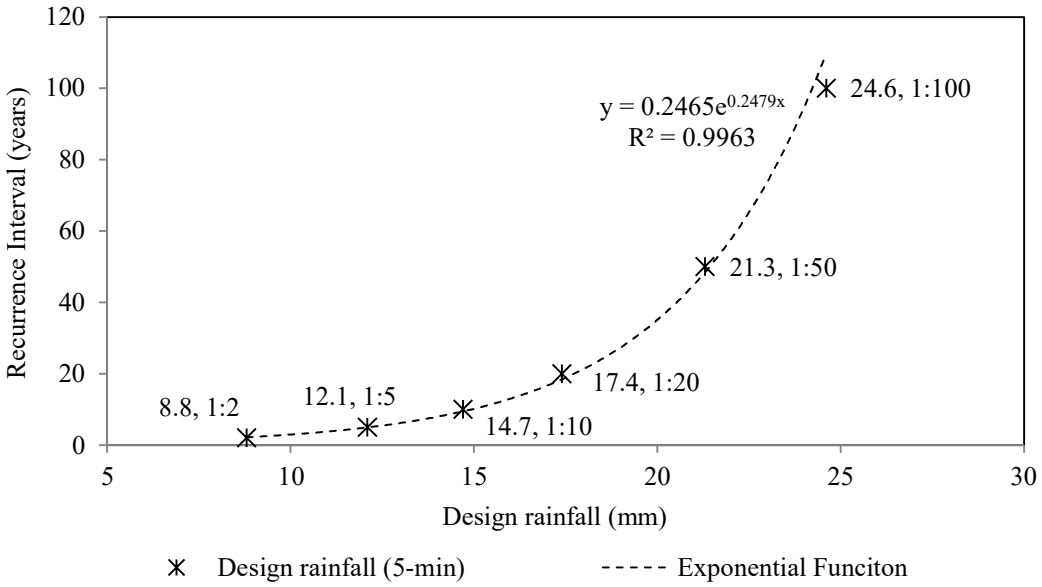

Figure 3.10: Typical depth-frequency relationship for O.R Tambo International Airport

The MRI criterion was applied to eliminate storm events with insignificant intensities considering the 5-min to 24-hour design rainfall for each station. This means that if the maximum RI of the event was less than two years, the storm event was ignored. A typical application of this criterion is depicted in Figure 3.11, which was applied to the storm event that occurred at the O.R Tambo station on 13 March 2011. The total storm duration for this event was 12 hours. A moving window period was used to extract the maximum rainfall for each of the standard time steps from 5 min to 12 hours. As depicted in Figure 3.11, as an example, the 5-min to 6-hour time steps were less than the specified threshold of two years. However, the 8, 10 and 12-hour time steps exceeded the threshold which therefore qualified this storm event.

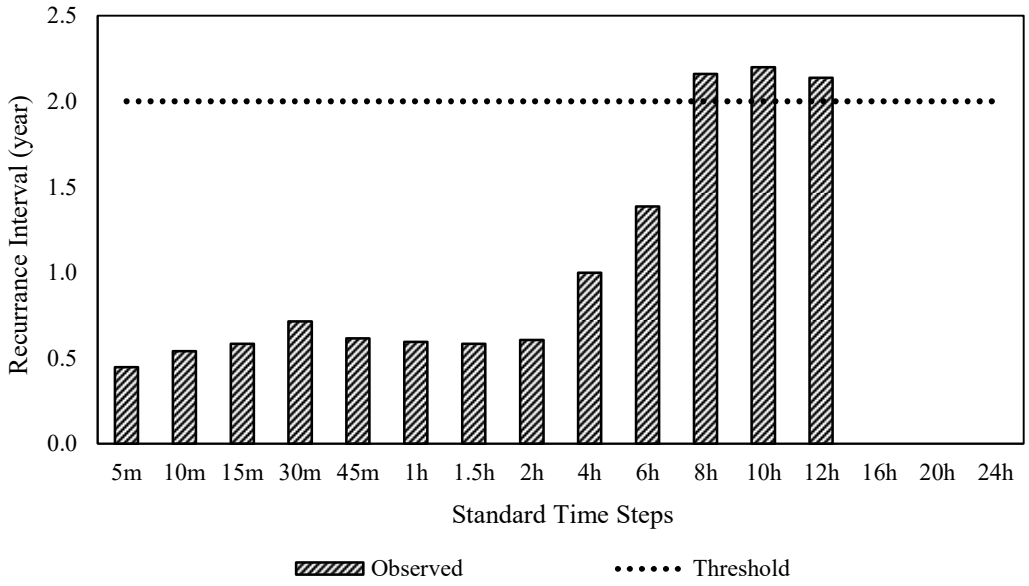

Figure 3.11: Typical maximum recurrence intervals per standard time step for the storm event that occurred on 13 March 2011 at O.R Tambo

3.6.4 Identification of single storm events

The Rain-Pro software was programmed to extract all data records with rainfall values of more than zero rainfall from the raw data set. A new data file was written to a separate text file (PROCESSED.txt) as described in more detail in Section 3.3. This process simplified the data file in terms of the number of line items, because the data loggers of the SAWS automatic rain gauges continuously records data in 5-min intervals. In any raw data file, more than 95% of the line items have zero rainfall. Because all these items have the same value, namely zero, these items are, therefore, not unique. All further processing of the new data set could, therefore, assume that all intermediate intervals of time have zero rainfall.

The processing of the PROCESSED.txt file was done in MS Excel. For an MDP of 0-min, which means that a storm event ended immediately when precipitation stopped, the total number of storm events identified from the 16 stations with good to average data sets, was 3 107 events. The number of events consistently increased as the MDP increased. This is because of the combined precipitation of short spells, forming a single event, that exceeds the threshold of 10 mm, whereas individually the spells do not meet the criterion. As a result, the total number of events for an MDP of 120-min was 4 560.

The total number of storm events for the selected stations are depicted in Figure 3.12. It is important to note that a large portion of the total number of events consisted of events for which the RI was less than two years, which are considered to be insignificant storm events for the purposes of this study. Over 80% of the events had a RI of less than two years. The storm events with RIs exceeding two years were considered significant, and the analyses were conducted on these events.

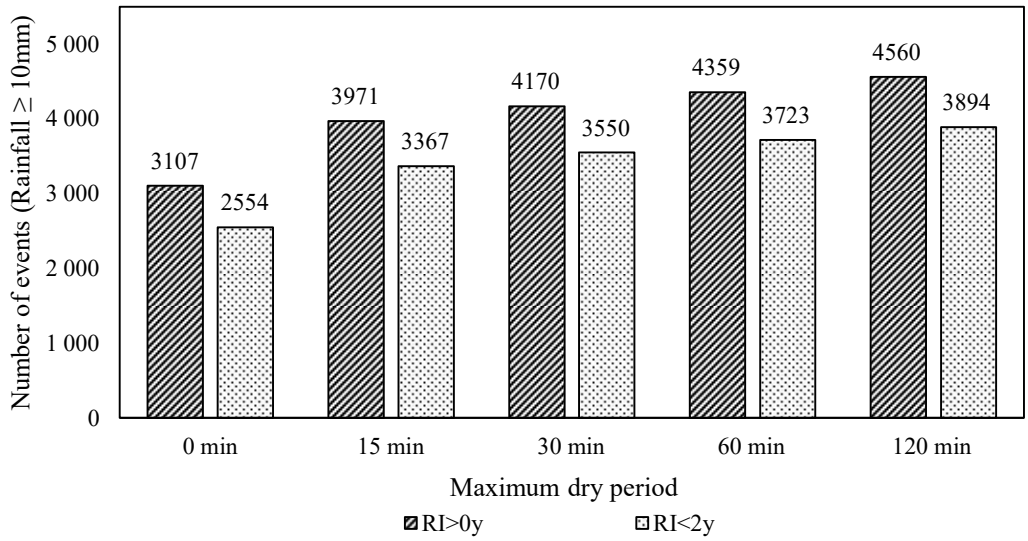

Figure 3.12: Total number of storm events and insignificant events identified based on different MDP criteria

The frequencies of events for the 16 stations with good to average data sets, considering different MDP criteria, are depicted in Figure 3.13. It can be seen that 82 to 85% of all events are deemed insignificant for the purposes of this study.

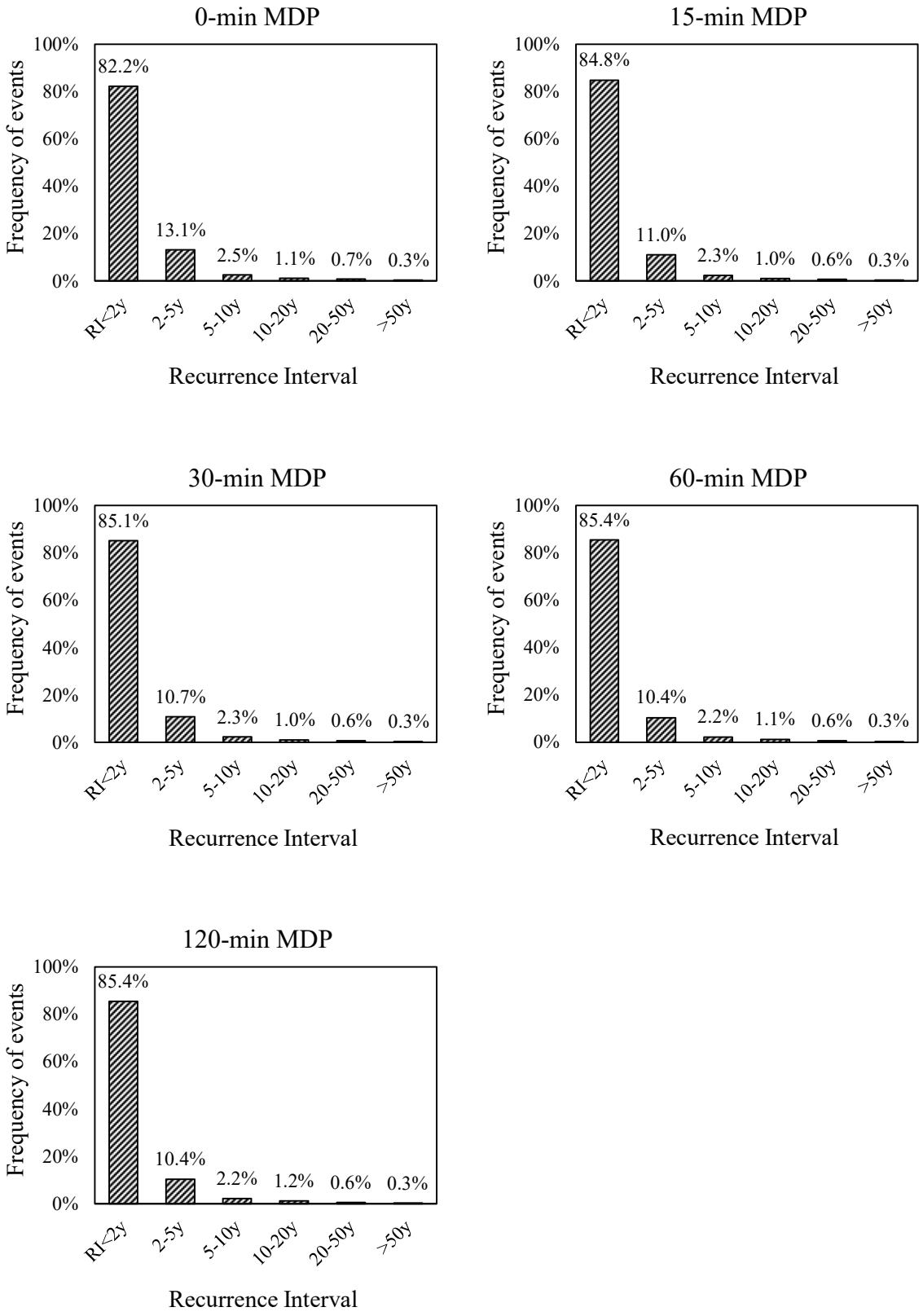

Figure 3.13: Frequency of events for different MDP criteria

3.7 CHAPTER SUMMARY

This chapter has provided details about the data source, the collation of the rainfall data, and an overview of the data processing. The missing data analysis was based on the total number of missing periods during 'wet' months. These months, consisting of October to April, were identified by considering the average monthly rainfall of the O.R Tambo, Irene, and Jhb Bot Gardens stations. The missing data as well as the data period of each station were used to classify the data quality of each rainfall station. A station was classified as either, good, average, or poor, depending on the selected classification criteria. In total 35 stations were assessed, with five having good data sets, 11 average, and 19 poor.

An assessment of the data quality was conducted by comparing the annual rainfall of each station, in hydrological years, with the annual rainfall from O.R Tambo and Irene. These two stations were used as baseline because of their long data periods and least missing data. A subjective assessment was conducted whereby a data set was thought to be unreliable if significant deviations from the baselines were observed which led to the downgrading of six stations' classification from average to poor. These stations are Lanseria, Fochville, Dobsonville, Magalies, Sandton, and Ivory Park. The stations with poor data sets were omitted from the study, whereas the good and average stations are used in Chapter 4 in subsequent investigations.

The criteria used for the identification of individual events were also described. These criteria consisted of an MDP ranging from 0 to 120-min, an MRD of 10 mm, and an MRI of 1:2 years. In Chapter 4 a single MDP was selected and subsequent analyses in the chapter, such as the advancement coefficient and dimensionless time to peak, were based on this MDP.

4 DATA ANALYSIS

The methods considered appropriate after completing the literature review consisted of the REC, TRI, CDS, SCS and SCS-SA rainfall distribution curves, and Huff curves. This chapter consists of seven sections that describe several aspects relating to the appropriate generation of synthetic design storms using these methods which provides the foundation for Chapter 5. This chapter also provides evidence of the inappropriateness of two of the methods, the SCS rainfall distribution curves, and Huff curves.

The first section of this chapter describes the extraction of the advancement coefficient relating to the CDS method, and the dimensionless time to peak relating to the TRI method. The significant storm events identified in the previous chapter were used to determine these storm parameters. The second section describes the design rainfall estimation of stations with good and average data sets as defined in the previous chapter, using Probability Distribution (PD) analysis. The third section describes the methodology that was developed to determine the regression coefficients associated with the CDS method. The fourth section describes the methodology that was adopted and adapted for the distribution of the design rainfall to create a 24-hour synthetic design storm. It also describes the process of extracting storm events from 24-hour distribution curves which is necessary for comparing the shape of synthetic design storms and significant storm events in the next chapter. The fifth section describes the comparison of the design rainfall ratios with the ratios of the SCS-SA curves and the recommendation with regards to the implementation of intermediate curve types. The sixth section describes the comparison of the SCS curves with (a) the SCS-SA curves and (b) the at-site design rainfall ratios, as well as the conclusion with regards to the use of the SCS curves. In section seven standardised mass curves are developed using the significant storm events identified in the previous chapter and compared with the at-site design rainfall ratios.

4.1 STORM PARAMETERS

In this section, an appropriate MPD, as defined in Section 3.6.1, was investigated and selected, and based on this finding, the storm parameters for the CDS and TRI methods were determined. The adaptations of the procedures to determine these parameters and the results are described below.

4.1.1 Selection of an appropriate maximum dry period criteria

As noted in Chapter 2, Ramlall (2020) based the decision to use an MDP of 1-hour instead of 6-hour, on the improved correlation between total rainfall depth and total storm duration.

A similar investigation was conducted whereby the correlation was determined using six different MDP criteria, namely, 0-min, 15-min, 30-min, 60-min, 120-min, and 360-min. The analysis was based on the significant storm events of five stations that were pooled together, namely: O.R Tambo, Irene, Vereeniging, Jhb Bot Gardens and Unisa. The results are summarised in Figure 4.1. The data were statistically significant with p-values less than 0.001.

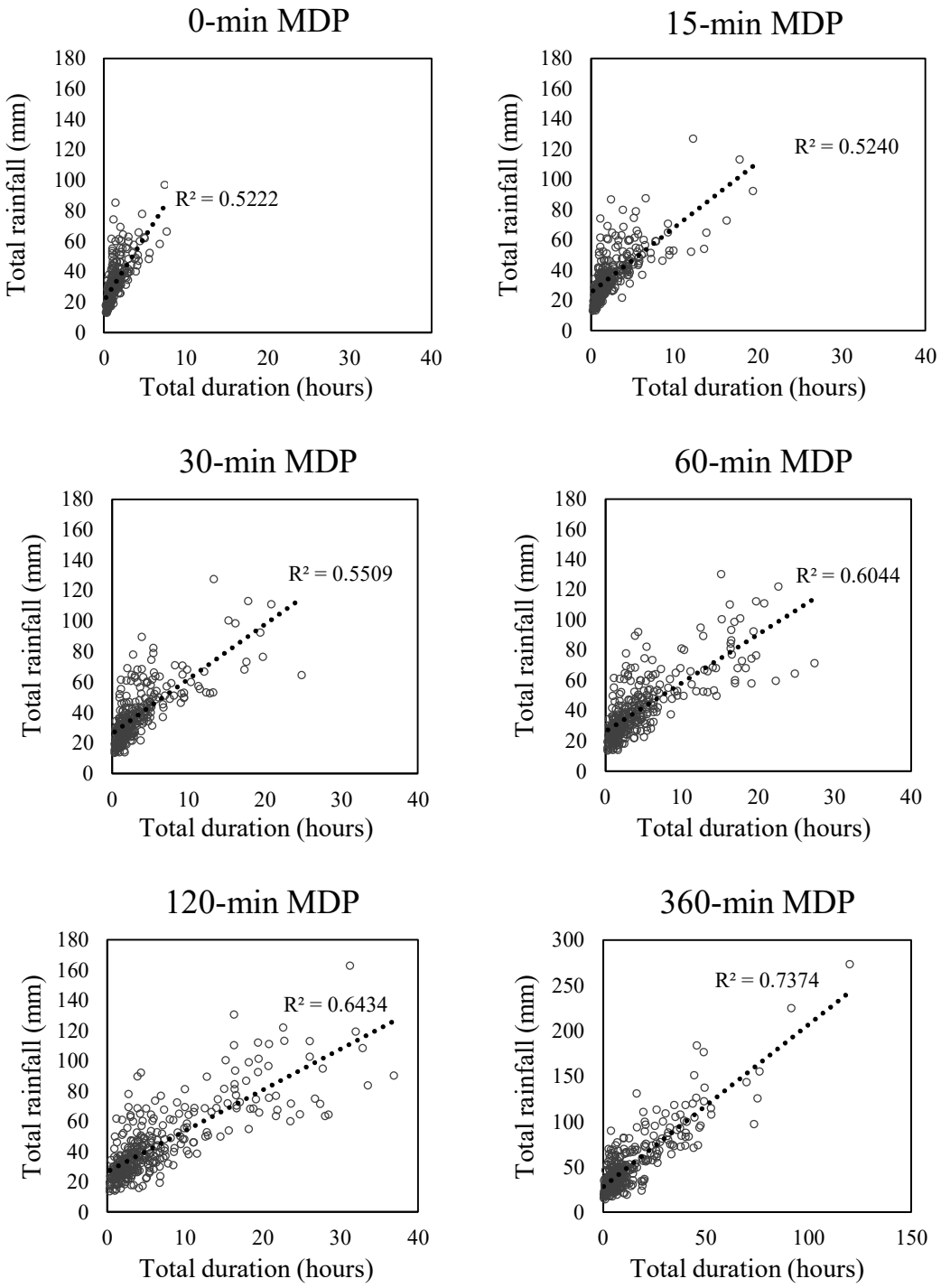

Figure 4.1: Correlation between total rainfall and duration for different MDP criterion

The results indicates that the correlation improves consistently as the MDP increases from an MDP of 0-min to 360-min. This finding was in contrast to the finding of Ramlall (2020), who found an increase in correlation by decreasing the MDP from 6-hour to 1-hour. This could be attributed to the difference in methodology. Ramlall (2020) used an MRD of 1 mm whereas in this study an MRD of 10 mm was used as well as an MRI of 1:2 year.

Subsequent to the above finding, an alternative approach was taken with this study which based the selection of the MDP on the response time of the catchment. It was argued that if the MDP is longer than the reaction time of a catchment, any rainfall after a dry period would not impact the peak discharge from the first spell. The second spell is rather seen as the start of the next event. The Antecedent Moisture Content (AMC) during the second spell is significantly impacted by the first event. The focus of this study is, however, not on the AMC but on the shape assessment of synthetic design storms. Therefore, the alternative approach is warranted.

The typical reaction time of small urban catchments are assumed to be approximately 15-min, and therefore, the 15-min MDP was selected for this study. The reaction of 15-min was also evident from the typical small urban catchment described in Section 5.7. However, the advancement coefficient tended to decrease as the MDP increase. Because permeable surfaces will reach higher levels of soil moisture content with a larger advancement coefficient, further research are recommended to investigate the effect of the advancement coefficient on runoff.

4.1.2 Storm advancement coefficient – Chicago Design Storm

As detailed in Section 2.2.2, Keifer and Chu (1957) determined the storm advancement coefficient for the City of Chicago using two different approaches. The first approach was, however, not considered for this study because of the following disqualifications:

a) According to their first approach, the antecedent rainfall was determined by first identifying the maximum rainfall within a 15, 30, 60 and 120-min period within each significant storm event. Each significant storm event was assumed to be 180 min in total, and the 180 min design rainfall for the 1:5 year storm event was divided on either side of the maximum intensity using the storm advancement coefficient. Since the significant storm events identified for this study were shown to vary significantly in terms of RI, a single RI would therefore be inappropriate.
b) There was an insignificant difference between the coefficients determined by Keifer and Chu (1957), which were 0.387 and 0.375 for the first and second approaches, respectively.

Therefore, the storm advancement coefficient was determined following Keifer and Chu's (1957) second approach.

The procedural steps that were followed to determine the advancement coefficient in this investigation, adopted from Keifer and Chu (1957), are summarised as follows:

a) The maximum rainfall within a 15, 30, 60 and 120-min period within each significant storm event, was identified.
b) For each of these periods, the ordinal position of the 5-min interval with the maximum rainfall was identified.
c) The location of the peak intensity for each period was determined per Equation 4.1. This concept is illustrated in Figure 4.2, which depicts a typical storm event for which the location of the peak intensity for a 30-min period was calculated.
d) The weighted average for each significant event was determined, using the location of peak intensity and weighted proportionally to 15, 30, 60 and 120-min per Equation 4.2.
e) The average for all significant events for each of the five best stations was determined per Equation 4.3.

$$r_d = \frac{t_i}{d_j}\left(n_j - 0.5\right) \qquad \text{(Equation 4.1)}$$

where:

r_d = location of peak intensity for the duration d,

d_j = specific duration (j_1 = 15-min, j_2 = 30-min, j_3 = 60-min, j_4 = 120-min),

n_j = ordinal position of 5-min interval with highest rainfall of storm event, and

t_i = duration of interval (5) (min).

$$r_s = \frac{\sum_{t=1}^{N_d} r_d \cdot d_j}{\sum_{t=1}^{N_d} d_j} \qquad \text{(Equation 4.2)}$$

where:

r_s = advancement coefficient of significant storm event s, and

N_d = Number of specific storm durations (4).

$$r = \frac{1}{N_s}\sum_{s=1}^{N_s} \frac{\sum_{j=1}^{N_d} t_i \cdot \left(n_{j,s} - 0.5\right)}{\sum_{j=1}^{N_d} d_{j,s}} \qquad \text{(Equation 4.3)}$$

where:

r = advancement coefficient, and

N_s = Number of significant storm events of station s.

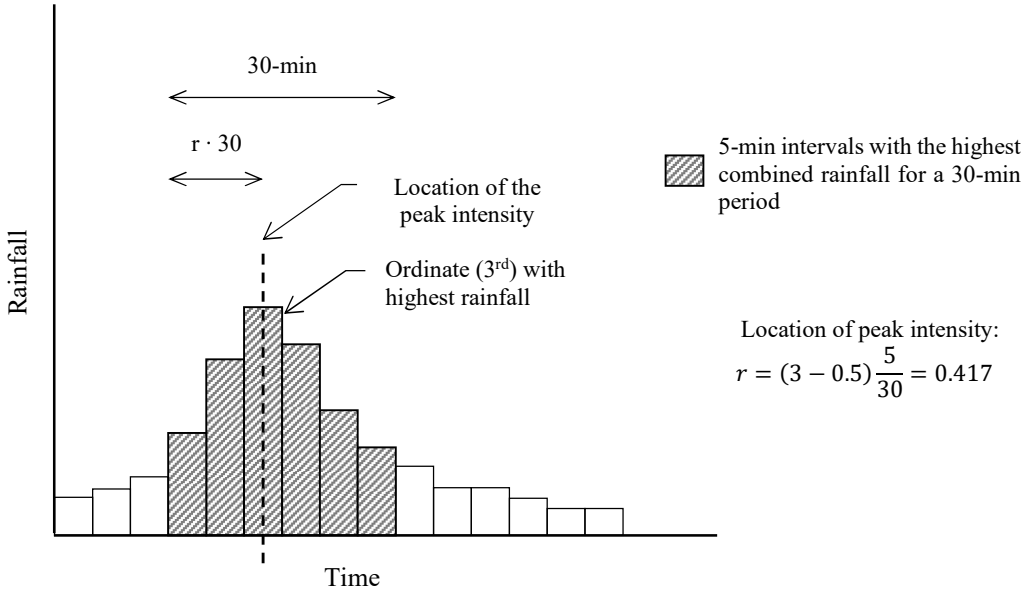

Figure 4.2: Typical location of the peak intensity within a 30-min duration

The storm advancement coefficient was calculated from the significant storm events identified from the five stations with good data sets in Gauteng, namely, O.R Tambo, Irene, Vereeniging, Jhb Bot Gardens and Unisa. The results, depicted in Figure 4.3, indicates minor differences between the average and median values that are similar to the coefficient proposed by Keifer and Chu (1957) of 0.375. As some variation of the advancement coefficient was evident, further analyses were conducted to determine whether different advancement coefficients could be applied in certain circumstances.

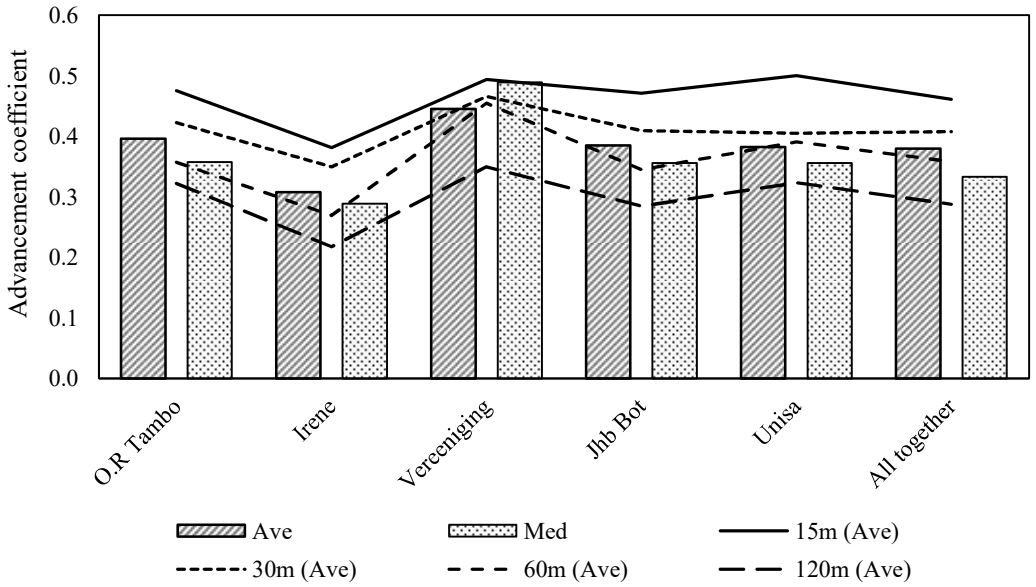

Figure 4.3: Average storm advancement coefficients, based on Keifer and Chu's (1957) second approach

In Figure 4.4 the frequency of events is depicted for various range classes. The results of the five stations are depicted individually and combined. This indicates the advancement coefficient has occurred most frequently in the four range classes between 0.1 and 0.5 with a slightly skewed distribution with a longer tail to the right (positively skewed).

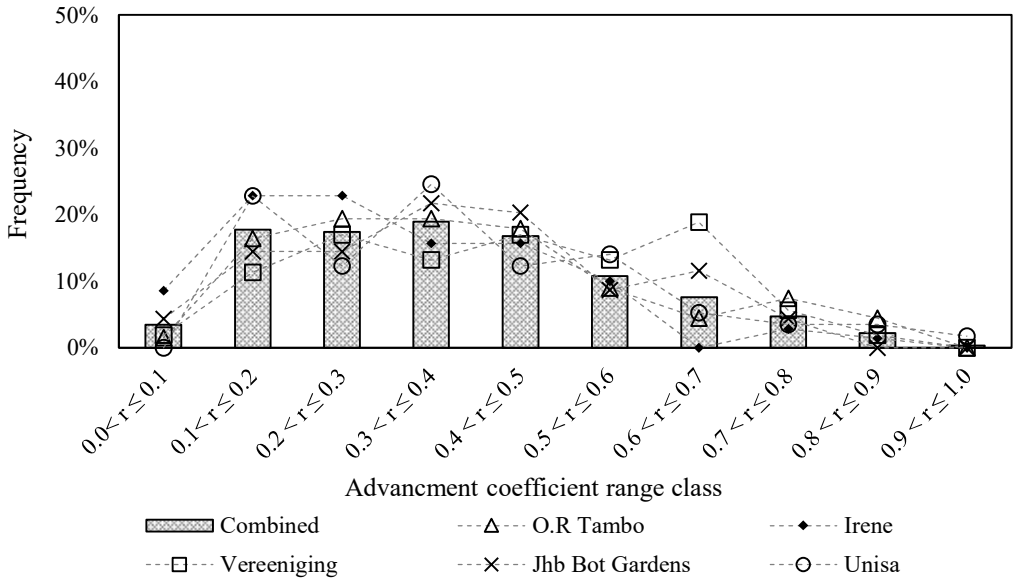

Figure 4.4: Frequency of storm advancement coefficient for different stations

In Figure 4.5 the frequency is depicted for different storm durations for the five stations combined. This indicates that for 2- to 3-hour and 3- to 4-hour events, the coefficient is likely to be between 0.1 to 0.2. However, for storm durations from 0 to 1-hour and 1 to 2-hour the coefficient is between 0.3 and 0.5.

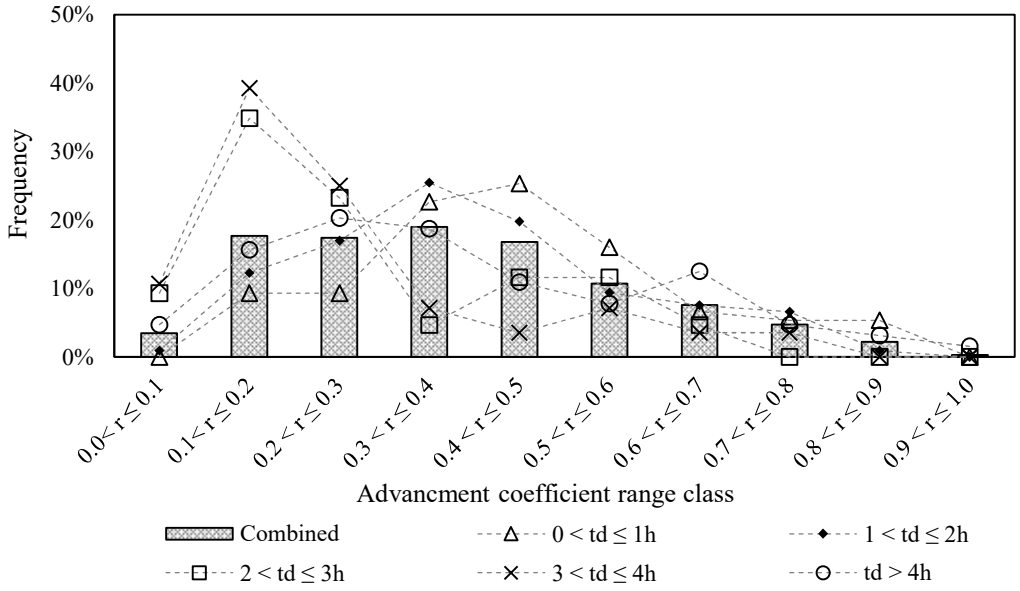

Figure 4.5: Frequency of storm advancement coefficient for different storm durations

The results depicted in Figure 4.4 and Figure 4.5 did not provide clear evidence about the most appropriate advancement coefficient. Therefore, the linear relationship between the advancement coefficient and the (a) storm duration, (b) the total rainfall, and (c) the recurrence interval was also investigated as depicted in Figure 4.6. It was observed that a poor relationship exists between these variables considering the coefficient of determination (R^2) value of 0.0054, 0.0081, and 0.0006. The p-values of 0.1924, 0.1112, and 0.6671 indicates the data are statistically insignificant. Therefore, the average coefficient of 0.380 for the five stations was accepted as the best result which are similar to 0.375 of Keifer and Chu (1957).

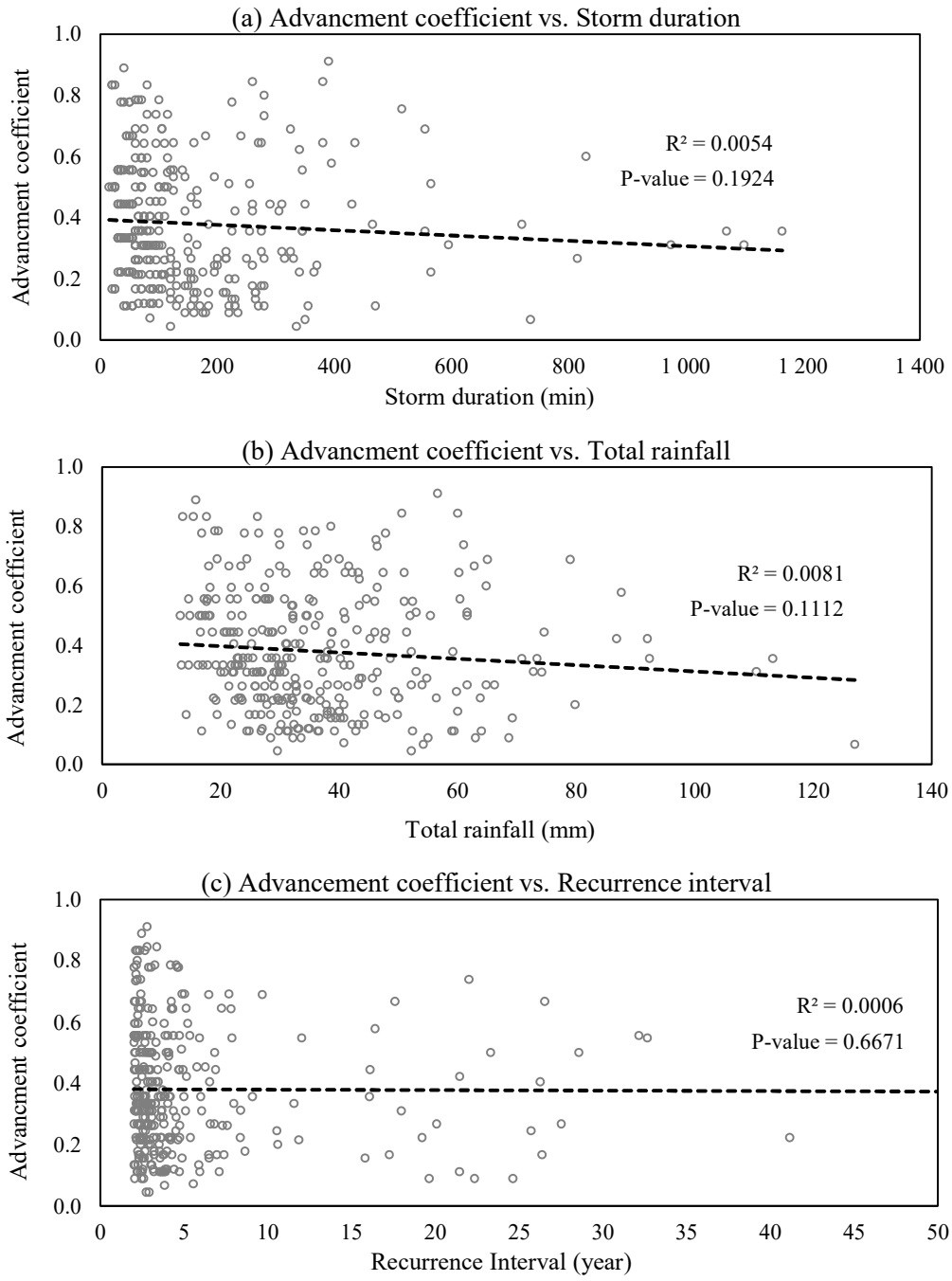

Figure 4.6: Storm advancement coefficients in relation to different parameters

4.1.3 Dimensionless time to peak - Triangular method

The hyetograph's first-moment arm for each significant storm event was calculated and related to a triangular representation of the hyetograph with an equal total rainfall volume and total storm duration, as described by Yen and Chow (1980).

However, for some events the first-moment arm was small which resulted in an obtuse type of triangle, meaning that one angle is larger than 90 degrees. This is, however, not possible, and therefore, in such instances, a right angle was assumed. An example of such an event was observed at O.R Tambo on 4 January 1997, which is depicted in Figure 4.7. The first-moment arm was calculated using Equation , which resulted in 43.2 minutes, and using Equation to calculate the time to peak intensity, yielded negative 40.3 minutes. The negative time to peak was adjusted to zero minutes as depicted in Figure 4.7. Approximately 46% of the significant single event-based events required this adjustment.

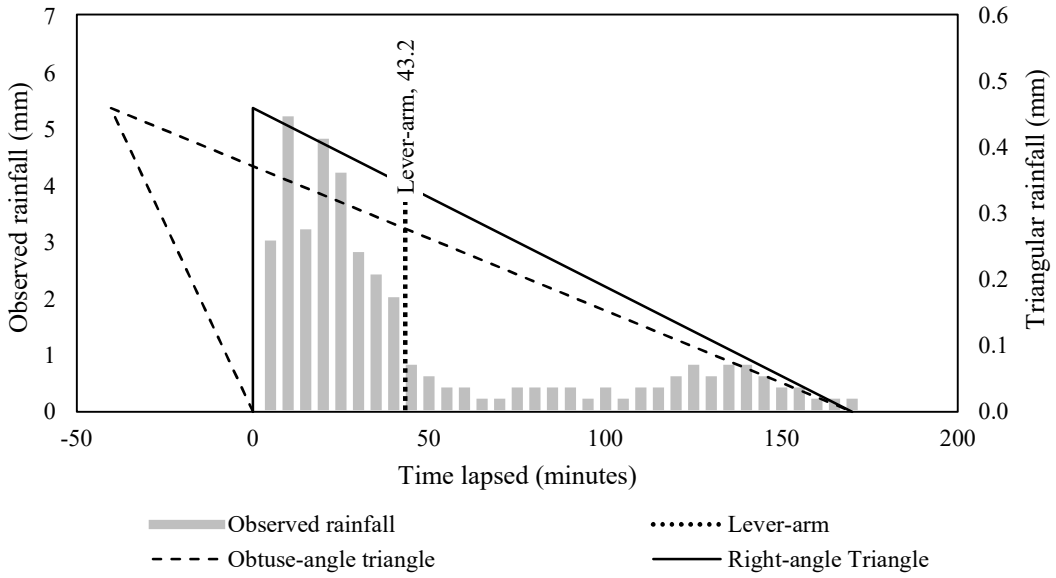

Figure 4.7: Correction of an obtuse triangle such as for the storm event at O.R. Tambo on 4 January 1997 at 00:50

Yen and Chow (1980) has determined the statistical mean values for the storm events sorted into various duration groups. The first group contained all events, the second group the 2-hour events, the third group the 3-hour events, etc. However, an insignificant difference was reported between the groups. Therefore, the effect of different total storm durations, total rainfall volumes and different seasons were not considered for this study, as proposed by Yen and Chow (1980). Instead, all events were grouped at each of the five best stations and the average time to peak ratio was computed as depicted in Figure 4.8. From the results the average for the five stations were 0.20, but large differences between the average and median values was observed.

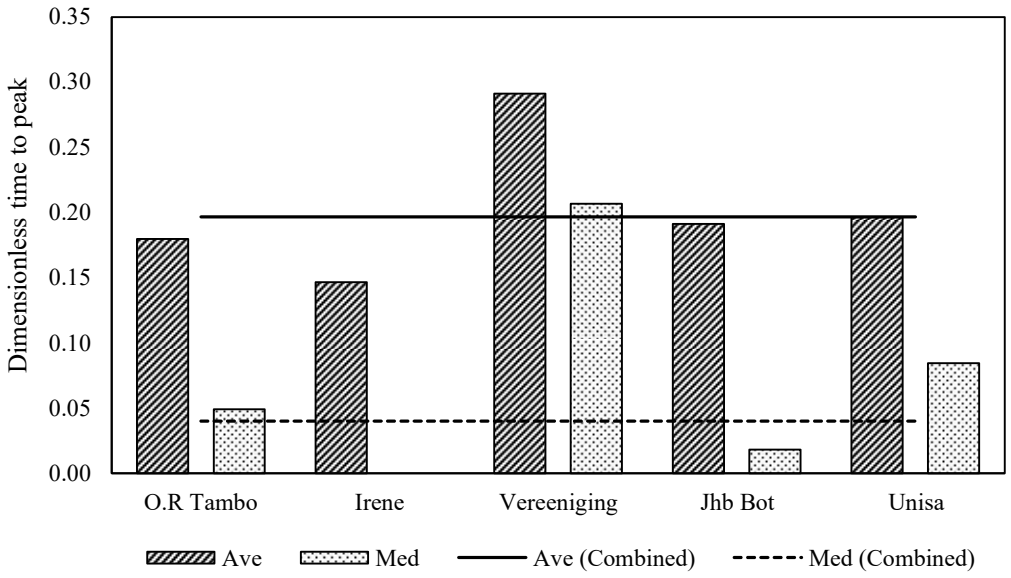

Figure 4.8: Time to peak intensity using method proposed by Yen and Chow (1980)

The frequency of events is depicted in Figure 4.9 for various range classes. The results indicate that the dimensionless time to peak between 0 and 0.1 has occurred most frequently. This is attributed to the correction of the obtuse triangles. This has resulted in large differences between the average and median values. The consequences of the large differences should be investigated in future research of the triangular method. However, the average of 0.20 value was used in subsequent analyses in this study.

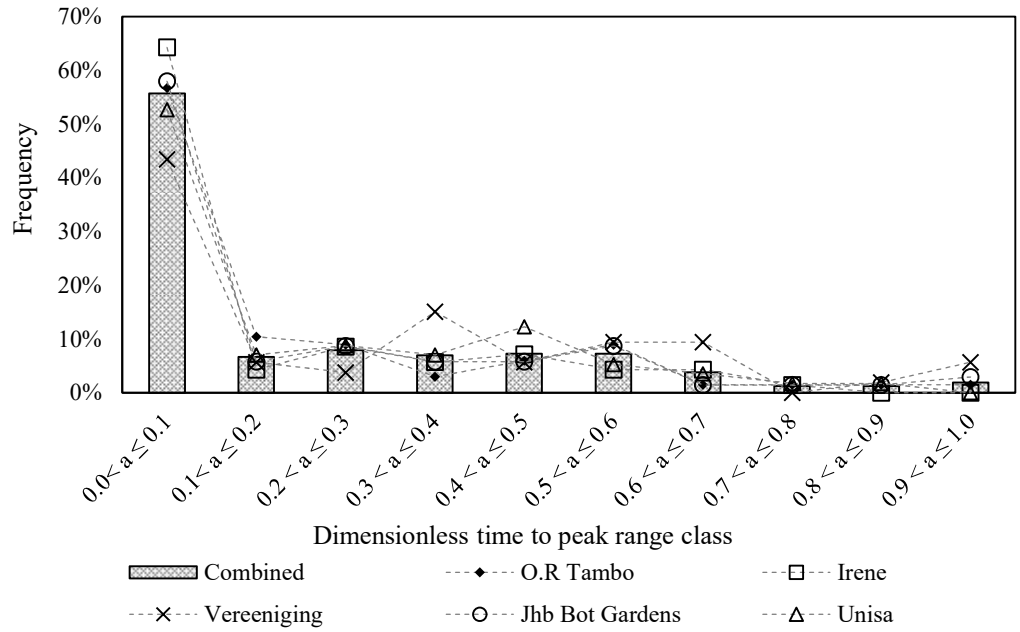

Figure 4.9: Frequency distribution of dimensionless time to peak for different stations

4.2 AT-SITE DESIGN RAINFALL

The development of short duration Depth-Duration-Frequency (DDF) curves for the rainfall stations in Gauteng is described in this section. The DDF curves were subsequently used for further analyses, namely:

a) Comparison with the Smithers and Schulze (2000) design rainfall,
b) Generating site-specific rainfall distribution curves, and
c) Determining the D-hour to 24-hour design rainfall ratios, compared with the ratios of the SCS-SA,SCS curves, and standardised mass curves.

Municipal stormwater infrastructure associated with minor stormwater drainage networks is generally designed to accommodate storm events with a return period of 1:5 up to 1:20 years. The DDF curves were, therefore, developed for stations that have a minimum data period of approximately 10 years. With a data period of at least 10 years the estimation of design events with a return period of up to 1:20 years is generally accepted, as estimation of return periods greater than twice the record length is generally not recommended (Smithers and Schulze, 2000). In terms of missing data, Smithers and Schulze (2000) found that there was no significant effect on design rainfall estimates if up to 20% of the years in the Annual Maximum Series (AMS) do not contain their true value. Even though this finding does not explicitly relate with the missing data in the context of this study, 16 stations were identified to comply with this criterion which are located as depicted in Figure 4.10.

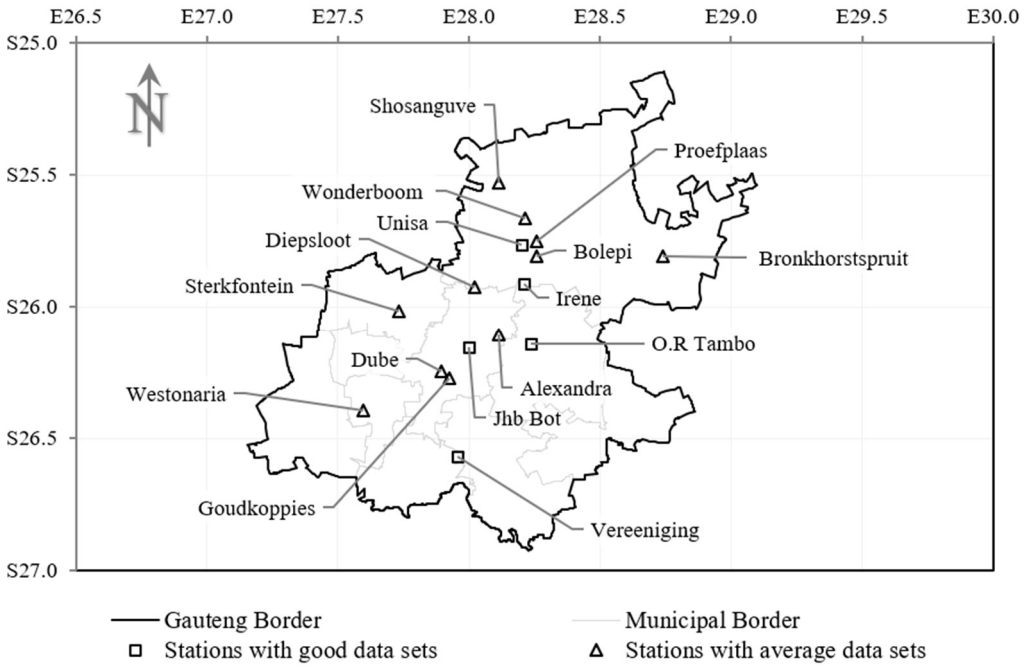

Figure 4.10: Rainfall stations (16) in Gauteng that were used for the at-site design rainfall

The AMS was extracted between 01 Oct and 30 Sep of each year (hydrological years) for 16 time steps ranging from 5-min to 24-hours (standard time steps) and a PD analysis was conducted on the AMS using the General Extreme Value (GEV) distribution. Based on Goodness-of-fit (GOF) tests and L-moments to fit the distributions to the data, Smithers (1996) recommended the GEV and the 3 parameter Log-Normal (LN3) distributions for short duration rainfall PD analysis in South Africa. In a further study, Smithers and Schulze (2000) concluded that if a single PD was to be adopted for all regions in South Africa, the GEV would be the most appropriate PD to use. Therefore, the GEV distribution with L-moments was used to estimate design rainfall in this study. The AMS of all 16 time steps and the design rainfall estimations are attached as Annexure B. Following the PD analysis of the 16 stations, the Relative Difference (RD) in the design rainfall obtained from the DRESA was computed for the 1:5, 1:10 and 1:20 year return periods, respectively. The RD was determined using Equation 4.4, and the average for all stations (ARD_t) was determined using Equation 4.5. The result of this analysis is depicted in Figure 4.11. This indicates that the ARD_t of the 5-min to 1.5-hour time steps range between a minimum of negative 17% and a maximum of 12%. These differences could be attributed to: (a) the inaccuracies in the 5-min rainfall data used in this study, (b) the data period of the rainfall records used in this study and differences in record length, (c) the GOF of the GEV distribution for short duration design rainfall, and (d) the use of a regional approach in the DRESA study compared to the at-site approach used in this study. The exact cause of the errors is yet to be determined. However, the ARD_t of all standard time steps are still within the RD associated with the 90% upper and lower bounds given by the DRESA software as depicted in Figure 4.11, except for the 5-min 1:20 year. Therefore, the estimation of the DRESA design rainfall following this analysis was deemed to be acceptable.

$$RD = \frac{P_{PD} - P_{SS}}{P_{SS}} \cdot 100 \qquad \text{(Equation 4.4)}$$

where:

RD = Relative difference of time step t, and return period T (%),

P_{PD} = Design rainfall obtained from the PD analysis (mm), and

P_{SS} = Mean design rainfall obtained from DRESA (mm).

$$ARD\_t = \frac{1}{N_t \cdot N_S} \cdot \sum_{t=1}^{N_t} \sum_{T=1}^{N_S} RE_{t,T} \qquad \text{(Equation 4.5)}$$

where:

ARD_t = RD of time step t, and return period T (%),

N_S = number of stations (16), and

N_t = number of time steps (16).

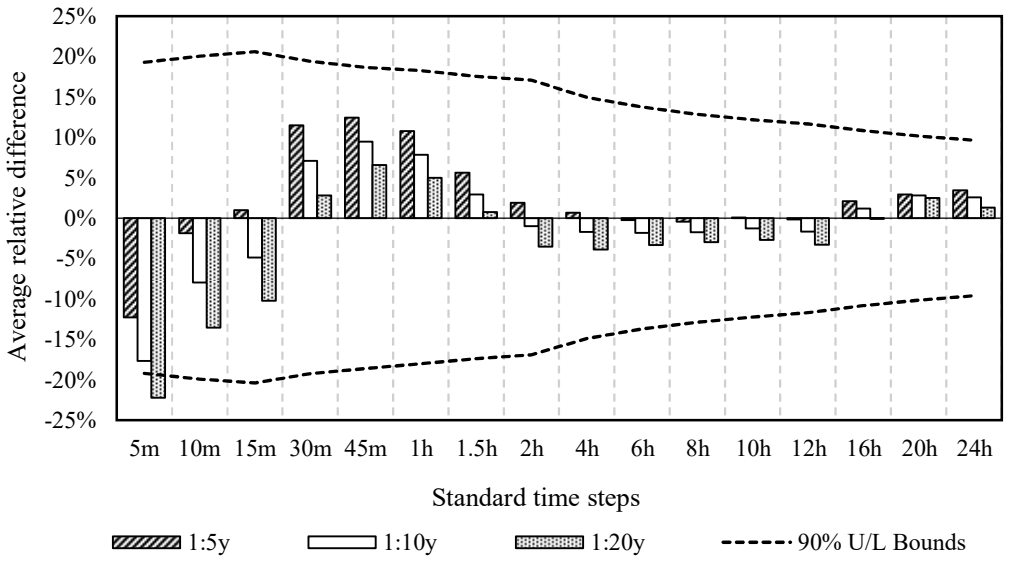

Figure 4.11: Average relative difference for each standard time step

The average RD per station (ARD_S) was determined using Equation 4.6 and the results are depicted in Figure 4.12. This indicates, for example, the 1:5 year at-site design rainfall for Alexandradepot are 47% higher than DRESA, and at Bolephi the 1:20 year is 28% lower. However, the cause of these differences needs to be further investigated.

$$ARD\_S = \frac{1}{N_t} \cdot \sum_{j=1}^{N_t} RD_{t,T} \qquad \text{(Equation 4.6)}$$

where:

ARD_S = Average relative difference of station S, and return period T (%), and

N_t = Number of time steps (16).

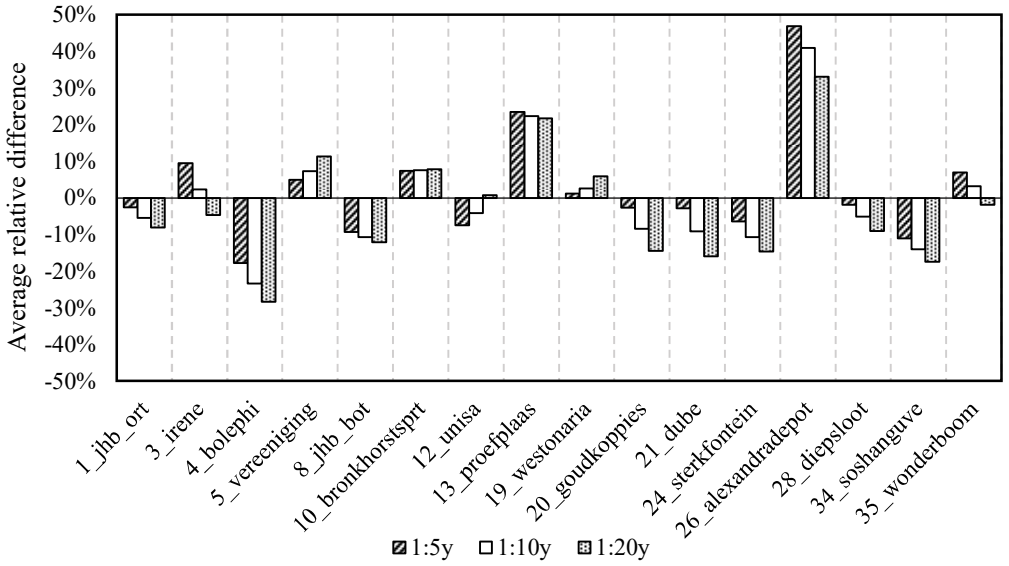

Figure 4.12: Average relative difference for each rainfall station

4.3 INTENSITY-DURATION-FREQUENCY REGRESSION COEFFICIENTS

A methodology of using a nonlinear algorithm to determine IDF regression coefficients as well as the Relative Error (RE) as a measure of their accuracy is presented in this section. IDF regression coefficients (a, b, and c) are needed to generate a synthetic design storm using the CDS method. These coefficients are associated with Equation 2.11. The DRESA and the at-site design rainfall depths were used to develop the regression coefficients. The design rainfall depths obtained from the DRESA were used to develop the regression coefficients. These were determined using an optimisation algorithm that adjusts the coefficients until the simulated intensities are approximately equal to the actual intensities. In this case, the actual intensities are the design rainfall obtained from the DRESA software, divided by their respective durations and the simulated intensities are the intensities that were simulated using Equation 2.11. The coefficients that yielded the best design intensities were found using the Generalised Reduced Gradient (GRG) nonlinear algorithm developed by Lasdon et al (1976). The GOF was determined using the Root Mean Square Error (RMSE) between the actual and simulated design intensities using Equation 4.7. The coefficients were adjusted until the RMSE was optimised by reaching a minimum. The built-in solver function of MS Excel, using the GRG nonlinear algorithm as the solving method and the calculated RMSE value as the objective value was used for this procedure. However, because the GRG algorithm finds a local optimum solution, the results are, therefore, dependent on the starting values of the coefficients. Recommended starting values for the a, b, and c coefficients are 1 000, 10, and 1, respectively. The regression coefficients for the DRESA design rainfall at 16 stations determined using this methodology are summarised in Table 4.1.

$$RMSE = \sqrt{\frac{\sum_{j=1}^{N_t}(IDF_A - IDF_S)^2}{N_t}} \qquad \text{(Equation 4.7)}$$

where:

$RMSE$ = Root Mean Square Error, and

N_t = Number of time steps (16).

Table 4.1: Regression coefficients determined from the DRESA design rainfall

ID	Name	a			b	c
		1:5	1:10	1:20		
1	Jhb OR Tambo	732	885	1047	4.269	0.726
3	Irene	745	901	1067	4.528	0.735
4	Bolepi House	988	1195	1414	5.621	0.756
5	Vereeniging	781	913	1040	5.086	0.752
8	Jhb Bot Gardens	723	874	1035	4.101	0.720
10	Bronkhorstspruit	991	1198	1418	5.693	0.757
12	Pretoria Unisa	992	1200	1420	5.710	0.757
13	Pretoria Proefplaas	979	1183	1400	5.757	0.760
19	Westonaria Kloof	738	862	982	4.339	0.729
20	Goudkoppies	741	895	1059	4.423	0.730
21	Dube	741	896	1060	4.430	0.731
24	Sterkfontein	715	850	988	3.926	0.715
26	Alexandra Depot	740	896	1060	4.437	0.731
28	Diepsloot	968	1170	1386	5.954	0.766
34	Shosanguve	988	1195	1414	5.686	0.757
35	Wonderboom	990	1196	1416	5.768	0.759

The RE of the simulated intensities, using the optimal regression coefficients presented in Table 4.1, was calculated per Equation 4.8 as follows:

$$RE = \frac{IDF_S - IDF_A}{IDF_A} \cdot 100 \qquad \text{(Equation 4.8)}$$

where:

RE = Relative error (%),

IDF_A = Actual design rainfall intensities (mm/hour), and

IDF_S = Simulated design rainfall intensities (mm/hour).

For example, the optimal coefficients from Table 4.1 for the 1:5-year design intensities for O.R. Tambo were 732, 4.269 and 0.726, respectively. Applying these coefficients, the simulated intensities were calculated for all standard time steps, and the RE concerning the actual intensities were determined. The same applies to the 1:10 and 1:20 year regression coefficients and the results are depicted in Figure 4.13.

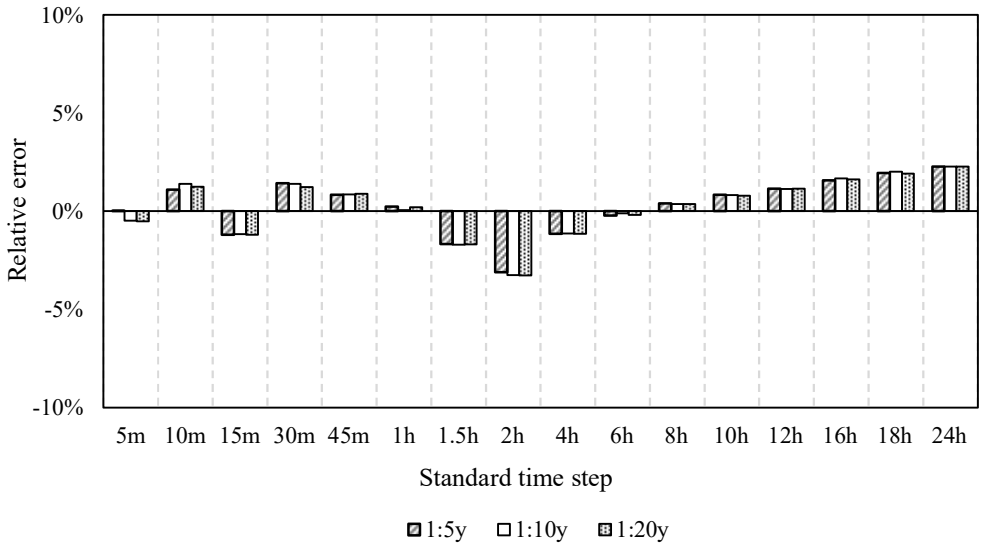

Figure 4.13: Relative error between actual and simulated design rainfall intensities for O.R. Tambo using the design rainfall from the DRESA software

The Average Relative Error (ARE_t) of each standard time step for the 1:5, 1:10 and 1:20 year return periods, respectively, of all stations, were determined following Equation 4.9 and the results are depicted in Figure 4.14. This indicates that the results are similar for all RIs, and the example results of O.R Tambo depicted in Figure 4.13.

$$ARE\_t = \frac{1}{N_S} \cdot \sum_{j=1}^{N_S} RE_{t,T} \qquad \text{(Equation 4.9)}$$

where:

ARE_t = Average relative error of time step t, and return period, T (%), and

N_S = Number of stations (16).

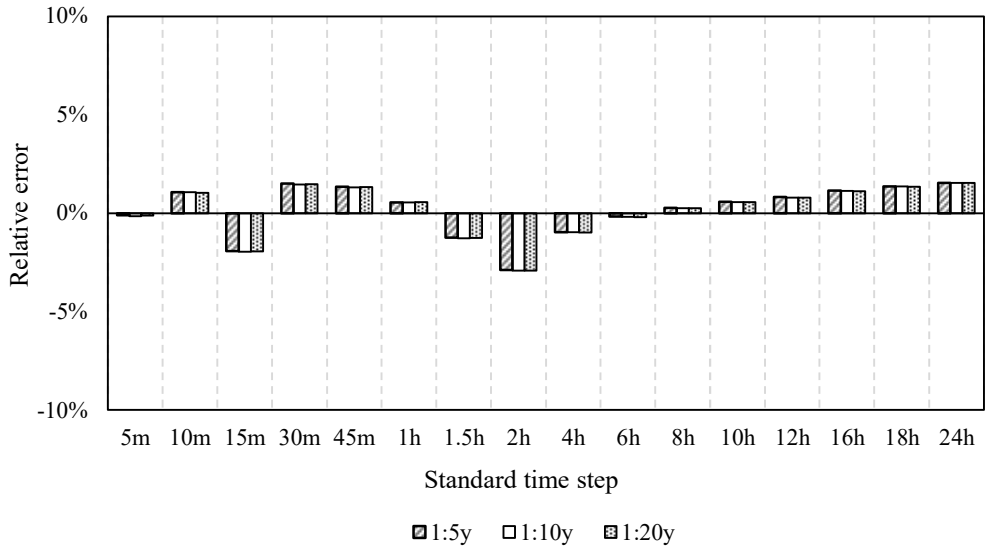

Figure 4.14: Average relative error for each standard time step (ARE_t)

The methodology of determining regression coefficients presented in this section has produced accurate simulated intensities. This was demonstrated by determining the GOF for all standard time steps with RIs of 1:5 to 1:20 year. It is, therefore, recommended that this methodology be incorporated into the DRESA software to provide the user with an opportunity to determine a synthetic design storm for a specific location.

4.4 RAINFALL DISTRIBUTION CURVES

The methodology of developing a rainfall Distribution Curve (DC) is described in this section which is divided into two parts. The first part describes the development of a 24-hour DC using the DDF curves described in Section 4.2. Each DC was subsequently used for the comparison between single event-based and continuous simulation modelling. The second part describes the methodology of developing a DC for a duration < 24-hour. This methodology was used for the comparison between observed and simulated storm events.

4.4.1 Development of a 24-hour distribution curve

The development of a 24-hour DC entails the embedment of the entire short duration DDF curve in a synthetic design storm. The peak intensity is located at the centre of the 24 hours and the design rainfall of shorter durations are divided equally on either side of the peak intensity. This process entails the interpolation of intermediate design rainfall for durations between the standard time steps (5, 10, 15, 30, 45-min, etc.). For example, the design rainfall for durations in 5-min intervals between 15 and 30-min is interpolated using a power regression function fitted through the incremental intensities of the standard time steps. This concept was adopted, and adapted, from the National Engineering Handbook (NRCS, 2019). The process is demonstrated in Table 4.2 and the procedural steps that were followed to complete Table 4.2 are summarised as follows:

a) Populate Column 1 and 2 with the standard time steps and design rainfall, respectively.
b) Calculated the rainfall ratios in Column 3 by dividing each rainfall value by the 24-hour rainfall value.
c) Calculate the non-dimensionalised incremental intensity in Column 4 by dividing the difference in ratio by the difference in duration. For example, the 0.5-hour non-dimensionalised incremental intensity is (0.386 - 0.445) / (0.50 – 0.25) = 0.351.
d) Calculate the logarithmic value of the duration and non-dimensionalised incremental intensity in Columns 5 and 6.
e) Determine the power regression coefficients in columns 7 and 8 for each duration and the next duration. For example, the coefficients 0.175 and -0.965 for duration = 0.083 hours, is applicable for all durations from 0.083 to 0.167 hours.

f) The LINEST function in MS Excel is suitable for this task, which uses the least square statistical procedure to calculate the regression coefficients that best fits the data.

The general power formula that applies to the regression coefficients summarised in Table 4.2, is shown in Equation 4.10.

$$I_{increment} = a \cdot (D_{intermediate})^b \qquad \text{(Equation 4.10)}$$

where:

$I_{increment}$ = Dimensionless incremental intensity,

a , b = Power regression coefficients, and

$D_{intermediate}$ = Intermediate storm duration. (hour).

Table 4.2: Example regression coefficients for incremental intensities

1	*2*	*3*	*4*	*5*	*6*	*7*	*8*
Duration (hour)	**Design Rainfall**	**Rainfall Ratio**	**Inc.Int.**	**log (hour)**	**log (Inc.Int.)**	**a**	**b**
0.083	12.1	0.161	1.928	-1.079	0.285	0.175	-0.965
0.167	18.3	0.243	0.988	-0.778	-0.005	0.177	-0.961
0.25	22.5	0.299	0.669	-0.602	-0.174	0.184	-0.933
0.5	29.1	0.386	0.351	-0.301	-0.455	0.175	-1.000
0.75	33.5	0.445	0.234	-0.125	-0.631	0.175	-1.000
1	36.8	0.489	0.175	0.000	-0.756	0.175	-0.890
1.5	41.4	0.550	0.122	0.176	-0.913	0.187	-1.051
2	44.8	0.595	0.090	0.301	-1.044	0.171	-0.918
4	52	0.691	0.048	0.602	-1.320	0.191	-1.000
6	56.8	0.754	0.032	0.778	-1.497	0.191	-1.000
8	60.4	0.802	0.024	0.903	-1.622	0.131	-0.817
10	63.4	0.842	0.020	1.000	-1.701	0.199	-1.000
12	65.9	0.875	0.017	1.079	-1.780	0.178	-0.954
16	69.7	0.926	0.013	1.204	-1.899	0.238	-1.059
20	72.7	0.965	0.010	1.301	-2.002	0.105	-0.785
24	75.3	1.000	0.009	1.380	-2.064		

Inc.Int. = Non-dimensionalised Incremental Intensity

Following the determination of the power regression coefficients, the design rainfall ratios are determined in 5-min intervals, for all durations from 5-min to 24-hour. The construction of the DC is initiated by positioning the peak ratio, namely the 5-min ratio, at the 12-hour mark. The difference between the 15-min and 5-min ratios is divided equally before and after the peak ratio so that the total is equal to the 15-min ratio. The difference between the 25-min and 15-min ratios is again divided equally on either side of the 15-min ratios so that the total is equal to the 25-min ratio, and so forth until the 24-hour ratio is distributed.

The distribution of the first 55 minutes of the D-hour to 24-hour design rainfall ratios is demonstrated in Figure 4.15. Finally, the DC is created by accumulating each 5-min ratio from the start to the end of the 24 hours. The distribution described in this section was subsequently applied to the construction of the 1:5 year DC (DC5), 1:10 year DC (DC10), and the 1:20 year DC (DC20) curves, as well as to constructing the SCS-SA curves in 5-min intervals.

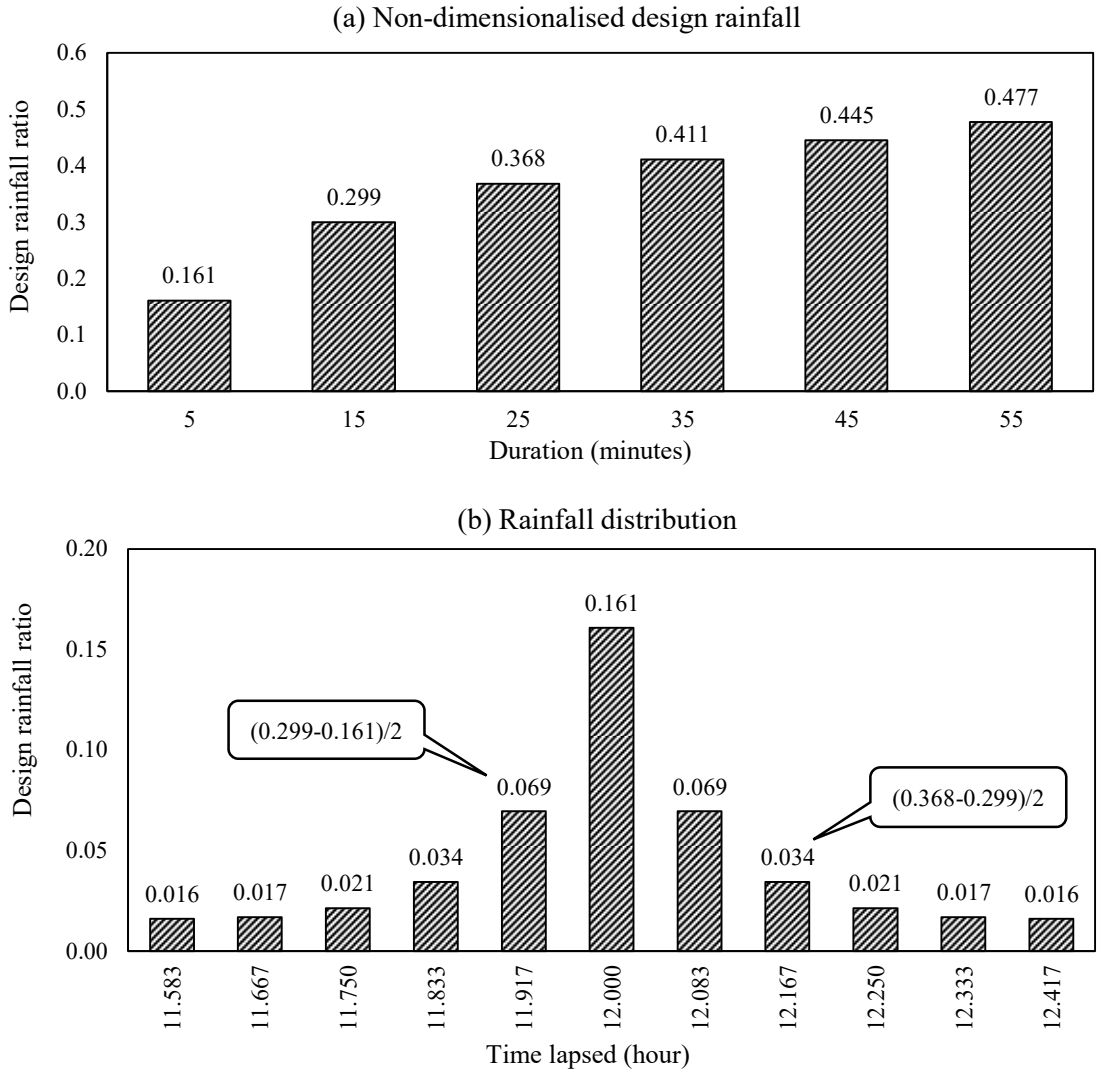

Figure 4.15: The general rainfall distribution process

4.4.2 Development of distribution curves for durations less than 24-hours

The procedure used to develop a DC for a synthetic design storm with durations < 24-hour was adopted from the National Engineering Handbook (NRCS, 2019). The extraction of a 6-hour rainfall distribution using the SCS-SA Type 2 curve is illustrated in Table 4.3 as an example.

Table 4.3: 6-hour DC extracted from a 24-hour DC (after NRCS, 2019)

Time lapsed (Hour)	SCS-SA Type 2	Unadjusted cumulative 6-hour rainfall ratio	6-hour distribution time (hour)	6-hour distribution cumulative rainfall ratio
0	0.0000			
0.5	0.0054			
1	0.0110			
1.5	0.0168			
2	0.0230			
2.5	0.0295			
3	0.0360			
3.5	0.0424			
4	0.0490			
4.5	0.0562			
5	0.0640			
5.5	0.0722			
6	0.0810			
6.5	0.0907			
7	0.1010			
7.5	0.1115			
8	0.1230			
8.5	0.1361			
9	0.1510	0.0000	0	0.0000
9.5	0.1679	0.0169	0.5	0.0242
10	0.1870	0.0360	1	0.0516
10.5	0.2100	0.0590	1.5	0.0845
11	0.2420	0.0910	2	0.1304
11.5	0.2920	0.1410	2.5	0.2020
12	0.5000	0.3490	3	0.5000
12.5	0.7080	0.5570	3.5	0.7980
13	0.7580	0.6070	4	0.8696
13.5	0.7900	0.6390	4.5	0.9155
14	0.8130	0.6620	5	0.9484
14.5	0.8321	0.6811	5.5	0.9758
15	0.8490	0.6980	6	1.0000
15.5	0.8639			
16	0.8770			
16.5	0.8884			
17	0.8990			
17.5	0.9094			
18	0.9190			
18.5	0.9272			
19	0.9350			
19.5	0.9432			
20	0.9510			
20.5	0.9577			
21	0.9640			
21.5	0.9705			
22	0.9770			
22.5	0.9832			
23	0.9890			
23.5	0.9946			
24	1.0000			

Although a DC at 5-min intervals is more appropriate, the example illustrated in Table 4.3 uses intervals at 30-min to shorten the example and still demonstrate the concept (NRCS, 2019). The procedural steps to complete Table 4.3 are summarised as follows:

a) Because the 24-hour distribution curve is centred around 12-hour, a 6-hour distribution curve will, therefore, start at 9-hour and end at 15-hour.
b) The new cumulative rainfall ratio at 9-hour become zero. The unadjusted ratio at 9.5-hour is equal to the difference between 9.5-hour and 9-hour, which is 0.0169.
c) The unadjusted ratio at 10-hour is equal to the sum of the unadjusted 9.5-hour ratio, and the difference between 10-hour and 9.5-hour, which is 0.0360.
d) The remainder of intervals, up to 15-hour is calculated in the same way, which has an unadjusted ratio of 0.6980.
e) Lastly, the adjusted ratios are calculated by dividing each unadjusted ratio by the unadjusted ratio of 15-hour of 0.6980, which results in the 6-hour DC. The extraction of a 6-hour event from the 24-hour SCS-SA Type 2 curve is depicted in Figure 4.16.

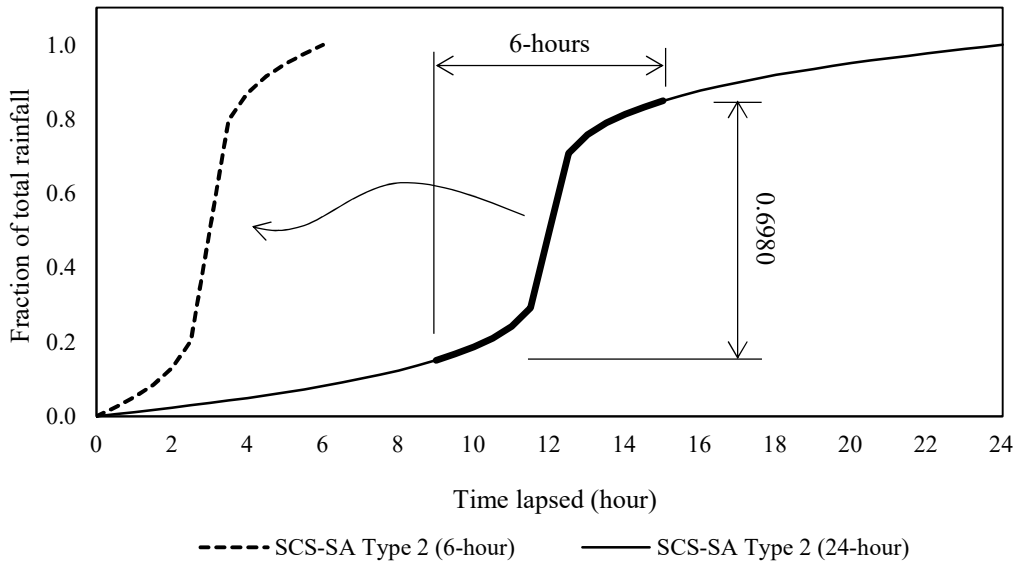

Figure 4.16: Typical adjusted six-hour distribution curve extracted from a 24-hour DC

4.5 SCS-SA CURVE COMPARISON

In this section, the D-hour to 24-hour ratios of the design rainfall at each station depicted in Figure 4.10 were calculated and compared with the ratios of the four SCS-SA curves. This was done to confirm the use of the Type 3 curve for the Gauteng province depicted in as recommended by Weddepohl (1988). The methodology that was used to achieve this was by comparing the D-hour to 24-hour ratios of the design rainfall with the SCS-SA curves.

Two sources of design rainfall were used for this analysis. The first being the design rainfall obtained from the DRESA software and the second is the at-site design rainfall, as describe in Section 4.2. The ratios for the SCS-SA curves were calculated using Equation and the coefficients listed in . These ratios are summarised in Table 4.4 and form the baseline ratios against which the two sources of design rainfall were compared.

Table 4.4: Sub-daily and sub-hourly ratios for the four SCS-SA curves

Duration	Type 1	Type 2	Type 3	Type 4
5m	0.084	0.135	0.174	0.209
10m	0.126	0.204	0.281	0.347
15m	0.155	0.249	0.355	0.444
30m	0.215	0.332	0.487	0.618
45m	0.256	0.384	0.561	0.710
1h	0.289	0.422	0.609	0.768
1.5h	0.341	0.478	0.672	0.835
2h	0.383	0.520	0.713	0.874
4h	0.502	0.629	0.802	0.938
6h	0.588	0.701	0.849	0.962
8h	0.657	0.755	0.881	0.974
10h	0.715	0.800	0.905	0.982
12h	0.767	0.838	0.925	0.987
16h	0.857	0.902	0.956	0.993
20h	0.933	0.955	0.980	0.997
24h	1.000	1.000	1.000	1.000

4.5.1 SCS-SA comparison with the DRESA software

The ratios for the design rainfall obtained from the DRESA software were calculated by dividing the rainfall for each duration by the 24-hour rainfall according to Equation 4.11:

$$RD_{t,T} = \frac{P_{t,T}}{P_{24,T}} \qquad \text{(Equation 4.11)}$$

where:

$RD_{t,T}$ = D-hour design rainfall ratio for duration t and recurrence interval T,

$P_{t,T}$ = Design rainfall for duration t and recurrence interval T (mm), and

$P_{24,T}$ = 24-hour Design rainfall for recurrence interval T (mm).

The position of the design rainfall ratios relative to the ratios of the four curves were linearly interpolated and were subsequently named Intermediate Curve (IC) values. Following the calculation of the D-hour design rainfall ratios, the IC value for each duration and RI was determined according to Equation 4.12.

$$IC_{t,T} = \frac{RD_{t,T} - RC_{i,t}}{RC_{i+1,t} - RC_{i,t}} + C_i \qquad \text{(Equation 4.12)}$$

where:

$IC_{t,T}$ = Intermediate curve type for duration t and recurrence interval *T*,

C_i = SCS-SA curve type *i* (1, 2, 3 or 4),

$RC_{i,t}$ = SCS-SA ratio for curve type i and duration *t*,

$RC_{i+1,t}$ = SCS-SA ratio for curve type *i+1* and duration *t*, and

$RD_{t,T}$ = D-hour design rainfall ratio for duration *t* and recurrence interval *T*.

The result of this analysis is summarised in Figure 4.17 and Figure 4.18. The values (1 to 4) on the vertical axis represents the four standard type curves. The D-hour to 24-hour ratio of each standard time step was linearly interpolated between the standard curve types using Equation 4.12 and was depicted as the IC value. For example, the 5-min ratio of Type 2 according to Table 4.4 is 0.135, but the number of the curve, which in this case is 2, is displayed on the figure, rather than the ratio. The same applies to all ratios of all standard time steps and standard type curves. If, for example, the IC value for the 1:5-year, 5-min DRESA design rainfall was 2.5, then the graph is depicted halfway between the value 2 and 3 on the vertical axis. The same applies to all standard time steps which then forms a continuous curve from 5-min to 20-hour. The IC value for the 24-hour time step is not depicted because it is always unity, and therefore, it is not applicable. The zero value on the vertical axis does not represent any standard curve type but rather a ratio value of zero. Minor volatility in the IC values was observed across all stations but there was no difference between RIs. For example, at O.R Tambo the IC value for the 5-min time step was 2.12 for the 1:5 to 1:20-year RIs. From 10-min to 1.5-hour the IC values were between 1.88 and 1.99 (approximately equal to Type 2). At 2-hour the IC value was 2.02 but from 4-hour to 20-hour it was between 1.94 and 1.98. The highest IC value was observed at Vereeniging which was 2.38 for the 5-min time step but the lowest for Vereeniging was 2.07. The lowest value overall was observed at Sterkfontein which was 1.78 for the 45-min time step. These minor volatility across all stations could be attributed to the smoothing of design rainfall applied following the regional approach. The smoothing of design rainfall estimation did not form part of this investigation. The methods of smoothing and the effect thereof is, however, recommended for future research.

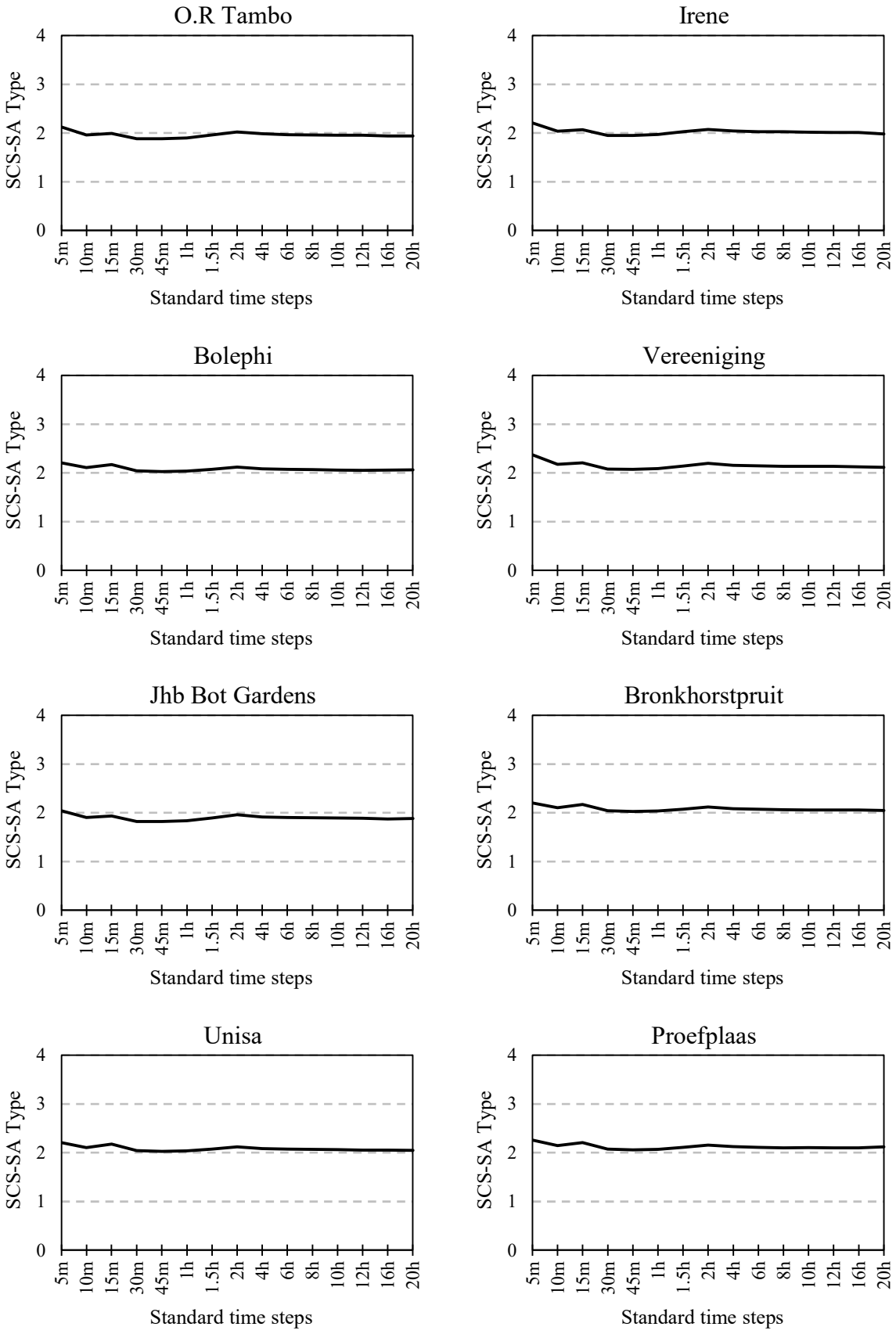

Figure 4.17: Comparison for SCS-SA curves and DRESA software design rainfall (1 of 2)

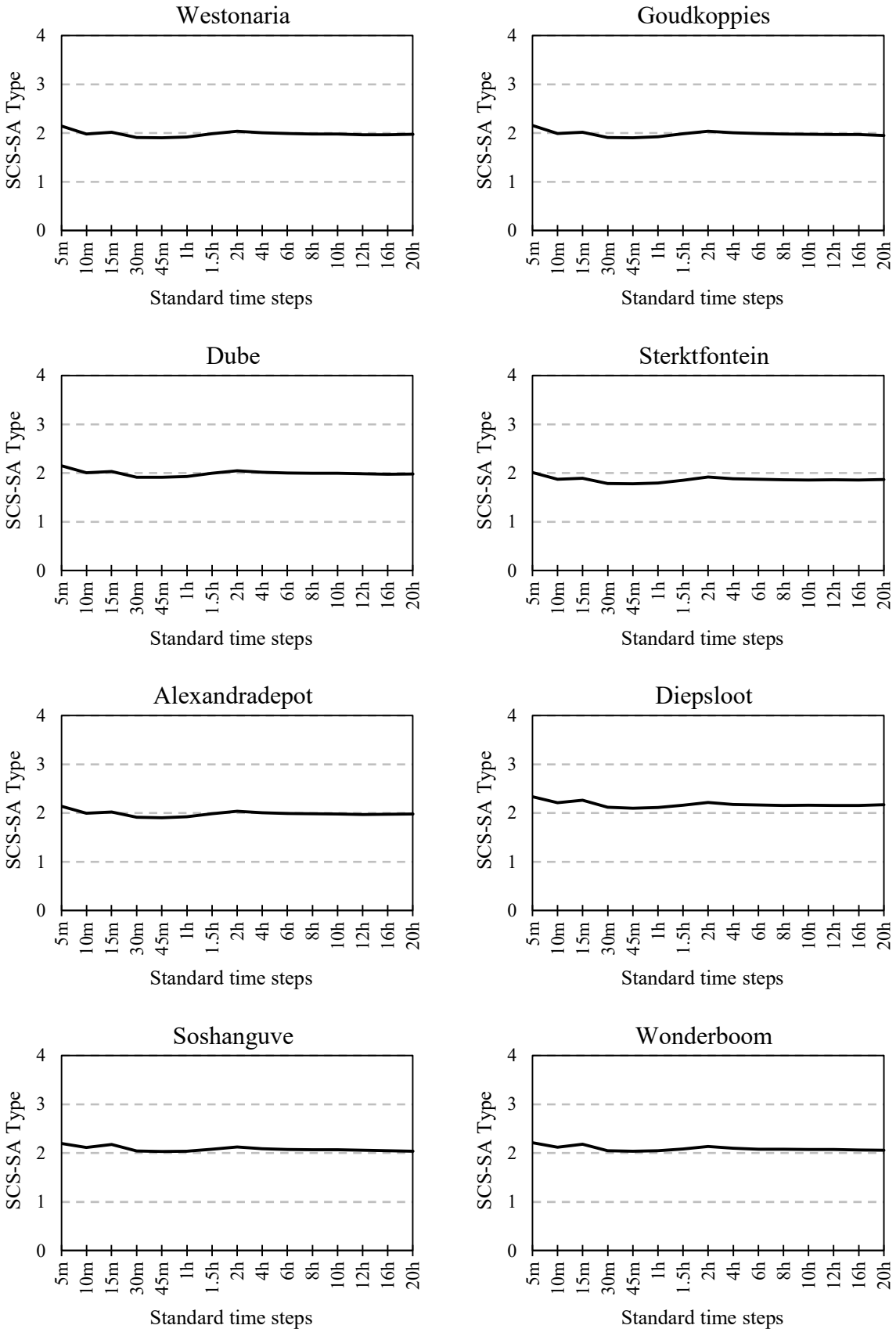

Figure 4.18: Comparison for SCS-SA curves and DRESA software design rainfall (2 of 2)

The average IC value for each standard time step (AIC_t) was determined using Equation 4.13 and the results are depicted in Figure 4.19. This indicates that the IC values range between 1.96 and 2.18 with an average (AIC_G) of 2.03 using Equation 4.14. The AIC_G value, therefore, represents the average of all standard time steps of the 16 stations in Gauteng. This concludes that the average IC value applicable to the Gauteng province, using the design rainfall from the DRESA software, was approximately equal to the Type 2 curve.

$$AIC\_t = \frac{1}{N_S} \cdot \frac{1}{N_T} \cdot \sum_{j=1}^{N_S} \sum_{i=1}^{N_T} IC_{T,S} \qquad \text{(Equation 4.13)}$$

where:

AIC_t = Average IC value for duration *t*,

IC_T = IC value for recurrence interval *T* and station *S*,

N_S = Number of stations (16), and

N_T = Number of recurrence intervals (3).

$$AIC\_G = \frac{1}{N_t} \cdot \sum_{k=1}^{N_t} AIC\_t \qquad \text{(Equation 4.14)}$$

where:

AIC_G = Average IC value for Gauteng,

ICT_T = IC value for recurrence interval *T* and station *S*, and

N_t = Number of standard time steps (16).

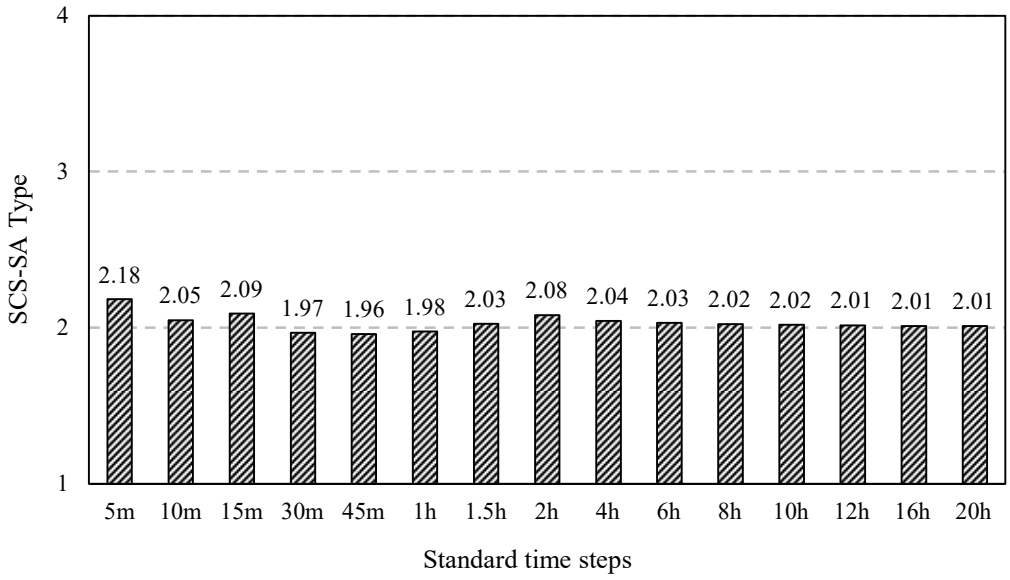

Figure 4.19: Average IC values for 16 stations according to the DRESA design rainfall

4.5.2 SCS-SA comparison with the at-site design rainfall

The same comparison was done using the at-site design rainfall described in Section 4.2. The AIC_t was determined using Equation 4.13 and the results are depicted in Figure 4.20 to Figure 4.22. The volatility in the IC values with regards to the standard time steps, summarised in Figure 4.20 to Figure 4.22, was much more noticeable compared to the results using the DRESA design rainfall. For example, the IC value at O.R Tambo for the 1:5 to 1:20 year, 5-min time step was similar at 1.95 (meaning it is approximately equal to Type 2) but increased to between 2.40 and 2.93 (between Type 2 and Type 3) at the 1-hour time step. Between the 1-hour and the 8-hour time steps the IC values decreased to between 1.52 and 2.07. Between the 8-hour and 20-hour it increased to a maximum of 2.60 and 3.68 (between Type 2 and Type 4). The variation in IC values differed at all stations, but the same volatility was observed. A general tendency at all stations was observed whereby the IC values for the 5-min to approximately 15-min time step was between Type 1 and 2. The IC values increased for longer time steps and generally exceeded Type 2 from the 45-min time step, for example, O.R Tambo, Irene, Bolephi, Vereeniging, Jhb Bot Gardens, Bronkhorstspruit, Unisa, Westonaria, Dube, Diepsloot, and Soshanguwe. From approximately 6-hour the IC values again decreased to below Type 2.

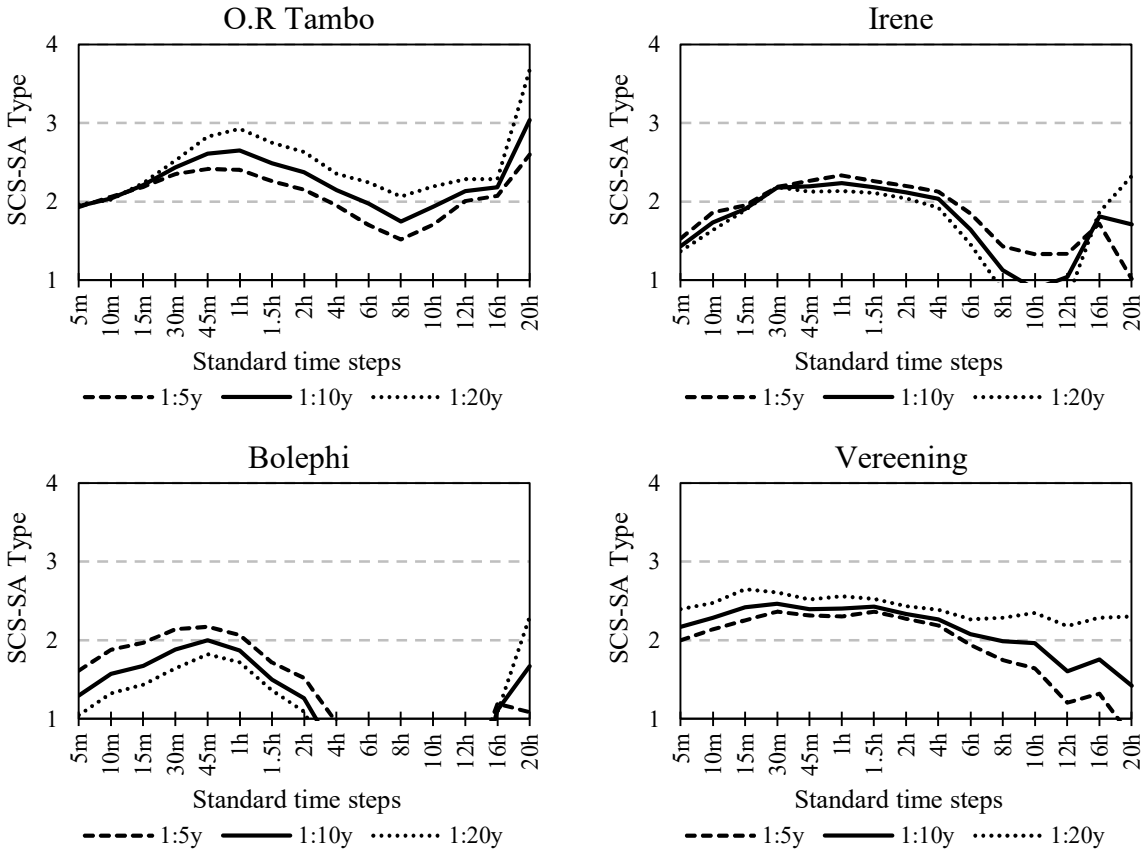

Figure 4.20: Comparison for SCS-SA curves and at-site design rainfall (1 of 3)

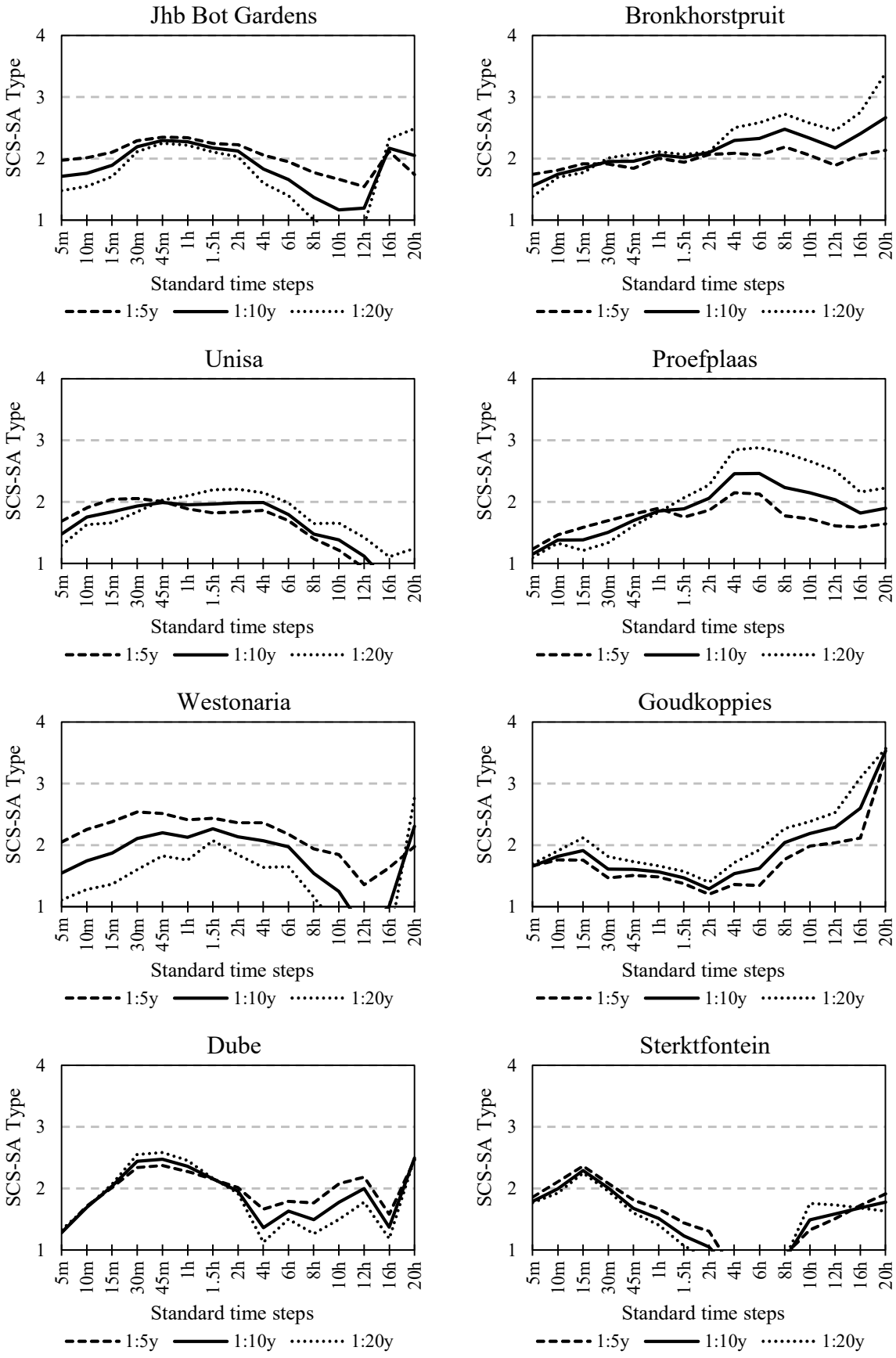

Figure 4.21: Comparison for SCS-SA curves and at-site design rainfall (2 of 3)

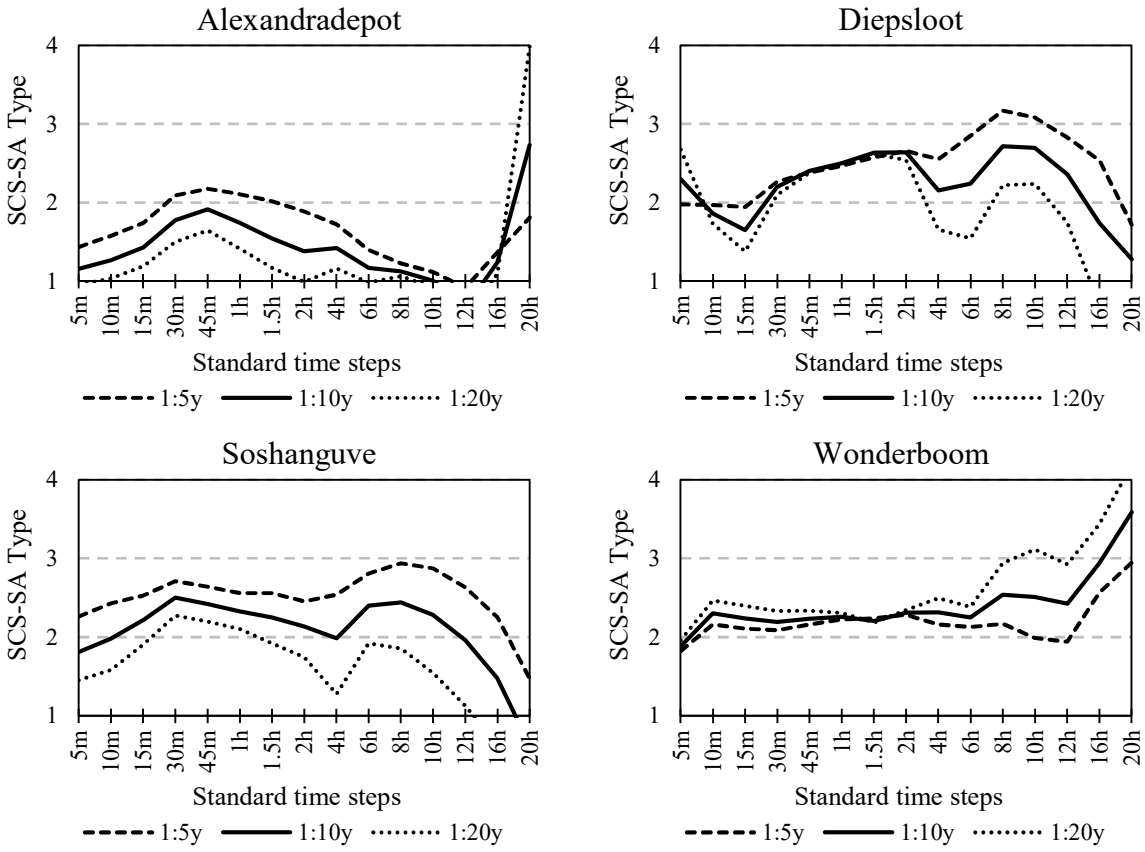

Figure 4.22: Comparison for SCS-SA curves and at-site design rainfall (3 of 3)

The AIC_t results for the at-site design rainfall are depicted in Figure 4.23. The majority of standard time steps had IC values less than Type 2 whereas the 30-min to 1.5-hour exceeded Type 2. However, the AIC_G value (average IC value for Gauteng) was 1.87 using Equation 4.14. This indicated that, on average, the curve type applicable to the Gauteng province, using the at-site design rainfall, was between Type 1 and 2. A single standard type SCS-SA curve could, therefore, not be assigned to the stations. A recommended solution is presented in the following section.

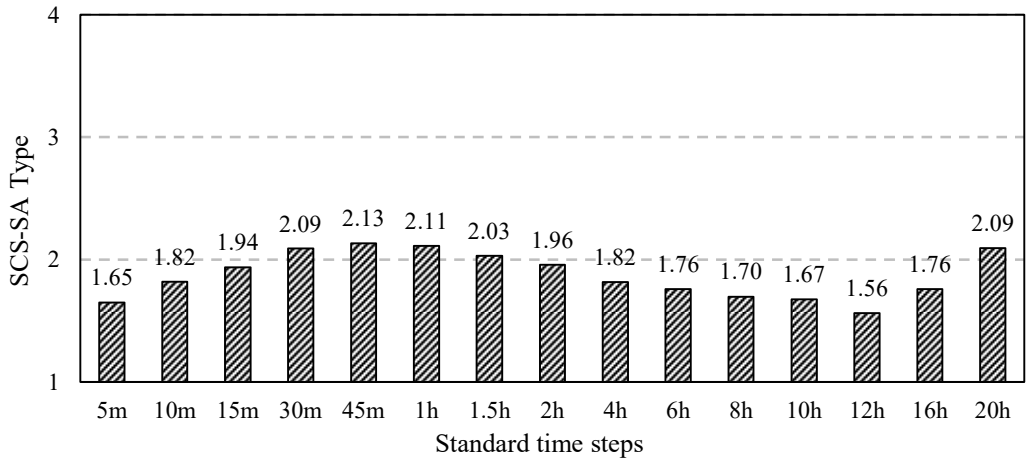

Figure 4.23: Average IC values for at-site design rainfall at 16 stations

4.5.3 Intermediate SCS-SA curves for Gauteng

The variation in IC value with duration and between sites in Gauteng is significant as it can lead to an underestimation or overestimation of the peak discharge. For example, if a stormwater network near O.R Tambo, with a reaction time of approximately 30-min, is simulated in a dynamic rainfall-runoff simulation model, using the SCS-SA Type 2 curve to generate a 1:20 year synthetic design storm, the peak discharge will be underestimated. This is because the IC value for the 30-min time step at O.R Tambo is 2.64, as depicted in Figure 4.20. Therefore, the Type 3 curve would be more appropriate from the four SCS-SA distributions. However, a linearly interpolated curve between the Type 2 and 3 curve that represents the intermediate curve of 2.64 is proposed. This means that an intermediate curve could be determined by following the rainfall distribution process described in Section 4.4. However, the curve is rather interpolated linearly between the cumulative rainfall ratios of the four standard curve types, using Equation 4.15 below. An example curve with IC value of 2.64 is depicted in Figure 4.24.

$$ICT_t = (IC - C_i) \cdot \left(RC_{i+1,t} - RC_{i,t}\right) + RC_{i,t} \qquad \text{(Equation 4.15)}$$

where:

ICT_t = Intermediate cumulative rainfall ratio for time step t,

C_i = SCS-SA curve type i (1, 2, 3 or 4),

C_{i+1} = SCS-SA curve type plus 1 (1, 2, 3 or 4), and

$RC_{i,t}$ = Cumulative rainfall ratio of SCS-SA curve i and time step t.

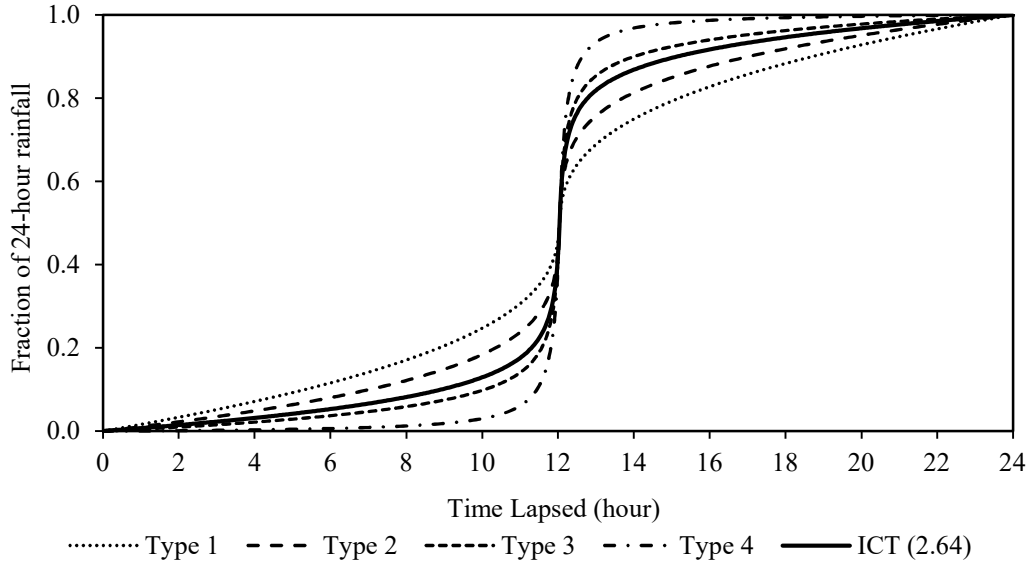

Figure 4.24: Example of an intermediate SCS-SA curve

To simplify the variation of the at-site IC values across Gauteng, the maximum of the 5-min to 30-min durations and for 1:5 to 1:20 year RIs at each site were determined, as depicted in Figure 4.25. For example, the IC value of 2.64 for O.R. Tambo would be applicable for all durations from 5-min to 30-min and RIs from 1:5 to 1:20 year. Although the use of the maximum value will result in an overestimation for certain durations and return periods, e.g. for the 1:20 year, 5-min IC value of 1.96, the use of the maximum value will result in a conservative (i.e. most intense) rainfall distribution. However, interpolating the 2.64 intermediate curve is an improvement from using the previously recommended Type 3 curve for Gauteng.

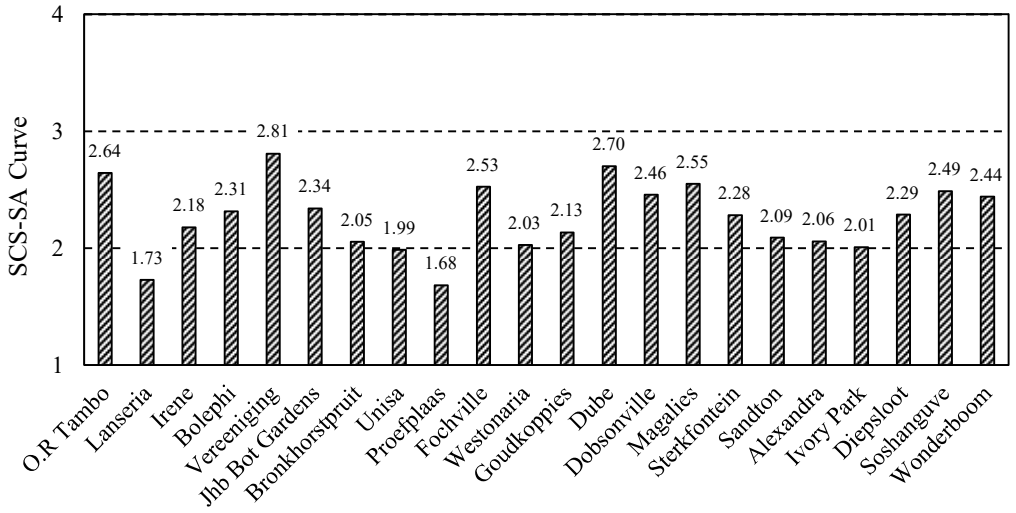

Figure 4.25: Maximum IC value for the 5-min to 30-min duration range

To envisage the variation of IC values, the maximum values from Figure 4.25 were geographically interpolated with the Inverse Distance Weighting (IDW) method by Shepard (1968) as per Equation 4.16.

$$IC_u = \frac{\sum_{i=1}^{n} \left(\frac{IC_i}{d_i}\right)^P}{\sum_{i=1}^{n} \left(\frac{1}{d_i}\right)^P} \qquad \text{(Equation 4.16)}$$

where:

IC_u = Predicted IC value at ungauged location *u*,

IC_i = IC value at station *i*,

d_i = Euclidean distance between ungauged location *u* and station *i*,

n = Number of stations (16),

P = IDW exponent,

The IDW exponent has a significant effect on the resulting surface. According to Shepard (1968) an exponent value higher than 2 resulted in even interpolated surfaces with abrupt changes near known points. A value lower than 2 resulted in flat surfaces with the known points appearing as blips (Shepard, 1968). Moeletsi et al. (2016) evaluated the IDW method for patching daily rainfall over the Free State Province, South Africa, and found the optimal exponents as both 2.0 and 2.5. This was achieved by assessing exponents at 0.5 intervals, starting from 1 to 5, using and average ranking system to find the optimal exponent. The accuracy of the predicted rainfall at targeted stations were compared to their measured rainfall. The average ranking was lowest for both 2.0 and 2.5. Therefore, and although the application of the IDW in this study is somewhat different, an exponent of 2.5 was used. The IC values across Gauteng were interpolated as depicted in Figure 4.26.

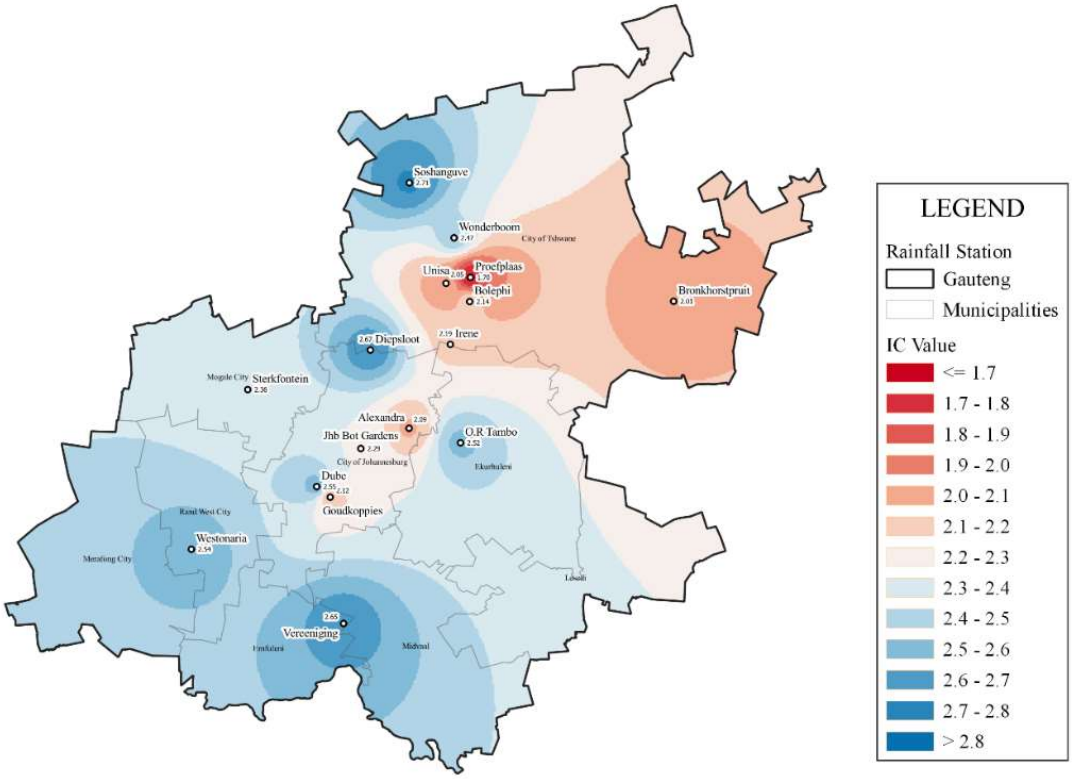

Figure 4.26: Maximum interpolated IC values for the 5-min to 30-min duration range using the IDW interpolation method

The IC value for any location within the boundary of the Gauteng Province can be estimated with Figure 4.26 which will result in a more accurate synthetic design storm. However, the appropriate exponent for this application needs to be determined in a future study. Smaller duration ranges for different RIs could also be considered, but further refinements of the IC values must be preceded by an investigation into the increase in RD between DRESA and at-site design rainfall.

Possible homogeneous regions and regional growth curves for the lower order standard time steps (< 2-hour) should be investigated as possible causes of the increase in RD. The impact of the discrepancies in the 5-min data and the effect of missing data on a PD analysis should also be investigation as it could impact the IC values. These causes, as well as the appropriateness of the IDW and its exponent, could contribute, for example, to the dramatic increase in IC values at Diepsloot and Soshanguve.

4.6 SCS CURVE COMPARISON

The use of the SCS curves is still preferred by some engineers (Brooker, 2021). Hence, the performance of the SCS curves were also investigated. The results of an analysis, similar to the analysis described in Section 4.5, are presented in this section. The development of the SCS curves is not the same as the SCS-SA curves. The approach used in the development of the SCS-SA curves follows the rainfall distribution procedure described in Section 4.4, whereas the SCS curves were based on the peak 30-min design rainfall for specific regions in the USA, as described in Section 1.1. The SCS curves for 6-min intervals were downloaded from the NRCS website (NRCS, 2020) and the maximum ratios were extracted from the data by using a moving window period. For standard time steps which are not multiples of six minutes, the ratios were determined using the incremental intensity concept as described in Section 4.4. The final ratios for the standard time steps of the four SCS curves are summarised in Table 4.5. The last column of Table 4.5 contains made-up ratios of an imaginary curve, II(x2), which are the ratios of the Type II curve multiplied by a factor of 2. The II(x2) ratios were utilized in Section 4.6.1 because several at-site design rainfall ratios exceeded the maximum SCS ratios.

Table 4.5: D-hour to 24-hour ratios for the four SCS curves

Duration	Type I	Type IA	Type II	Type III		II(x2)
5m	0.061	0.020	0.116	0.070		0.232
10m	0.113	0.040	0.204	0.140		0.408
15m	0.150	0.060	0.278	0.197		0.555
30m	0.213	0.115	0.380	0.287		0.760
45m	0.252	0.147	0.423	0.359		0.847
1h	0.281	0.171	0.454	0.404		0.908
1.5h	0.330	0.215	0.501	0.458		1.000 #
2h	0.370	0.252	0.538	0.500		1.000 #
4h	0.492	0.371	0.639	0.622		1.000 #
6h	0.578	0.468	0.707	0.709		1.000 #
8h	0.647	0.548	0.760	0.772		1.000 #
10h	0.707	0.621	0.803	0.819		1.000 #
12h	0.761	0.687	0.841	0.856		1.000 #
16h	0.857	0.811	0.904	0.914		1.000 #
20h	0.935	0.917	0.955	0.961		1.000 #
24h	1.000	1.000	1.000	1.000		1.000 #

Ratio of >1 is not possible. Therefore, the ratio is set to a maximum of 1.000

The ratios summarised in Table 4.5 are depicted in Figure 4.27. It is observed that the ratios for Type IA, I and II are evenly spaced, whereas the ratios of the Type III curve appear different from the ratios of the other curves. The ratios for all standard time steps are increasing from Type IA as the minimum to Type II as the maximum. However, the Type III curve ratios start near Type I, increasing steadily and exceeding Type II at the 6-hour time step.

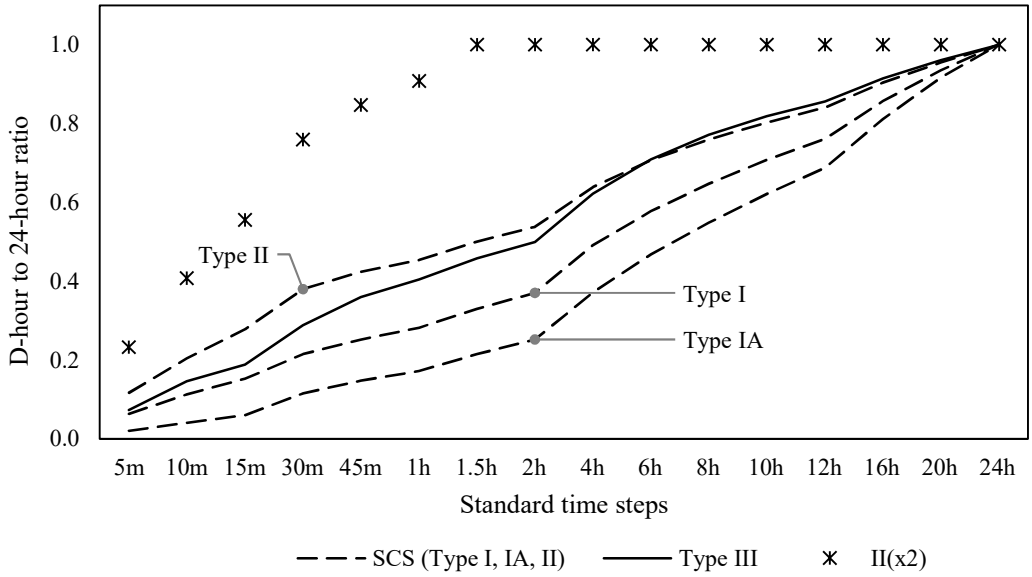

Figure 4.27: D-hour to 24-hour ratios of SCS curves

The comparison of the SCS curve ratios for the standard time steps is described in the following two sections. The first section is the comparison with the ratios of the at-site design rainfall. The second section describes the comparison with the SCS-SA curve ratios.

4.6.1 SCS comparison with at-site design rainfall

In this analysis the ratios of the SCS curves were compared with the ratios of the at-site design rainfall described in Section 4.2. Only the SCS Types I, IA and II ratios were considered because, as depicted in Figure 4.27, Type III ratios appear to be a hybrid of Types I and II ratios. This means the Types I, IA, and II ratios increase proportionally and appear nearly parallel. However, the Type III agree closest to Type I at the 5-min time step but deviates rapidly with higher time steps. Conversely, from the 6-hour time step and onwards the Type III agree closest to Type II. Therefore, the positions of the at-site ratios were interpolated linearly, relative to the ratios of Types I, IA and II ratios, as depicted in Figure 4.28 and Figure 4.29. The Type II ratios are the highest of all SCS types. Therefore, the imaginary curve was used as an upper limit for the ratios in case the at-site ratios exceeded Type II. The results depicted in Figure 4.28 and Figure 4.29 indicate that the majority of stations agree closest to Type II with several stations marginally below Type II.

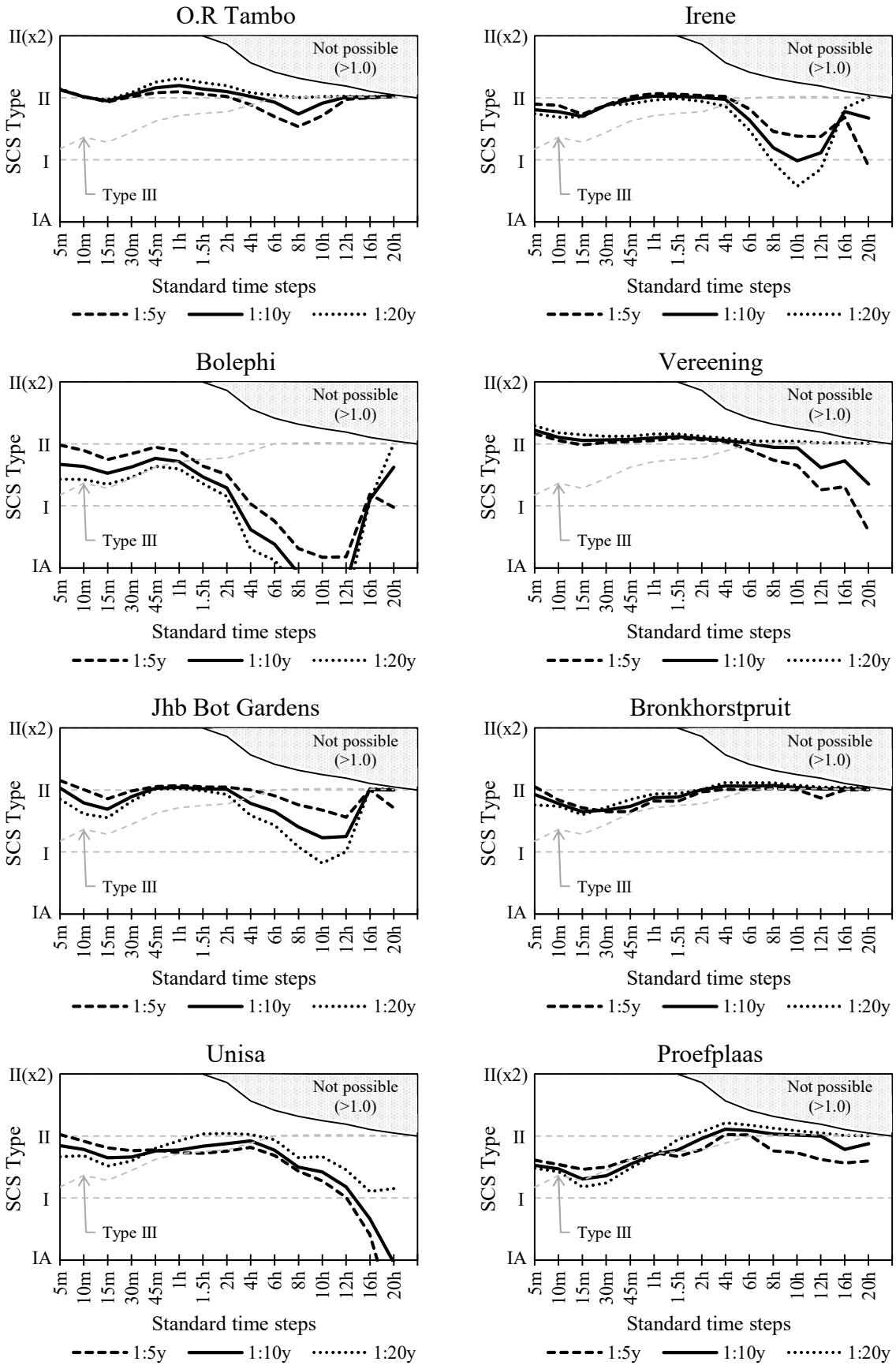

Figure 4.28: Comparison for SCS curves and at-site design rainfall (1 of 2)

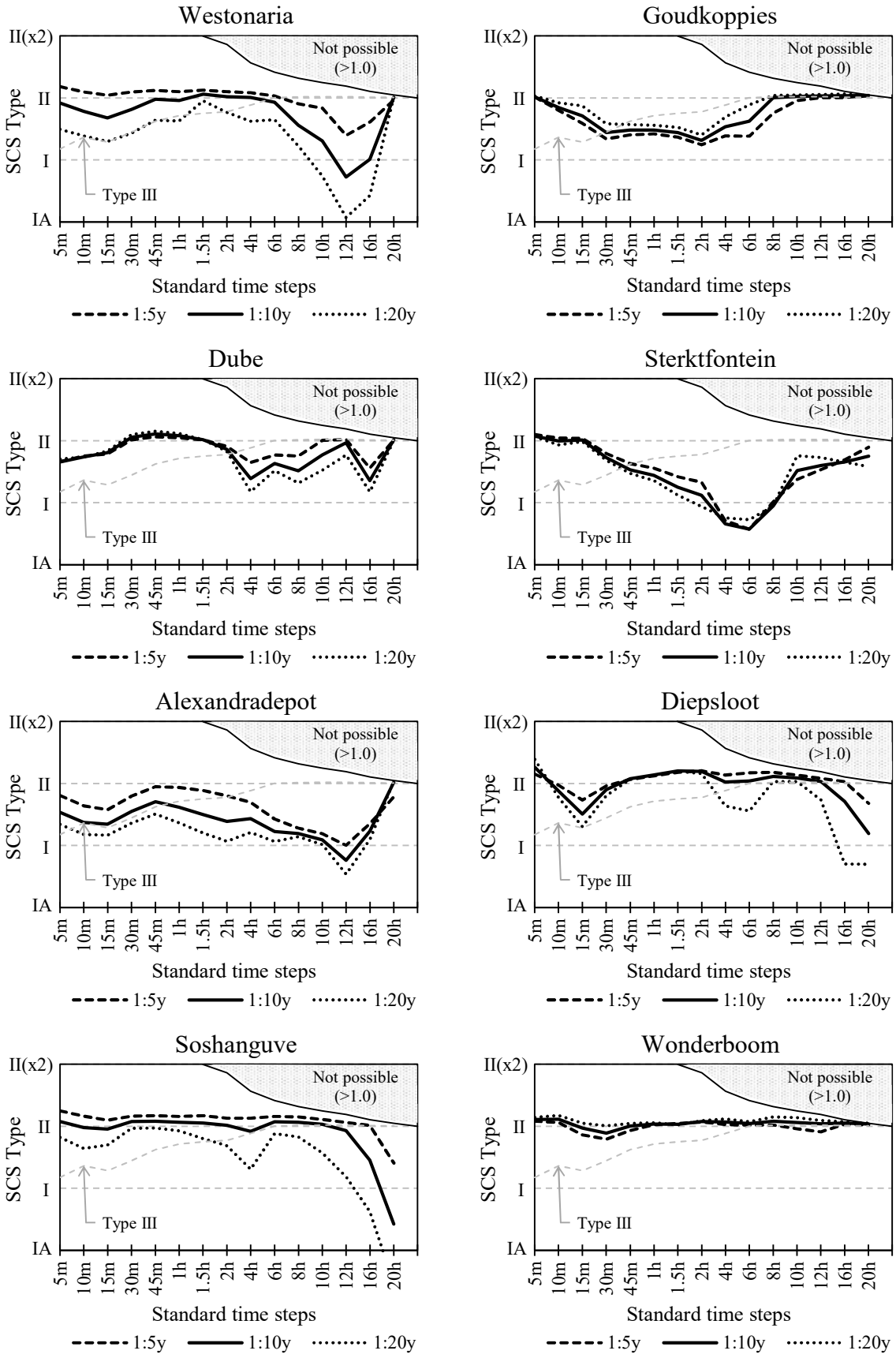

Figure 4.29: Comparison for SCS curves and at-site design rainfall (2 of 2)

In order to determine the relationship between the Type II curve and the at-site design rainfall, the ratio between the ratio of each standard time step was determined per Equation 4.17.

$$RA(TII)_{t,T} = \frac{R_{PD}}{R_{TII}} \qquad \text{(Equation 4.17)}$$

where:

$RA(TII)_{t,T}$ = Ratio of at-site design rainfall ratio and SCS Type II ratio for time step t, and return period T,

R_{PD} = At-site D-hour to 24-hour design rainfall ratio, and

R_{TII} = SCS Type II D-hour to 24-hour ratio.

The maximum for the 5 to 30-min range (associated with small catchments with rapid response times) was identified for each station which is depicted in Figure 4.30. This indicates that only Bolephi and Unisa's ratios are approximately equal to the Type II curve ratios. The ratios for the Irene, Proefplaas and Alexandradepot stations are marginally less than the Type II ratios. At several stations, like Bronkhorstspruit, Dube and Sterkfontein, the at-site design rainfall ratios are marginally higher, approximately 10%. At the remaining stations the values are much larger. It can, therefore, be concluded from this analysis that the SCS curves must be used with caution.

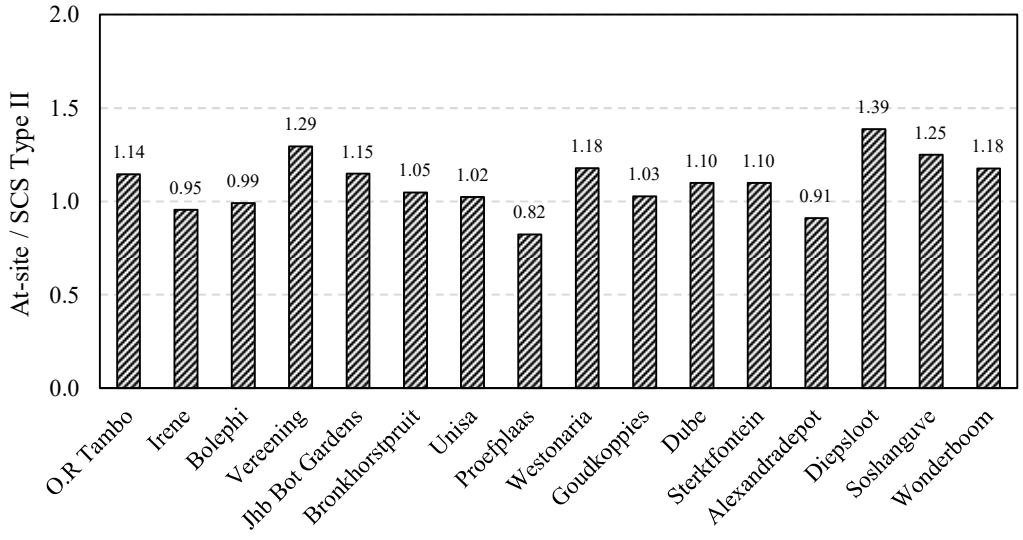

Figure 4.30: Maximum at-site / SCS Type II ratio for the 5-min to 30-min duration range

4.6.2 SCS comparison with SCS-SA

In this section the SCS curve ratios were compared with the ratios of the SCS-SA curve ratios. The ratios of the SCS and SCS-SA curves were combined as depicted in Figure 4.31. This indicates that the SCS Type II is approximately equal to the SCS-SA Type 2.

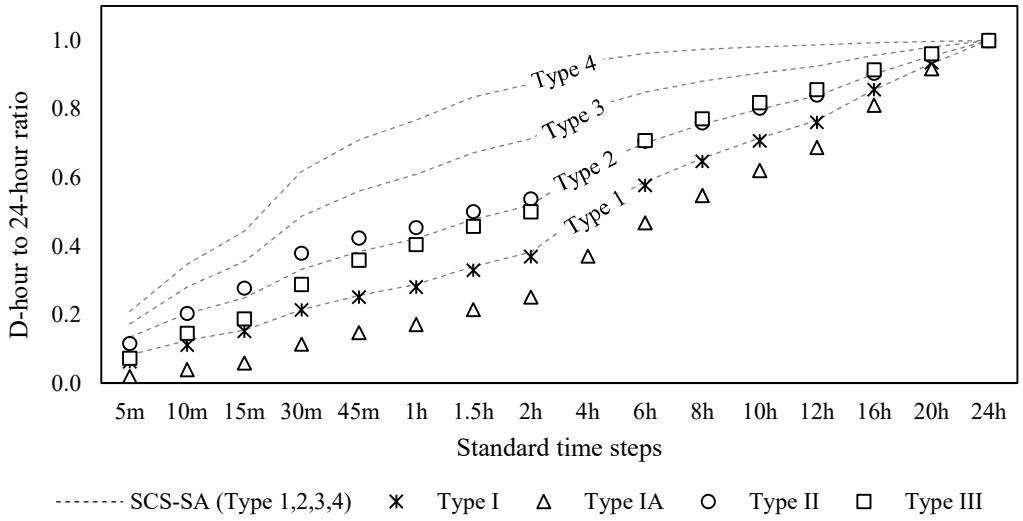

Figure 4.31: D-hour to 24-hour ratios of SCS curves compared to SCS-SA curves

However, by interpolating, linearly, the positions of the ratios of the four SCS curves, relative to the ratios of the SCS-SA curves, it was observed that the 30-min IC value was 2.31 as depicted in Figure 4.32. This was the maximum ratio that could be achieved with the SCS curves which decreases towards the 5-min as well as towards the 20-hour ratio. The IC values for the Type III curve were all less than 2.00 for all durations less than 6-hours. The Type I curve was less than SCS-SA Type 1 for all durations less than 16-hour whereas Type IA never exceeded SCS-SA Type 1.Therefore, based on the comparison with the SCS-SA curves, the SCS Type III as well as the Type 1 and Type 1A, are not recommended in Gauteng. Therefore, the use of the Type II curve is limited and it must be used with caution.

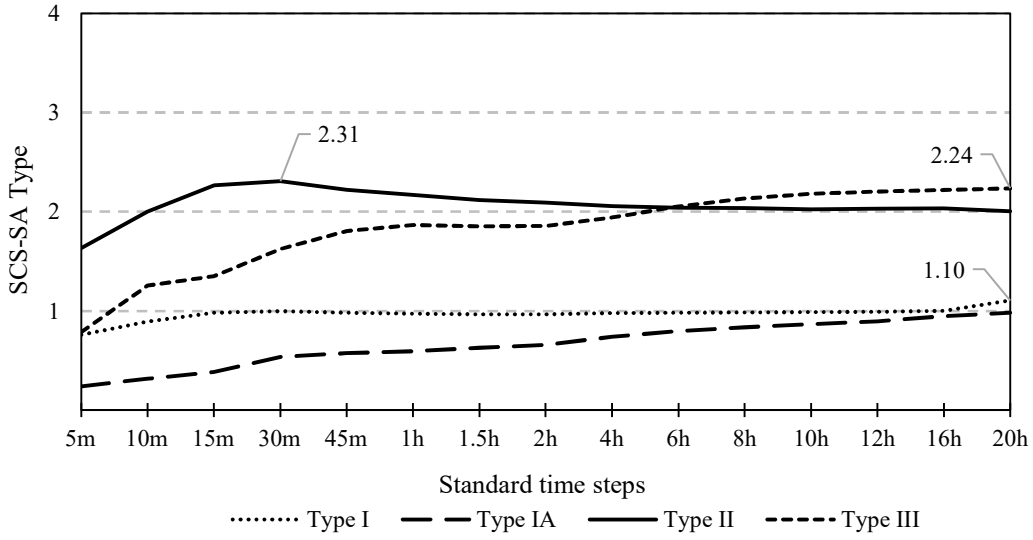

Figure 4.32: IC values associated with the SCS curves

4.7 STANDARDISED MASS CURVES

The ability of standardised mass curves, more commonly known as Huff curves, to generate short duration design rainfall were evaluated in this section. These curves were developed by non-dimensionalising all significant storm events concerning the total duration and total rainfall depth. The 10, 50 and 90 percentiles were determined at 0.05 dimensionless time intervals along the horizontal axis. Curves were developed for the 316 significant storm events identified at the five best stations in Gauteng described in Section 3.6. Guidance is lacking in terms of the minimum sample size that is required for the development of stable curves. Bonta (2004) has, however, shown that a sample size of 10 storm events agree poorly compared to a base set of 182 storm events, and has emphasised the need for guidelines for estimating the minimum sample size. A threshold of 11 storm events was considered for this study because stations were analysed separately and only significant events were used. The classification of events is depicted in Figure 4.33. Most events are classified as 2nd quartile events and exceed the threshold, whereas the 4th quartile had the least number of events with all stations having less events than the threshold. Some 1st and 3rd quartile stations also have 10 or fewer events, for example, Vereeniging has seven 1st quartile events whereas O.R Tambo and Irene have nine and ten 3rd quartile events, respectively, which does not meet the threshold.

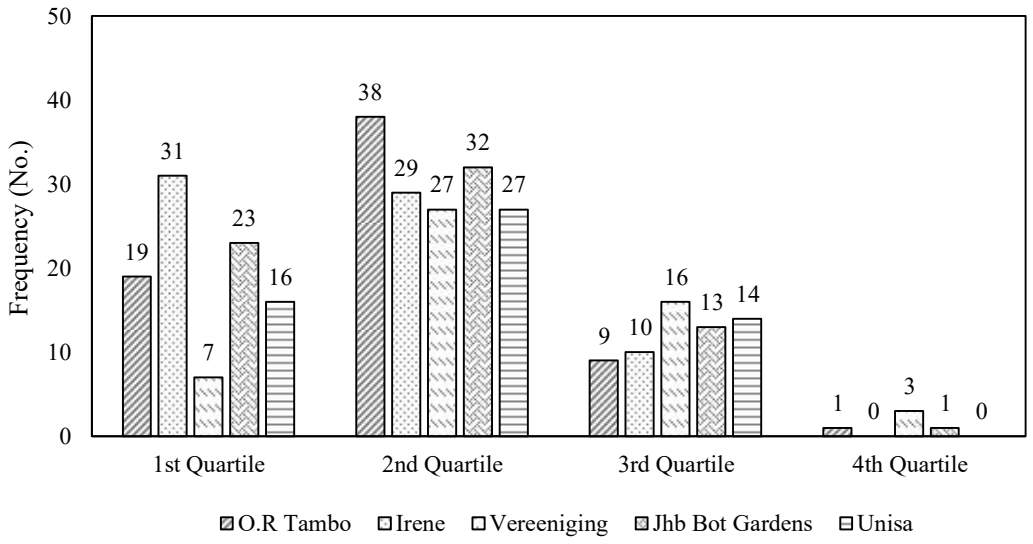

Figure 4.33: Frequency of Huff curve quartiles

The curves for O.R. Tambo are depicted as examples in Figure 4.34. The first quartile has 19 storm events, and the 2nd quartile has 38 events. The spread of breakpoints in both the 1st and 2nd quartile curves appear even and therefore produced seemingly smooth curves. Conversely, the 3rd quartile curves were produced from nine events and contains large open spaces between the breakpoints, and the 4th quartile curve has only one event. Therefore, a sample size of ten events or less, was accepted as an insufficient sample size to produce stable curves.

Even though the minimum sample size that is required is unknown, it was accepted that anything more than ten events are adequate to produce stable curves for this investigation. The 4th quartile curves were, therefore, ignored because of insufficient storm events. The 1st quartile curves for Vereeniging and the 3rd quartile curves for O.R Tambo and Irene were also ignored because of an insufficient sample size.

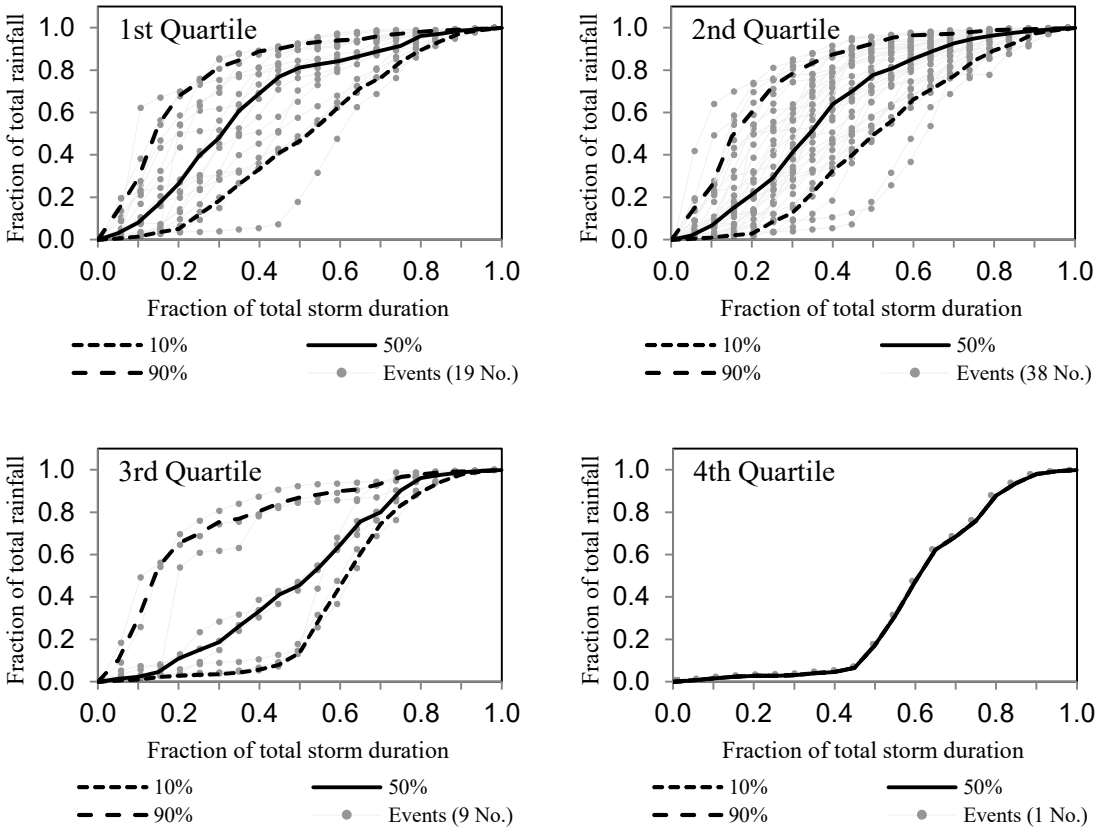

Figure 4.34: Standardised mass curves (Huff curves) for O.R. Tambo

Bonta (2004) has successfully fitted tenth order polynomials to Huff curves which simplifies their use. However, an analysis was conducted to determine the nth order polynomial that best fitted the ordinates of the curves. The general tenth order polynomial is presented in Equation 4.18 and similar equations were used for lower-order polynomials.

$$P = a \cdot T^{10} + b \cdot T^{9} + c \cdot T^{8} + d \cdot T^{7} + e \cdot T^{6} + f \cdot T^{5} + g \cdot T^{4} + h \cdot T^{3} + i \cdot T^{2} + j \cdot T \qquad \text{(Equation 4.18)}$$

where:

P = Fraction of total rainfall,

$a - j$ = Regression coefficients, and

T = Fraction of total duration.

The absolute RE (ABS) was determined for each ordinate from 0.05 to 0.95 for all five stations using Equation 4.19 and the results for O.R. Tambo, using the 90-percentile curve and the nth order polynomials as an example, are depicted in Figure 4.35.

$$ABS = \frac{100}{N_o} \cdot \sum_{i=1}^{N_o} \frac{|NP_i - HC_i|}{HC_i} \qquad \text{(Equation 4.19)}$$

where:

ABS = Average absolute RE of nth order polynomial,

N_o = number of ordinates (16), and

NP_i = Simulated fraction of total rainfall with the nth polynomial for ordinal i,

HC_i = Fraction of total rainfall according to the standardised mass curve for ordinal i.

It is observed in Figure 4.35 that the third to fifth-order polynomials performed poorly for the lower fractions of the total duration, and the second order for the higher fractions. The ABS for the sixth to tenth polynomials were below 15% and decreased for higher fractions.

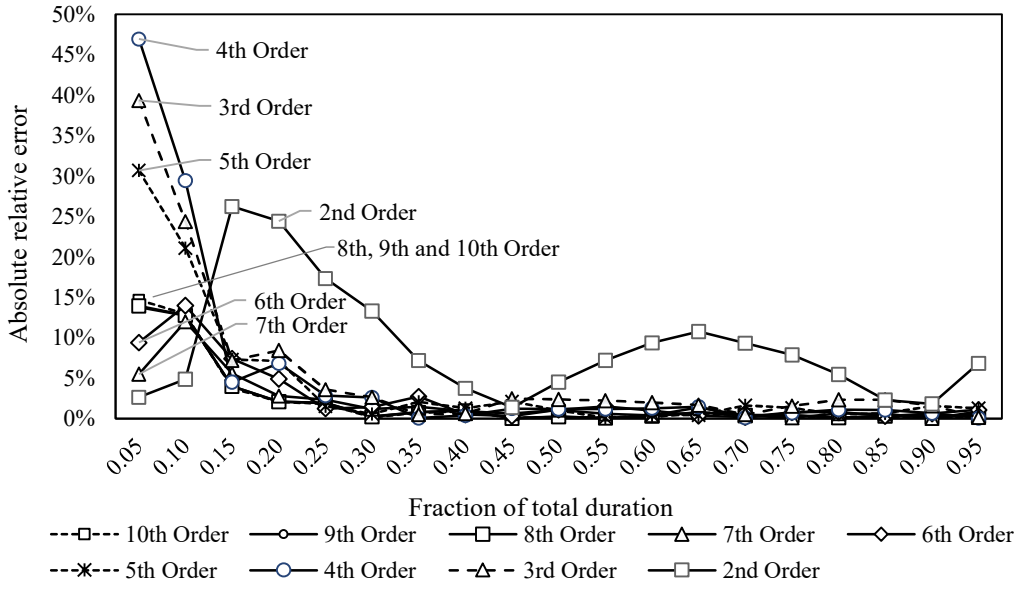

Figure 4.35: ABS for nth order polynomials developed for the 1st quartile, 90-percentile curve for O.R. Tambo

The results were similar for other percentiles and was typical of all stations. For example, the ABS for the nth polynomials for the 2nd quartile, and 50-pecentile curves for Jhb Bot Gardens are depicted in Figure 4.36. The second, third, fifth, and seventh order polynomials performed poorly compared to the eighth, ninth and tenth polynomials. The ABS decreased for all polynomials for higher fractions. Based on these preliminary results it was determined that the higher-order polynomials performed much better than the lower order polynomials, but the best could not be identified.

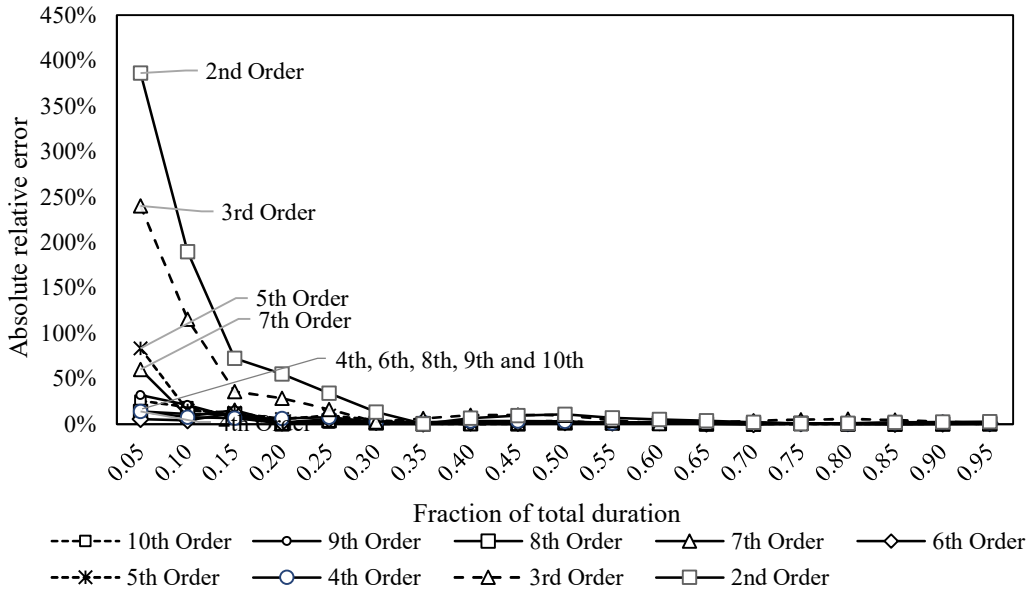

Figure 4.36: ABS for nth order polynomials developed for the 2nd quartile, a 50-percentile curve for Jhb Bot Garden

Therefore, the average ABS value was determined for all ordinates of the nth polynomial and the results for O.R Tambo as an example is depicted in Figure 4.37. It is observed that the seventh order polynomial fitted the 90 percentile curve for O.R Tambo the best with an average ABS value of 1.9%. A similar analysis was conducted for the 1st, 2nd and 3rd quartile events, 10, 50 and 90 percentile curves, for O.R Tambo, Irene, Vereeniging, Jhb Bot Gardens and Unisa stations.

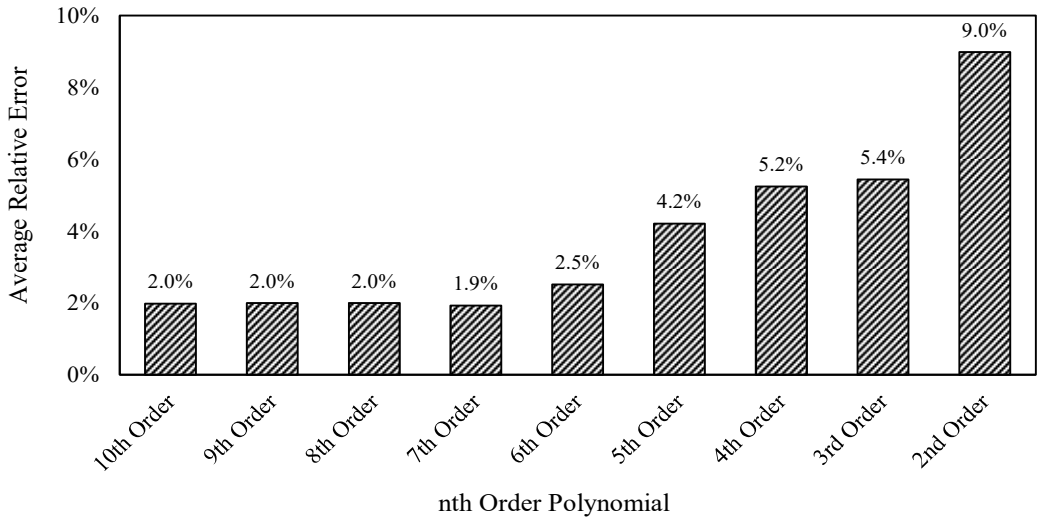

Figure 4.37: Average RE for nth order polynomials developed for the 1st quartile, 90-percentile curve for O.R. Tambo

The average ABS values for the n^{th} polynomial of the three percentiles and the five stations were ranked, and the lowest rank was assigned to the polynomial which resulted in the lowest average ABS value. The result of this analysis is, summarised in Table 4.6 to Table 4.8.

For the 1st quartile events, 10 percentile curves were best fitted by the seventh order polynomial, and for the 50 and 90 percentile curves, the ninth order polynomial was the best on average. In Table 4.7 the 2nd quartile events, 10 and 90 percentile curves were best fitted by the ninth order polynomial, and for the 50 percentile it was the tenth order polynomial. In Table 4.8 the 3rd quartile events, 10 and 50 percentile curves were best fitted by the tenth order polynomial, and for the 90 percentile it was the ninth order polynomial.

Table 4.6: Ranking of n^{th} order polynomials for the 1st quartile curves

Station	n^{th} Order polynomial								
	10th	**9th**	**8th**	**7th**	**6th**	**5th**	**4th**	**3rd**	**2nd**
10-Percentile curves									
O.R Tambo	3	2	4	1	5	8	7	6	9
Irene	7	6	2	4	8	3	1	5	9
Vereeniging	(Insufficient sample size)								
Jhb Bot Gardens	3	4	1	5	2	6	8	7	9
Unisa	3	2	7	1	8	4	6	5	9
Average ranking	**4.0**	**3.5**	**3.5**	**2.8**	**5.8**	**5.3**	**5.5**	**5.8**	**9.0**
50-Percentile curves									
O.R Tambo	3	2	1	4	5	6	7	8	9
Irene	3	2	5	4	1	6	7	8	9
Vereeniging	(Insufficient sample size)								
Jhb Bot Gardens	2	1	6	4	3	5	7	8	9
Unisa	3	2	1	4	6	5	7	8	9
Average ranking	**2.8**	**1.8**	**3.3**	**4.0**	**3.8**	**5.5**	**7.0**	**8.0**	**9.0**
90-Percentile curves									
O.R Tambo	2	3	4	1	5	6	7	8	9
Irene	2	1	3	4	6	5	7	8	9
Vereeniging	(Insufficient sample size)								
Jhb Bot Gardens	2	1	3	4	5	6	7	8	9
Unisa	2	1	3	4	6	5	7	8	9
Average ranking	**2.0**	**1.5**	**3.3**	**3.3**	**5.5**	**5.5**	**7.0**	**8.0**	**9.0**

Table 4.7: Ranking of n^{th} order polynomials for the 2^{nd} quartile curves

Station	n^{th} Order polynomial								
	10th	**9th**	**8th**	**7th**	**6th**	**5th**	**4th**	**3rd**	**2nd**
10-Percentile curves									
O.R Tambo	2	1	3	5	4	6	8	7	9
Irene	4	1	7	3	5	6	2	8	9
Vereeniging	4	5	7	3	8	2	1	6	9
Jhb Bot Gardens	3	2	1	4	5	7	8	6	9
Unisa	4	2	5	3	1	7	6	8	9
Average ranking	**3.4**	**2.2**	**4.6**	**3.6**	**4.6**	**5.6**	**5.0**	**7.0**	**9.0**
50-Percentile curves									
O.R Tambo	2	3	5	6	1	7	4	8	9
Irene	2	1	4	3	6	7	5	8	9
Vereeniging	1	2	3	5	4	8	7	6	9
Jhb Bot Gardens	3	4	2	6	1	7	5	8	9
Unisa	1	5	4	2	6	3	7	8	9
Average ranking	**1.8**	**3.0**	**3.6**	**4.4**	**3.6**	**6.4**	**5.6**	**7.6**	**9.0**
90-Percentile curves									
O.R Tambo	2	1	5	4	3	6	8	7	9
Irene	2	1	3	4	5	6	7	8	9
Vereeniging	1	2	3	4	5	7	6	8	9
Jhb Bot Gardens	3	2	4	1	5	6	8	7	9
Unisa	2	1	3	4	5	6	7	8	9
Average ranking	**2.0**	**1.4**	**3.6**	**3.4**	**4.6**	**6.2**	**7.2**	**7.6**	**9.0**

Table 4.8: Ranking of n^{th} order polynomials for the 3^{rd} quartile curves

Station	n^{th} Order polynomial								
	10th	**9th**	**8th**	**7th**	**6th**	**5th**	**4th**	**3rd**	**2nd**
10-Percentile curves									
O.R Tambo	(Insufficient sample size)								
Irene	(Insufficient sample size)								
Vereeniging	3	5	7	6	8	4	1	9	2
Jhb Bot Gardens	1	3	2	6	5	4	8	7	9
Unisa	3	4	1	5	6	2	7	8	9
Average ranking	**2.3**	**4.0**	**3.3**	**5.7**	**6.3**	**3.3**	**5.3**	**8.0**	**6.7**
50-Percentile curves									
O.R Tambo	(Insufficient sample size)								
Irene	(Insufficient sample size)								
Vereeniging	1	2	7	3	6	5	8	4	9
Jhb Bot Gardens	1	2	5	6	3	7	4	8	9
Unisa	3	4	2	1	5	7	6	8	9
Average ranking	**1.7**	**2.7**	**4.7**	**3.3**	**4.7**	**6.3**	**6.0**	**6.7**	**9.0**
90-Percentile curves									
O.R Tambo	(Insufficient sample size)								
Irene	(Insufficient sample size)								
Vereeniging	2	1	3	8	7	6	4	5	9
Jhb Bot Gardens	2	1	3	4	6	5	7	8	9
Unisa	2	1	3	4	7	6	5	8	9
Average ranking	**2.0**	**1.0**	**3.0**	**5.3**	**6.7**	**5.7**	**5.3**	**7.0**	**9.0**

As depicted in Figure 4.38, the ninth order polynomial generally fits all ordinates in the 1st, 2nd, and 3rd quartile events, 10, 50, and 90 percentile curves the best with an average of 2.3 for all stations and quartiles with sufficient sample size. The tenth-order polynomial fits the second-best with an average of 2.5 and then followed by the eight order polynomial, and so forth. Therefore, further analyses were based on the ninth order polynomial in contrast to Bonta's (2004) tenth order polynomial.

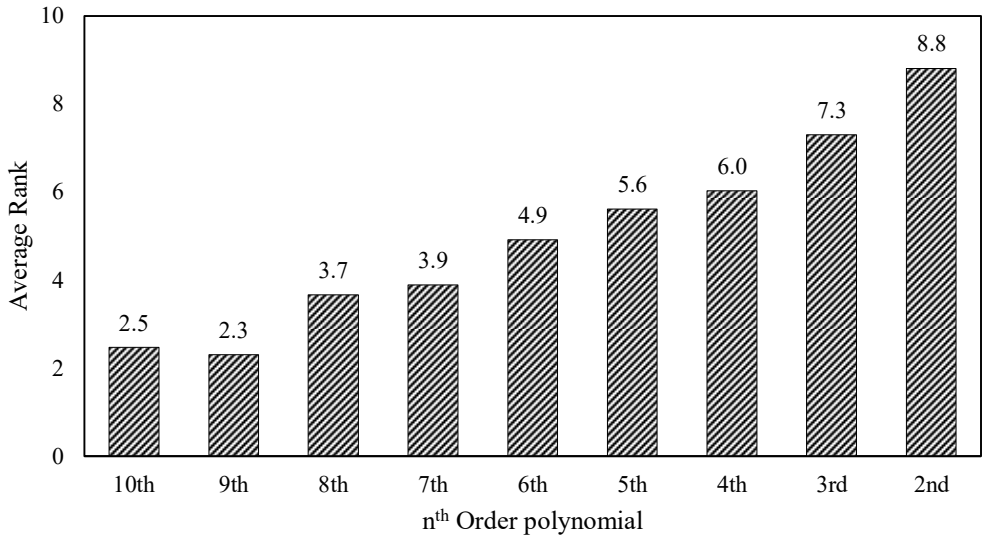

Figure 4.38: Average rank of all stations and quartiles with sufficient sample size (> 10)

Design storms of 24-hour duration were generated from the standardised mass curves, using the 9th order polynomial, and a moving window period was used to determine the maximum ratio for the standard time steps. These ratios were compared with the D-hour to 24-hour ratios of the at-site design rainfall described in Section 4.2. O.R Tambo's results for the 10 and 90 percentile curves are depicted in Figure 4.39 as an example. Similar results were obtained for Irene, Vereeniging, Jhb Bot Gardens and Unisa. It is observed that all the standardised mass curves, 1st to 3rd quartile as well as 10 and 90 percentile curves, are underestimating the short duration time step ratios, compared with the at-site design rainfall ratios. The ratios from the 8-hour time step and onwards, of the 90 percentile curves in all quartiles, agrees well with the ratios of the design rainfall.

However, the response time for small urban catchments necessitates the use of accurate short duration time step ratios, because the peak discharge will also be underestimated if the short time step ratios are underestimated. Therefore, it can be concluded from this analysis that the 24-hour design storms generated from standardised mass curves are inadequate for small urban catchments.

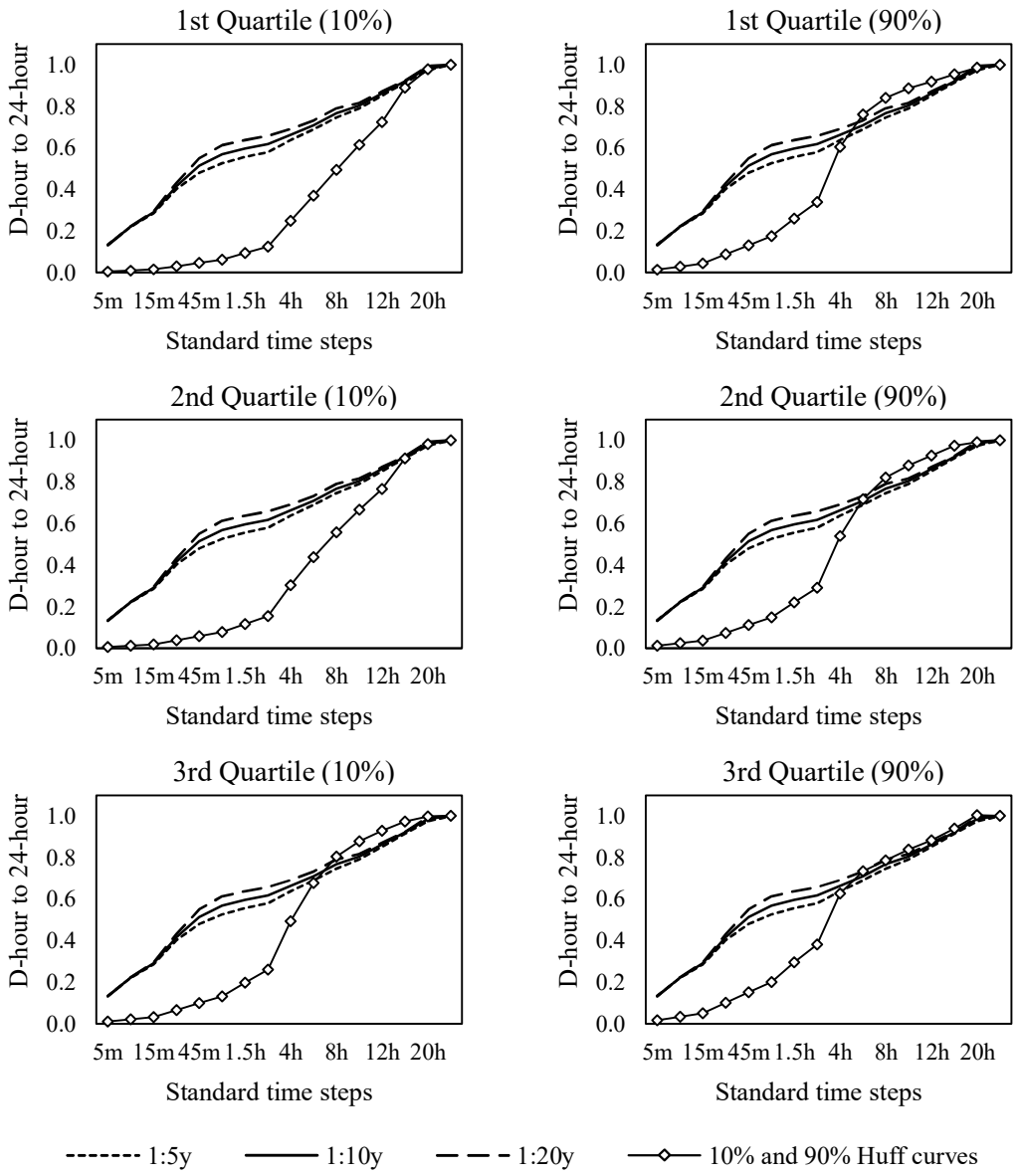

Figure 4.39: D-hour to 24-hour ratios of the standardised mass curves for O.R Tambo

It was, however, possible to increase the ratios of the standardised mass curves by generating shorter design storms, like 2-hour instead of 24-hour. This means that the D-hour to 2-hour ratios of the standardised mass curves would correlate better with the design rainfall. However, this would result in the storm duration becoming a critical parameter for accurate design rainfall estimation. This would increase the complexity of synthetic design storms because of the impact the storm duration has on the antecedent moisture content when applied to a SWMM model. The difficulty of generating a 9th order polynomial will also add to this complexity. Hence, it was concluded from this investigation that the use of standardised mass curves is not recommended for use in small urban catchments.

4.8 CHAPTER SUMMARY

This chapter has provided the basis to generate synthetic design storms using the methods that are considered for this study, and to assess the performance of the methods. The primary storm parameters consisting of the storm advancement coefficient and the dimensionless time to peak were determined to be 0.38 and 0.20, respectively. It can be seen that the two coefficients, although similar by definition, are not similar. This is because of the difference in the calculation procedure. Storm events, identified in the previous chapter, with an MDP of 15-min, were used to determine these parameters. The use of this MDP was based on the argument that if the MDP exceeds the time of concentration, any rainfall after the dry period could no longer influence the peak discharge of the previous spell. The reaction time of the SWMM model considered in the next chapter, which is representative of the catchment size targeted in this study, was found to have a reaction time of 15-min, and therefore, the 15-min MDP was selected. The storm shape and average intensity assessments in the next chapter was, therefore, also be based on the 15-min MDP.

A methodology for determining regression coefficients for the CDS method, using the GRG non-linear solver, was developed. These coefficients, together with the storm advancement coefficient, was be used for the CDS method in the next chapter. The simulated design rainfall intensities, using the regression coefficients, were evaluated by determining the RE of the actual design rainfall intensities obtained from the DRESA software. From this analysis it was evident that the results obtained from the methodology, involving the GRG non-linear solver, was sufficiently accurate to determine the regression coefficients required by the CDS method.

Design rainfalls were determined using the at-site AMS for 16 standard time steps for each station and compared with the design rainfall obtained from the DRESA software. It was found that the average RD was within the 90% upper and lower bounds given by the DRESA software. Short duration design rainfall of between 5 and 30-min was identified to be substantially lower than the DRESA software and further investigation is recommended to identify the cause of the discrepancy.

The procedure to distribute design rainfall equally around the peak intensity was adapted to utilize the concept of incremental intensities for the interpolation of design rainfall for intermediate time steps. This was subsequently used to generate the DC5, DC10 and the DC20 curves from the at-site design rainfall developed from the PD analysis. The procedure to extract an event of less than 24-hour, adopted from NRCS (2019), was also illustrated. This procedure will be used in the next chapter to extract synthetic design storms from the SCS-SA, DC5, DC10 and the DC20 curves, for durations equal to the significant events.

The D-hour to 24-hour design rainfall ratios, using the design rainfall of the DRESA software as well as the at-site design rainfall, were calculated and their position relative to the four standard SCS-SA curves were determined. The results from both sources of design rainfall indicated that, on average, Gauteng conforms more closely to the SCS-SA Type 2 curve, rather than Type 3. However, a significant variation in the ratios for the various durations were observed because the derived ratios plotted between standard SCS-SA type curves. This led to the development of intermediate curves whereby a curve is linearly interpolated between two standard type curves. The method of interpolating between standard type curves and the spatial interpolation between stations was documented. Similar analyses were conducted by comparing the SCS curves with the SCS-SA curves as well as the at-site design rainfall ratios. It was observed that the Type II curve contains the highest ratios for the 5-min to 6-hour time steps, and that they marginally exceed the ratios of the SCS-SA Type 2 curve. The highest IC value achieved with the Type II curve was 2.31 for the 30-min time step. The Type II curve can, therefore, only be applied to areas with a similar IC value, and to catchments with a 30-min response time. From the comparison with the at-site design rainfall ratios, it was observed that very few stations conform to the Type II curve, and that the majority exceeds the 30-min ratio. This analysis has, therefore, shown that the use of the SCS curves is very limited and must be used with caution.

Standardised mass curves (Huff curves) were developed for quartiles with a sufficient sample size. These curves were successfully fitted to 9^{th} order polynomials using a ranking system to find the n^{th} polynomial that fitted the data points the best. The polynomials were subsequently used to generate 24-hour synthetic design storms. Since standardised mass curves are dimensionless in respect of time and depth, the storm duration and depth of a 24-hour event were multiplied with the dimensionless time and depth factors of each ordinate, respectively. The maximum ratios for the standard time steps were compared with the at-site design rainfall ratios. Based on this analysis it was concluded that standardised mass curves underestimate short duration design rainfall. Therefore, this method was not considered any further because it will lead to an underestimation of the peak discharge when applied to a single event-based model of a small urban stormwater network.

In the next chapter, the flow results from single event-based modelling, using the standard type curves and the intermediate curves, will be demonstrated.

5 EVALUATION OF SYNTHETIC DESIGN STORMS

This chapter contains details of the evaluation of synthetic design storms by comparison between mass curves and average intensities, as well as simulated peak discharge and runoff volumes. The evaluation of the synthetic design storms was conducted by considering two characteristics of an event, namely the shape of the mass curves, and the average intensities of standard time steps. This was achieved by non-dimensionalising each significant event in terms of rainfall and generating a synthetic storm event matching the total duration. The simulated peak discharge and runoff volume generated with different synthetic design storms were also compared with results from continuous simulation using observed rainfall data as input. The methods used to generate synthetic design storms include the following:

a) the CDS method, using the regression coefficients from Table 4.1, and an average advancement coefficient of 0.38,

b) standard curves, including the SCS-SA Type 2 [SA(T2)] and 3 [SA(T3)],

c) DCs developed using the methodology described in Section 4.4, and the on-site design rainfall described in Section 4.3,

d) the REC method, and

e) the TRI method using a dimensionless time to peak of 0.20.

5.1 MASS CURVE COMPARISON

The evaluation of the shape of the mass curves was conducted by considering each significant storm event with an MDP of 15-min. The GOF of the shape of the synthetic storm event compared to the observed storm event at 5-min intervals were determined using the Mean Absolute Relative Error (MARE) technique. The average of all significant events was the final score given to the method used to generate the synthetic storm event. The general MARE formula for the shape of the mass curve (MARE_S) is expressed in Equation 5.1.

$$MARE\_S = \frac{1}{N_s \cdot \overline{N_d}} \sum_{j=1}^{N_s} \sum_{i=1}^{N_d} \left[\frac{\left| S_{(ij)} - O_{(ij)} \right|}{O_{(ij)}} \right] \qquad \text{(Equation 5.1)}$$

where:

$S_{(ij)}$ = Synthetic depth for duration *i* and storm *j* (mm),

$O_{(ij)}$ = Observed depth for duration *i*, and storm *j* (mm),

$\overline{N_d}$ = Average number of 5-minute data points per storm, and

N_s = Number of storms.

A typical result of the GOF between an observed individual storm event and the synthetic design storms is depicted in Figure 5.1. The storm event that occurred on 29 October 1994 at O.R. Tambo is used to illustrate the assessment process followed for all significant events identified in Section 3.6. This event had a total duration of 50-min and the total rainfall was 17 mm. Considering the results presented in Figure 5.1, the DC5 best represents the shape of the observed mass curve with a MARE_S of 0.311. The DC10, and DC20 curves performed slightly worse with values of 0.326 and 0.350, respectively. The SA(T2) and SA(T3) also showed good correlations with values of 0.366 and 0.337, respectively. The CDS method performed better than the REC and TRI, with values of 0.431, 0.535, 0.494, respectively. Therefore, considering this single event at the O.R Tambo station, the DC5 presented the best fit of all the methods, and the REC the worst.

To determine the overall performance of the methods, the average and median MARE_S values were determined for all the significant events from the five best stations in Gauteng, namely O.R Tambo, Irene, Vereeniging, Jhb Bot Gardens, and Unisa. The significant events from the five stations were pooled together before the analysis was conducted. The result of this analysis is depicted in Figure 5.2. It is seen that the TRI best represents observed events when analysed in this manner with the lowest MARE_S values, followed by the REC. The results of both TRI and REC outperformed CDS, DC5, DC10, DC20, SA(T2) and SA(T3). It is important to note that this means the methods that use a single point on the IDF curve according to , performed better than the methods that use the entire IDF curve. This is, however, attributed to the position of the peak intensity relative to the total duration. For DC5, DC10, DC20, SA(T2) and SA(T3) the peak intensity is in the middle of 24-hours, whereas with CDS it is slightly earlier. Therefore, the effect of adjusting the position of the peak, was investigated. This is described in the next section.

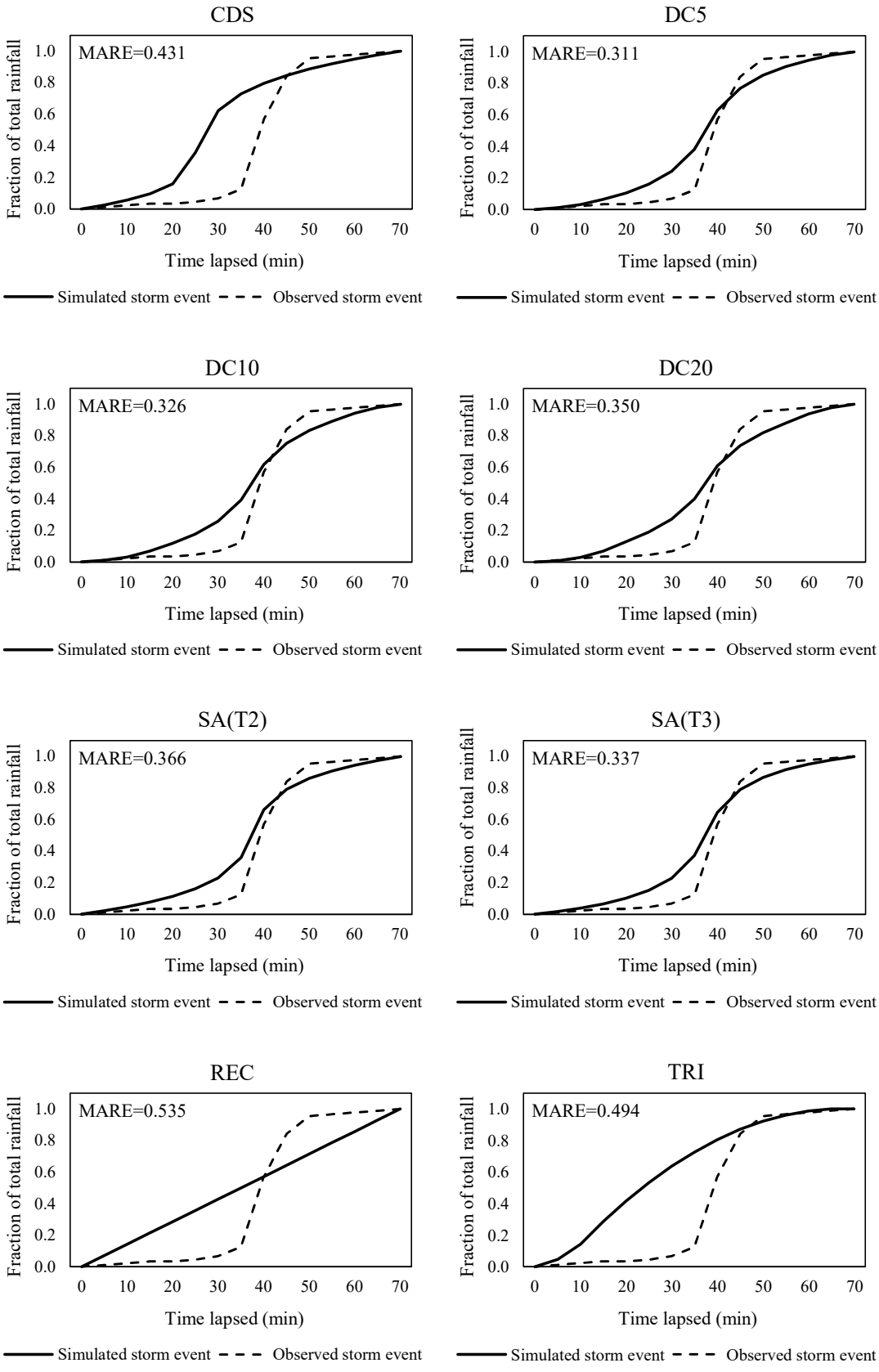

Figure 5.1: Typical GOF between the shape of an observed individual storm event at O.R Tambo on 29 October 1994, and a synthetic storm event

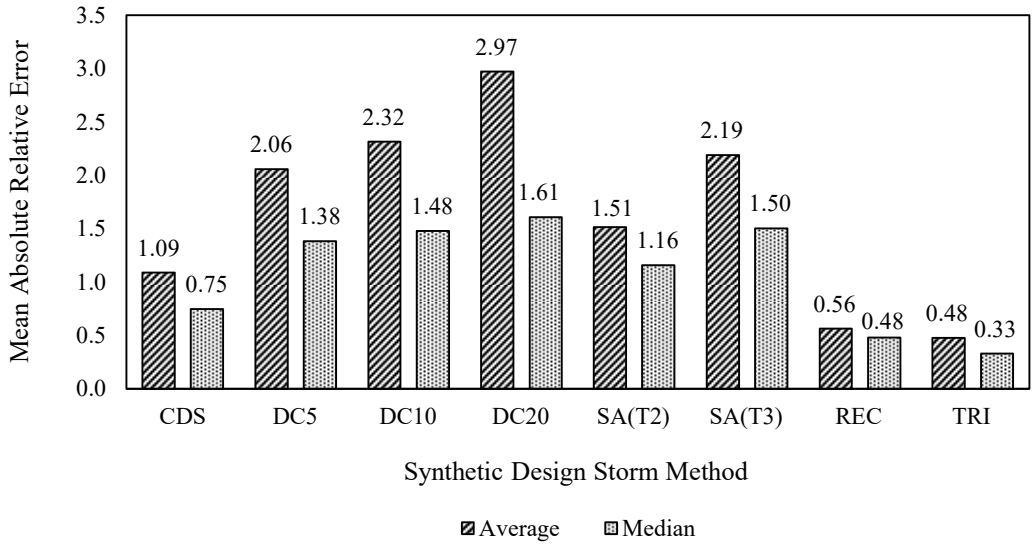

Figure 5.2: MARE_S between observed storm events and synthetic design storms at the five best stations in Gauteng

5.2 ADJUSTMENT OF THE PEAK INTENSITY'S POSITION

This section describes the development of a procedure to adjust the position of the peak intensity of the SCS-SA curves in an attempt to improve their performance. The updated results of the mass curve comparison, described in Section 5.1, using the modified curves are also presented below.

As described in Section 1.1 of the literature review, the SCS-SA curves were developed with the peak intensity at the centre of 24-hour and the design rainfall of increasing durations divided equally on either side of the peak intensity. Conversely, with the CDS method the peak intensity can be positioned anywhere between the start and end of the event, but with the average intensities of all durations still embedded in the event as depicted in Figure 2.8. Therefore, the same methodology used to determine regression coefficients described in Section 4.3 was used to determine the coefficients of the SCS-SA curves. This means that the SCS-SA curves were recreated using the CDS method, but with the peak earlier during the event. The optimised regression coefficients of the SCS-SA curves are summarised in Table 5.1.

Table 5.1: CDS Regression coefficients for the SCS-SA curves

Description	SCS-SA curves	
	Type 2	Type 3
a	10.079	27.517
b	6.470	11.686
c	0.755	0.891

The CDS method with IDF regression coefficients described in Section 4.3 were also re-evaluated, but with an optimized advancement coefficient. The updated results for the mass curve comparison are depicted in Figure 5.3. It is seen that the results for the CDS, SA(T2) and SA(T3) improved significantly. An advancement coefficient of 0.01 was found to give the best results with improved average GOF values. The same optimization procedure was, however, not attempted for the DC5, DC10 and DC20 curves. This will entail the smoothing of the DDF curves which falls outside the scope of this study. Therefore, only improved results for the CDS, SA(T2) and SA(T3) are depicted in Figure 5.3.

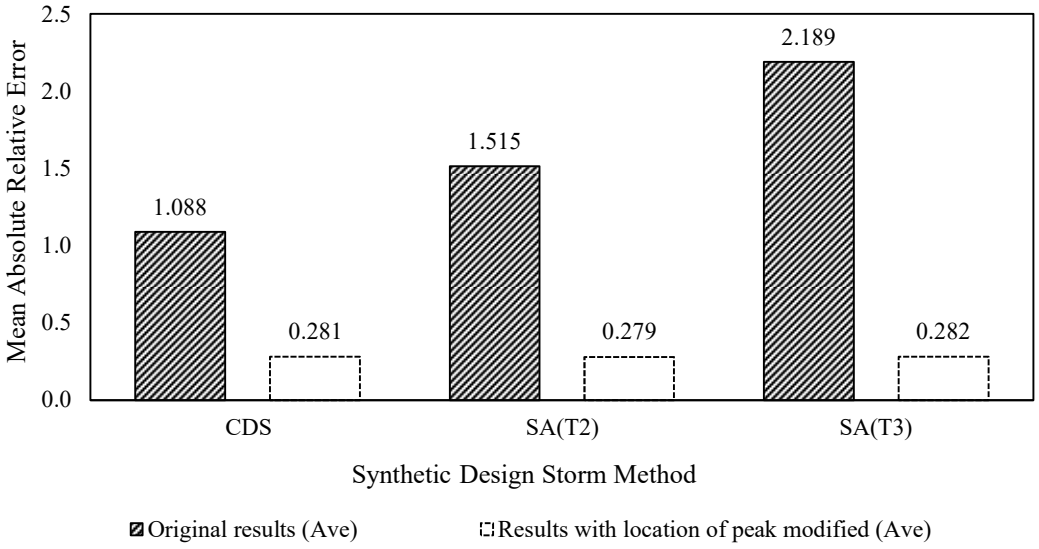

Figure 5.3: Synthetic design storms modified with peak earlier during an event

It can be concluded that the performance of the methods that use the entire IDF curve can be altered and improved by modifying the position of the peak intensity relative to the total duration of an event. However, any value of MARE_S above zero implies that the shape of a synthetic design storm does not represent observed hyetographs. Another factor that contributes to an MARE_S value above zero is the variation of RI within observed storm events. Conversely, synthetic design storms assume that intensities of increasing durations, embedded in an event, have the same RI. This can lead to overcompensation by reducing the advancement coefficient to a value beyond the true optimum point. This phenomenon is explained in detail in Section 5.3 which describes the assessment of the average intensities between observed storm events and synthetic design storms.

5.3 AVERAGE INTENSITY COMPARISON

The evaluation of the intensities was conducted by considering the ratios of average intensities of the standard time steps (5, 10, 15, 30, 45-min, etc.) of each significant storm event. The GOF of the ratios of the synthetic design storms compared to the observed storm events was determined using the general MARE formula for the average intensity ratios (MARE_I), expressed in Equation *5.2*.

$$MARE\_I = \frac{1}{N_s}\sum_{j=1}^{N_s}\left[\frac{\left|S_{(j)} - O_{(j)}\right|}{O_{(j)}}\right] \qquad \text{(Equation 5.2)}$$

where:

$S_{(j)}$ = Synthetic intensity for storm j,

$O_{(j)}$ = Observed intensity for storm j, and

N_s = Number of storms.

Similar to the mass curve assessment, the average intensity ratio assessment was conducted considering the CDS, DC5, DC10, DC20, SA(T2), SA(T3), REC and TRI methods. The same storm event, depicted in Figure 5.1, is used to illustrate the comparison of the average intensity ratios, although all significant storm events were used for the assessment. The results for the example event are depicted in Figure 5.4. In contrast to MARE_S, the MARE_I result for REC is the worst. This is attributed to the uniform intensity assumed by the REC method. The result for TRI is slightly better than REC because of the minor increase in variation of intensities. This can be seen by considering Equation which stipulates that the peak intensity of a triangular hyetograph is twice the total rainfall depth of the event, divided by the total duration. This means the longer the duration of an event, the lower the peak intensity becomes, which explains the poor MARE_I for the TRI method. The results for the CDS, DC5, DC10, DC20, SA(T2) and SA(T3), depicted in Figure 5.4, are all similar with MARE_I ranging from a minimum of 0.218 for SA(T2) to a maximum of 0.307 for DC20.

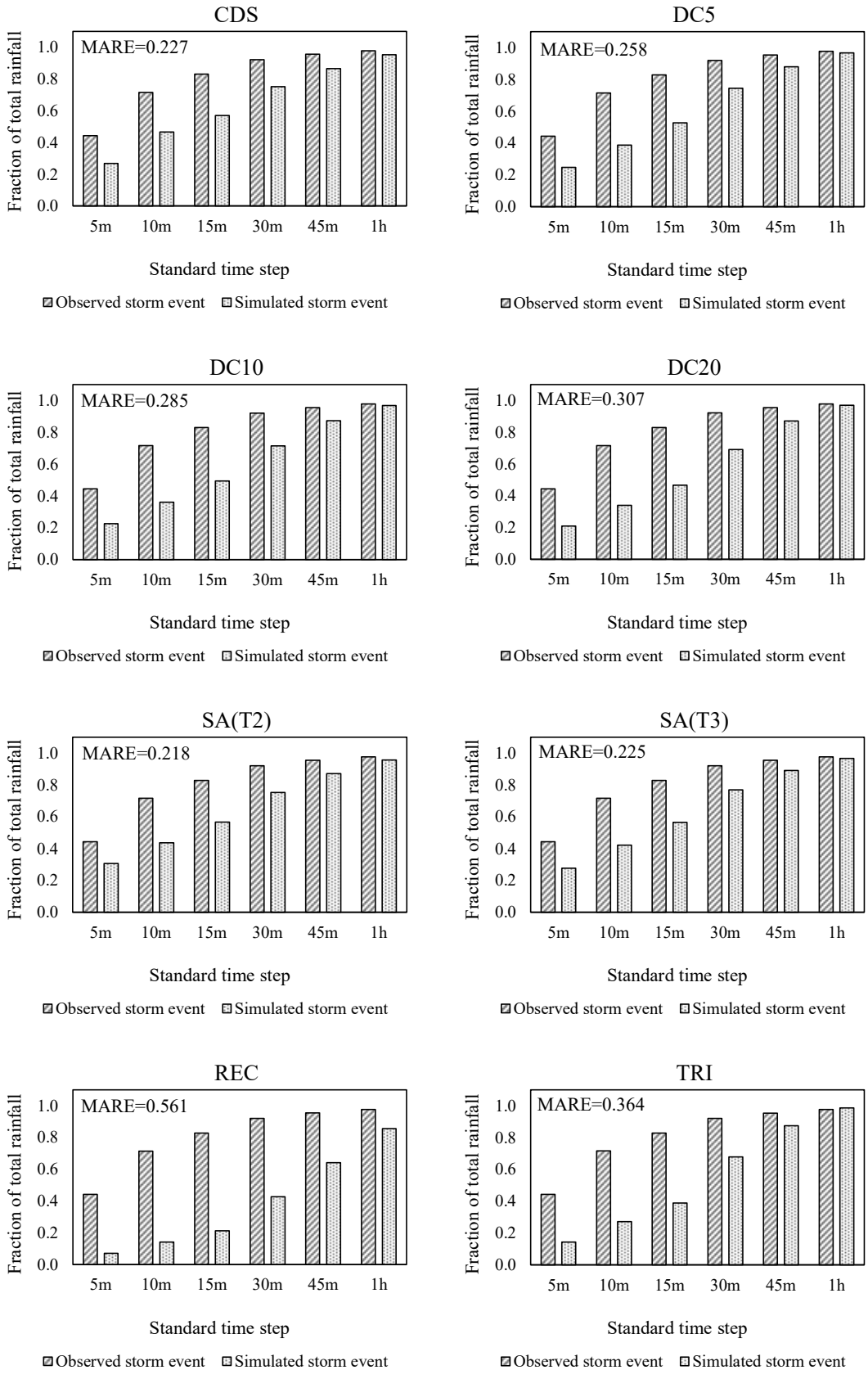

Figure 5.4: Typical GOF between the average intensities of an observed individual storm event at O.R Tambo on 29 October 1994, and a synthetic storm event

Following the analysis of individual storm events, the average and median values of the five stations with the best data sets were determined and the results for significant events at these sites are shown in Figure 5.5. The average and median values for the REC and TRI methods are approximately equal, which indicates an approximately symmetrical frequency distribution. According to these results the REC method has the worst representation of average intensities, followed by the TRI method. The median values for the CDS, DC5, DC10, DC20, SA(T2) and SA(T3) methods are similar and much lower than the REC and TRI methods. This indicates a much better representation of average intensities. However, a significant difference between the average and median values for these methods can be observed. This shows that the results are skewed, which is confirmed by considering the frequency distributions depicted in Figure 5.6.

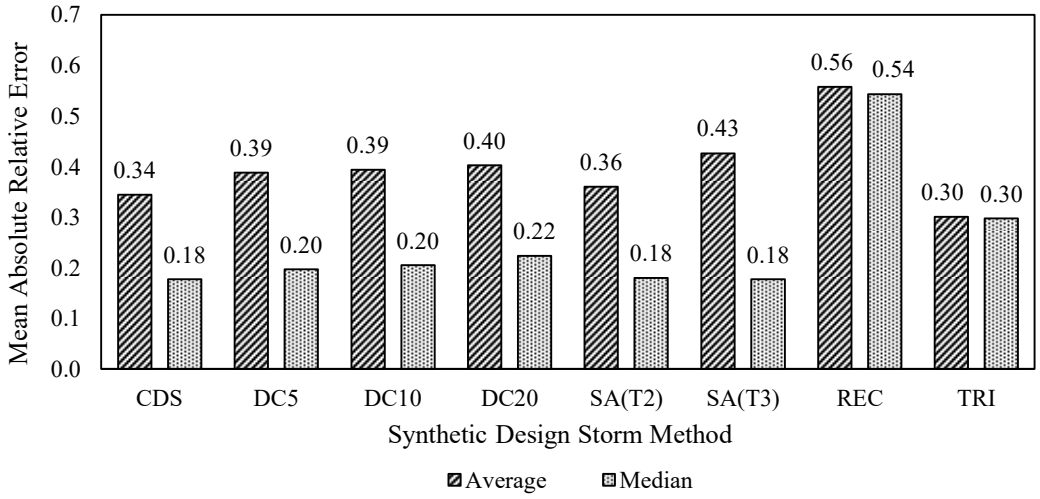

Figure 5.5: MARE_I between observed storm events and synthetic design storms at the five best stations in Gauteng

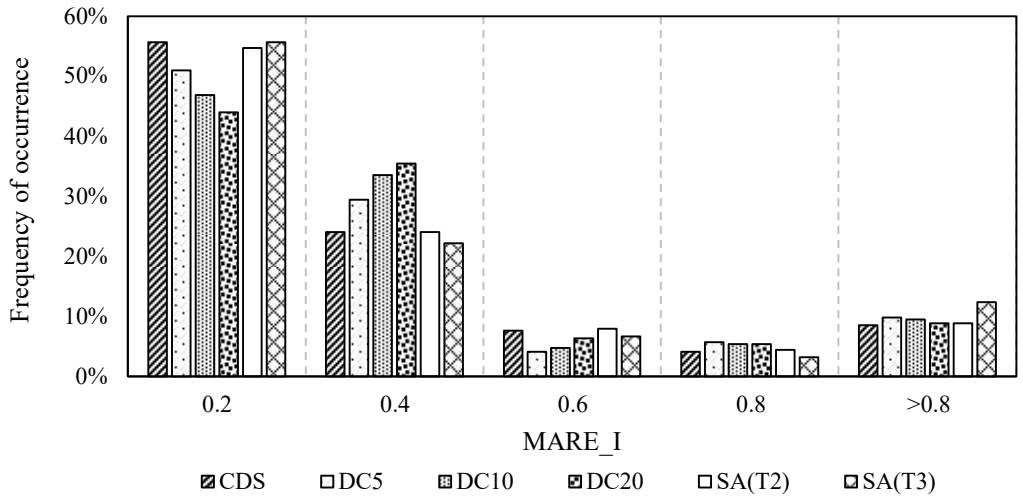

Figure 5.6: MARE_I frequency of occurrence for methods based on entire IDF curve

The results depicted in Figure 5.5 show that the CDS, SA(T2) and SA(T3) performed the best of all the methods considering the MARE_I. The modification to the location of the peak intensity applied in Section 5.2 will not improve the MARE_I value. This is because of the embedment of all intensities with increasing duration in a single event associated with the methods that utilize the entire IDF curve. This procedure, therefore, does not alter the intensities of the synthetic design storm but merely the location of the peak. The variation of the RI of average intensities during an observed event was therefore further investigated in Section 5.4 to see the causes of the MARE_I value.

5.4 VARIATION IN RECURRENCE INTERVAL OF AVERAGE INTENSITIES

To determine the variation in RI of the average intensities during a storm event, the MRI criterion described in Section 3.6.3 was applied. This was done by determining the RI Ratio (RIR) of the standard time steps relative to the RI Maximum (RIM) of each storm event with the same maximum standard duration. The average RIR of the five best stations in Gauteng is depicted in Figure 5.7, which was determined using Equation 5.3.

$$RIR_{t,D} = \frac{1}{N_s \cdot N_{SD}} \sum_{j=1}^{N_S} \sum_{i=1}^{N_{SD}} \frac{RI_{t,i}}{RIM_i} \qquad \text{(Equation 5.3)}$$

where:

RIR = Recurrence interval ratio of time step t, and total duration D,

N_{SD} = Number of storm events with total duration D,

N_S = Number of stations (5),

$RI_{t,i}$ = Recurrence interval of time step t, and storm event i, (year), and

RIM_i = Maximum recurrence interval of storm event i, (year).

The results depicted in Figure 5.7 show that, on average, the highest RIR is located at the longest standard time steps for 6, 8, 12 and 16-hour events, and the smallest duration the lowest RIR. For example, storm events with a total duration of more than 12 but less than 16 hours, denoted by the 12h curve, have a 12-hour RIR of approximately 1.0, but a 5-min RIR of approximately 0.1. This finding contradicts the assumption that the RI of all standard time steps have the same RI, which is associated with the methods that utilize the entire IDF curve. For storm events with a total duration of less than 6-hours, the RI of the maximum time steps starts to decrease which indicates a tendency for the maximum RI to shift to the shorter time steps. Considering the 1h and 2h curves, the RIR of the 1 and 2-hour time steps are lower than the 30-min and 1-hour RIR, respectively. This effect is presented as the cause of an MARE_I above zero, as described in Section 5.3.

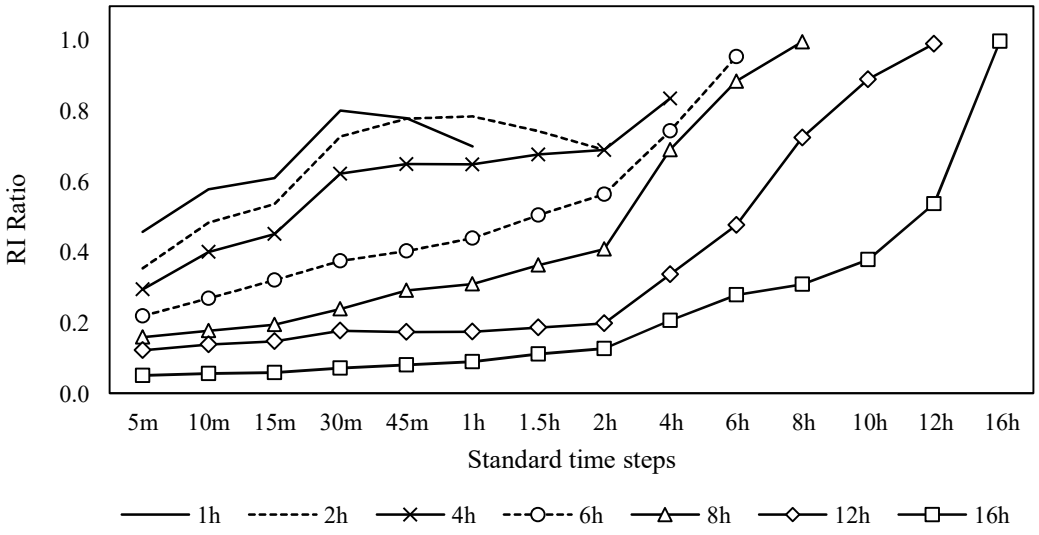

Figure 5.7: Variation in RI for the five best stations in Gauteng

5.5 EVENT-BASED AND CONTINUOUS SIMULATION

An assessment was conducted in terms of the peak discharge and runoff volume simulated from a SWMM model of a hypothetical catchment area. This was achieved by comparing the result of an event-based simulation, using each of the synthetic design storms, with the results from a continuous simulation application of the model. The observed rainfall data for the five best stations, namely O.R. Tambo, Irene, Vereeniging, Jhb Bot Gardens and Unisa, and the hydrological urban catchment defined by Gironas et al. (2009) as depicted in Figure 5.8 was used in this assessment. The catchment has a total area of 11.6 ha which was divided into seven sub-catchment areas. The characteristics of the sub-catchments are summarised in Table 5.2.

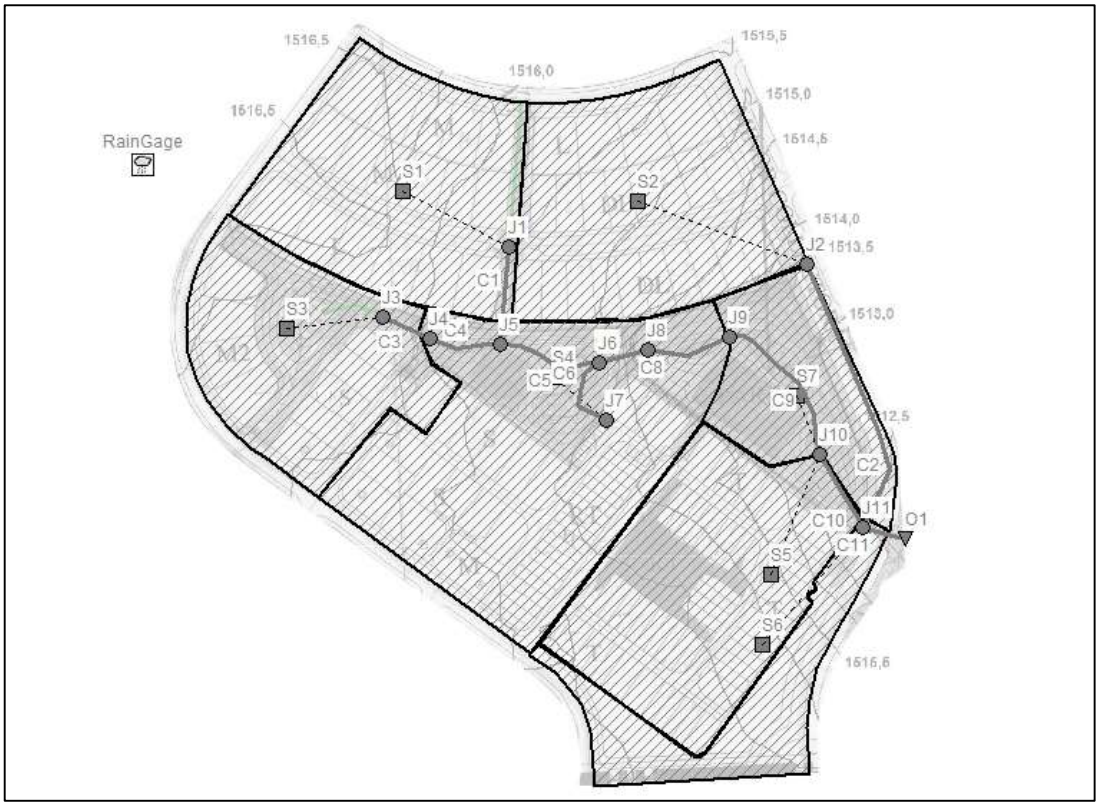

Figure 5.8: The catchment used for the SWMM modelling

Table 5.2: Sub-catchment SWMM characteristics

Description	Sub-catchment						
	S1	S2	S3	S4	S5	S6	S7
Area (ha)	1.829	1.906	1.505	2.740	1.930	0.793	0.935
Width (m)	480.1	500.3	438.8	706.2	506.6	208.1	273.4
Slope (%)	2.5	2.5	4.5	4.0	2.5	2.5	3.8
Imperv (%)	56.8	63.0	39.5	49.9	87.7	95.0	0.0
N-Imperv	0.015	0.015	0.015	0.015	0.015	0.015	0.015
N-Perv	0.240	0.240	0.240	0.240	0.240	0.240	0.240
Dstore-Imperv (mm)	1.5	1.5	1.5	1.5	1.5	1.5	1.5
Dstore-Perv (mm)	7.5	7.5	7.5	7.5	7.5	7.5	7.5
Zero-Imperv (%)	25	25	25	25	25	25	25
Subarea Routing	Outlet	Outlet	Outlet	Outlet	Outlet	Outlet	Outlet
Percent Routed (%)	100	100	100	100	100	100	100
Suction head (mm)	110	110	110	110	110	110	110
Conductivity (mm/h)	11	11	11	11	11	11	11
Initial deficit (m/m) Note	0.263	0.263	0.263	0.263	0.263	0.263	0.263

Note: Difference between porosity and field capacity

5.6 PEAK RUNOFF COMPARISON

The catchment depicted in Figure 5.8 has a single outfall node, namely O1. This node was selected to conduct the flow comparison between the continuous simulation and the event-based model. The time step used in the simulations was 5-min. The observed rainfall data of five stations with the best available data sets were used as input data for five different continuous simulation models, namely O.R. Tambo, Irene, Vereeniging, Jhb Bot Gardens and Unisa. Small continuity errors existed following the simulations which confirm the validity of the analysis results. The AMS of the flow rates in hydrological years, using the five different rainfall data sets, were extracted. This was followed by a PD analysis using the GEV distribution with L-moments to estimate the design peak discharges. The result of the PD analysis is summarized in Table 5.3.

Table 5.3: Estimated runoff at node O1 using the GEV probability distribution for the five best stations in Gauteng

RI (years)	FLOW RATE (m^3/s)				
	O.R Tambo	Irene	Vereeniging	Jhb Bot	Unisa
1:2	1.219	1.372	1.285	1.284	1.384
1:5	1.757	1.840	1.887	1.813	1.958
1:10	2.204	2.180	2.432	2.202	2.461
1:20	2.717	2.531	3.102	2.605	3.062
1:50	3.530	3.023	4.249	3.177	4.059

The same catchment depicted in Figure 5.8 was simulated using a single event-based approach, using synthetic design storms as input data. Synthetic design storms for the 1:5, 1:10 and 1:20-year RIs were generated using SA(T2), SA(T3), CDS, DC5, DC10, DC20, REC, and TRI. A storm duration of 2-hours was used for SA(T2), SA(T3), CDS, DC5, DC10 and DC20 since it will generally be adequate to exceed the longest time of concentration (Watson, 1981). Longer durations will lead to higher levels of soil moisture content, and therefore, the 24-hour storm duration was also used to evaluate the effect on the peak discharge. The REC and TRI methods were applied by finding the critical duration for the REC method and determining the minimum duration for the TRI method. These procedures are explained in detail in Sections 5.7 and 5.8, respectively. Again, small continuity errors were obtained after each simulation which confirms the validity of the analysis results. The peak discharge at node O1 from the event-based simulation was obtained which was compared to the peak discharge obtained from the continuous simulation which used the observed rainfall from each rainfall station. The average percentage RE between the results from the continuous simulation for each station, and the results from the REC and TRI methods, are depicted in Figure 5.9. Both methods underestimated the peak discharge at all five stations.

Since the same parameters were used in both the continuous simulation and single event-based modelling, the initial deficit applicable to single event-based modelling, using REC and TRI synthetic design storms, is questioned. Therefore, further research into the initial deficit associated with the infiltration parameters of the Green-Ampt model is recommended.

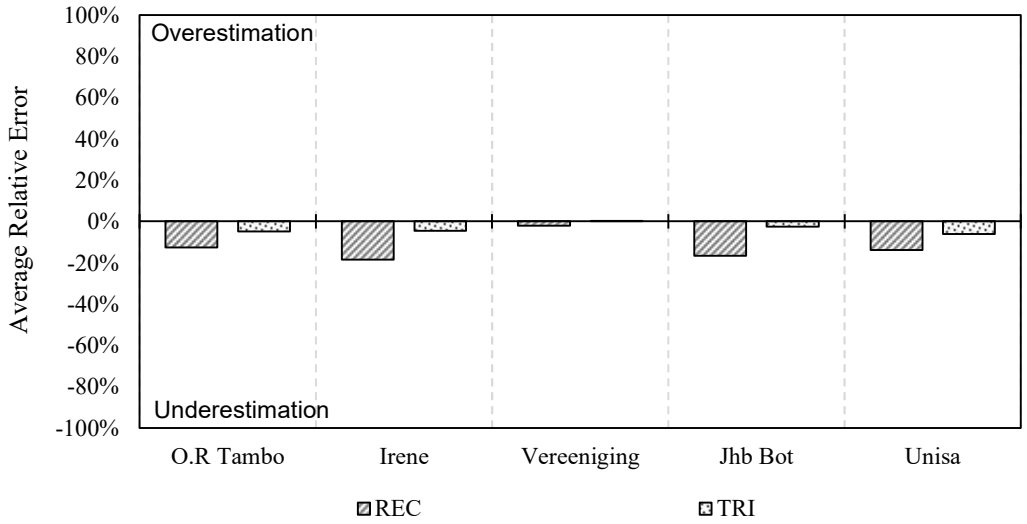

Figure 5.9: Average RE of the peak runoff at node O1 between continuous simulation and single event-based modelling using the REC and TRI methods

The results using the CDS, SA(T2), SA(T3), DC5, DC10 and DC20 methods for the 2-hour and 24-hour single event-based modelling, are depicted in Figure 5.10 and Figure 5.11, respectively. The difference between SA(T2) and SA(T3) for the 24-hour event was much greater than the difference for the 2-hour event. This is attributed to the change in the ratio characteristics which is described in detail in Section 5.9. The RE for the CDS method was much greater for the 24-hour event compared to the RE for the 2-hour event, which is expected because of the consistency provided by the CDS method in terms of average intensities. In other words, the average intensities of the 5, 10, 15-min, etc. remains constant, irrespective of the total duration of the event. This means the soil has reached a higher level of soil moisture content during a 24-hour event compared to a 2-hour event. The results of the DC5, DC10 and the DC20 curves relative to SA(T2) and SA(T3) is consistent with the SCS-SA design rainfall ratio comparison described in Section 4.5. The cause for the larger overestimation by the CDS, SA(T2), SA(T3), DC5, DC10 and DC20 at the Unisa station relative to the other stations is unknown but could be attributed to excessive missing data during 1999/00, 2000/01 and 2018/19, which led to a substantial deviation between the annual rainfall, as depicted in Figure 3.4. Although the number of locations used for the comparison was limited, the results indicated good peak discharge estimates. The comparison could be expanded to more locations considering different reaction times and catchment characteristics.

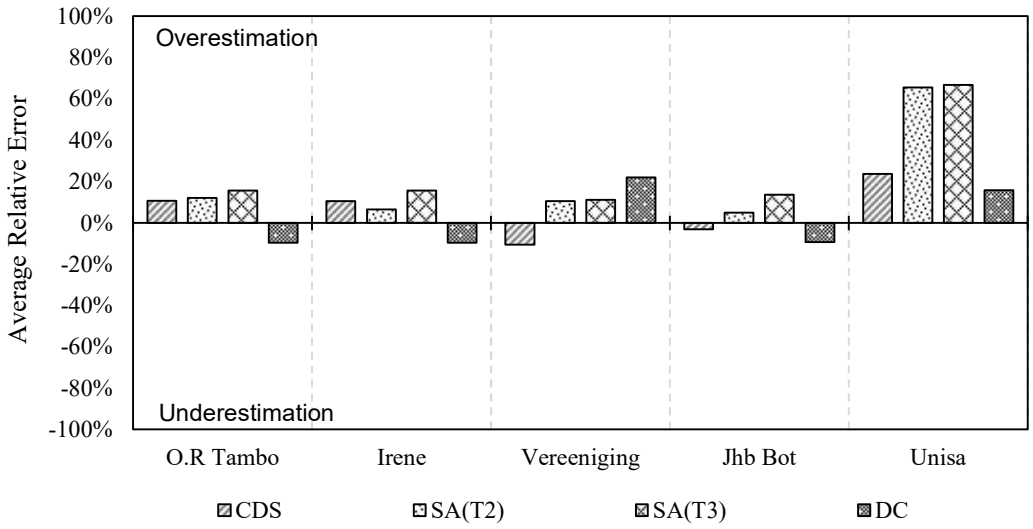

Figure 5.10: Average RE of the peak discharge at node O1 between continuous simulation and single event-based modelling using a 2-hour storm event

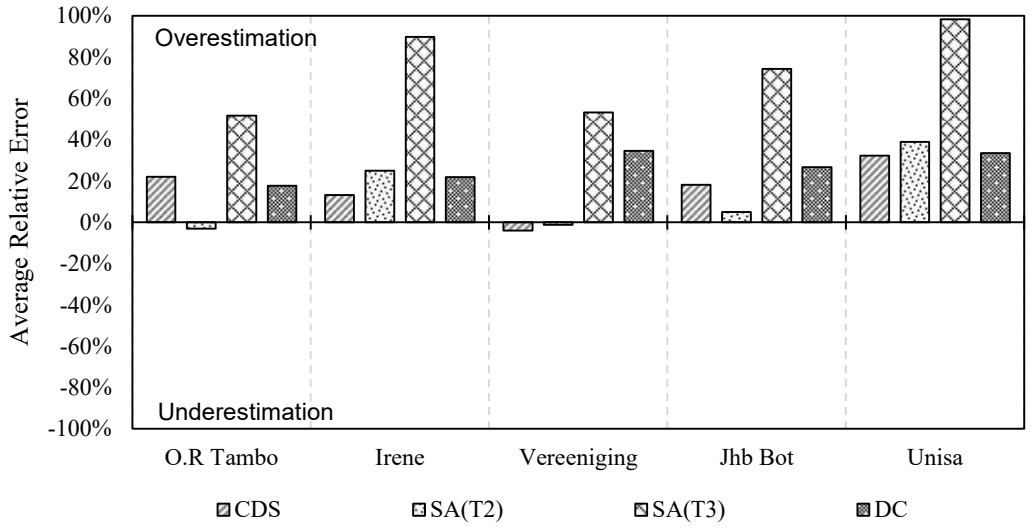

Figure 5.11: Average RE of the peak discharge at node O1 between continuous simulation and single event-based modelling using a 24-hour storm event

5.7 CRITICAL STORM DURATION

The critical duration refers to the duration which allows sufficient time for discharge to reach the outlet point. However, the duration must be as short as possible so that the discharge is not underestimated. This involves the simulation of multiple REC synthetic design storms, starting at 5-min and systematically increasing the duration until the discharge has reached a maximum.

If the duration of the REC synthetic design storm is less than the critical duration, the discharge from the remote parts of the catchment has not yet reached the point of discharge. This is according to Mulvaney (1851), as cited by Dooge (1974), who states that the peak discharge from the catchment will occur when the discharge from every portion of the catchment arrives simultaneously at the point of discharge. Conversely, if the duration exceeds the critical duration, the intensity of the synthetic design storm will be lower which will result in a lower peak discharge. The results of applying this concept to the catchment are shown in Figure 5.8, and using the design rainfall estimation for O.R Tambo described in Section 4.2 as input data, the critical storm duration was found to be 15-min, as shown in Figure 5.12.

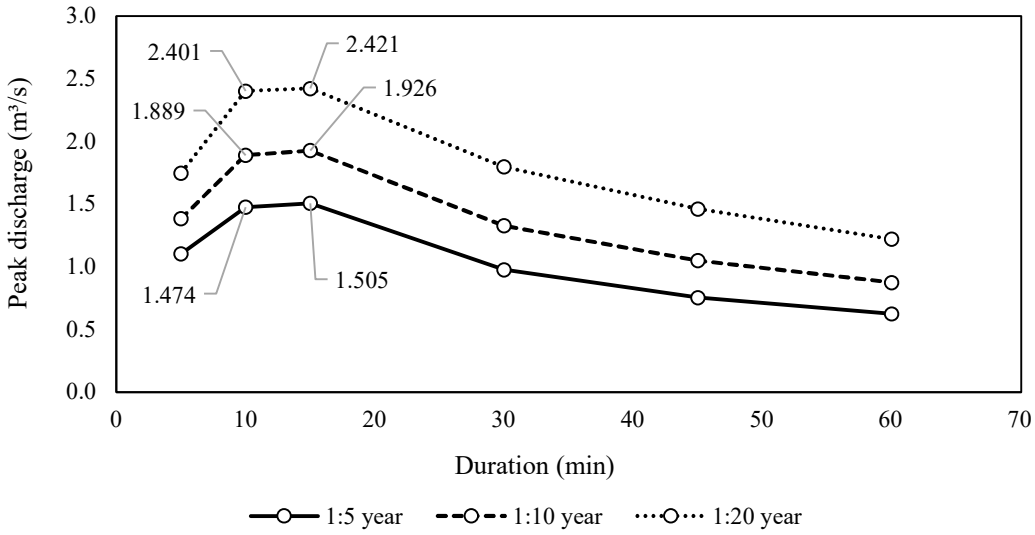

Figure 5.12: Critical storm duration for O.R Tambo according to the REC method

5.8 MINIMUM STORM DURATION FOR A TRIANGULAR HYETOGRAPH

The minimum duration applicable to the TRI method was determined by limiting the maximum intensity of the triangular hyetograph expressed in Equation to the maximum intensity following the PD analysis described in Section 4.2. An example of this limitation is depicted in Figure 5.13. From the IDF graph, the intensity of the 5-min duration is equal to 125 mm/h. However, the maximum intensity for a 5-min triangular hyetograph computed using Equation , is 250 mm/h. Therefore, generating a 5-min triangular hyetograph is incorrect. Limiting the triangular hyetograph to 30-min as shown in Figure 5.13, will therefore ensure that the peak intensity is not exceeded. The results for the five best stations, following this methodology, are depicted in Figure 5.14.

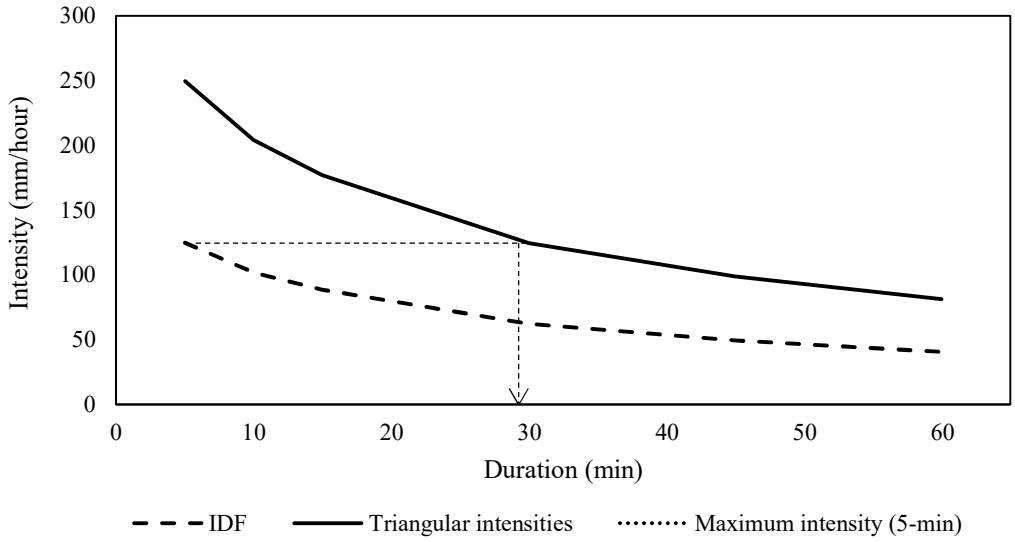

Figure 5.13: Example of determining the minimum storm duration for the TRI method

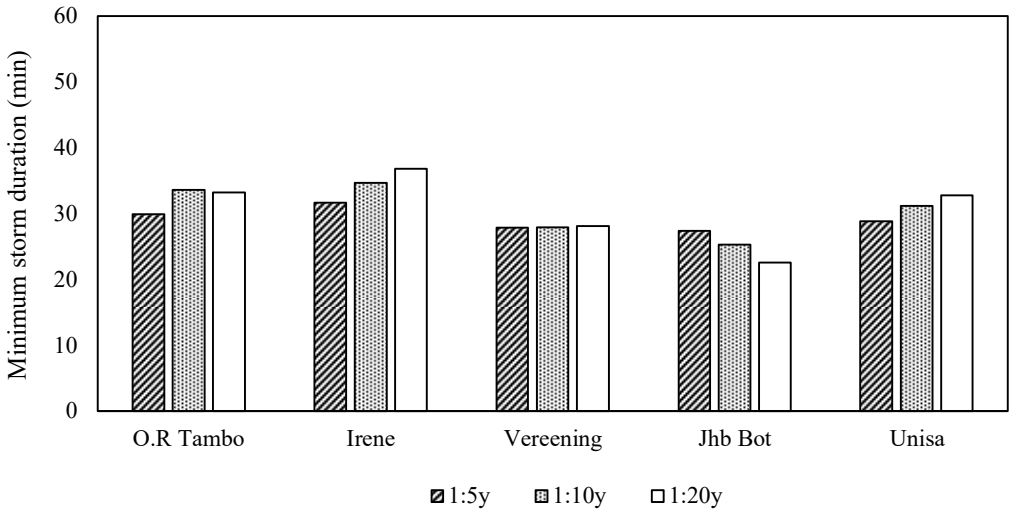

Figure 5.14: Result of the minimum storm durations for the five best stations in Gauteng

5.9 SCS-SA RATIOS FOR 2-HOUR EVENTS

To create 2-hour storm events from the standard SCS-SA curves, the development of a DC for a duration < 24-hours, as described in Chapter 4.4, was applied. This involved determining the D-hour to 2-hour ratios as depicted in Figure 5.15. Considering the critical storm duration of 15-min depicted in Figure 5.12, the ratios for the 2-hour, Types 2, 3 and 4 curves at 15-min duration, as depicted in Figure 5.15, are approximately equal. The 15-min ratios for the 24-hour storm event are, however, very different. This explains the difference between the peak discharge comparison for the SA(T2) and SA(T3) considering a 24-hour event compared to a 2-hour event, as described in Section 5.6.

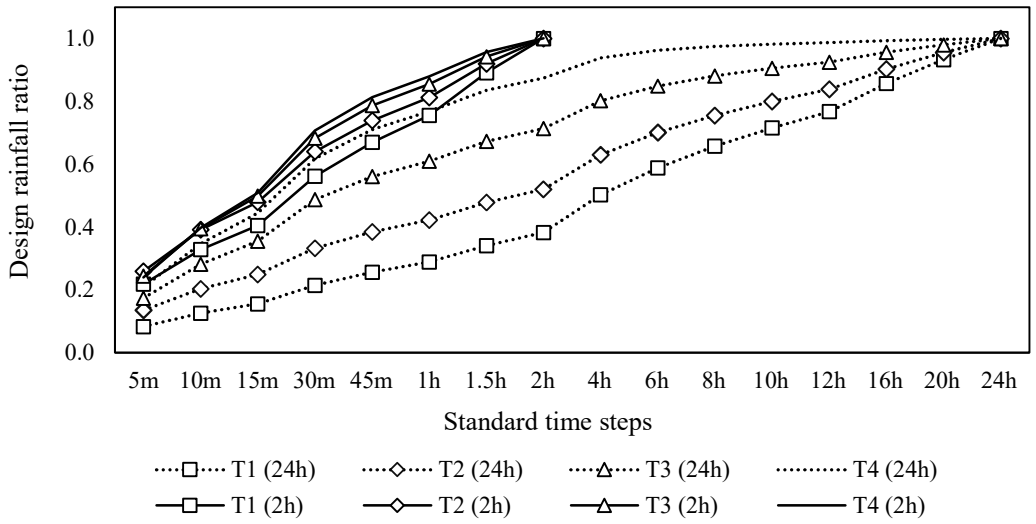

Figure 5.15: Design rainfall ratios in relation to 2-hour rainfall

5.10 SMOOTHED-PROBABILITY-INHERITED RUNOFF VOLUME

The methodology that was developed to determine the runoff volume from a continuous simulation model with a certain RI, is described in this section. Because the runoff volume from a single event-based model increases proportionally as the RI increases, the Smoothed-Probability-Inherited (SPI) methodology was developed to improve the consistency between runoff volume and peak discharge. This process is summarised as follows:

a) Identify each event from the continuous simulation model that resulted in the annual peak discharge and determine the limits of each event graphically.
b) Determine the RI of each event using the PD analysis results of the peak discharge. The runoff volume, therefore, automatically inherits the same RI as the peak discharge.
c) The runoff volume is smoothed using a logarithmic regression line, and the SPI runoff volume is determined using the general equation expressed in terms of Equation 5.4 as follows:

$$V_T = a \cdot ln(RI) + b \qquad \text{(Equation 5.4)}$$

where:

V_T = SPI runoff volume for recurrence interval T, and

a,b = logarithmic regression constants.

The event that resulted in the annual peak discharge is obtained from the continuous simulation model by extracting a three-day time series, one day before and one day after the date of the maximum. After the three-day time-series extraction, the limits of the event are determined by identifying the points of approximate zero discharge before and after the peak discharge. This process is illustrated using, for example, the rainfall event of 9 February 2020 for O.R Tambo. The three-day time series is depicted in Figure 5.16, the start and end of the event were identified, and the event was extracted for which the cumulative runoff volume was calculated as depicted in Figure 5.17.

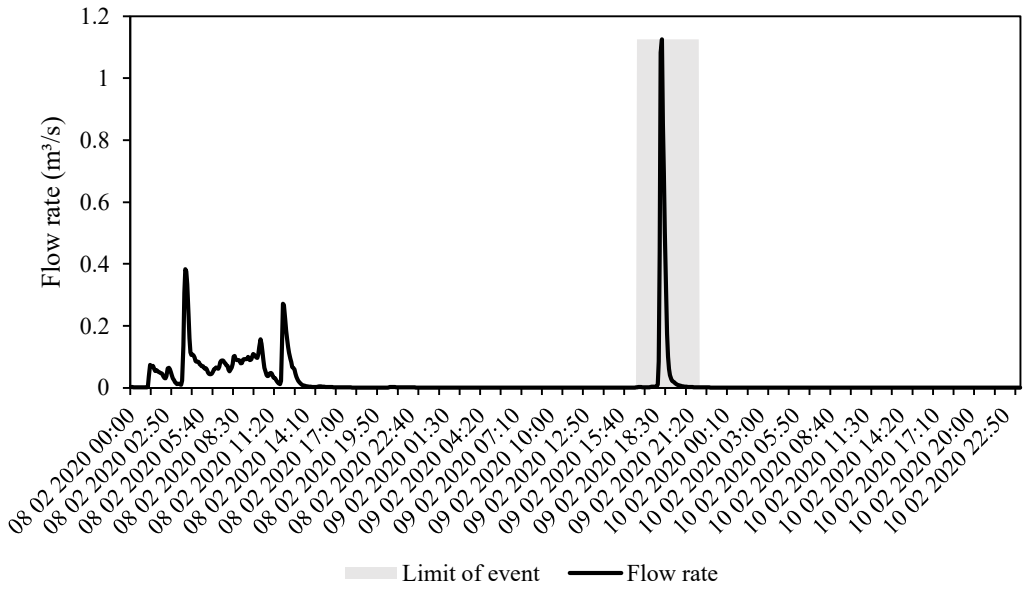

.

Figure 5.16: Three-day time series containing the event that resulted in the peak runoff at O.R. Tambo in the year 2020

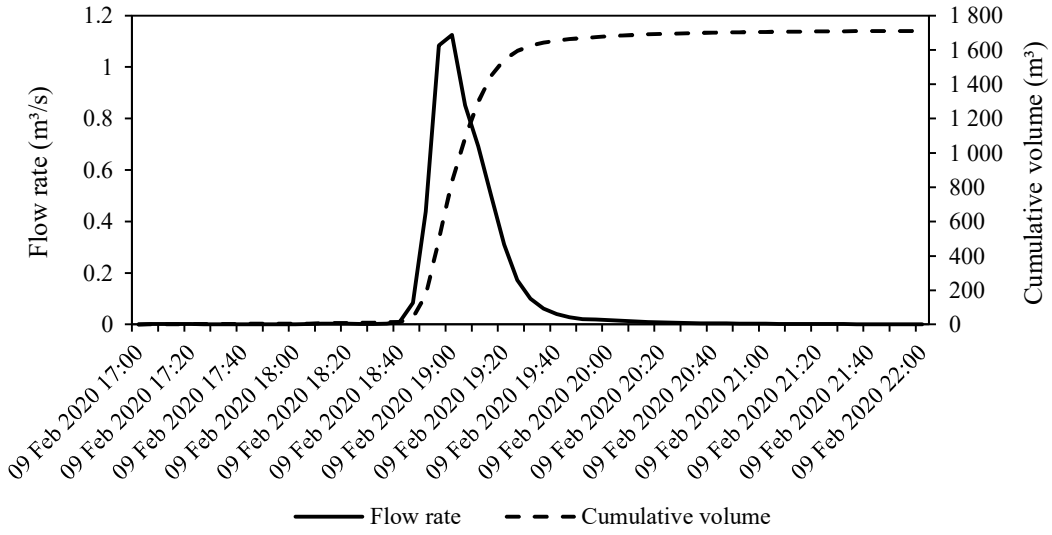

Figure 5.17: Extracted event that resulted in the peak runoff at O.R. Tambo in 2020

The process of extracting, identifying, and determining the runoff volume was repeated for each annual maximum peak discharge at each station. The scatter plots of the peak discharge and runoff volumes of the five stations are depicted in Figure 5.18. It was observed that a reasonable correlation exists between the peak discharge and runoff volumes with R^2 ranging between 0.439 and 0.795. The data at all five stations were statistically significant with p-values less than 0.001.

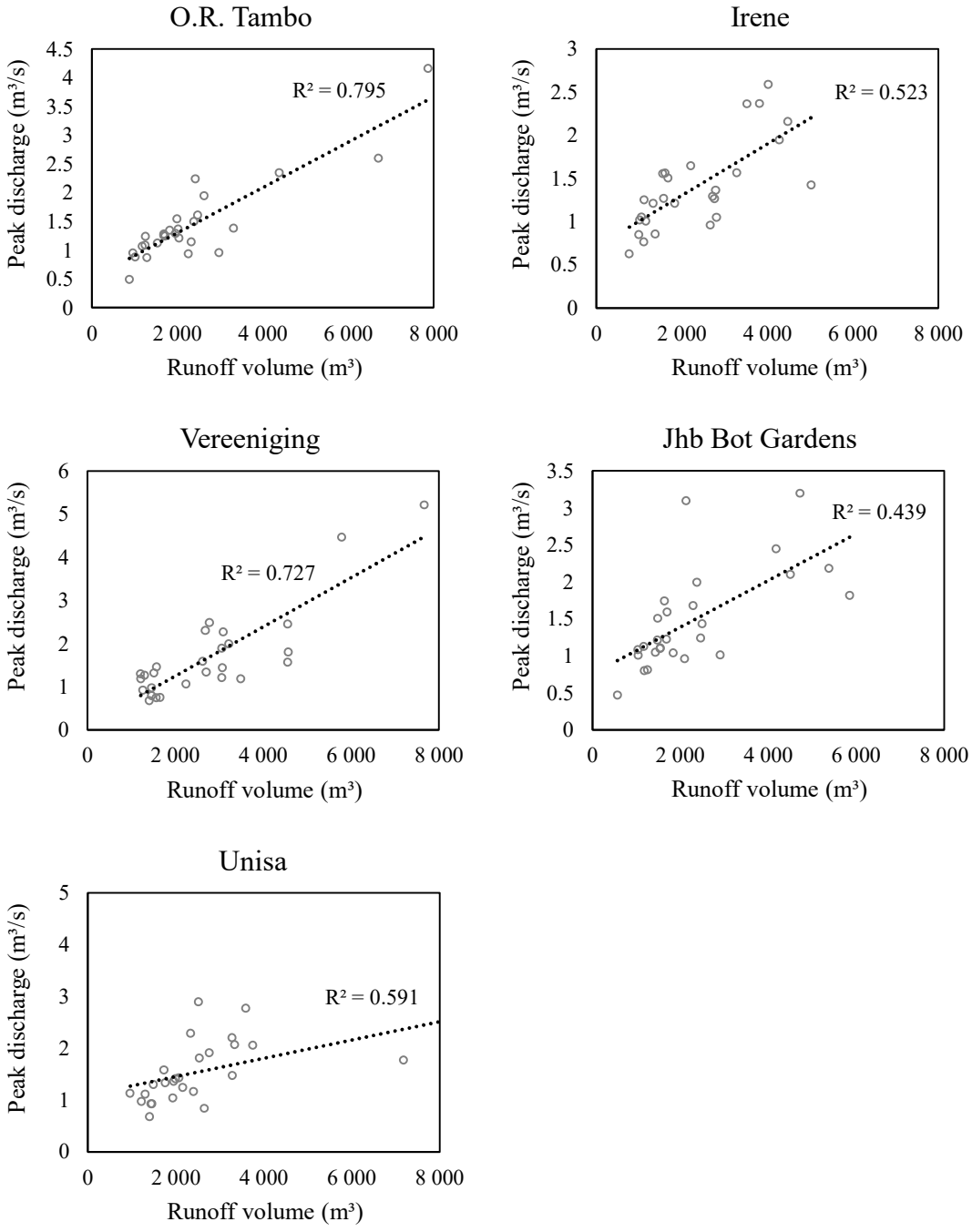

Figure 5.18: Annual maximum runoff rate and associated runoff volume obtained from a continuous simulation for O.R. Tambo

Following the calculation of each event's RI, using the PD analysis results to characterise the events, the inconsistency in the runoff volume's RI was observed by ranking the events in descending order as depicted in Figure 5.19. For example, the runoff volume in the years 2009, 1998 and 1995 for O.R Tambo should be ranked much higher considering the volume of runoff.

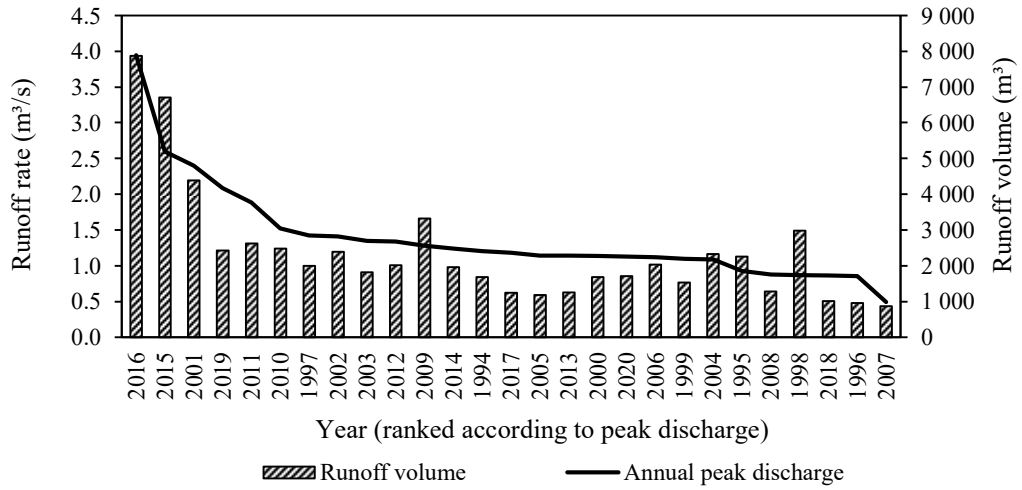

Figure 5.19: Annual peak discharge and corresponding runoff volume for O.R Tambo

Therefore, to prevent some runoff volumes with lower RIs to be more than others with higher Ris, the smoothing of the runoff volume was necessary to improve the consistency. A logarithmic regression line for the runoff volume with the RI as the dependent variable and runoff volume as the independent variable was determined. For example, the smoothing of O.R Tambo's runoff volume is depicted in Figure 5.20. The R^2 value of 0.802 indicated a reasonable fit to the data. The data was statistically significant with a p-value less than 0.001. The same process was followed for Irene, Vereeniging, Jhb Bot Gardens and Unisa for which the SPI runoff volumes with their respective R^2 values are summarised in Table 5.4.

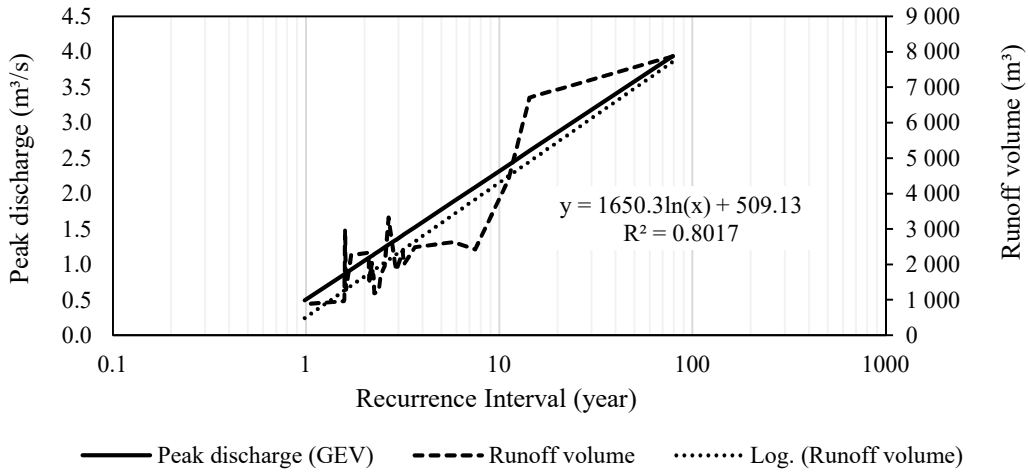

Figure 5.20: Typical smoothing of the probability-inherited runoff volume at O.R Tambo

Table 5.4: SPI runoff volumes

RI (years)	SPI RUNOFF VOLUME (m³)				
	O.R Tambo	Irene	Vereeniging	Jhb Bot	Unisa
1:5	3 165	3 072	3 047	2 750	1.958
1:10	4 309	3 713	3 991	3 328	2.461
1:20	5 453	4 354	4 936	3 907	3.062
R^2	0.802	0.522	0.727	0.439	0.591

5.11 RUNOFF VOLUME COMPARISON

The SPI runoff volumes summarised in Table 5.4 were used for comparison with the runoff volumes obtained from the single event-based simulations. The runoff volumes were determined at the outfall node O1 depicted in Figure 5.8, using all the synthetic design storms as input data. The average RE runoff volumes of the single event-based simulations is depicted in Figure 5.21. The 2-hour rather than the 24-hour event was used for the SA(T2), SA(T3), CDS and DC methods because the runoff volume from a 24-hour event would be much higher. This is because the total rainfall for a 24-hour synthetic design storm is equal to the 24-hour design rainfall which must exceed the 2-hour rainfall. As depicted in Figure 3.9, the 2-hour design rainfall was equal to approximately 50% of the 24-hour rainfall. The runoff volume from a 24-hour synthetic design storm must, therefore, also exceed the runoff volume from a 2-hour synthetic design storm. It was observed that the peak discharge was underestimated by between 47% and 72% using the REC and TRI methods. The peak discharge obtained from the SA(T2) and SA(T3) were overestimated by up to 19%. With the CDS it was generally underestimated by up to 22%, but for Irene and Jhb Bot Gardens, it was overestimated by up to 15%.

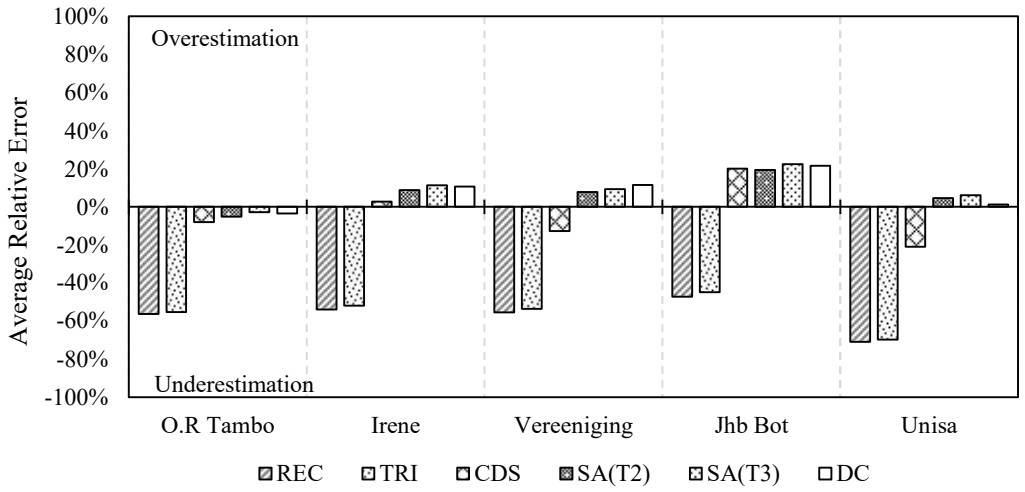

Figure 5.21: Average RE of the runoff volume between continuous simulation and single event-based modelling

This result was, however, not without doubt an indication of a method's failure to generate an accurate synthetic design storm. Instead, it indicated the accuracy of the end result of applying a method to a dynamic rainfall-runoff simulation model whilst ignoring other factors, like infiltration characteristics. It was also assumed that the result of a continuous simulation modelling, followed by the PD analysis of the peak discharge and the application of the SPI methodology, provided the true runoff volume for a particular RI. However, the results for the REC and TRI methods are certainly an indication of their inability to produce accurate runoff volumes, whereas the results for CDS and SCS-SA are much closer to the SPI runoff volume. Therefore, it can be safely concluded that the CDS and SCS-SA are appropriate methods for the generation of synthetic design storms for single event-based simulation modelling.

5.12 CHAPTER SUMMARY

This chapter has provided details of the synthetic design storm evaluations. The shape and average intensities of synthetic design storms were compared with observed storm events. It was concluded that the shape and average intensities of the REC method least represents observed events. It was, however, further demonstrated that the REC method can be used to determine the response time of a catchment. This was based on the concept of the critical duration which allows sufficient time for discharge from the entire catchment to reach the point of discharge.

The methods that consider an entire IDF curve, which includes the CDS, SA(T2), SA(T3) and DC methods, were also shown to be a poor representation of observed events. By manipulating the position of the peak intensity, it was demonstrated that the GOF was improved considerably. However, the variation of the RI relative to the average intensities of the standard time steps, also contributes to the poor GOF. It was demonstrated that the maximum RI of 6-hour and longer events is likely to be associated with the maximum standard duration. It was, however, concluded that the shape of synthetic design storms is not similar to observed events.

Following the shape and average intensity assessments, the synthetic design storms were used in a dynamic rainfall-runoff simulation model. A stormwater network in a catchment was simulated in SWMM. The rainfall data from the five best stations in Gauteng was used as input data for the model. The AMS of the flows and volumes were determined following a continuous simulation and a PD analysis was conducted. The results from the analysis were used as a baseline for the comparison with the results of single event-based simulations. The REC, TRI, CDS, SA(T2), SA(T3), DC5, DC10 and DC20 methods were used to generate synthetic design storms.

The results of the SA(T2) and SA(T3) was successfully related to the IC value, and it was demonstrated that the characteristics of 2-hour events were very different to 24-hour events.

The peak discharge results of the REC and TRI methods were underestimated, and therefore, the initial deficit associated with the infiltration parameters of the Green-Ampt model is questioned, for which further research is recommended. The effect of the location of peak intensity and the total duration of the storm event should also be further investigated as it was shown that these two parameters can have a significant effect on the peak discharge.

The next chapter contains a general discussion and conclusions drawn from the findings of this study and includes areas recommended for future research.

6 DISCUSSION, CONCLUSIONS, AND RECOMMENDATIONS

This chapter presents a discussion of the results of the study and conclusions that emanated from this study. The proposed way forward is also described.

6.1 OBJECTIVE

This study aimed to test the performance of the existing synthetic design storm generation methods, and to identify the method, or methods, most suited for conditions in small catchments in Gauteng, using the 5-min interval rainfall records obtained from the SAWS. The specific objectives of the study to meet this aim were to: (a) identify and assess the performance of currently available methods to estimate synthetic design storms used as input for single-event modelling in the selected pilot study area; and (b) to propose an improved procedure to generate a more accurate synthetic design storm applicable to small catchment areas in the study area.

6.2 DISCUSSION

The literature review found that existing synthetic design storms have a strong scientific basis, with synthetic design storms being classified into three categories: (a) methods that are derived from the IDF curves which includes the CDS, REC, TRI, SCS and SCS-SA; (b) standardised mass curves generated directly from rainfall records, which includes the Huff and NOAA Atlas 14 curves; and (c) the simulation from a stochastic rainfall model, which includes the daily rainfall disaggregation model for South Africa.

Although the existing synthetic design storms were developed using the best data, technology, and engineering judgement available at the time, they do present a degree of insufficiency. For example, the total precipitation volume is systematically underestimated by the rectangular hyetograph (Arnell, 1982), and it was also realised that it gives a wrong picture of a hyetograph (Niemczynowicz, 1982). In terms of the triangular hyetograph method, Veneziano and Villani (1999) have noticed that, although it is quite simple and intuitive, it does not have a strong conceptual basis and may produce biased flow estimates. The CDS method, on the other hand, uses point rainfall data that applies to a particular site and therefore the variability and unique character of the rainfall patterns will automatically be embedded in the CDS method. Methods that use the entire IDF curve to generate a synthetic design storm hold much potential since the design rainfall has been regionalised by Smithers and Schulze (2000). Some of the variability and unique character of the rainfall pattern will therefore automatically be embedded in these methods.

The first aim of this study was to identify and assess the performance of currently available methods to estimate synthetic design storms used as input for single-event modelling in the selected pilot study area. In order to achieve this aim, short-duration observed rainfall data recorded at 35 automatic rainfall stations situated in the Gauteng province, were collected, and assessed in terms of completeness. The missing data and the data period of each station were used to classify the data quality of each rainfall station. A station was classified as either good, average or poor, depending on the selected classification criteria. The stations with poor data sets were omitted from the study, whereas the good and average stations were used in subsequent investigations. Five stations have good data sets with each having a data period of 26 years and less than 5% of missing data during the rainy months. A further 17 stations were identified with average quality data sets but six stations were downgraded because of substantial deviations in their annual rainfall data.

The criteria used for the identification of individual events were also described. These criteria consisted of: (a) an MDP ranging from 0 to 120-min; (b) an MRD of 10 mm; and (c) an MRI of 1:2 years. The correlation between the total storm duration and total rainfall depth increased as the MDP increased, which contradicts the findings from Ramlall (2020), perhaps because of the difference in the storm event identification criteria. However, this study is based on an MDP associated with the reaction time of a small urban catchment. The use of an MDP of 15-min, which is representative of the catchment size targeted in this study, was based on the argument that if the MDP exceeds the time of concentration, any rainfall after the dry period could no longer influence the peak discharge of the previous spell. Appropriate storm parameters were determined which were 0.38 for the advancement coefficient and 0.20 for the dimensionless time to peak. The determination of regression coefficients for any DDF curve, using the GRG nonlinear algorithm to determine appropriate coefficients, was demonstrated.

Design rainfalls were determined using the at-site AMS for 16 standard durations for each station and compared with the design rainfall obtained from the DRESA software. It was found that the average RD was within the 90% upper and lower bounds given by the DRESA software. Short duration design rainfall of between 5-min and 1.5-hour was identified to deviate substantially from the DRESA software and further investigation is recommended to identify the cause.

The procedure to distribute design rainfall equally around the peak intensity was adapted to utilize the concept of incremental intensities for the interpolation of design rainfall for intermediate time steps. This was subsequently used to generate the DC5, DC10 and the DC20 curves from the design rainfall developed from the PD analysis. The procedure to extract an event of less than 24-hour was also illustrated.

The D-hour to 24-hour ratios were also determined and their position relative to the four standard SCS-SA curves were determined, using the design rainfall of the DRESA software as well as the at-site design rainfall analysis. The results from both sources of design rainfall indicated that, on average, Gauteng conforms more closely to the SCS-SA Type 2 curve, rather than Type 3. However, a significant variation in the ratios for the various durations were observed because the derived ratios plotted between standard SCS-SA type curves. This led to the development of IC values and intermediate curves whereby a curve is linearly interpolated between two standard type curves. The method of interpolating between standard type curves was also documented.

The design rainfall ratios of the SCS curves were compared with the SCS-SA curves as well as the at-site design rainfall ratios. It was observed that the Type II curve contains the highest ratios for the 5-min to 6-hour time steps which marginally exceed the ratios of the SCS-SA Type 2 curve. The highest IC value achieved with the Type II curve was 2.31 for the 30-min time step. The Type II curve can, therefore, only be applied to areas with a similar IC value, and to catchments with a 30-min response time. From the comparison with the at-site design rainfall ratios, it was observed that very few stations conform to the Type II curve, and that the majority exceeds the 30-min ratio. This analysis has, therefore, shown that the use of the SCS curves is very limited and must be used with caution.

A methodology for determining regression coefficients for the CDS method, using the GRG non-linear solver was also developed. The simulated design rainfall intensities, using the regression coefficients, were evaluated by determining the RE of the actual design rainfall intensities obtained from the DRESA software. From this analysis it was evident that the results obtained from the methodology, involving the GRG non-linear solver, were sufficiently accurate to determine the regression coefficients required by the CDS method.

Standardised mass curves (Huff curves) were developed for quartiles with sufficient sample sizes. These curves were successfully fitted to 9th order polynomials using a ranking system to find the n^{th} polynomial that fitted the data points the best. The polynomials were subsequently used to generate 24-hour synthetic design storms and the maximum ratios for the standard time steps were compared with the at-site design rainfall ratios. Based on this analysis it was concluded that standardised mass curves underestimate short duration design rainfall and will, therefore, result in an underestimation of the peak discharge if used for single event-based modelling of a small urban stormwater network.

The synthetic design storm evaluation was conducted by comparing the synthetic design storms with the observed rainfall events. Two aspects were evaluated, namely the shape of the mass curves, as well as the average intensities embedded in each synthetic design storm. It was concluded that the shape and average intensities of the REC method least represents observed events. It was, however, further demonstrated that the REC method can be used to determine the response time of a catchment. This was based on the concept of the critical duration which allows sufficient time for discharge from the entire catchment to reach the point of discharge.

The methods that consider an entire IDF curve, which include the CDS, SA(T2), SA(T3) and DC methods, were also shown to be a poor representation of observed events. By manipulating the position of the peak intensity, it was demonstrated that the GOF has improved considerably. However, the variation of the RI relative to the average intensities of the standard time steps, also contributes to the poor GOF. It was also demonstrated that the maximum RI of 6-hour and longer events is likely to be associated with the maximum standard duration. It was, however, concluded that the shapes of synthetic design storms are not similar to observed events. This analysis provided evidence that synthetic design storms do not exist in nature.

Following the shape and average intensity assessments, the synthetic design storms were used in a dynamic rainfall-runoff simulation model. A stormwater network in a catchment was simulated in SWMM. The rainfall data from the five best stations in Gauteng was used as input data for the model. The AMS of the flows and volumes were determined following a continuous simulation and a PD analysis was conducted. The results from the analysis were used as a baseline for the comparison with the results of single event-based simulations. The REC, TRI, CDS, SA(T2), SA(T3), DC5, DC10 and DC20 methods were used to generate synthetic design storms.

The results of the SA(T2) and SA(T3) were successfully related to the IC values, and it was demonstrated that the characteristics of 2-hour events were very different to 24-hour events. Various observations were made from these results of which the most important was that the suggested values for the initial deficit associated with the Green-Ampt infiltration parameters did not result in good simulations. This, however, falls outside the scope of this study and further investigation is recommended. The effect of the location of peak intensity and the total duration of the storm event should also be further investigated as it was shown that these two parameters can have a significant effect on the peak discharge.

The CDS method was also shown to provide consistent results compared to continuous simulation. However, a sensitivity analysis must be conducted to determine the effect of the advancement coefficient and total storm duration on the peak discharge. The advantages of the CDS method are summarised as follows:

a) The IDF coefficients can be accurately determined from the design rainfall obtained from the DRESA software, which can be used to generate a synthetic design storm.

b) The location of the peak intensity concerning the total duration of the event can be adjusted to be anywhere between the start and end of the event.

6.3 CONCLUSIONS

It is, in general, concluded that synthetic design storms, applied to a single event-based model, provides the engineer with the ability to assess the complex hydrological and hydraulic characteristics of an urban stormwater network. Despite its unrealistic assumptions, shortcomings, and the criticism the synthetic design storm concept has received, applying it to a single event-based model has resulted in good peak discharge and runoff volume estimates. Two methods to generate synthetic design storms were identified that could be applied to a single event-based model. They are the SCS-SA and CDS methods. The methodology that was used to determine the CDS regression coefficients from the DRESA design rainfall was sufficient and resulted in good results when applied to a single event-based simulation. The design rainfall ratio comparisons from both the at-site and DRESA design rainfall, provided the bases to conclude the inappropriateness of the SCS-SA Type 3 curve for Gauteng. However, it was also concluded that interpolation between the standard type curves is needed for better single event-based simulation results. The REC method provides a means of evaluating the response time of an urban catchment, but the initial deficit defined as the difference between the porosity and field capacity, associated with the Green-Ampt infiltration method, did not result in good simulations.

It can, therefore, be concluded that the project aims were achieved, namely:

a) The performance of currently available methods to estimate synthetic design storms was assessed and used as input for single-event modelling in the selected pilot study area.

b) An improved procedure to generate a synthetic design storm applicable to small catchment areas in the study area was proposed through the development of intermediate SCS-SA curve types. The intermediate curves could be used in combination with the interpolated map of Gauteng with lower values to the north of the province and higher values to the south.

The objective of the study was therefore successfully achieved by the identification of the two methods that are suitable for single event-based modelling. These methods are the CDS with location-specific regression coefficients and the SCS-SA curves with intermediate curves that was developed for better modelling of different regions in Gauteng.

6.4 RECOMMENDATIONS

Recommendations that emanated from this study are summarised as follows:

a) The impact the advancement coefficient and total storm duration have on the peak discharge must be investigated by conducting a sensitivity analysis. Other parameters that could also be considered for the analysis includes the size of the catchment, slope, roughness, and soil types.

b) The impact that missing data has on the design rainfall estimation and by implication the design rainfall ratios, in the context of this study, should be investigated.

c) The current DRESA software, be further developed to provide the user with an opportunity to determine a synthetic design storm for a specific location.

d) The discrepancy between the dates of the daily and 5-min data, and the annual maximum daily rainfalls from the daily and the 5-min data should be further investigated.

e) The effect of data smoothing on design rainfall estimation must be investigated.

f) The appropriateness of the GEV PD for short duration rainfall should be re-confirmed.

g) An appropriate exponent for the IDW interpolation technique should be investigated, as well as the appropriateness of the technique itself to interpolate IC values.

h) The suggested values for the initial deficit associated with the Green-Ampt infiltration parameters should be investigated.

i) The relevance of the CDS and SCS-SA methods for generating synthetic design storms applicable to single event-based modelling of small urban catchments must be expanded on a national scale, with the possibility of following a regional approach and ensemble modelling investigated.

j) The interrelatedness of a PD analysis, missing data, discrepancies in the 5-min rainfall data, the RD between DRESA and at-site design rainfall, and the classification of a hydrological year should be investigated.

k) The increase in RD between DRESA and at-site design rainfall, possible homogeneous regions, and regional growth curves for the lower order standard times steps (< 2-hour) should be investigated.

7 REFERENCES

Adamson, P. T. 1981. *Southern African storm rainfall.* Technical Report No TR 102, Department of Environment Affairs, Pretoria, RSA. pp 19.

Adams, B.J. and Howard, C.D., 1986. Design storm pathology. *Canadian Water Resources Journal*, Vol 11, No 3, pp 49-55.

Al-Saadi, R. 2002. *Hyetograph estimation for the State of Texas.* Texas Tech University, Department of Civil Engineering, Lubbock, Texas, United States.

Arnell, V. 1982. Estimating runoff volumes from urban areas. *Journal of the American Water Resource Association,* Vol 18, No 3, June, pp 383-387.

Asquith, W. H. Bumgarner, J. R. and Fahlquist, L. S. 2003. A triangular model of dimensionless runoff producing rainfall hyetographs in Texas. *Journal of the American Water Resources Association,* Vol 39, No 4, June, pp 911-921.

Balbastre-Soldevila, R., García-Bartual, R. and Andrés-Doménech, I., 2019. A comparison of design storms for urban drainage system applications. *Water*, Vol 11, No 4, pp 757.

Bonnin, M. Martin, D. Lin, B. Parzybok, T. Yekta, M. and Riley, D. 2011. NOAA Atlas 14 Volume 1 Version 5, *Precipitation-Frequency Atlas for the United States.* NOAA, National Weather Service, Silver Spring, MD, USA.

Bonta, J. V. 1997. Proposed use of Huff Curves for hyetograph characterization. pp 111-124. In: C.W. Richardson *et al. (ed.)* Proceedings of the Workshop on Climate and Weather Research. Denver, Colorado. July 17-19, 1995. USDA-Agricultural Research Services, 1996-03, pp 223.

Bonta, J. V. 2004. Development and utility of Huff curves for disaggregating precipitation amounts. *Applied Engineering in Agriculture*, Vol 20, No 5, pp 641-653.

Bonta, J. V. and Shahalam, A. 2003. Cumulative storm rainfall distributions: comparison of Huff curves.*Journal of Hydrology*, Vol 42, No 1, June, pp 65-74.

Boughton, W. 2000. *A model for disaggregating daily to hourly rainfall for design flood estimation.* Cooperative Research Centre for Catchment Hydrology, Monash University, Clayton, Victoria, Australia. Report 00/15, 36 pp.

Boussinesq, J. and Flamant, A. 1886. Notice sur la vie et les travaux de Barré de Saint-Venant. *Annales des ponts et chaussées*, Vol 12, pp 557-595.

Brooker, C. 2021. Personal communication, 22 February 2021, Mr Chris Brooker, CBA Specialist Engineering, Gauteng, South Africa, 2055.

Cordery, I. and Pilgrim, D. 1993. *Handbook of hydrology.* McGraw-Hill, New York, USA.

Cronshey, R. 1986. *Urban hydrology for small watersheds*. US Dept. of Agriculture, Soil Conservation Service, Engineering Division.

Dooge, J.C. 1974. The development of hydrological concepts in Britain and Ireland between 1674 and 1874. *Hydrological Sciences Journal*, Vol 19, No 3, pp 279-302.

Ellouze, E. Azri, C. and Abida, H. 2009. Spatial variability of monthly and annual rainfall data over Southern Tunisia. *Atmospheric Research,* Vol 93, No 4, pp 832-839.

El-Sayed, E. A. H. 2017. Development of synthetic rainfall distribution curves for Sinai area. *Ain Shams Engineering Journal*, Vol 9, No 4, December, pp 1949-1957.

Gironás, J., Roesner, L.A., Davis, J., Rossman, L.A. and Supply, W. 2009. *Storm water management model applications manual*. Cincinnati, OH: National Risk Management Research Laboratory, Office of Research and Development, US Environmental Protection Agency.

Gomez, M. and Sanchez, X. 2014. *Rational method application (Lecture notes).*5 December 2020, https://ocw.camins.upc.edu/ocw/home.htm?execution=e1s6.

Green, W. H. and Ampt, G.A. 1911. Studies on Soil Physics. *The Journal of Agricultural Science,* Vol 4, No 1, pp 1-24.

Horton, R. E. 1933. The role of infiltration in the hydrologic cycle. *Transactions American Geophysical Union,* Vol 14, No 1, June, pp 446-460.

Huff, F. A. 1967. Time distribution of rainfall in heavy storms. *Water Resources Research*, Vol 3, No 4, December, pp 1007-1019.

Huff, F. A. 1990. *Time distributions of heavy rainstorms in Illinois.* Department of energy and natural resources, Champaign.

Hydrological Research Unit. 1972. Design flood determination in South Africa: Report No 1/72.

Izzard, C. F. 1946. Hydraulics of runoff from developed surfaces. *Proceedings, highway research board,* Vol 26, pp 129-146.

Keifer, C. J. and Chu, H. H. 1957. Synthetic storm pattern for drainage design. *ASCE Journal of the hydraulics division,* Vol 83, No 4, pp 1332.1-1332.25.

Knoesen, D.M. 2005. *The development and assessment of techniques for daily rainfall disaggregation in South Africa.* University of KwaZulu-Natal, School of Bioresources Engineering and Environmental Hydrology, Pietermaritzburg.

Lasdon, L.S., Waren, A.D., Jain, A. and Ratner, M. 1978. Design and testing of a generalized reduced gradient code for nonlinear programming. *ACM Transactions on Mathematical Software (TOMS)*, Vol 4, No 1, pp 34-50.

Linnerts, S. 2022. Personal communication, 23 September 2022, Me Samantha Linnerts, South African Weather Service, Gauteng, South Africa, 0157.

Males, R. Braune, M. van Bladeren, D. and Mahlangu, D.J. 2004. Regional hydrological modelling of City of Tshwane municipality using Visual SWMM. *Journal of Water Management Modelling,* Vol 12, No R220-30, pp 627-649.

Malik, U. and James, W. 2007. Reliability of design storms used to size urban stormwater system elements. *Journal of water management modelling*, pp 309-326.

Mhlongo, P. 2022. Personal communication, 6 January 2022, Ms Prisca Mhlongo, Ilifa Africa Engineers, Gauteng, South Africa, 1734.

Moeletsi, M.E.A.R.C., Shabalala, Z.P.A.R.C., De Nysschen, G.A.R.C., Moeletsi, M.E. and Walker, S. 2016. Evaluation of an inverse distance weighting method for patching daily and dekadal rainfall over the Free State Province, South Africa. *Water SA*, Vol 42, No 3, pp 466-474.

Mulvaney, T.J. 1851. On the use of self-registering rain and flood gauges in making observations of the relations of rainfall and flood discharges in a given catchment. *Proceedings of the institution of Civil Engineers of Ireland*, No *4*, pp 19-31.

Munro, G. 2021. Personal communication, 23 August 2021, Mr Gerhard Munro, Oracle Java Certified SE Programmer, Gauteng, South Africa, 1709.

Niemczynowicz, J. 1982. *Areal intensity duration frequency curves for short term rainfall events in Lund.* Hydrology Research, Sweden.

NRCS. 2019. National Engineering Handbook. Part 630 Hydrology. *Chapter 4: Storm rainfall depth and distribution.* Department of Agriculture, Washington.

NRCS, 2020. United States Department of Agriculture, September 2021, https://www.nrcs.usda.gov/wps/portal/nrcs/detailfull/national/water/manage/hydrology/?cid=stelprdb1044959.

Pan, C. Wang, X. Liu, L. Huang, H. and Wang, D. 2017. Improvement to the Huff curve for design storms and urban flooding simulations in Guangzhou, China. Water, Vol 9, No 6. pp 411.

Perica, S. Pavloci, S. St. Laurent, M. Trypaluk, C. Unruh, D. and Wilhite, O. 2018. NOAA Atlas 14 Volume 11 Version 2, *Precipitation-Frequency Atlas for the United States, Texas.* National Weather Service, Silver Spring, MD.

Prodanovic, P. and Simonovic, S.P. 2004. *Generation of synthetic design storms for the Upper Thames River basin*. Department of Civil and Environmental Engineering, The University of Western Ontario.

Ramlall, R. 2020. *Assessing the performance of techniques for disaggregating daily rainfall for design flood estimation in South Africa.* University of KwaZulu-Natal, School of Agricultural Earth and Environmental Sciences, Pietermaritzburg.

Restrepo, P. J. and Eagleson, P. S. 1982. Identification of independent rainstorms.*Journal of Hydrology*, Vol 55, pp 303-319.

Schmidt, E.J. and Schulze, R. E. 1987. *Design stormflow and peak discharge rates for small catchments in Southern Africa.* Water Research Commission. WRC Report No. TT 31/87. Pretoria. pp 65-70.

Schulze, R. E. 1984. *Hydrological models for application to small rural catchments in southern Africa: Refinements and development.* University of Natal, Department of Agricultural Engineering, Pietermaritzburg.

Schulze, R. E. and Arnold, H. 1979. *Estimation of volume and rate of runoff in small catchments in South Africa, based on the SCS technique.* University of Natal, Department of Agricultural Engineering, Pietermaritzburg.

SCS. 1973. *A method for estimating volume and rate of runoff in small watersheds.* US Department of Agriculture, Soil Conservation Service, Washington, D.C.

Shepard, D. 1968. A two-dimensional interpolation function for irregularly-spaced data. *In Proceedings of the 1968 23rd ACM national conference*, pp. 517-524.

Sherman, C. 1931. Frequency and intensity of excessive rainfall at Boston, Massachusetts. *American Society of Civil Engineers,* Vol 95, No 1, pp 951-960.

Sherman, C. 1932. The relation of hydrographs of runoff to size and character of drainage-basins, Eos. *Transactions American Geophysical Union,* Vol 13, No 1, pp 332-339.

Silveira, A. L. L. 2016. Cumulative equations for continuous time Chicago hyetograph method. *Brazilian Journal of Water Resources,* Vol 21, No 3, pp 646-651.

Smith, A. A. 2004. MIDUSS Version 2, Reference Manual. Alan A. Smith Inc., Dundas, Ontario, Canada.

Smithers, J.C., 1996. Short-duration rainfall frequency model selection in Southern Africa. *Water SA*, Vol 22*, No* 3, pp 211-217.

Smithers, J. C. 2012. *Methods for design flood estimation in South Africa.* Water Research Commission, Vol 38, No 4, July, pp 633-646.

Smithers, J. C. and Schulze, R. E. 2000. *Development and evaluation of techniques for estimating short duration design rainfall in South Africa.* Water Research Commission.WRC Report No. 681/1/00. Pretoria.

Smithers, J.C. and Schulze, R.E. 2002. *The estimation of design rainfall for Tshwane – Report to SRK Consulting*. School of Bioresources Engineering and Environmental Hydrology. Pietermaritzburg. ACRUcons Report 38.

Smithers, J. C. and Schulze, R. E. 2003. *Design rainfall and flood estimation in South Africa.* Water Research Commission.WRC Report No 1060/01/03. Pretoria.

Veneziano, D. and Villani, P. 1999. Best linear unbiased design hyetograph. *Water Resources Research*, Vol 35, No 9, September, pp 2725-2738.

Wartalska, K. Kaźmierczak, B. Nowakowska, M. and Kotowski, A. 2020. Analysis of hyetographs for drainage system modeling. Water, Vol 12, No 1, pp 149.

Watson, M. D. 1981. *Application of ILLUDAS to stormwater drainage design in South Africa.* University of the Witwatersrand, Johannesburg.

Watt, E. and Marsalek, J. 2013. Critical review of the evolution of the design storm event concept. *Canadian Journal of Civil Engineering*, Vol 40, No 2, pp 105-113.

Weddepohl, J. P. 1988. *Design rainfall distributions for southern Africa.* University of Natal, Department of Agricultural Engineering, Pietermaritzburg.

Weesakul, U. Chaowiwat, W. Rehan, M.M. and Weesakul, S. 2017. Modification of a design storm pattern for urban drainage systems considering the impact of climate change. *Engineering and Applied Science Research,* Vol 44, No 3, pp 161-169.

U.S. Weather Bureau. 1961. Generalised Estimates of Probable Maximum Precipitation and Rainfall-Frequency Data for Puerto Rico and Virgin Islands. *U.S. Department, Soil Conservation Service,* Technical paper, No 42.

Yen, B. C. and Chow, V. T. 1980. Design hyetographs for small drainage structures. *ASCA Journal of the hydraulics division,* Vol 106, No HY6, pp 1055-76.

Yu, Y. S. and McNown, J. S. 1964. Runoff from impervious surfaces. *Journal of hydraulic research,* Vol 2, No 1, pp 3-23.

ANNEXURE A

AN ALTERNATIVE DEVELOPMENT OF THE CUMULATIVE RAINFALL FORMULAE FOR THE CHICAGO DESIGN STORM METHOD

The development of the instantaneous intensity formula associated with the CDS method is well documented by Keifer and Chu (1957), and other authors like Watson (1981), Smith (2004) and Silveira (2016). The instantaneous intensity formula is based on the Sherman (1931) average intensity function, which can be proven by using the quotient rule for differentiation of functions (Mhlongo, 2022).

Keifer and Chu (1957) also introduced the advancement coefficient that was used to develop formulae for the instantaneous intensity before and after the peak intensity. Silveira (2016) integrated the formulae from the start of an event, which results in the cumulative rainfall formulae expressed in Equations A.1 and A.2 as follows:

$$P_t(t_0 < t \leq t_p) = r \cdot P - \frac{a(t_p - t)}{60 \cdot \left(b + \frac{t_p - t}{r}\right)^c} \qquad \text{(Equation A.1)}$$

and:

$$P_t(t > t_p) = r \cdot P + \frac{a(t - t_p)}{60 \cdot \left(b + \frac{t - t_p}{1 - r}\right)^c} \qquad \text{(Equation A.2)}$$

where:

P_t = cumulative rainfall from the start to any time interval of the storm event (mm),

P = total rainfall (mm),

r = storm advancement coefficient.

t = any time interval measured from the start of the event (min), and

t_p = time to peak intensity (min).

a,b,c = IDF regression coefficients.

However, an alternative and simpler development of Equations A.1 and A.2 is proposed which is independent of the instantaneous formulae. As before, the relationship between the average intensity and duration has a sigmoidal shape which is defined by Sherman (1931) in terms of the storm duration and the IDF regression coefficients as follows:

$$i_{av} = \frac{a}{(b + t_d)^c} \qquad \text{(Equation A.3)}$$

where:

i_{av} = average rainfall intensity (mm/hour),

However, if the peak intensity of a synthetic design storm is located anywhere between the start and end of the event, the storm duration is equal to the sum of the time before and after the peak intensity as follows:

$$t_d = t_b + t_a \qquad \text{(Equation A.4)}$$

where:

t_b = storm duration before the peak intensity (min), and

t_a = storm duration after the peak intensity (min).

And, if the advancement coefficient is defined as the ratio between the time before the peak intensity and the storm duration as follows:

$$\frac{t_b}{t_d} = r$$

$$\therefore t_d = \frac{t_b}{r} \qquad \text{(Equation A.5)}$$

Then, by substituting Equation A.5 in A.3, the average intensity before the peak intensity is as follows:

$$i_{b\,av} = \frac{a}{\left(b + \frac{t_b}{r}\right)^c} \qquad \text{(Equation A.6)}$$

where:

$i_{b\,av}$ = average intensity before the peak intensity (mm/hour).

However, by multiplying the average intensity with the duration before the peak intensity, the cumulative rainfall before the peak intensity, measured backwards from the peak intensity, is therefore:

$$P_b = \frac{t_b}{60} \cdot \frac{a}{\left(b + \frac{t_b}{r}\right)^c} \qquad \text{(Equation A.7)}$$

where:

P_b = total rainfall before the peak intensity (mm).

Because of similarity, the total rainfall before the peak intensity can also be expressed in terms of the storm advancement coefficient as follows:

$$P_b = r \cdot P \qquad \text{(Equation A.8)}$$

Therefore, for any duration measured backwards from the peak intensity, the cumulative rainfall is defined as the difference between Equations A.8 and A.7 as follows:

$$P_b = r \cdot P - \frac{t_b \cdot a}{60 \cdot \left(b + \frac{t_b}{r}\right)^c} \qquad \text{(Equation A.9)}$$

However, if time is measured from the start of the event (t_0) to the peak intensity, the time measure backwards from the peak intensity is as follows:

$$t_b = t_p - t \qquad \text{(Equation A.10)}$$

where:

t_p = duration from the start of the event to the peak intensity (min).

And, by substituting Equation A.10 in A.9, the cumulative rainfall for any time interval measured from the start of the event up to the peak intensity are expressed in terms of Equation A.1. The cumulative rainfall formula for any time interval after the peak intensity, expressed in terms of Equation A.2, is developed in a similar way. The cumulative rainfall formulae are depicted in Figure A.1

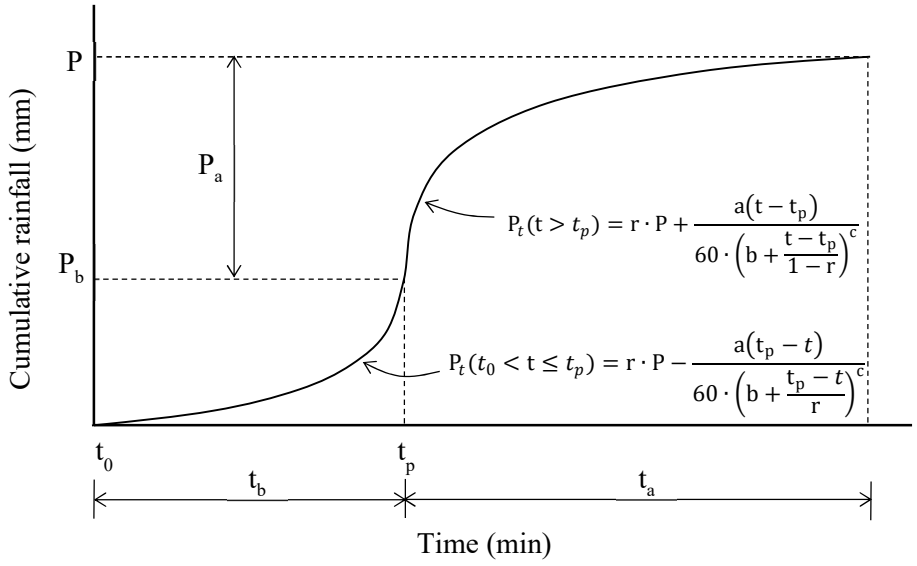

Figure A.1: Cumulative curve for the Chicago Design Storm method

ANNEXURE B

AT-SITE DESIGN RAINFALL FOR RAINFALL STATIONS IN GAUTENG

This annexure provides details of the AMS, and the design rainfall estimates of 16 stations depicted in Figure B.1. The AMS was extracted between 01 Oct and 30 Sep of each year (hydrological years) for 16 time steps ranging from 5-min to 24-hours (standard time steps). The PD analysis results for the GEV distribution with L-moments and ordinary product moments, and their respective Kolmogorov-Smirnof (K-S) test statistic, are provided. However, the design rainfall with ordinary product moments is provided for information purposes only because the design rainfall with L-moments were used in further analyses. The analyses were conducted using the software program HEC-SSP version: 2.3-beta.3 Build: 42393 Date: 20 Jun 2022. Hydrological years with large percentages of missing data periods and / or incomplete hydrological years, which are filled with a light diagonal pattern e.g., Bolephi, Bronkhorstspruit, Sterkfontein, Soshanguve, and Wonderboom, were excluded from an analysis.

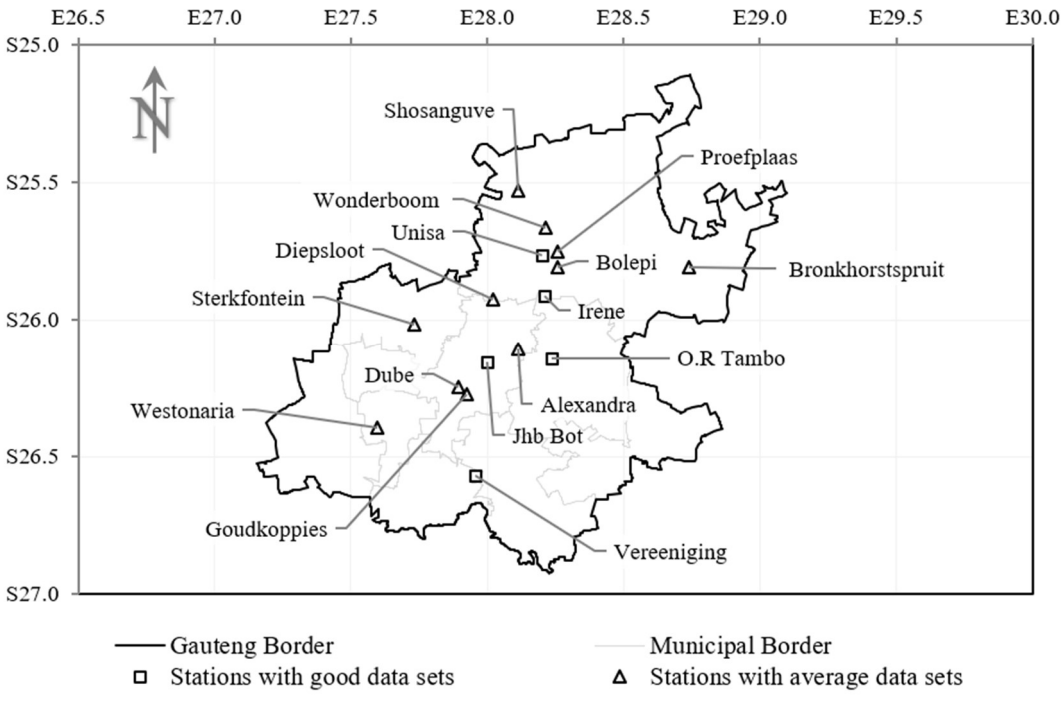

Figure B.1: Rainfall stations in Gauteng that were used for the at-site design rainfall

Station: 1_O.R Tambo **Period:** 23 Oct 1994 to 31 Dec 2020

Year	Standard time step (min/hour)															
	5m	10m	15m	30m	45m	60m (1h)	90m (1.5h)	120m (2h)	240m (4h)	360m (6h)	480m (8h)	600m (10h)	720m (12h)	960m (16h)	1200m (20h)	1440m (24h)
1994/95	7.8	12.6	16.8	21.6	31.0	33.6	34.0	34.0	36.8	39.0	41.8	45.8	48.0	59.4	60.8	80.0
1995/96	8.0	11.0	13.4	17.6	19.8	21.4	29.2	34.4	40.8	44.6	55.4	69.0	76.8	86.2	86.8	87.0
1996/97	8.0	11.6	14.4	23.2	28.4	29.8	32.4	34.0	41.4	46.0	55.6	60.8	65.0	76.6	92.0	93.6
1997/98	7.4	12.8	18.8	27.2	27.4	33.0	36.2	36.6	41.2	54.2	62.0	64.0	64.2	64.2	64.2	64.2
1998/99	6.4	11.6	15.4	21.8	22.6	22.8	25.8	28.4	41.2	43.0	43.2	50.4	58.2	59.0	59.2	62.6
1999/00	7.6	12.4	17.2	20.6	22.2	23.2	29.2	34.0	41.6	42.6	43.6	45.6	64.8	73.4	75.4	80.2
2000/01	11.6	16.6	18.4	26.2	32.8	37.2	41.0	43.0	56.4	67.8	70.8	86.4	94.2	99.0	111.0	112.4
2001/02	8.6	17.0	22.8	35.8	40.0	42.4	49.0	51.0	51.0	51.0	51.0	51.0	51.2	52.4	80.6	80.6
2002/03	9.6	16.4	18.8	25.4	30.0	31.4	32.0	32.0	32.2	36.4	44.0	49.2	49.6	53.6	53.6	53.6
2003/04	10.2	12.8	16.2	18.0	18.8	19.6	21.6	24.8	30.4	39.4	43.2	45.0	46.8	50.2	55.0	57.2
2004/05	7.8	13.2	16.2	22.8	23.4	25.8	28.8	31.0	49.8	54.2	54.4	55.8	56.0	56.2	56.4	57.0
2005/06	7.4	11.6	15.8	24.6	28.6	29.4	35.2	36.0	38.0	38.0	38.0	38.0	38.0	38.0	42.8	42.8
2006/07	3.6	3.6	4.2	7.0	10.0	11.8	14.8	17.0	20.8	24.6	26.4	26.4	29.6	33.2	33.2	33.2
2007/08	4.8	9.0	12.6	18.6	19.4	19.4	19.6	19.6	23.6	27.2	28.8	32.0	34.6	42.6	48.6	52.4
2008/09	9.0	13.4	18.6	25.8	32.6	37.4	40.2	41.4	42.2	42.2	42.2	43.0	46.4	46.8	46.8	47.6
2009/10	9.6	13.4	14.6	25.0	33.8	38.6	42.4	45.8	48.0	48.8	48.8	49.0	49.0	49.0	49.6	53.4
2010/11	9.0	16.8	24.0	31.2	33.4	33.8	34.0	34.0	41.2	54.6	59.2	62.6	65.6	71.8	71.8	71.8
2011/12	7.4	13.6	16.4	23.8	28.6	31.2	32.6	33.6	38.0	38.8	42.4	42.4	42.4	43.2	46.6	47.6
2012/13	10.0	15.8	19.2	26.2	28.4	29.6	29.6	29.6	31.4	32.8	40.8	46.4	53.6	62.8	65.6	66.0
2013/14	9.8	14.4	18.2	25.0	26.2	26.4	26.8	26.8	36.2	40.6	42.6	44.0	44.6	44.6	45.0	49.6
2014/15	9.8	17.2	23.2	42.2	63.2	73.4	74.2	76.8	78.0	79.0	80.6	82.0	82.0	82.0	82.0	82.0
2015/16	6.6	9.6	11.0	15.6	17.0	17.4	17.4	18.0	25.2	33.0	41.2	51.2	57.6	64.6	68.2	68.6
2016/17	17.2	26.6	37.4	57.4	75.2	83.4	85.2	86.4	89.6	89.6	89.6	89.6	89.6	89.8	89.8	90.2
2017/18	9.0	13.4	14.2	15.6	15.8	15.8	17.6	17.8	22.4	28.8	39.0	44.6	50.8	61.0	76.6	76.8
2018/19	7.8	12.2	17.2	27.0	29.8	32.8	34.0	35.0	35.8	35.8	35.8	35.8	35.8	35.8	42.8	53.8
2019/20	13.6	19.6	24.4	28.4	28.4	28.4	28.6	28.8	28.8	32.8	38.4	47.6	53.4	53.8	53.8	54.0
RI	**GEV distribution (L-Moments)**															
1:100	16.5	24.5	33.9	54.1	76.9	89.7	93.3	95.3	95.6	103.7	105.6	108.8	108.8	112.7	123.3	121.1
1:50	15.2	23.0	31.3	48.7	66.2	75.9	79.2	81.1	83.9	90.2	92.5	97.2	99.5	104.3	113.6	112.8
1:20	13.4	20.8	27.7	41.8	53.5	60.1	63.0	64.9	69.8	74.4	77.1	82.8	87.2	92.7	100.2	101.0
1:10	12.0	18.9	24.8	36.5	44.9	49.7	52.4	54.1	59.8	63.7	66.7	72.6	77.6	83.3	89.6	91.3
1:5	10.6	16.8	21.7	31.2	36.9	40.2	42.7	44.3	50.3	53.9	57.2	62.6	67.8	73.2	78.3	80.8
1:2	8.4	13.4	16.9	23.5	26.5	28.1	30.4	31.9	37.5	41.0	44.7	48.8	52.9	57.1	60.8	63.7
K-S	0.171	0.155	0.142	0.138	0.153	0.125	0.162	0.137	0.136	0.084	0.142	0.140	0.090	0.068	0.078	0.108
RI	**GEV distribution (Product-Moments)**															
1:100	17.1	25.5	36.2	56.8	76.9	86.9	88.7	90.7	93.3	95.0	95.5	100.2	103.2	107.0	116.4	116.4
1:50	15.6	23.8	32.9	50.6	66.8	75.1	77.3	79.3	82.9	85.4	87.0	92.2	95.9	100.4	108.9	109.5
1:20	13.7	21.3	28.6	42.7	54.5	60.9	63.4	65.3	69.8	73.2	75.8	81.4	85.6	90.7	97.9	99.4
1:10	12.2	19.3	25.3	37.0	46.0	50.9	53.5	55.3	60.3	64.1	67.3	72.8	77.3	82.5	88.8	90.7
1:5	10.6	17.0	21.8	31.3	37.7	41.4	44.0	45.7	50.9	55.0	58.6	63.8	68.2	73.3	78.6	80.9
1:2	8.3	13.3	16.7	23.3	26.6	28.5	31.0	32.4	37.7	41.9	45.8	49.8	53.5	57.8	61.7	64.2
K-S	0.184	0.172	0.147	0.142	0.164	0.130	0.152	0.149	0.143	0.091	0.174	0.155	0.086	0.079	0.080	0.120

Station: 3_Irene **Period:** 27 Oct 1994 to 31 Dec 2020

Year	Standard time step (min/hour)															
	5m	10m	15m	30m	45m	60m (1h)	90m (1.5h)	120m (2h)	240m (4h)	360m (6h)	480m (8h)	600m (10h)	720m (12h)	960m (16h)	1200m (20h)	1440m (24h)
1994/95	12.6	18.2	20.6	27.8	34.0	51.8	60.2	62.2	68.6	68.6	68.6	68.6	68.6	69.2	70.6	84.2
1995/96	10.8	18.6	26.4	39.8	43.6	44.4	45.2	46.8	59.6	63.8	64.2	78.0	86.6	93.2	93.6	94.0
1996/97	8.4	13.8	19.2	34.6	40.2	40.8	45.6	55.6	79.8	82.4	82.8	84.4	94.4	110.8	112.6	122.8
1997/98	9.2	16.8	19.0	27.0	32.0	36.0	40.8	40.8	41.0	41.0	41.0	41.0	41.0	41.2	43.0	43.0
1998/99	7.4	12.0	18.0	27.8	40.2	49.6	60.0	61.0	61.0	61.0	61.2	61.2	62.2	66.2	66.2	66.2
1999/00	8.0	15.4	21.2	39.4	45.0	48.6	51.8	53.2	56.6	56.8	56.8	56.8	59.0	66.0	68.4	84.0
2000/01	11.2	20.2	28.0	39.6	42.6	43.4	44.8	48.0	56.6	58.4	60.4	60.8	60.8	60.8	60.8	60.8
2001/02	11.0	19.0	20.6	22.0	22.2	22.2	22.4	22.4	22.4	24.4	24.4	24.4	24.4	25.6	25.8	31.4
2002/03	5.4	8.6	11.2	16.0	17.8	18.0	18.8	20.0	24.0	27.8	30.8	32.2	35.2	35.4	49.6	52.8
2003/04	7.4	13.8	14.0	14.6	15.2	19.0	22.0	25.0	29.8	33.0	43.6	46.4	46.4	47.8	53.8	61.2
2004/05	8.0	13.4	14.8	24.4	29.8	31.0	31.2	31.4	31.4	37.6	41.4	42.4	42.8	42.8	42.8	50.4
2005/06	9.8	15.6	18.8	20.0	20.6	23.0	27.4	31.6	41.0	42.6	44.0	44.8	46.0	46.2	46.2	46.6
2006/07	8.4	13.6	15.2	22.0	26.2	31.4	37.6	41.4	57.8	66.2	67.6	67.6	67.6	67.6	67.6	67.6
2007/08	8.4	11.4	13.6	18.2	25.8	27.2	28.4	29.6	29.6	34.4	37.2	38.0	41.6	52.6	59.2	67.2
2008/09	7.2	13.0	15.6	16.4	16.8	24.0	30.8	32.6	34.0	35.2	35.6	35.6	35.6	35.6	35.6	38.2
2009/10	7.2	12.6	17.4	27.6	33.4	37.0	37.2	38.0	41.8	41.8	41.8	41.8	41.8	41.8	41.8	64.4
2010/11	7.6	10.6	15.0	22.6	29.0	32.8	35.2	36.8	42.4	52.2	53.6	56.4	59.2	68.4	68.6	68.6
2011/12	7.8	14.4	17.2	22.4	25.8	27.6	32.4	34.6	40.4	43.8	44.0	44.0	44.0	44.0	44.8	46.8
2012/13	6.4	9.4	11.8	21.0	25.4	31.0	33.0	33.8	34.6	34.6	35.8	36.4	37.8	45.4	47.8	71.8
2013/14	12.2	20.8	27.8	38.8	42.2	44.6	46.2	46.4	53.6	55.0	55.2	60.8	64.8	80.6	81.6	86.0
2014/15	10.0	19.6	29.2	40.4	43.0	46.4	47.6	50.6	58.4	59.6	61.0	61.2	61.2	61.6	62.8	62.8
2015/16	10.4	15.4	18.6	20.6	21.4	23.6	27.6	34.8	46.4	53.2	55.4	66.4	85.8	104.8	111.6	113.2
2016/17	7.6	13.6	17.8	23.0	31.6	44.8	54.4	61.8	71.2	74.6	76.8	76.8	76.8	77.6	80.4	82.8
2017/18	6.6	11.4	15.4	25.4	29.2	33.6	38.8	40.6	49.0	49.4	56.0	65.4	75.0	104.4	120.4	122.4
2018/19	8.0	12.6	15.2	19.2	19.8	20.8	23.6	25.6	37.4	49.8	53.6	58.6	62.8	68.2	72.0	73.8
2019/20	9.4	18.8	24.8	40.6	48.8	49.8	49.8	49.8	49.8	50.0	50.0	60.8	65.0	81.0	99.2	107.0
RI	**GEV distribution (L-Moments)**															
1:100	14.5	23.7	35.6	53.9	55.9	60.1	68.8	73.2	86.2	87.7	87.0	88.4	104.1	132.7	147.3	147.8
1:50	13.5	22.6	32.5	49.2	53.0	57.6	65.2	69.1	81.3	83.2	83.0	85.3	98.3	121.9	133.4	135.9
1:20	12.2	20.9	28.5	43.0	48.5	53.4	59.5	62.9	73.9	76.3	76.7	80.0	89.4	106.9	114.9	119.3
1:10	11.2	19.4	25.5	38.2	44.3	49.4	54.4	57.5	67.3	70.0	70.9	74.8	81.6	94.6	100.4	105.9
1:5	10.1	17.6	22.4	33.0	39.4	44.3	48.3	51.0	59.5	62.5	63.9	68.0	72.3	81.3	85.3	91.4
1:2	8.4	14.5	17.8	25.2	30.3	34.5	37.4	39.6	45.8	49.0	51.0	54.3	55.9	59.9	62.2	68.4
K-S	0.122	0.115	0.085	0.139	0.128	0.124	0.103	0.080	0.095	0.088	0.109	0.127	0.144	0.105	0.080	0.101
RI	**GEV distribution (Product-Moments)**															
1:100	13.6	23.0	33.1	50.0	54.5	59.3	67.0	70.7	84.5	86.4	86.3	88.8	101.5	125.4	136.7	140.4
1:50	13.0	22.1	30.9	46.7	51.9	56.8	63.7	67.3	80.0	82.1	82.4	85.5	96.4	117.0	126.5	130.9
1:20	12.0	20.6	27.9	42.0	47.7	52.8	58.6	61.8	73.0	75.5	76.2	79.9	88.3	104.5	111.8	116.9
1:10	11.2	19.2	25.3	37.9	43.9	48.9	53.8	56.9	66.7	69.4	70.6	74.5	81.0	93.8	99.6	105.1
1:5	10.2	17.6	22.6	33.4	39.2	44.0	48.1	50.9	59.3	62.2	63.7	67.7	72.2	81.5	86.0	91.7
1:2	8.5	14.6	18.1	25.7	30.4	34.5	37.6	39.9	45.9	49.1	51.0	54.1	56.2	60.8	63.5	69.3
K-S	0.145	0.126	0.102	0.144	0.133	0.131	0.105	0.087	0.098	0.086	0.113	0.133	0.138	0.115	0.098	0.089

Station: 4_Bolephi **Period:** 26 Aug 2000 to 12 Apr 2018

Year	Standard time step (min/hour)															
	5m	10m	15m	30m	45m	60m (1h)	90m (1.5h)	120m (2h)	240m (4h)	360m (6h)	480m (8h)	600m (10h)	720m (12h)	960m (16h)	1200m (20h)	1440m (24h)
1999/00	0.0	0.0	0.0	0.0	0.0	0.0	0.0	0.0	0.0	0.0	0.0	0.0	0.0	0.0	0.0	0.0
2000/01	0.0	0.0	0.0	0.0	0.0	0.0	0.0	0.0	0.0	0.0	0.0	0.0	0.0	0.0	0.0	0.0
2001/02	0.0	0.0	0.0	0.0	0.0	0.0	0.0	0.0	0.0	0.0	0.0	0.0	0.0	0.0	0.0	0.0
2002/03	6.0	6.2	7.8	12.0	12.2	14.2	16.2	16.2	17.2	20.6	31.0	31.8	36.0	36.0	36.0	36.0
2003/04	3.8	7.0	9.8	16.8	19.4	20.4	23.6	27.4	36.0	36.2	36.2	36.2	36.2	36.2	36.2	36.2
2004/05	9.8	18.2	24.4	31.8	36.8	37.4	37.4	37.4	39.2	39.4	39.4	39.4	50.2	74.4	74.4	74.4
2005/06	9.8	15.8	17.4	24.6	26.0	27.2	29.0	30.8	37.6	45.2	49.4	54.0	55.8	57.0	58.0	61.8
2006/07	8.6	13.8	21.2	30.2	31.6	32.2	32.4	32.4	32.4	34.2	36.2	38.4	42.2	42.2	43.2	44.0
2007/08	9.0	14.8	18.6	28.6	34.4	36.8	39.6	41.0	41.6	41.6	41.8	41.8	42.0	42.6	44.6	53.0
2008/09	7.6	11.4	17.4	27.2	28.2	28.4	28.8	29.4	32.8	35.6	36.4	38.0	38.0	38.0	38.0	38.0
2009/10	6.4	11.6	14.8	26.0	34.2	38.8	40.6	41.2	41.4	41.4	41.4	41.4	41.4	44.6	47.4	47.8
2010/11	9.6	18.4	23.8	39.6	50.2	50.6	50.6	50.8	55.2	63.0	63.2	67.2	75.8	99.0	99.8	99.8
2011/12	9.8	17.8	19.4	22.6	25.2	26.8	28.6	28.8	28.8	29.2	29.8	29.8	30.2	30.4	30.4	33.8
2012/13	8.6	14.0	19.2	30.0	30.4	30.4	30.6	31.0	31.6	31.6	36.0	37.6	41.0	41.4	43.0	60.2
2013/14	9.6	15.0	17.6	25.2	38.2	43.6	44.0	44.8	46.2	46.2	47.2	55.0	64.6	90.4	93.6	100.6
2014/15	10.4	17.0	22.8	30.4	34.4	34.6	34.8	39.6	41.4	41.4	41.6	46.4	46.4	46.6	48.6	52.2
2015/16	5.8	10.4	11.2	18.4	24.6	26.4	27.4	31.8	41.4	53.2	56.4	61.8	64.6	79.4	91.8	100.4
2016/17	11.0	16.0	17.4	24.4	26.2	27.0	27.2	30.0	32.4	38.8	47.4	52.8	58.0	71.0	81.8	82.4
2017/18	6.4	11.0	15.2	22.6	28.6	31.2	32.4	36.4	41.8	54.2	61.6	70.2	79.2	97.8	119.6	126.2
RI	**GEV distribution (L-Moments)**															
1:100	10.9	19.7	26.1	40.3	54.4	59.4	61.6	61.4	57.8	73.7	80.2	90.7	102.7	145.2	168.6	168.1
1:50	10.9	19.4	25.6	38.8	50.5	54.5	55.9	56.1	55.0	67.9	73.2	82.5	93.2	128.7	147.1	149.4
1:20	10.8	18.9	24.5	36.3	45.2	48.1	48.9	49.5	51.0	60.3	64.3	72.1	80.9	107.7	120.5	125.2
1:10	10.6	18.2	23.4	34.1	41.1	43.3	43.8	44.8	47.7	54.6	57.8	64.2	71.6	92.2	101.4	107.0
1:5	10.2	17.2	21.8	31.4	36.7	38.5	38.9	40.2	44.0	48.8	51.3	56.3	62.1	76.7	82.8	88.6
1:2	9.0	14.6	18.3	26.3	30.0	31.3	32.1	34.0	37.9	40.3	42.2	44.9	48.2	54.5	57.0	61.8
K-S	0.172	0.116	0.155	0.120	0.111	0.146	0.114	0.141	0.159	0.108	0.143	0.147	0.148	0.185	0.177	0.135
RI	**GEV distribution (Product-Moments)**															
1:100	11.3	19.8	26.0	41.3	53.8	55.3	55.8	55.7	58.5	69.2	72.7	81.3	92.3	124.7	142.4	148.2
1:50	11.2	19.5	25.4	39.4	50.0	51.9	52.3	52.5	55.4	64.9	68.4	76.5	86.4	115.6	130.8	136.4
1:20	11.0	18.9	24.4	36.6	44.9	47.0	47.4	48.1	51.1	59.0	62.4	69.5	77.9	102.4	114.2	119.5
1:10	10.7	18.2	23.3	34.1	40.9	43.0	43.5	44.5	47.6	54.2	57.4	63.6	70.7	91.1	100.4	105.4
1:5	10.2	17.1	21.7	31.2	36.6	38.7	39.3	40.7	43.8	49.0	51.9	57.0	62.7	78.4	85.1	89.8
1:2	8.8	14.5	18.3	26.1	30.1	31.8	32.8	34.6	37.8	40.8	43.0	46.0	49.4	57.0	60.1	64.1
K-S	0.148	0.119	0.154	0.121	0.111	0.139	0.125	0.174	0.168	0.130	0.153	0.178	0.171	0.214	0.209	0.137

Station: 5_Vereeniging **Period:** 28 Oct 1994 to 31 Dec 2020

Year	Standard time step (min/hour)															
	5m	10m	15m	30m	45m	60m (1h)	90m (1.5h)	120m (2h)	240m (4h)	360m (6h)	480m (8h)	600m (10h)	720m (12h)	960m (16h)	1200m (20h)	1440m (24h)
1994/95	20.4	36.4	51.0	64.4	68.2	78.4	80.6	83.0	83.0	83.2	83.2	83.2	83.2	83.2	83.2	84.4
1995/96	8.6	14.6	19.2	23.8	26.8	28.6	36.2	42.6	46.2	47.4	47.6	47.6	47.6	48.6	48.6	50.4
1996/97	8.2	11.2	14.8	22.0	22.8	23.0	23.4	24.8	29.8	31.8	35.4	36.6	43.4	54.2	55.6	66.6
1997/98	13.6	20.0	22.2	38.2	42.0	46.0	52.4	52.4	64.0	64.0	64.0	64.0	64.0	68.4	74.6	85.4
1998/99	6.8	11.2	15.6	22.2	25.6	26.8	29.2	30.2	36.2	43.2	49.2	50.6	50.6	56.0	56.6	64.8
1999/00	11.4	16.6	25.6	36.8	38.0	38.4	41.0	41.0	45.4	45.6	45.6	45.6	45.6	45.6	47.0	53.6
2000/01	6.8	11.6	15.4	23.8	24.8	25.2	26.8	31.2	36.2	36.8	36.8	36.8	36.8	36.8	51.2	60.2
2001/02	10.6	15.2	16.4	17.4	20.2	22.6	24.4	24.8	25.4	26.4	29.0	29.2	30.8	32.6	37.0	37.0
2002/03	5.6	7.4	10.4	16.6	23.0	28.6	33.8	36.0	43.2	43.2	43.2	43.2	43.2	43.2	43.2	43.4
2003/04	6.8	9.2	11.2	20.0	21.2	22.2	23.6	24.0	31.2	33.6	36.6	39.0	40.0	46.4	49.8	50.6
2004/05	5.6	9.8	13.4	19.6	22.4	24.4	29.8	32.0	32.2	35.4	41.0	49.6	49.8	64.2	74.6	75.4
2005/06	5.4	8.8	11.4	17.6	20.2	29.4	30.0	30.8	37.2	41.2	41.2	41.2	41.2	53.8	69.0	75.8
2006/07	5.8	9.8	13.2	17.4	19.6	20.2	22.0	23.4	31.0	31.6	35.0	35.8	41.4	42.6	46.4	52.0
2007/08	6.4	11.0	15.4	21.6	23.6	28.2	37.0	37.4	47.6	47.6	47.8	47.8	47.8	47.8	47.8	51.0
2008/09	9.0	10.0	11.2	16.8	21.4	25.2	30.6	30.8	32.2	36.8	36.8	36.8	36.8	38.0	39.6	39.6
2009/10	10.0	18.0	21.8	30.4	38.4	43.4	46.4	46.6	47.4	47.4	47.4	47.4	47.4	47.4	51.2	53.2
2010/11	7.8	12.4	16.2	18.8	21.6	26.8	37.2	42.2	76.6	94.2	109.2	121.0	126.8	130.4	130.6	131.4
2011/12	7.0	12.6	16.0	23.8	28.6	30.0	30.8	35.2	50.2	56.8	62.4	65.0	65.2	65.2	66.6	66.6
2012/13	13.0	20.6	31.2	34.4	34.4	34.4	34.4	34.4	43.8	48.2	60.6	68.2	71.4	82.6	84.8	89.2
2013/14	6.4	12.4	18.2	30.4	40.2	45.8	54.0	57.0	62.8	62.8	63.0	63.0	63.0	63.0	63.0	63.0
2014/15	14.4	21.6	26.6	32.6	35.4	36.4	36.4	36.4	36.4	36.4	36.4	36.4	36.4	36.4	36.4	36.4
2015/16	10.0	14.4	18.4	28.4	29.8	30.4	33.6	35.2	39.2	40.8	41.6	42.2	44.0	52.4	62.8	65.2
2016/17	8.4	16.2	20.6	27.8	32.4	33.2	37.0	38.2	40.4	44.4	57.0	64.4	65.0	65.8	67.8	76.2
2017/18	7.2	11.0	15.8	27.4	33.4	35.8	35.8	35.8	36.4	37.4	41.2	49.4	57.2	79.2	92.4	95.8
2018/19	11.2	16.4	17.8	28.4	37.8	46.4	55.8	59.6	61.2	64.4	64.4	65.2	65.8	67.6	67.6	74.2
2019/20	7.2	13.0	17.0	20.4	22.0	23.6	38.4	40.0	41.6	42.8	43.2	45.4	45.8	52.8	54.8	55.4
RI	**GEV distribution (L-Moments)**															
1:100	23.7	38.1	53.5	66.7	73.1	84.2	86.0	89.1	102.3	111.8	123.3	129.6	134.7	133.4	137.0	133.4
1:50	20.0	32.0	43.7	56.3	62.2	70.3	74.4	77.2	88.8	95.8	104.1	109.9	113.1	116.5	120.8	121.2
1:20	15.8	25.3	33.4	44.9	50.0	55.4	61.0	63.5	73.2	77.9	83.2	88.0	89.8	96.5	101.3	105.2
1:10	13.2	21.0	27.3	37.6	42.2	46.3	52.1	54.3	62.8	66.2	70.1	74.1	75.3	82.8	87.6	93.0
1:5	10.8	17.2	22.2	31.2	35.3	38.5	44.1	46.0	53.2	55.8	58.7	61.8	62.8	70.0	74.5	80.4
1:2	8.0	12.7	16.3	23.5	26.9	29.4	33.8	35.4	40.8	42.8	45.0	46.9	48.0	53.1	57.0	61.6
K-S	0.101	0.082	0.152	0.109	0.117	0.065	0.108	0.112	0.095	0.111	0.092	0.121	0.110	0.090	0.088	0.099
RI	**GEV distribution (Product-Moments)**															
1:100	20.7	35.1	48.4	61.9	66.7	75.8	80.5	83.1	90.6	99.7	109.8	118.9	122.9	128.2	130.5	132.1
1:50	18.4	30.6	41.7	54.0	58.9	66.4	71.5	74.1	82.3	89.5	97.4	104.6	107.7	113.7	117.0	120.2
1:20	15.4	25.1	33.7	44.7	49.4	55.1	60.5	62.8	71.4	76.5	82.2	87.4	89.5	95.8	100.0	104.6
1:10	13.3	21.3	28.3	38.2	42.7	47.3	52.6	54.8	63.1	67.0	71.3	75.3	76.9	83.0	87.5	92.6
1:5	11.2	17.8	23.3	32.1	36.3	39.9	44.9	46.9	54.6	57.5	60.8	63.7	65.0	70.7	75.1	80.2
1:2	8.3	13.0	16.8	24.0	27.5	30.1	34.3	36.0	42.0	44.0	46.3	48.0	49.1	53.6	57.6	61.7
K-S	0.124	0.079	0.134	0.100	0.123	0.104	0.127	0.111	0.110	0.152	0.118	0.126	0.115	0.079	0.081	0.094

Station: 8_Jhb Botanical Gardens **Period:** 23 Oct 1994 to 31 Dec 2020

Year	Standard time step (min/hour)															
	5m	10m	15m	30m	45m	60m (1h)	90m (1.5h)	120m (2h)	240m (4h)	360m (6h)	480m (8h)	600m (10h)	720m (12h)	960m (16h)	1200m (20h)	1440m (24h)
1994/95	6.4	10.4	14.8	22.4	25.4	25.8	27.0	27.4	27.4	29.2	39.8	44.2	46.0	52.0	57.0	72.6
1995/96	8.2	11.4	16.2	25.2	30.6	34.6	35.8	36.8	44.4	49.2	56.2	60.0	62.4	72.6	74.4	76.2
1996/97	8.6	14.2	19.6	33.4	51.4	55.0	55.4	55.4	55.6	55.6	57.2	57.2	57.2	57.2	59.4	68.2
1997/98	8.6	14.6	19.2	30.6	35.2	38.0	38.6	38.8	41.6	42.4	42.4	42.4	42.4	47.8	49.2	50.6
1998/99	9.2	12.4	15.2	17.2	18.4	21.0	21.4	21.6	21.8	27.4	29.8	32.4	34.6	40.0	41.2	46.6
1999/00	7.2	13.4	16.8	25.0	27.8	34.8	41.2	52.0	69.2	86.8	90.2	92.2	97.4	110.4	113.4	117.2
2000/01	5.4	9.6	12.4	15.4	17.6	19.0	22.0	24.2	27.8	27.8	28.0	28.2	30.4	31.4	33.2	34.0
2001/02	3.6	6.0	7.0	10.2	13.2	18.0	21.0	23.4	25.0	26.0	29.6	29.6	29.6	29.8	29.8	29.8
2002/03	9.8	12.2	13.2	16.0	18.6	19.2	19.2	20.4	29.0	29.4	29.6	32.0	33.0	33.0	33.0	33.0
2003/04	5.6	10.8	15.0	21.2	22.2	22.4	22.6	22.6	22.8	27.8	30.6	32.6	33.4	37.8	38.6	39.8
2004/05	8.6	16.8	25.0	41.0	49.2	52.0	52.0	52.0	52.2	52.2	52.2	52.2	52.2	52.2	52.2	52.2
2005/06	7.6	12.2	12.6	13.0	13.0	13.4	17.2	18.8	25.2	26.0	26.0	26.0	26.4	26.4	26.4	26.4
2006/07	5.6	10.2	11.8	14.6	15.4	15.6	18.2	20.4	23.8	23.8	28.0	37.2	37.4	37.6	37.6	37.6
2007/08	10.0	17.2	19.6	23.0	29.6	35.4	49.4	53.6	58.4	60.2	60.2	60.2	60.2	60.4	60.4	61.2
2008/09	6.2	10.2	13.2	19.6	26.8	29.8	30.6	32.8	38.8	40.0	40.2	40.2	40.2	40.2	40.2	40.2
2009/10	13.6	24.0	31.0	43.4	46.8	49.0	51.0	53.4	59.8	59.8	59.8	59.8	59.8	60.2	60.4	60.4
2010/11	10.8	15.6	21.6	42.4	51.0	53.6	60.6	64.0	64.8	65.0	67.2	78.4	94.4	109.8	110.4	110.4
2011/12	7.4	11.4	15.0	19.2	20.6	22.2	26.8	28.8	34.8	37.8	40.0	45.4	46.0	46.6	51.0	52.2
2012/13	6.2	10.4	14.6	17.2	17.6	17.6	18.6	19.2	23.8	25.0	25.8	30.2	30.2	30.6	31.4	32.4
2013/14	11.6	15.4	18.0	25.4	26.4	27.4	30.0	35.0	36.6	36.6	36.6	36.6	36.6	47.4	47.4	47.4
2014/15	7.2	13.4	16.8	24.2	28.8	30.6	31.4	32.4	39.8	40.0	40.0	40.0	40.0	40.0	40.4	41.8
2015/16	12.4	13.6	14.6	16.6	19.4	22.4	25.0	26.6	39.0	50.6	52.6	58.6	68.4	100.4	101.2	101.4
2016/17	9.8	13.8	16.6	22.8	26.8	28.0	31.2	38.0	48.6	58.2	65.4	68.2	71.4	91.6	99.2	102.4
2017/18	10.0	16.6	22.4	25.8	29.6	33.4	35.0	35.0	35.0	40.4	52.2	60.6	70.2	90.8	109.6	111.0
2018/19	9.2	16.2	18.2	22.0	22.6	24.2	29.4	30.8	39.8	50.8	51.8	51.8	52.0	52.0	53.2	59.6
2019/20	7.2	10.4	13.6	16.8	18.0	18.4	18.4	19.4	27.4	32.0	33.4	36.8	38.4	38.4	38.6	38.6
RI	**GEV distribution (L-Moments)**															
1:100	14.4	23.3	32.1	55.0	69.9	74.3	80.0	82.3	87.5	96.6	98.4	104.1	123.0	161.1	169.7	169.2
1:50	13.7	21.7	29.3	48.5	60.7	65.0	70.0	72.8	78.6	86.4	88.7	93.6	107.2	135.5	142.8	144.8
1:20	12.5	19.5	25.6	40.5	49.5	53.5	57.7	60.8	66.9	73.2	76.0	80.1	88.1	106.4	111.9	115.7
1:10	11.5	17.7	22.9	34.7	41.8	45.4	49.0	52.1	58.2	63.4	66.4	69.9	74.8	87.3	91.6	95.8
1:5	10.3	15.8	20.0	29.1	34.3	37.4	40.5	43.4	49.3	53.6	56.5	59.5	62.1	70.0	73.2	77.1
1:2	8.1	12.7	15.9	21.3	24.3	26.5	29.0	31.1	36.2	39.2	41.9	44.3	45.1	48.3	49.9	52.4
K-S	0.077	0.112	0.106	0.107	0.092	0.091	0.096	0.130	0.119	0.137	0.149	0.114	0.089	0.105	0.116	0.110
RI	**GEV distribution (Product-Moments)**															
1:100	14.2	23.7	31.3	50.3	62.2	65.5	69.6	72.8	78.5	89.7	92.8	97.2	109.0	134.1	141.6	143.1
1:50	13.5	22.0	28.8	45.7	56.2	59.7	63.7	66.9	72.7	82.0	85.1	89.3	98.9	120.5	127.2	129.5
1:20	12.4	19.6	25.5	39.6	48.1	51.6	55.4	58.6	64.5	71.4	74.5	78.2	85.3	102.4	107.9	110.8
1:10	11.4	17.7	22.9	34.7	41.9	45.2	48.8	51.8	57.6	63.0	66.0	69.4	74.7	88.3	92.8	96.0
1:5	10.3	15.8	20.2	29.6	35.3	38.3	41.6	44.3	50.0	54.0	56.8	59.9	63.5	73.5	77.0	80.1
1:2	8.2	12.7	16.0	21.8	25.2	27.5	30.1	32.2	37.3	40.0	42.5	45.0	46.6	51.2	52.9	55.3
K-S	0.076	0.114	0.101	0.131	0.123	0.112	0.112	0.133	0.132	0.142	0.139	0.105	0.114	0.136	0.155	0.126

Station: 10_Bronkhorstpruit **Period:** 15 Apr 2009 to 31 Dec 2020

Year	Standard time step (min/hour)															
	5m	10m	15m	30m	45m	60m (1h)	90m (1.5h)	120m (2h)	240m (4h)	360m (6h)	480m (8h)	600m (10h)	720m (12h)	960m (16h)	1200m (20h)	1440m (24h)
2008/09	1.8	3.0	4.0	6.2	8.2	9.0	10.0	10.6	11.0	11.0	11.4	12.4	15.6	18.4	22.2	23.6
2009/10	13.0	18.8	24.6	37.0	42.4	48.2	53.6	54.8	63.0	65.0	65.0	65.0	65.0	65.2	65.2	65.2
2010/11	8.2	12.8	16.6	22.6	29.2	34.8	40.8	54.6	75.4	79.8	80.0	81.0	82.2	83.0	83.2	83.2
2011/12	8.8	13.6	19.2	32.2	37.4	44.0	47.2	51.4	53.4	53.4	54.4	65.2	75.6	90.6	99.6	101.2
2012/13	13.8	19.8	21.4	21.4	21.6	22.8	25.4	26.2	33.6	33.6	33.8	40.8	43.4	46.2	66.0	68.4
2013/14	14.2	26.0	33.6	52.8	65.4	69.4	71.6	72.4	73.8	73.8	86.2	86.2	86.2	86.4	86.8	86.8
2014/15	11.0	12.6	13.6	17.0	17.4	18.6	21.4	24.0	31.0	34.8	42.0	44.0	44.0	44.0	44.0	48.4
2015/16	7.8	14.2	17.4	23.0	24.0	25.6	25.8	33.0	50.4	66.0	80.2	82.8	86.0	99.0	100.8	102.6
2016/17	12.6	19.8	26.2	30.8	32.0	42.0	55.8	71.4	109.4	126.4	134.0	139.4	144.2	152.4	163.2	166.6
2017/18	12.4	22.6	27.6	33.0	33.6	33.8	34.2	34.2	37.8	45.4	50.0	53.6	56.6	69.6	81.8	89.8
2018/19	8.0	14.0	18.4	22.8	25.4	27.8	28.8	29.2	29.2	29.8	30.0	33.0	41.6	50.6	50.8	51.0
2019/20	7.4	11.8	15.4	19.0	22.4	26.8	27.4	27.4	32.4	37.6	43.4	47.0	56.2	60.8	65.0	81.6
RI	**GEV distribution (L-Moments)**															
1:100	17.1	35.4	43.6	72.6	92.5	94.6	103.8	108.4	162.9	178.2	184.6	186.4	191.5	200.9	208.8	203.2
1:50	16.4	31.5	39.3	61.8	76.4	81.4	89.8	96.1	136.5	149.7	157.7	159.6	163.2	173.1	180.3	178.7
1:20	15.3	26.7	33.9	49.6	59.0	65.8	73.0	80.4	106.4	117.0	125.8	128.0	130.5	140.1	146.7	148.7
1:10	14.3	23.4	29.8	41.6	48.2	55.1	61.3	68.7	86.6	95.4	103.8	106.3	108.7	117.7	123.8	127.4
1:5	13.0	20.2	25.8	34.4	38.9	45.2	50.2	56.9	68.8	75.8	83.2	86.1	88.7	96.7	102.4	106.9
1:2	10.6	15.8	20.0	25.4	27.8	32.1	35.3	39.8	46.4	50.9	55.9	59.5	63.2	69.2	74.4	78.7
K-S	0.195	0.206	0.120	0.173	0.114	0.113	0.152	0.185	0.145	0.156	0.140	0.128	0.133	0.136	0.164	0.178
RI	**GEV distribution (Product-Moments)**															
1:100	16.6	30.5	38.9	62.0	77.2	82.1	86.4	93.0	132.1	151.2	160.4	165.3	169.7	179.1	190.7	193.4
1:50	16.1	28.4	36.3	55.8	68.1	73.8	79.0	86.2	118.6	134.0	143.0	147.0	150.6	159.9	169.7	172.7
1:20	15.1	25.6	32.5	47.7	56.8	62.9	68.8	76.2	100.4	111.7	120.2	123.2	126.4	135.2	143.0	146.2
1:10	14.1	23.2	29.4	41.6	48.6	54.6	60.5	67.7	86.4	95.0	102.8	105.5	108.6	116.8	123.5	126.8
1:5	13.0	20.6	26.0	35.5	40.5	46.0	51.5	58.0	71.7	78.1	84.9	87.6	90.7	98.2	103.9	107.4
1:2	10.6	16.3	20.5	26.5	29.2	33.3	37.1	41.7	49.5	53.5	58.3	61.6	65.3	71.3	76.1	79.7
K-S	0.205	0.238	0.137	0.207	0.116	0.134	0.181	0.217	0.170	0.136	0.124	0.120	0.147	0.111	0.146	0.164

Station: 12_Unisa **Period:** 23 Oct 1994 to 31 Dec 2020

Year	Standard time step (min/hour)															
	5m	10m	15m	30m	45m	60m (1h)	90m (1.5h)	120m (2h)	240m (4h)	360m (6h)	480m (8h)	600m (10h)	720m (12h)	960m (16h)	1200m (20h)	1440m (24h)
1994/95	12.6	23.2	28.6	37.0	39.8	41.2	43.6	48.6	58.8	63.2	64.0	73.4	79.8	81.4	81.4	83.6
1995/96	13.4	26.6	39.4	68.4	103.2	133.8	180.4	186.4	187.2	187.2	193.4	195.0	195.0	196.4	196.4	196.4
1996/97	9.2	17.4	22.4	36.8	43.0	45.2	46.0	46.0	46.0	46.0	46.0	46.0	46.2	46.4	46.8	64.0
1997/98	7.0	11.8	15.2	24.8	27.4	27.4	32.0	32.8	40.4	45.0	49.8	51.0	52.0	56.2	58.2	60.0
1998/99	7.6	13.4	17.8	23.2	27.2	29.2	30.0	30.0	30.8	32.8	33.4	34.0	37.6	45.0	48.0	50.8
1999/00	5.6	7.8	9.0	17.4	20.8	22.2	26.0	30.0	35.4	37.8	40.0	40.2	42.2	52.8	61.3	68.3
2000/01	13.2	13.2	13.2	19.0	20.4	20.6	20.8	21.6	21.8	21.8	21.8	21.8	23.2	27.0	28.0	30.0
2001/02	9.2	15.4	18.2	26.4	31.0	32.4	32.6	33.0	33.2	33.2	33.2	33.2	33.2	33.2	33.2	33.2
2002/03	12.4	20.0	22.8	27.8	28.4	29.0	32.2	38.2	45.2	48.8	54.8	55.4	55.4	55.6	60.2	66.0
2003/04	9.4	15.8	21.0	30.2	39.6	50.8	65.4	69.2	69.4	69.4	69.4	69.4	69.6	70.8	86.0	88.8
2004/05	7.6	13.2	18.4	22.0	23.6	24.8	30.2	35.2	49.8	50.6	50.6	50.6	50.6	56.4	56.4	67.2
2005/06	10.6	16.2	20.6	28.2	33.2	35.2	37.2	39.4	50.8	59.4	65.8	77.8	80.6	81.2	81.2	81.2
2006/07	7.6	11.8	14.2	19.2	20.0	20.0	20.0	20.4	28.4	34.6	36.6	36.6	37.0	37.8	40.6	41.2
2007/08	9.4	16.8	24.4	37.6	41.0	41.8	41.8	41.8	50.4	52.4	52.6	52.6	52.6	52.6	52.6	53.8
2008/09	12.0	21.6	26.2	35.2	40.6	43.0	44.2	44.2	47.4	48.6	48.6	48.6	48.6	48.6	48.6	48.6
2009/10	7.2	12.6	17.0	22.8	22.8	26.0	28.6	28.6	28.6	28.6	28.6	28.6	28.6	29.2	32.0	37.0
2010/11	9.0	14.6	19.2	24.2	27.6	29.0	34.2	40.2	56.2	64.0	64.2	67.4	68.8	88.0	88.6	88.8
2011/12	10.0	14.8	18.8	23.6	26.8	28.0	29.0	29.4	30.0	35.2	38.4	38.8	39.6	46.2	47.6	48.6
2012/13	8.2	12.4	19.4	25.8	27.4	28.2	30.2	33.0	33.8	34.2	38.0	40.0	45.0	45.4	46.6	63.8
2013/14	16.0	30.0	30.0	30.0	30.0	33.0	41.6	47.8	65.6	73.4	73.6	73.6	73.6	77.6	95.4	98.8
2014/15	7.6	13.6	18.8	28.0	29.8	29.8	33.8	45.8	46.8	46.8	49.6	51.0	51.4	51.4	51.4	74.4
2015/16	5.4	9.2	13.4	19.4	23.2	27.0	31.0	34.0	39.2	45.4	47.8	48.8	55.0	71.4	78.8	87.0
2016/17	9.0	14.0	20.0	24.2	24.8	25.2	27.2	28.0	31.0	37.0	39.4	42.8	44.0	51.4	60.4	70.6
2017/18	9.2	15.0	16.6	23.6	27.4	28.0	29.2	30.2	42.0	54.8	59.8	66.8	81.2	101.8	118.8	128.2
2018/19	6.4	10.6	12.4	14.6	15.6	16.4	18.2	22.0	24.4	30.0	35.6	36.2	36.2	44.0	44.8	44.8
2019/20	5.8	11.2	14.2	18.4	19.8	25.0	33.8	36.0	61.2	76.2	79.2	96.2	99.4	110.6	129.2	154.8
RI	**GEV distribution (L-Moments)**															
1:100	17.8	35.4	40.8	67.0	96.9	124.7	159.4	165.8	168.9	174.8	176.5	190.8	195.5	208.7	225.5	224.0
1:50	16.4	30.9	36.8	57.0	76.9	93.1	114.5	121.5	132.4	139.0	141.6	152.5	157.0	168.5	182.9	187.7
1:20	14.4	25.6	31.7	45.9	57.0	64.5	75.6	81.9	95.9	102.4	105.5	112.9	116.8	126.2	137.4	146.5
1:10	12.9	22.0	27.9	38.7	45.7	49.6	56.5	61.8	75.0	80.9	84.0	89.3	92.6	100.5	109.4	119.4
1:5	11.3	18.6	24.1	32.4	36.6	38.7	43.1	47.2	58.2	63.3	66.2	69.7	72.4	78.9	85.5	95.0
1:2	8.8	14.2	18.5	24.6	26.8	28.0	30.8	33.4	39.9	43.8	46.1	47.6	49.4	54.0	57.6	64.4
K-S	0.105	0.091	0.104	0.121	0.153	0.159	0.201	0.132	0.121	0.144	0.116	0.097	0.083	0.135	0.107	0.106
RI	**GEV distribution (Product-Moments)**															
1:100	16.9	32.1	40.0	64.7	91.6	115.3	151.7	157.6	163.0	166.3	171.4	177.6	180.0	186.8	195.2	202.9
1:50	15.8	29.1	36.3	56.2	76.9	95.1	123.3	128.5	134.7	138.7	143.0	149.0	151.7	159.2	168.4	176.9
1:20	14.2	25.1	31.6	46.2	60.3	72.5	91.8	96.1	102.9	107.2	110.7	116.1	118.9	126.6	135.7	144.4
1:10	12.8	22.1	27.9	39.4	49.4	57.9	71.5	75.3	82.2	86.6	89.6	94.3	97.0	104.3	112.6	121.1
1:5	11.3	19.1	24.2	33.1	39.6	45.0	53.6	56.9	63.7	68.0	70.6	74.3	76.8	83.4	90.5	98.3
1:2	8.9	14.6	18.6	24.8	27.4	29.0	31.7	34.3	40.7	44.7	46.7	48.9	50.9	56.0	60.4	66.5
K-S	0.121	0.097	0.098	0.118	0.157	0.221	0.258	0.249	0.158	0.135	0.144	0.124	0.121	0.147	0.141	0.112

Station: 13_Proefplaas **Period:** 25 Feb 2011 to 31 Dec 2020

Year	Standard time step (min/hour)															
	5m	10m	15m	30m	45m	60m (1h)	90m (1.5h)	120m (2h)	240m (4h)	360m (6h)	480m (8h)	600m (10h)	720m (12h)	960m (16h)	1200m (20h)	1440m (24h)
2010/11	10.0	18.4	23.6	35.0	48.2	64.0	85.6	102.4	139.4	155.4	163.6	163.6	163.6	163.6	163.6	163.8
2011/12	10.0	17.0	23.0	36.2	49.0	55.2	56.4	57.4	58.6	58.6	58.6	58.6	58.6	58.6	58.6	58.6
2012/13	6.4	11.6	15.0	24.0	26.4	27.8	31.0	31.8	31.8	32.4	37.6	44.4	47.8	50.2	52.6	52.6
2013/14	10.6	18.6	26.0	35.6	41.4	49.6	59.6	68.4	99.6	101.4	101.4	101.4	101.4	101.6	105.6	106.0
2014/15	9.0	15.0	19.4	28.0	31.2	35.4	38.8	52.8	58.4	58.6	58.6	74.2	75.8	76.0	76.6	76.8
2015/16	17.2	27.2	30.4	33.0	33.0	33.0	35.0	39.6	55.2	61.0	61.4	61.4	65.2	94.8	96.6	100.4
2016/17	10.4	17.0	23.0	27.2	31.2	34.2	34.6	34.6	45.4	65.4	73.4	85.6	87.6	88.0	88.0	88.2
2017/18	10.4	19.8	24.6	43.4	52.0	54.0	57.6	61.2	75.6	76.0	76.0	79.6	91.6	110.4	129.6	140.8
2018/19	7.6	14.2	20.4	23.8	25.8	33.6	33.6	33.6	33.8	39.6	44.6	45.2	45.2	54.8	55.4	63.8
2019/20	10.2	13.2	15.4	18.4	22.0	25.6	29.2	33.8	55.0	71.2	75.8	76.4	77.4	81.8	99.4	116.2
RI	**GEV distribution (L-Moments)**															
1:100	18.9	32.4	32.2	47.9	68.7	88.1	131.0	158.3	217.0	226.5	241.4	231.2	223.2	213.0	217.2	220.6
1:50	17.2	29.5	31.3	46.2	63.9	79.5	108.3	128.9	176.2	186.1	194.9	191.8	189.4	187.3	194.1	199.3
1:20	15.1	25.8	29.9	43.4	57.0	68.2	83.9	97.8	132.4	142.0	146.1	148.6	150.7	155.6	164.1	170.8
1:10	13.6	23.1	28.4	40.7	51.3	59.8	68.7	78.9	105.3	114.3	116.7	121.3	125.1	132.9	141.6	148.7
1:5	12.0	20.3	26.4	37.2	45.0	51.2	55.7	62.9	82.2	90.3	92.0	97.5	101.8	110.9	118.9	125.5
1:2	9.7	16.3	22.2	30.4	34.7	38.6	40.4	44.3	55.1	61.6	63.8	68.9	72.2	80.4	85.6	90.3
K-S	0.256	0.166	0.162	0.138	0.161	0.207	0.207	0.181	0.199	0.251	0.207	0.178	0.151	0.138	0.136	0.106
RI	**GEV distribution (Product-Moments)**															
1:100	19.7	31.1	32.5	47.7	63.7	77.5	103.9	124.4	173.1	189.6	198.6	196.9	196.3	194.3	195.2	197.5
1:50	17.8	28.6	31.5	46.0	60.3	72.5	93.6	110.8	152.6	166.4	173.2	173.2	173.8	175.3	179.4	183.3
1:20	15.5	25.4	29.9	43.1	55.1	65.2	80.0	93.2	126.3	137.2	141.9	143.6	145.4	150.3	157.2	162.7
1:10	13.7	22.9	28.3	40.3	50.5	59.0	69.7	80.0	106.8	115.9	119.5	122.3	124.7	131.3	139.1	145.3
1:5	12.0	20.3	26.2	36.9	45.0	51.9	59.0	66.8	87.3	94.8	97.7	101.3	104.0	111.6	119.5	125.6
1:2	9.6	16.4	22.1	30.3	35.3	39.9	43.0	47.5	59.1	65.0	67.6	72.0	74.7	82.3	88.0	92.8
K-S	0.263	0.156	0.175	0.136	0.184	0.241	0.209	0.181	0.208	0.208	0.193	0.133	0.118	0.127	0.145	0.118

Station: 19_Westonaria **Period:** 01 Oct 2011 to 31 Dec 2020

Year	Standard time step (min/hour)															
	5m	10m	15m	30m	45m	60m (1h)	90m (1.5h)	120m (2h)	240m (4h)	360m (6h)	480m (8h)	600m (10h)	720m (12h)	960m (16h)	1200m (20h)	1440m (24h)
2011/12	8.4	9.6	11.6	18.8	24.4	27.8	33.0	33.0	40.2	42.6	46.8	53.8	56.4	56.4	59.4	59.4
2012/13	8.0	13.4	19.6	30.4	32.4	32.4	35.2	37.4	43.6	45.6	49.0	49.0	49.0	49.2	49.4	49.4
2013/14	12.0	19.0	21.4	33.4	45.4	48.2	59.2	61.4	63.0	63.4	63.4	63.4	63.4	63.4	63.6	63.6
2014/15	10.2	15.0	22.2	26.8	27.4	28.4	28.4	28.8	29.0	30.2	38.0	38.2	38.2	38.2	38.2	38.2
2015/16	9.8	16.6	18.8	26.4	28.4	29.0	32.2	37.0	44.8	47.2	55.8	60.2	62.6	83.4	101.8	106.2
2016/17	10.4	19.0	26.0	37.2	43.8	48.6	62.6	62.6	79.2	95.4	97.4	97.6	99.8	119.0	142.4	143.4
2017/18	9.2	11.6	14.2	22.0	24.6	25.4	25.4	25.4	26.0	26.0	32.2	35.0	40.6	54.2	55.0	62.4
2018/19	10.8	16.0	21.2	31.8	34.0	35.2	37.8	39.6	42.2	42.2	42.2	42.2	42.2	42.2	42.2	50.0
2019/20	7.2	14.0	17.0	18.6	18.6	18.8	23.6	30.6	38.8	40.0	40.0	43.6	44.8	44.8	44.8	44.8
RI	**GEV distribution (L-Moments)**															
1:100	12.9	21.2	27.0	42.5	61.0	68.0	102.4	99.0	113.2	143.9	150.5	144.9	151.4	197.5	258.1	254.8
1:50	12.6	20.8	26.6	41.1	55.9	61.4	85.3	84.2	97.5	117.6	121.0	119.6	122.8	154.5	192.7	193.6
1:20	12.1	20.0	25.7	38.7	49.0	52.8	66.8	67.6	79.2	89.7	91.2	92.9	94.0	112.7	132.3	135.7
1:10	11.6	19.1	24.7	36.4	43.7	46.5	55.2	56.9	66.8	72.7	74.0	76.7	77.2	89.3	100.3	104.2
1:5	11.0	17.9	23.2	33.3	38.1	40.0	45.1	47.3	55.5	58.3	60.1	63.1	63.6	71.0	76.5	80.2
1:2	9.6	15.2	19.6	27.3	29.5	30.7	33.1	35.6	40.8	41.6	44.9	47.5	48.6	51.8	53.0	55.7
K-S	0.120	0.114	0.170	0.119	0.150	0.151	0.144	0.148	0.216	0.232	0.134	0.102	0.134	0.113	0.126	0.142
RI	**GEV distribution (Product-Moments)**															
1:100	12.9	21.3	27.6	41.7	55.6	61.4	82.0	82.0	97.4	118.0	118.8	118.3	120.6	147.9	182.6	184.1
1:50	12.6	20.8	26.9	40.3	52.2	57.1	74.1	74.6	88.2	104.1	105.1	105.4	107.4	130.5	159.2	161.2
1:20	12.0	19.9	25.8	38.1	47.2	51.0	63.7	64.7	76.0	86.6	88.1	89.2	90.9	108.8	130.1	132.5
1:10	11.5	19.0	24.6	35.8	43.0	46.0	55.7	57.1	66.7	74.0	75.9	77.6	79.0	93.1	109.0	111.5
1:5	10.9	17.7	23.0	33.0	38.2	40.4	47.5	49.2	57.0	61.5	64.1	66.0	67.4	77.7	88.3	90.9
1:2	9.6	15.0	19.4	27.3	30.1	31.4	35.1	37.3	42.4	43.9	47.6	49.8	51.3	56.0	59.4	61.8
K-S	0.117	0.124	0.148	0.122	0.135	0.159	0.196	0.205	0.215	0.205	0.132	0.123	0.149	0.160	0.220	0.253

Station: 20_Goudkoppies **Period:** 28 Dec 2009 to 31 Dec 2020

Year	Standard time step (min/hour)															
	5m	10m	15m	30m	45m	60m (1h)	90m (1.5h)	120m (2h)	240m (4h)	360m (6h)	480m (8h)	600m (10h)	720m (12h)	960m (16h)	1200m (20h)	1440m (24h)
2009/10	14.2	20.8	26.4	31.0	33.0	34.8	36.6	37.4	42.8	43.8	44.8	52.2	56.0	58.4	58.8	59.0
2010/11	7.4	14.4	15.8	17.2	17.2	22.0	31.2	39.0	59.4	74.8	85.4	92.0	93.8	93.8	95.6	96.4
2011/12	10.0	16.6	23.2	26.4	30.8	32.0	34.0	34.6	54.6	61.6	68.8	73.2	73.6	74.6	89.4	89.4
2012/13	9.2	13.6	16.0	16.0	16.0	16.0	20.0	23.0	38.2	45.6	63.6	68.8	79.8	97.2	98.0	99.8
2013/14	6.4	12.0	14.8	18.8	22.6	23.8	25.2	25.6	28.4	37.6	45.4	50.8	51.2	51.4	51.4	56.4
2014/15	9.6	11.4	12.4	14.2	15.6	16.0	16.4	19.8	25.0	27.8	29.6	29.8	29.8	29.8	30.0	30.0
2015/16	9.4	15.4	17.8	24.2	33.2	38.6	46.0	46.6	53.4	53.8	57.8	58.6	58.6	67.2	72.0	73.8
2016/17	8.6	9.4	11.6	14.6	19.2	25.0	26.4	27.2	27.4	27.4	30.8	30.8	32.2	41.8	44.8	47.0
2017/18	9.8	18.4	24.6	29.4	31.8	32.2	32.2	32.2	44.2	51.0	59.6	66.0	71.6	79.6	91.0	93.4
2018/19	9.6	12.8	14.0	15.8	16.0	16.0	16.2	17.0	20.4	23.2	26.4	29.8	30.6	34.6	38.6	46.6
2019/20	7.2	10.2	12.2	18.4	22.2	24.2	25.8	26.4	31.4	41.0	49.8	59.0	60.4	60.6	72.0	72.2
RI	**GEV distribution (L-Moments)**															
1:100	14.9	25.6	38.4	45.4	46.0	48.2	53.5	56.0	76.2	91.2	100.4	104.1	109.1	119.0	116.4	117.6
1:50	14.1	23.7	33.7	39.9	42.5	45.1	50.2	52.4	71.3	84.3	94.3	98.9	103.8	113.0	112.9	114.1
1:20	12.8	21.1	28.1	33.4	37.6	40.6	45.2	47.1	63.9	74.5	84.9	90.5	95.2	103.3	106.6	107.7
1:10	11.8	19.1	24.3	28.9	33.7	36.7	40.8	42.6	57.5	66.4	76.7	82.7	87.1	94.3	99.8	100.9
1:5	10.7	16.9	20.7	24.6	29.3	32.3	35.9	37.5	50.1	57.3	66.9	73.0	76.9	83.0	90.2	91.4
1:2	9.0	13.5	15.8	19.0	22.4	24.7	27.3	28.9	37.4	42.4	49.7	54.8	57.4	61.9	69.0	70.8
K-S	0.213	0.072	0.150	0.150	0.204	0.156	0.135	0.120	0.128	0.124	0.132	0.161	0.151	0.081	0.154	0.138
RI	**GEV distribution (Product-Moments)**															
1:100	15.8	23.7	32.5	38.1	42.3	45.1	51.9	53.1	71.4	86.1	96.9	102.2	105.9	115.3	118.4	118.2
1:50	14.6	22.4	30.2	35.5	40.0	42.8	48.9	50.2	67.7	80.6	91.5	97.3	101.2	109.8	114.1	114.2
1:20	13.0	20.4	26.8	31.7	36.4	39.3	44.3	45.8	61.7	72.3	83.0	89.3	93.3	100.9	106.5	107.1
1:10	11.9	18.8	24.1	28.7	33.3	36.1	40.3	41.9	56.3	65.2	75.4	81.8	85.8	92.5	98.9	99.8
1:5	10.7	16.9	21.2	25.3	29.5	32.2	35.6	37.3	49.8	57.0	66.3	72.5	76.3	82.0	88.8	90.2
1:2	8.9	13.7	16.5	19.8	22.9	25.1	27.4	29.2	37.9	42.9	50.0	54.9	57.7	62.0	67.9	70.1
K-S	0.208	0.069	0.174	0.206	0.203	0.160	0.126	0.136	0.147	0.135	0.143	0.168	0.160	0.091	0.171	0.154

Station: 21_Dube **Period:** 04 Nov 2011 to 31 Dec 2020

Year	Standard time step (min/hour)															
	5m	10m	15m	30m	45m	60m (1h)	90m (1.5h)	120m (2h)	240m (4h)	360m (6h)	480m (8h)	600m (10h)	720m (12h)	960m (16h)	1200m (20h)	1440m (24h)
2011/12	8.6	16.4	23.2	35.8	41.6	44.0	46.0	47.6	49.8	50.4	50.4	52.2	57.4	59.6	59.6	59.6
2012/13	5.6	7.8	8.6	11.8	14.4	15.2	17.2	17.2	20.4	24.0	24.0	24.0	24.4	25.8	26.4	27.8
2013/14	9.8	16.0	23.4	37.8	42.0	43.8	44.4	44.4	44.4	53.2	61.2	64.8	67.4	67.4	76.6	77.6
2014/15	6.2	9.6	11.8	14.6	17.2	19.2	24.4	29.2	48.8	64.8	65.0	69.0	77.4	83.4	86.4	92.8
2015/16	6.4	12.4	17.6	33.4	42.4	44.4	45.2	45.2	47.8	49.0	50.6	60.0	61.0	66.8	73.0	75.2
2016/17	5.8	8.4	12.6	19.0	19.8	24.2	34.0	36.0	39.4	39.4	39.4	39.4	39.4	39.4	40.2	45.0
2017/18	8.0	15.6	19.8	22.8	24.8	25.0	25.0	25.2	25.2	25.2	35.4	39.8	39.8	39.8	40.0	40.0
2018/19	5.4	8.4	10.6	16.8	18.8	19.0	20.2	26.2	28.4	28.4	28.4	28.4	28.4	35.8	39.8	45.8
2019/20	7.4	12.4	15.2	22.2	28.2	29.4	30.4	30.6	37.2	49.8	60.4	70.8	72.8	73.0	87.6	88.0
RI	**GEV distribution (L-Moments)**															
1:100	13.2	21.3	31.2	53.9	62.6	64.2	60.4	58.8	55.0	72.4	75.3	83.5	92.7	99.4	113.1	117.1
1:50	11.9	20.2	29.2	49.3	57.3	59.1	57.2	56.2	54.4	70.1	73.4	81.5	89.7	95.4	107.8	111.5
1:20	10.3	18.4	26.3	42.8	49.9	51.8	52.2	52.0	53.0	65.9	69.9	77.5	84.2	88.5	99.0	102.3
1:10	9.2	16.8	23.7	37.5	43.8	45.8	47.5	48.1	51.3	61.7	66.0	73.0	78.4	81.7	90.5	93.6
1:5	8.1	14.9	20.7	31.7	37.0	39.0	41.8	43.0	48.4	55.8	60.3	66.6	70.4	72.8	79.7	82.4
1:2	6.6	11.6	15.4	22.5	26.2	27.9	31.3	33.3	40.1	43.3	47.4	51.5	53.1	54.8	58.6	60.9
K-S	0.131	0.175	0.137	0.169	0.207	0.210	0.184	0.165	0.149	0.201	0.135	0.162	0.170	0.200	0.219	0.173
RI	**GEV distribution (Product-Moments)**															
1:100	11.4	20.3	29.3	49.0	57.8	60.2	58.8	57.3	57.6	73.3	76.6	85.2	92.6	97.9	110.0	113.4
1:50	10.8	19.4	27.8	45.8	54.0	56.3	55.9	55.0	56.4	70.5	74.2	82.5	89.3	93.9	105.1	108.3
1:20	9.8	17.9	25.3	40.9	48.1	50.3	51.1	51.1	54.1	65.9	69.8	77.6	83.3	87.2	97.0	99.9
1:10	9.0	16.5	23.1	36.6	43.0	45.1	46.7	47.3	51.5	61.3	65.4	72.4	77.3	80.5	89.0	91.7
1:5	8.2	14.9	20.5	31.7	37.1	39.0	41.3	42.6	47.7	55.2	59.3	65.4	69.2	71.9	78.9	81.3
1:2	6.8	11.7	15.6	23.0	26.7	28.4	31.4	33.4	38.9	42.9	46.6	50.5	52.5	54.6	58.7	61.0
K-S	0.177	0.183	0.156	0.176	0.214	0.216	0.196	0.177	0.142	0.217	0.154	0.162	0.176	0.210	0.230	0.186

Station: 24_Sterkfontein **Period:** 22 Sep 2009 to 31 Dec 2020

Year	Standard time step (min/hour)															
	5m	10m	15m	30m	45m	60m (1h)	90m (1.5h)	120m (2h)	240m (4h)	360m (6h)	480m (8h)	600m (10h)	720m (12h)	960m (16h)	1200m (20h)	1440m (24h)
2008/09	0.6	1.0	1.4	1.6	1.8	1.8	1.8	1.8	2.8	3.2	3.4	3.6	3.6	3.6	3.6	3.6
2009/10	6.6	12.8	16.4	25.0	27.2	27.8	27.8	27.8	29.6	29.8	32.2	36.2	36.2	36.4	36.6	36.6
2010/11	10.0	19.8	22.8	24.2	24.4	24.4	26.2	33.0	47.6	60.2	68.4	78.6	87.8	98.6	100.2	101.8
2011/12	10.0	14.4	19.2	24.2	26.2	26.4	35.2	36.2	36.6	38.0	56.6	56.6	56.6	56.6	56.8	64.4
2012/13	8.8	13.6	16.6	21.6	24.6	29.4	31.6	36.0	41.6	49.6	62.4	62.8	62.8	63.6	65.0	66.2
2013/14	9.2	13.6	15.4	18.0	18.4	18.8	20.6	21.0	32.0	33.0	33.4	34.6	35.2	39.4	39.4	46.4
2014/15	7.0	11.4	12.4	16.6	26.8	29.4	30.0	30.2	31.2	31.2	31.2	31.2	31.2	31.2	31.4	31.6
2015/16	10.4	17.2	26.0	31.8	33.0	33.8	36.0	36.4	36.4	39.2	45.0	55.0	61.8	65.2	71.0	74.4
2016/17	7.6	13.8	17.6	21.4	23.4	24.2	24.2	24.4	30.4	38.2	45.0	50.0	55.2	74.4	84.8	85.2
2017/18	15.0	21.2	25.2	29.0	29.2	29.2	29.2	29.2	29.8	38.8	40.8	50.0	57.0	64.8	69.4	72.6
2018/19	9.6	18.8	27.4	33.8	34.6	35.0	35.6	36.6	36.8	36.8	36.8	43.0	46.2	47.2	53.2	54.2
2019/20	12.6	21.6	31.4	37.4	39.2	41.6	41.6	44.4	56.2	63.0	68.0	92.0	95.0	97.8	105.0	116.2
RI	**GEV distribution (L-Moments)**															
1:100	18.0	27.7	38.9	46.0	46.5	46.7	45.2	45.5	78.5	91.2	94.4	123.1	123.1	128.2	135.2	144.0
1:50	16.5	25.9	36.3	43.0	43.5	44.2	43.8	44.6	66.8	78.6	86.5	109.4	111.9	118.7	125.8	133.5
1:20	14.5	23.3	32.5	38.6	39.3	40.6	41.4	42.8	54.6	64.7	75.8	92.1	96.8	104.9	111.9	118.2
1:10	13.0	21.3	29.4	35.1	36.0	37.5	39.1	40.9	47.3	55.8	67.4	79.5	85.0	93.3	99.8	105.1
1:5	11.5	19.1	25.9	31.2	32.5	34.1	36.2	38.3	41.2	47.9	58.6	67.1	72.5	80.3	86.0	90.3
1:2	9.3	15.7	20.2	24.8	27.0	28.4	30.6	32.7	34.3	38.3	44.9	49.6	53.5	58.7	62.4	65.3
K-S	0.144	0.189	0.134	0.127	0.149	0.164	0.119	0.193	0.170	0.188	0.133	0.147	0.171	0.127	0.109	0.123
RI	**GEV distribution (Product-Moments)**															
1:100	17.1	25.5	36.2	43.0	43.6	45.5	44.9	47.0	64.6	76.7	85.1	109.5	114.8	121.9	127.2	136.4
1:50	15.9	24.4	34.3	40.8	41.5	43.3	43.4	45.6	59.5	70.6	80.2	100.6	106.3	113.9	119.7	127.8
1:20	14.2	22.6	31.5	37.5	38.4	40.1	41.0	43.3	52.9	62.5	72.8	88.3	94.1	102.1	108.2	114.6
1:10	12.9	21.1	28.9	34.5	35.7	37.3	38.8	41.0	47.9	56.2	66.3	78.4	83.9	91.8	97.8	103.1
1:5	11.5	19.2	25.9	31.1	32.6	34.1	35.9	38.0	42.9	49.7	58.9	67.7	72.7	79.9	85.4	89.6
1:2	9.4	15.9	20.5	25.2	27.4	28.5	30.6	32.3	35.6	39.8	46.0	51.0	54.4	59.4	63.2	66.1
K-S	0.151	0.215	0.149	0.148	0.148	0.171	0.130	0.173	0.164	0.251	0.165	0.113	0.160	0.128	0.122	0.111

Station: 26_Alexandra Depot **Period:** 17 Nov 2011 to 31 Dec 2020

Year	Standard time step (min/hour)															
	5m	10m	15m	30m	45m	60m (1h)	90m (1.5h)	120m (2h)	240m (4h)	360m (6h)	480m (8h)	600m (10h)	720m (12h)	960m (16h)	1200m (20h)	1440m (24h)
2011/12	10.4	16.8	21.0	28.6	34.4	38.2	41.0	42.0	43.4	44.6	45.6	45.6	45.6	46.4	56.2	62.8
2012/13	4.6	5.0	6.2	8.2	9.6	10.0	10.4	10.6	10.8	16.4	17.2	17.2	17.2	22.8	25.8	27.2
2013/14	9.6	16.2	17.6	20.4	23.6	25.4	27.6	31.0	42.6	44.0	44.0	44.0	44.2	44.8	46.4	51.2
2014/15	8.0	11.8	15.0	22.0	25.2	25.8	26.2	26.2	29.2	33.4	36.0	36.6	36.6	36.6	36.6	37.0
2015/16	13.2	26.2	34.6	41.8	44.0	47.8	49.8	51.4	51.8	51.8	51.8	51.8	55.0	60.6	64.8	70.2
2016/17	12.8	20.6	27.4	47.6	61.0	64.0	68.8	71.4	71.8	71.8	72.0	72.0	72.0	95.8	107.6	122.0
2017/18	11.8	20.2	26.8	49.6	57.2	58.2	60.6	61.2	63.2	73.6	81.0	94.0	108.4	143.4	178.4	180.0
2018/19	11.0	20.0	25.6	41.6	53.0	55.6	59.4	64.2	102.8	112.0	121.2	121.6	122.2	135.8	141.4	141.4
2019/20	16.2	16.2	22.4	31.0	37.2	45.8	58.8	63.0	71.8	82.6	98.4	112.8	114.8	115.0	115.0	115.4
RI	**GEV distribution (L-Moments)**															
1:100	17.0	26.3	36.0	57.8	73.5	71.8	74.6	77.9	121.2	144.4	173.5	184.3	183.1	224.0	279.7	264.9
1:50	16.6	25.9	35.3	56.4	71.0	70.4	73.6	77.0	114.0	132.3	155.0	165.2	166.4	200.8	242.7	235.6
1:20	15.9	25.1	33.9	53.6	66.4	67.4	71.4	74.7	102.4	114.8	129.9	138.9	142.4	168.7	195.3	195.9
1:10	15.1	24.1	32.2	50.4	61.5	63.8	68.4	71.6	91.6	100.0	110.2	117.9	122.5	142.9	160.3	164.7
1:5	13.9	22.5	29.6	45.6	54.6	58.2	63.3	66.4	78.2	83.3	89.4	95.5	100.2	115.0	125.2	131.7
1:2	11.2	18.0	23.0	34.0	39.5	43.9	48.9	51.2	53.1	55.6	57.4	60.5	63.7	71.0	74.7	80.9
K-S	0.163	0.216	0.184	0.146	0.106	0.132	0.148	0.139	0.153	0.140	0.126	0.154	0.177	0.165	0.164	0.169
RI	**GEV distribution (Product-Moments)**															
1:100	17.0	26.8	36.5	58.8	72.9	73.3	78.8	82.4	120.0	135.4	152.3	161.2	166.0	195.1	232.2	230.3
1:50	16.6	26.3	35.7	56.9	70.2	71.3	76.9	80.4	112.6	125.5	140.2	149.0	154.0	180.5	211.3	211.5
1:20	15.9	25.3	34.0	53.6	65.4	67.6	73.1	76.5	100.9	110.6	122.3	130.6	135.7	158.3	181.0	183.6
1:10	15.0	24.2	32.0	49.9	60.4	63.3	68.8	72.0	90.1	97.6	107.0	114.5	119.3	138.6	155.6	159.5
1:5	13.8	22.4	29.2	44.7	53.6	57.2	62.3	65.2	77.0	82.6	89.6	95.8	100.0	115.5	127.2	132.0
1:2	11.1	17.8	22.6	33.2	39.0	42.8	46.9	49.0	52.9	56.5	59.9	63.2	65.8	74.6	80.0	84.8
K-S	0.149	0.202	0.166	0.169	0.124	0.139	0.180	0.174	0.142	0.139	0.156	0.184	0.183	0.188	0.178	0.171

Station: 28_Diepsloot **Period:** 04 Nov 2011 to 31 Dec 2020

Year	Standard time step (min/hour)															
	5m	10m	15m	30m	45m	60m (1h)	90m (1.5h)	120m (2h)	240m (4h)	360m (6h)	480m (8h)	600m (10h)	720m (12h)	960m (16h)	1200m (20h)	1440m (24h)
2011/12	11.0	16.2	18.2	22.8	25.0	34.6	38.4	41.2	41.6	61.6	79.8	84.2	84.2	89.0	102.0	108.6
2012/13	20.0	20.4	21.4	38.2	47.4	54.0	58.6	58.6	58.6	58.6	58.6	58.8	58.8	58.8	58.8	58.8
2013/14	6.8	13.4	17.8	29.6	39.0	42.6	51.0	55.4	61.2	63.8	63.8	63.8	63.8	66.6	71.0	87.2
2014/15	8.6	15.0	18.8	26.2	26.2	26.2	26.2	27.0	43.6	46.2	46.2	47.2	47.2	47.2	48.0	48.2
2015/16	10.2	13.8	18.8	28.6	38.8	42.2	54.8	61.8	61.8	61.8	61.8	61.8	61.8	62.0	62.0	62.0
2016/17	5.6	9.4	11.6	11.8	15.8	17.0	19.0	25.2	30.0	30.6	32.0	33.2	33.4	33.4	36.2	39.0
2017/18	4.6	7.6	8.8	11.8	12.4	13.4	13.4	13.4	15.2	21.2	26.4	31.4	34.0	41.2	48.0	48.6
2018/19	7.0	10.8	14.2	16.0	16.8	16.8	17.4	18.0	29.8	34.0	34.4	39.8	45.0	49.8	50.2	51.2
2019/20	4.4	8.0	11.4	17.6	21.2	22.2	23.6	29.6	47.8	72.8	81.8	85.8	85.8	86.0	86.0	86.0
RI	**GEV distribution (L-Moments)**															
1:100	32.8	25.5	22.8	48.9	68.6	77.6	90.5	89.0	71.4	77.6	102.3	113.1	112.7	117.4	146.8	161.8
1:50	25.7	23.6	22.5	45.2	61.4	69.6	81.3	81.9	70.0	76.6	97.6	105.7	105.1	108.9	128.6	140.2
1:20	18.5	21.0	21.8	39.9	51.8	58.7	68.6	71.5	67.1	74.4	89.8	94.6	94.0	96.7	106.6	114.7
1:10	14.2	18.7	21.0	35.3	44.3	50.2	58.5	62.6	63.8	71.6	82.2	84.9	84.5	86.6	91.3	97.2
1:5	10.8	16.3	19.7	30.2	36.5	41.2	47.7	52.3	58.6	66.8	72.5	73.7	73.6	75.3	76.7	80.9
1:2	7.0	12.2	16.3	21.5	24.8	27.5	30.8	34.9	45.5	53.6	53.6	54.4	55.1	56.9	57.2	59.4
K-S	0.136	0.161	0.185	0.126	0.169	0.148	0.170	0.169	0.135	0.166	0.145	0.136	0.126	0.119	0.173	0.173
RI	**GEV distribution (Product-Moments)**															
1:100	25.2	23.9	23.8	45.6	60.2	67.8	79.1	82.3	73.1	82.1	100.0	107.0	106.3	109.6	124.4	134.2
1:50	21.9	22.5	23.2	42.7	55.6	62.7	73.4	76.9	71.2	80.2	95.5	101.0	100.3	103.1	114.6	123.4
1:20	17.7	20.3	22.2	38.4	48.9	55.3	64.6	68.6	67.5	76.4	88.0	91.6	91.1	93.3	100.9	108.3
1:10	14.7	18.4	21.1	34.5	43.2	48.8	57.0	61.0	63.4	72.1	80.7	83.2	82.9	84.8	90.0	96.2
1:5	11.8	16.2	19.5	29.9	36.7	41.4	48.0	51.9	57.7	66.0	71.5	73.1	73.1	74.9	78.2	83.1
1:2	7.7	12.4	16.0	21.9	25.7	28.6	32.2	35.6	44.5	51.7	53.6	55.0	55.8	57.7	59.6	62.3
K-S	0.148	0.152	0.218	0.134	0.172	0.151	0.195	0.186	0.152	0.206	0.159	0.130	0.132	0.131	0.146	0.173

Station: 34_Soshanguve **Period:** 11 Sep 2009 to 31 Dec 2020

Year	Standard time step (min/hour)															
	5m	10m	15m	30m	45m	60m (1h)	90m (1.5h)	120m (2h)	240m (4h)	360m (6h)	480m (8h)	600m (10h)	720m (12h)	960m (16h)	1200m (20h)	1440m (24h)
2008/09	0.8	1.4	1.8	3.0	3.8	5.0	6.8	8.6	16.2	21.6	25.6	26.4	26.4	26.4	26.4	26.4
2009/10	10.0	17.4	24.8	36.0	38.4	38.4	39.0	39.0	39.2	41.0	41.0	41.0	41.2	41.8	43.8	43.8
2010/11	11.6	17.6	22.2	33.6	40.2	46.4	47.0	50.6	60.8	84.0	87.2	87.2	87.2	87.4	87.4	87.4
2011/12	8.6	12.6	15.8	18.2	20.6	21.4	21.8	22.6	23.8	23.8	29.2	29.8	32.0	32.8	34.0	34.4
2012/13	7.8	15.4	16.0	24.6	34.4	39.4	48.8	51.4	53.0	53.6	54.2	56.2	56.2	56.2	61.2	61.2
2013/14	12.6	21.6	29.4	45.0	49.4	49.8	50.2	50.4	50.6	50.6	50.6	50.6	50.6	50.6	50.6	51.2
2014/15	4.0	6.2	7.0	10.8	15.4	19.6	21.8	22.6	25.4	25.4	25.4	29.0	37.4	38.4	38.4	38.8
2015/16	7.0	13.0	16.4	19.8	24.2	29.4	43.8	46.0	46.4	50.2	60.8	60.8	60.8	60.8	60.8	60.8
2016/17	8.6	14.2	17.4	28.8	31.2	31.8	32.0	32.0	57.8	64.8	69.6	71.8	72.2	72.2	72.6	93.6
2017/18	8.4	15.2	20.0	27.4	27.8	27.8	28.4	31.0	48.6	59.0	66.4	73.4	78.6	95.0	110.0	120.2
2018/19	11.0	14.0	17.2	20.0	20.8	20.8	21.0	22.0	22.8	22.8	28.6	33.4	34.6	35.4	35.6	36.2
2019/20	6.6	10.0	12.6	16.6	19.0	23.8	24.2	24.2	28.6	31.6	33.2	34.8	35.2	35.4	35.4	35.6
RI	**GEV distribution (L-Moments)**															
1:100	14.1	22.2	33.9	57.2	64.2	68.1	66.7	69.5	71.1	103.9	112.6	117.8	124.9	146.1	169.3	195.1
1:50	13.7	21.7	31.9	52.2	58.4	61.7	62.5	65.1	68.9	95.5	102.9	106.8	111.1	125.5	140.9	159.3
1:20	12.9	20.6	28.9	45.2	50.5	53.2	56.3	58.5	64.8	83.4	89.3	91.8	93.6	101.2	109.4	120.6
1:10	12.1	19.5	26.2	39.6	44.2	46.6	50.8	52.7	60.5	73.3	78.2	80.1	80.6	84.8	89.2	96.5
1:5	11.0	17.9	23.1	33.5	37.6	39.9	44.4	46.0	54.7	62.1	66.2	67.6	67.7	69.4	71.5	75.8
1:2	8.8	14.5	17.6	24.0	27.5	29.7	33.4	34.5	42.2	43.7	46.8	48.3	49.1	49.3	49.8	51.2
K-S	0.166	0.148	0.199	0.122	0.126	0.132	0.153	0.175	0.168	0.170	0.134	0.143	0.139	0.128	0.141	0.143
RI	**GEV distribution (Product-Moments)**															
1:100	13.7	22.3	32.4	52.6	58.1	60.3	62.4	65.4	71.0	97.7	102.7	104.6	106.6	118.8	133.9	149.2
1:50	13.4	21.7	30.9	48.9	54.1	56.4	59.4	62.0	68.5	90.9	95.8	97.7	99.2	109.0	120.7	133.9
1:20	12.6	20.6	28.4	43.4	48.3	50.6	54.5	56.8	64.3	80.8	85.5	87.3	88.3	95.1	103.0	113.4
1:10	11.9	19.5	26.1	38.8	43.3	45.7	49.9	51.9	59.9	72.0	76.5	78.3	79.2	83.9	89.3	97.5
1:5	10.9	17.9	23.2	33.5	37.7	40.1	44.3	46.0	54.1	61.9	66.1	67.9	68.8	71.7	75.0	80.9
1:2	8.8	14.5	17.8	24.5	28.2	30.7	33.9	35.1	42.0	44.4	48.0	49.9	51.3	52.2	53.3	55.7
K-S	0.173	0.149	0.186	0.143	0.144	0.127	0.165	0.184	0.177	0.162	0.151	0.159	0.169	0.163	0.151	0.166

Station: 35_Wonderboom **Period:** 21 Jun 2008 to 04 Feb 2019

Year	Standard time step (min/hour)															
	5m	10m	15m	30m	45m	60m (1h)	90m (1.5h)	120m (2h)	240m (4h)	360m (6h)	480m (8h)	600m (10h)	720m (12h)	960m (16h)	1200m (20h)	1440m (24h)
2007/08	0.4	0.8	1.0	1.2	1.2	1.2	1.2	1.2	1.4	1.4	1.4	1.4	1.4	1.4	1.4	1.6
2008/09	16.2	29.0	34.4	45.0	49.4	51.4	54.8	55.8	56.8	58.8	59.8	59.8	59.8	59.8	61.4	62.2
2009/10	9.0	14.2	19.0	24.2	24.8	25.8	26.6	27.8	28.6	29.6	31.4	32.6	33.6	34.2	37.4	37.4
2010/11	8.0	15.2	18.4	29.0	35.0	41.4	52.0	70.2	99.8	107.8	107.8	109.6	110.4	114.4	115.4	115.4
2011/12	14.6	24.8	32.2	44.4	53.2	57.4	58.4	58.4	58.6	58.8	58.8	59.0	63.6	74.0	74.6	78.0
2012/13	9.4	13.4	16.0	23.8	33.8	38.0	40.2	44.8	48.0	48.0	48.2	48.6	48.6	48.6	48.6	54.0
2013/14	9.4	16.2	18.2	23.2	28.6	31.0	32.6	35.4	53.6	54.0	54.4	54.4	63.0	76.2	86.0	86.4
2014/15	10.2	17.2	20.0	26.8	35.6	41.8	53.8	57.6	58.4	63.2	96.4	103.6	103.6	103.6	109.4	110.0
2015/16	11.4	21.8	26.2	31.4	33.2	40.4	44.4	45.6	46.8	60.8	62.8	64.2	66.4	90.2	92.4	97.8
2016/17	6.0	10.6	14.2	17.8	19.6	22.6	30.4	33.6	45.6	58.0	59.2	65.0	69.6	76.8	84.0	84.8
2017/18	3.2	6.2	7.8	12.6	16.2	18.6	22.4	24.2	25.2	25.2	25.2	25.4	25.4	25.6	25.8	25.8
2018/19	6.0	9.6	13.2	18.8	19.8	20.0	20.2	20.2	21.0	21.0	23.4	26.8	28.4	33.8	36.0	41.0
2019/20																
RI	**GEV distribution (L-Moments)**															
1:100	19.7	37.8	46.8	61.9	68.1	69.7	70.7	83.8	109.9	111.5	138.5	148.0	141.9	140.4	141.4	138.6
1:50	18.4	34.3	42.1	55.6	62.5	65.5	68.0	79.4	100.9	104.4	125.6	133.0	130.2	132.6	134.7	133.1
1:20	16.4	29.6	35.9	47.3	54.6	59.1	63.3	72.3	88.1	93.4	107.7	112.7	113.3	119.9	123.4	123.3
1:10	14.6	25.8	31.1	41.1	48.3	53.3	58.7	65.7	77.6	83.7	93.4	96.8	99.3	108.1	112.3	113.4
1:5	12.6	21.6	26.1	34.6	41.3	46.5	52.5	57.6	65.8	72.1	77.8	80.1	83.6	93.5	98.1	100.2
1:2	9.1	15.2	18.6	25.1	30.1	34.4	39.9	42.4	46.7	51.6	53.2	54.5	57.8	66.0	70.0	72.9
K-S	0.129	0.119	0.155	0.146	0.149	0.148	0.154	0.135	0.205	0.222	0.180	0.172	0.165	0.144	0.117	0.107
RI	**GEV distribution (Product-Moments)**															
1:100	19.0	34.7	42.4	56.6	64.3	67.0	70.3	81.5	115.6	123.8	132.2	138.4	136.2	135.4	138.3	137.3
1:50	17.8	32.2	39.2	52.1	59.7	63.3	67.5	77.4	104.4	112.6	121.3	126.5	126.0	128.4	131.8	131.5
1:20	16.0	28.4	34.6	45.8	53.1	57.6	62.6	70.7	89.3	97.1	105.6	109.6	110.9	116.9	120.8	121.5
1:10	14.4	25.3	30.7	40.6	47.5	52.4	57.9	64.5	77.5	84.6	92.5	95.7	98.0	106.0	110.2	111.5
1:5	12.5	21.6	26.3	34.9	41.2	46.1	51.8	56.9	65.1	71.2	77.9	80.4	83.3	92.3	96.6	98.5
1:2	9.2	15.5	19.1	25.7	30.5	34.6	39.6	42.5	46.0	49.9	54.0	55.6	58.4	66.3	69.9	72.3
K-S	0.121	0.130	0.181	0.122	0.155	0.146	0.168	0.146	0.220	0.208	0.188	0.184	0.164	0.145	0.127	0.117